frontiers | Research Topics

Cardiovascular sequelae of chemotherapy and radiotherapy in cancer survivors: Current evidence and perspectives

Edited by
Antonella Lombardo, Péter Ferdinandy and Rod Skinner

Published in
Frontiers in Cardiovascular Medicine
Frontiers in Oncology

ISSN 1664-8714
ISBN 978-2-8325-2905-8
DOI 10.3389/978-2-8325-2905-8

About Frontiers

Frontiers is more than just an open access publisher of scholarly articles: it is a pioneering approach to the world of academia, radically improving the way scholarly research is managed. The grand vision of Frontiers is a world where all people have an equal opportunity to seek, share and generate knowledge. Frontiers provides immediate and permanent online open access to all its publications, but this alone is not enough to realize our grand goals.

Frontiers journal series

The Frontiers journal series is a multi-tier and interdisciplinary set of open-access, online journals, promising a paradigm shift from the current review, selection and dissemination processes in academic publishing. All Frontiers journals are driven by researchers for researchers; therefore, they constitute a service to the scholarly community. At the same time, the *Frontiers journal series* operates on a revolutionary invention, the tiered publishing system, initially addressing specific communities of scholars, and gradually climbing up to broader public understanding, thus serving the interests of the lay society, too.

Dedication to quality

Each Frontiers article is a landmark of the highest quality, thanks to genuinely collaborative interactions between authors and review editors, who include some of the world's best academicians. Research must be certified by peers before entering a stream of knowledge that may eventually reach the public - and shape society; therefore, Frontiers only applies the most rigorous and unbiased reviews. Frontiers revolutionizes research publishing by freely delivering the most outstanding research, evaluated with no bias from both the academic and social point of view. By applying the most advanced information technologies, Frontiers is catapulting scholarly publishing into a new generation.

What are Frontiers Research Topics?

Frontiers Research Topics are very popular trademarks of the *Frontiers journals series*: they are collections of at least ten articles, all centered on a particular subject. With their unique mix of varied contributions from Original Research to Review Articles, Frontiers Research Topics unify the most influential researchers, the latest key findings and historical advances in a hot research area.

Find out more on how to host your own Frontiers Research Topic or contribute to one as an author by contacting the Frontiers editorial office: frontiersin.org/about/contact

Cardiovascular sequelae of chemotherapy and radiotherapy in cancer survivors: Current evidence and perspectives

Topic editors

Antonella Lombardo — Agostino Gemelli University Polyclinic (IRCCS), Italy
Péter Ferdinandy — Semmelweis University, Hungary
Rod Skinner — Newcastle University, United Kingdom

Topic coordinator

Massimiliano Camilli — Agostino Gemelli University Polyclinic (IRCCS), Italy

Citation

Lombardo, A., Ferdinandy, P., Skinner, R., eds. (2023). *Cardiovascular sequelae of chemotherapy and radiotherapy in cancer survivors: Current evidence and perspectives*. Lausanne: Frontiers Media SA. doi: 10.3389/978-2-8325-2905-8

Table of contents

frontiers | Frontiers in Cardiovascular Medicine

TYPE Editorial
PUBLISHED 20 June 2023
DOI 10.3389/fcvm.2023.1230862

OPEN ACCESS

EDITED AND REVIEWED BY
Chiara Lestuzzi,
Santa Maria degli Angeli Hospital Pordenone, Italy

*CORRESPONDENCE
Massimiliano Camilli
massimiliano.camilli91@gmail.com

RECEIVED 29 May 2023
ACCEPTED 12 June 2023
PUBLISHED 20 June 2023

CITATION
Felici T, Skinner R, Ferdinandy P, Varga ZV, Lombardo A and Camilli M (2023) Editorial: Cardiovascular sequelae of chemotherapy and radiotherapy in cancer survivors: current evidence and perspectives.
Front. Cardiovasc. Med. 10:1230862.
doi: 10.3389/fcvm.2023.1230862

Editorial: Cardiovascular sequelae of chemotherapy and radiotherapy in cancer survivors: current evidence and perspectives

Tamara Felici[1,2], Roderick Skinner[3,4], Péter Ferdinandy[5,6,7], Zoltan V. Varga[5,8,9], Antonella Lombardo[1,2] and Massimiliano Camilli[1,2]*

[1]Department of Cardiovascular and Pulmonary Sciences, Catholic University of the Sacred Heart, Rome, Italy, [2]Department of Cardiovascular Medicine, Fondazione Policlinico Universitario A. Gemelli IRCCS, Rome, Italy, [3]Department of Paediatric and Adolescent Haematology and Oncology, Great North Children's Hospital, Newcastle upon Tyne, United Kingdom, [4]Translational and Clinical Research Institute, Newcastle University Centre for Cancer, Newcastle University, Newcastle upon Tyne, United Kingdom, [5]Department of Pharmacology and Pharmacotherapy, Semmelweis University, Budapest, Hungary, [6]Pharmahungary Group, Szeged, Hungary, [7]MTA-SE System Pharmacology Research Group, Department of Pharmacology and Pharmacotherapy, Semmelweis University, Budapest, Hungary, [8]HCEMM-SU Cardiometabolic Immunology Research Group, Budapest, Hungary, [9]MTA-SE Momentum Cardio-Oncology and Cardioimmunology Research Group, Budapest, Hungary

KEYWORDS

cancer survivors, cardiotoxicity, radiotherapy, cardio-oncology, cardiac imaging, early diagnosis

Editorial on the Research Topic
Cardiovascular sequelae of chemotherapy and radiotherapy in cancer survivors: current evidence and perspectives

Cardiovascular diseases and cancer are the two leading causes of morbidity and premature death worldwide (1, 2). In the past decade, the survival of cancer patients has impressively increased, mainly through screening modalities improvement and development of novel anticancer drugs (1, 2). This inevitably brought to a growing population of cancer survivors, burdened by long-term sequelae due to chemotherapy and radiotherapy (1–3). Indeed, chest malignancies, including lung, esophageal and breast cancers, as well as lymphomas, usually require radiotherapy as part of their treatment regimen. Even though advanced radiation techniques have provided better protective effects for the heart, the risk of delayed heart disease still represents a considerable concern.

Therefore, we should take into account the potential synergic effect of anticancer agents and radiotherapy (4–6). Moon-Sing Lee et al. in their population-based study, identified 158,798 breast cancer patients and using a propensity score match of 1:1, included 21,123 patients in each left and right breast radiation cohort. Previous heart disease and anticancer agents, including epirubicin, doxorubicin and trastuzumab, were taken into account for the analysis. Patients who received left radiation demonstrated an increased risk of ischemic heart disease compared with patients who received right breast radiation. Furthermore, in those undergoing left breast radiation dose >6,040 Gray, subsequent epirubicin might show a tendency to increase the risk of heart failure, whereas doxorubicin and trastuzumab did not. Further studies appear to be needed to confirm these hypothesis-generating results.

In the arena of emerging mechanisms involved in cardiotoxicity, the inflammatory cascade seems to be a common denominator in the pathogenesis of cardiovascular events during treatment of various types of tumors. In particular, Torrente et al. conducted a single-institution retrospective study in order to assess the incidence and identify risk factors for cardiac events in patients treated with Immune checkpoint inhibitors (ICIs) for hematological and solid tumors. These agents produce a wide spectrum of inflammatory and immune-related adverse events (7), mainly due to aberrant autoreactive T-cell activation, eventually affecting any organ or tissue. Among the various forms of ICI toxicities, myocarditis brings high risk of morbidity and mortality. In this study, 378 patients were analyzed and it was found that the incidence of cardiac events (CEs) was 16.7%, during a median follow-up of 50.5 months. The multivariable analysis showed that age, history of arrhythmia or ischemic heart disease, as well as prior immune-related adverse events, were predictors of CEs. Moreover, it appeared that CEs during ICI treatment, in particular atrial fibrillation, were more common than currently appreciated. Thus, a thorough cardiovascular evaluation is strongly recommended before ICI treatment and, in high-risk patients, a closer follow-up and prompt referral to cardio-oncology specialists, as soon as cardiotoxicity is suspected. Risk stratification using a scoring system may improve the cardiovascular outcomes of patients treated with ICIs, by identifying those at higher risk for cardiovascular complications.

In the field of innovative immunological treatment, another topic of current interest is represented by chimeric antigen receptor-T (CAR-T) cells infusion for patients affected by advanced and refractory onco-hematological malignancies. CAR-T cell-related cardiovascular toxicities are now emerging as significantly affecting patients' prognosis. Mechanisms involved are still under investigation, although the aberrant inflammatory activation observed in cytokine release syndrome (CRS) seems to play a pivotal role. The most frequently reported cardiac events, observed both in adults and in the pediatric population, are represented by hypotension, arrhythmias and left ventricular systolic dysfunction, sometimes associated with overt heart failure. Therefore, there is an increasing need to understand the pathophysiological basis of these events and risk factors related to their development, in order to identify most vulnerable patients requiring a close cardiological monitoring and long-term follow-up. A multidisciplinary approach focused on the management of this selected population is now needed to optimize outcomes Camilli et al.

The inflammatory hypothesis may be also applied to the therapeutic field. Aspirin, through its anti-inflammatory effect, can inhibit tumor cell growth and prevent the development of cardiovascular diseases (8). By suppressing cyclooxygenase 1/2, some preclinical studies have found possible antitumor mechanisms in subjects affected by prostate cancer. Wei-Ting Chang et al. starting from a reported increased risk of incident coronary heart disease and myocardial infarction in association with Gonadotropin Releasing Hormone (GnRH) antagonists treatment, aimed at studying whether regular aspirin use was associated with a risk reduction of major adverse cardiovascular and cerebrovascular events (MACCEs) by using a nationwide database. In their study, they observed that, despite a higher risk of MACCEs among irregular aspirin users, after adjusting for age, cancer stage and comorbidities, there was a trend to MACCEs reduction among those who received aspirin regularly.

Among the numerous pathological changes that occur to the myocardium during cardiotoxic therapy, oedema is considered an early manifestation of myocardial damage and a precursor of cardiac dysfunction and fibrosis (9, 10). Cardiac magnetic resonance (CMR) T2 mapping technique can characterize myocardial oedema *in vivo* and potentially provide additional insights beyond functional evaluation (9, 10). In the field of gynecological malignancies, Meng-Xi Young et al. enrolled 73 cancer patients and 41 healthy volunteers. All participants underwent CMR imaging. CMR sequences included cardiac cine, T2 mapping, and late gadolinium enhancement. In patients with gynecological malignancies, myocardial oedema developed with increasing chemotherapy cycles and was associated with decreased left ventricular mass. This report represents one of the few examples of T2 mapping application in cardio-oncology and above all in the gynecological population.

At the same time, in order to confirm the ability of native T1 and T2 values in detecting and monitoring early myocardial injury of chest radiotherapy, Yaotian Tian et al. in their prospective observational study, enrolled fifteen participants who received non-anthracycline chemotherapy and chest radiotherapy, and 30 age/gender-matched controls. Cardiac magnetic resonance scans were performed within 2 days, 3 months, and 6 months after chest radiotherapy. They demonstrated that native T1 and T2 values increased at 3 months after radiotherapy, whereas LVEF showed no significant changes during the 6-month follow-up.

Rapid development of microarray and sequencing technologies has revolutionized the complexity of collecting and examining molecular data in current biomedical research. Hongyan Qian et al. aimed at understanding the differences in the molecular mechanisms involved in doxorubicin-induced acute and chronic cardiotoxicity, through mouse models and Ribonucleic acid (RNA)-sequencing data. Mice were injected intraperitoneally with doxorubicin [(20 mg/kg, once) or (5 mg/kg/week, three times)] to simulate acute and chronic cardiotoxicity. Left ventricular myocardium samples were analyzed by RNA-sequencing to identify differentially-expressed genes. *Alas1*, *Atp5g1*, and *Ptgds* revealed to be ideal biomarkers in acute cardiotoxicity, while *Hsph1* and *Vegfa* were identified as potential biomarkers of chronic toxicity. This report first provided bioinformatics and clinical evidence for differences in mechanisms of doxorubicin-induced acute and chronic cardiotoxicity.

The increasing need to understand the pathophysiological basis of cardiotoxicity and its early detection serves to identify most vulnerable patients requiring a close cardiological monitoring and, above all, a long-term follow-up (2). With improved cancer survival, non-cancer events, especially heart diseases, have become a leading cause of death in neoplastic patients and require long-term follow-up. Bei Chen et al. in the first large population-based study on the risk of fatal cardiac events in sarcoma patients, suggested that the risk of death is higher than

that observed in the general population, and progressively increased with longer follow-up times. However, in patients with bone and soft tissue sarcoma, the risk of cardiac death varied mainly in patients with different histological subtypes of sarcoma and disease stages. Subgroup analyses indicated that chemotherapy increased the risk of events in patients with localized osteosarcoma, but not in those with other histological sarcoma subtypes and clinical characteristics. Thus, to mitigate the risk of death in sarcoma patients, enhanced multidisciplinary cooperation is warranted.

Similarly, Xuezhen Wang et al. explored the impact of chemotherapy on the risk of cardiac-related death in astrocytoma patients, by retrospectively evaluating astrocytoma patients diagnosed between 1975 and 2016 in the Surveillance, Epidemiology, and End Results (SEER) database. They found that age at diagnosis plays a crucial role in determining the risk of subsequent cardiac death rather than chemotherapy, highlighting that cardio–oncologists must provide comprehensive care and long-term monitoring for cancer patients, especially those at an increased cardiovascular risk.

This special issue again sheds light on the emerging role of cardio-oncology teams, always more necessary to reduce the burden of cardiovascular diseases in cancer patients through surveillance strategies implementation and cardiotoxicity management protocols.

Author contributions

TF, RS, PF, ZV, AL and MC wrote the original draft of the Editorial and made critical revisions to the draft. All authors contributed to the article and approved the submitted version.

Conflict of interest

The authors declare that the research was conducted in the absence of any commercial or financial relationships that could be construed as a potential conflict of interest.

Publisher's note

References

1. Bray F, Laversanne M, Cao B, Varghese C, Mikkelsen B, Weiderpass E, et al. Comparing cancer and cardiovascular disease trends in 20 middle- or high-income countries 2000–19: a pointer to national trajectories towards achieving sustainable development goal target 3.4. *Cancer Treat Rev*. (2021) 100:102290. doi: 10.1016/j.ctrv.2021.102290

2. Lyon AR, López-Fernández T, Couch LS, Asteggiano R, Aznar MC, Bergler-Klein J, et al. 2022 ESC guidelines on cardio-oncology developed in collaboration with the European hematology association (EHA), the European society for therapeutic radiology and oncology (ESTRO) and the international cardio-oncology society (IC-OS). *Eur Heart J*. (2022) 43(41):4229–361. doi: 10.1093/eurheartj/ehac244

3. Liang Z, He Y, Hu X. Cardio-oncology: mechanisms, drug combinations, and reverse cardio-oncology. *Int J Mol Sci*. (2022) 23(18):10617. doi: 10.3390/ijms231810617

4. Delaney G, Jacob S, Featherstone C, Barton M. The role of radiation therapy in cancer treatment: estimating optimal use from an evidence-based review of clinical guidelines. *Cancer*. (2005) 104(6):1129–37. doi: 10.1002/cncr.21324

5. Minotti G, Reggiardo G, Camilli M, Salvatorelli E, Menna P. From cardiac anthracycline accumulation to real-life risk for early diastolic dysfunction: a translational approach. *JACC CardioOncol*. (2022) 4(1):139–40. doi: 10.1016/j.jaccao.2021.12.002

6. Minotti G, Menna P, Camilli M, Salvatorelli E, Levi R. Beyond hypertension: diastolic dysfunction associated with cancer treatment in the era of cardio-oncology. *Adv Pharmacol*. (2022) 94:365–409. doi: 10.1016/bs.apha.2022.02.002

7. Tedeschi A, Camilli M, Ammirati E, Gentile P, Palazzini M, Conti N, et al. Immune checkpoint inhibitor-associated myocarditis: from pathophysiology to rechallenge of therapy—a narrative review. *Future Cardiol*. (2023) 19(2):91–103. doi: 10.2217/fca-2022-0120

8. Camilli M, Iannaccone G, La Vecchia G, Cappannoli L, Scacciavillani R, Minotti G, et al. Platelets: the point of interconnection among cancer, inflammation and cardiovascular diseases. *Expert Rev Hematol*. (2021) 14(6):537–46. doi: 10.1080/17474086.2021.1943353

9. Camilli M, Skinner R, Iannaccone G, La Vecchia G, Montone RA, Lanza GA, et al. Cardiac imaging in childhood cancer survivors: a state-of-the-art review. *Curr Probl Cardiol*. (2023) 48(4):101544. doi: 10.1016/j.cpcardiol.2022.101544

10. Baldassarre LA, Ganatra S, Lopez-Mattei J, Yang EH, Zaha VG, Wong TC, et al. Advances in multimodality imaging in cardio-oncology: JACC state-of-the-art review. *J Am Coll Cardiol*. (2022) 80(16):1560–78. doi: 10.1016/j.jacc.2022.08.743

frontiers | Frontiers in Oncology

TYPE Original Research
PUBLISHED 12 September 2022
DOI 10.3389/fonc.2022.952370

OPEN ACCESS

EDITED BY
Antonella Lombardo,
Agostino Gemelli University Polyclinic (IRCCS), Italy

REVIEWED BY
Gareth Morgan,
Hywel Dda University Health Board, United Kingdom
Andrea Paccone,
G. Pascale National Cancer Institute Foundation (IRCCS), Italy

*CORRESPONDENCE
You-Cheng Lin
cmcvecho3@gmail.com

SPECIALTY SECTION
This article was submitted to Cardio-Oncology, a section of the journal Frontiers in Oncology

RECEIVED 25 May 2022
ACCEPTED 19 August 2022
PUBLISHED 12 September 2022

CITATION
Chang W-T, Hong C-S, Hsieh K-L, Chen Y-C, Ho C-H, Shih J-Y, Kan W-C, Chen Z-C and Lin Y-C (2022) Regular use of aspirin is associated with a lower cardiovascular risk in prostate cancer patients receiving gonadotropin-releasing hormone therapy. *Front. Oncol.* 12:952370. doi: 10.3389/fonc.2022.952370

Regular use of aspirin is associated with a lower cardiovascular risk in prostate cancer patients receiving gonadotropin-releasing hormone therapy

Wei-Ting Chang[1,2,3], Chon-Seng Hong[1,4], Kun-Lin Hsieh[5,6], Yi-Chen Chen[7], Chung–Han Ho[7,8], Jhih-Yuan Shih[1,4], Wei-Chih Kan[9,10], Zhih-Cherng Chen[1] and You-Cheng Lin[11]*

[1]Division of Cardiology, Department of Internal Medicine, Chi Mei Medical Center, Tainan, Taiwan, [2]Department of Biotechnology, Southern Taiwan University of Science and Technology, Tainan, Taiwan, [3]Institute of Clinical Medicine, College of Medicine, National Cheng Kung University, Tainan, Taiwan, [4]Department of Health and Nutrition, Chia Nan University of Pharmacy and Science, Tainan, Taiwan, [5]Division of Urology, Department of Surgery, Chi-Mei Medical Center, Tainan, Taiwan, [6]Department of Environmental and Occupational Health, College of Medicine, National Cheng Kung University, Tainan, Taiwan, [7]Department of Medical Research , Chi-Mei Medical Center, Tainan, Taiwan, [8]Department of Health and Nutrition , Chia Nan University of Pharmacy and Science, Tainan, Taiwan, [9]Division of Nephrology, Department of Internal medicine, Chi Mei Medical Center, Tainan, Taiwan, [10]Department of Biological Science and Technology, Chung Hwa University of Medical Technology, Tainan, Taiwan, [11]Division of Plastic Surgery, Department of Surgery, Chi-Mei Medical Center, Tainan, Taiwan

Gonadotropin-releasing hormone (GnRH) therapy has been known to increase risks of major adverse cardiovascular and cerebrovascular events (MACCEs). Herein, we aim to estimate whether regular use of aspirin attenuates risks of MACCEs in prostate cancer patients receiving GnRHs. Using Taiwanese National Health Insurance Research Database (NHIRD), we identified 7719 patients diagnosed with prostate cancer who were either aspirin-naïve, received irregular or regular aspirin from 2008 to 2015. Through a multivariable logistic regression model, we investigated the impact of aspirin on MACCEs. Compared with nonusers and irregular users, most patients receiving regular aspirin were older and had more comorbidities. The crude incidence of one-year MACCEs was lowest in aspirin nonusers but highest in irregular users of aspirin compared with regular users of aspirin (2.65% vs. 4.41% vs. 2.85%, p=0.0099). After adjusting for age, cancer stage and comorbidities, irregular aspirin users had a higher risk of one-year MACCEs (adjusted OR: 1.33; 95% CI: 0.93-1.90, p=0.1139) than aspirin nonusers, but conversely, there was a trend of reducing the risk of MACCEs among those who received regular aspirin (adjusted OR: 0.79; 95% CI: 0.44-1.42, p=0.4256). In the subgroup analysis, there were age- and cancer stage-independent higher risks of MACCEs in patients who took aspirin irregularly compared to those in patients who did not take aspirin. The risks were attenuated in patients

receiving regular aspirin. Collectively, regular use of aspirin presented a trend of reducing risks of MACCEs in prostate cancer patients receiving GnRHs. However, irregular use of aspirin diminished the benefits.

KEYWORDS

prostate cancer, GnRH therapy, aspirin, cardiotoxicity, MACCEs

Introduction

With a high prevalence, prostate cancer affects approximately one man in eight during his lifetime (1, 2). Notably, at the average age of 66 at diagnosis, most prostate cancer patients were at old ages and had comorbidities (2). Medical castration, including gonadotropin-releasing hormone (GnRH) therapy, has significantly improved cancer-free survival (3, 4). Nevertheless, since the first observational study in a Surveillance, Epidemiology, and End Results-Medicare database, numerous studies, including randomized controlled trials, have identified an increased risk of incident coronary heart disease and myocardial infarction in association with GnRH therapy (5–7). To date, the cornerstone of management of GnRH therapy-associated cardiovascular complications relies on prevention (6, 7). Before initiating GnRH therapy, a multidisciplinary discussion with the patient, especially those with multiple cardiovascular risk factors, about the risks and benefits of GnRH therapy should be carried out (6). Additionally, increasing the awareness of patients of the signs of cardiovascular disease and screening for undiagnosed risk factors are essential (6, 8). Notably, evidence suggests that, in patients diagnosed with high-risk prostate cancer, aspirin may be associated with lower prostate cancer-specific mortality (9, 10). Although this has yet to be validated in other populations, it is possible that select patients may benefit from aspirin for primary and secondary prevention of cardiovascular diseases and possibly for reduced cancer-related mortality.

Aspirin, through its anti-inflammatory effect, can inhibit tumor cell growth and the development of cardiovascular diseases (9, 10). By suppressing cyclooxygenase 1/2, some preclinical studies have found some possible antitumor mechanisms of aspirin in prostate cancer (11, 12). Downer et al. suggested that regular aspirin lowers the risk of lethal prostate cancer (13). Additionally, evidence suggests that, in patients diagnosed with high-risk prostate cancer, aspirin may be associated with lower prostate cancer-specific mortality (9, 10). Nevertheless, it remains uncertain whether prostate cancer patients may benefit from aspirin for primary and secondary prevention of cardiovascular diseases. Hereby, using a nationwide database, we aimed to study whether regular aspirin use is associated with a risk reduction of major adverse cardiovascular and cerebrovascular events (MACCEs) in prostate cancer patients receiving GnRH therapy.

Method

Data source

This study was a real-world database study using Taiwan's National Health Insurance Research Database (NHIRD) and the Taiwan Cancer Registry (TCR), which are released by the Health and Welfare Data Science Center (HWDC). The NHIRD includes age, sex, medications, procedures and all medical diagnoses from Taiwan's single-payer National Health Insurance program. The diagnosis of diseases and procedures in the NHIRD was based on the International Classification of Diseases (ICD) codes, so high reliability could be confirmed (14). In addition, the TCR is a high-quality registry database that includes almost 97% of cancer patients and has been established by Taiwan's Ministry of Health and Welfare since 1979 (15, 16). Information on age at cancer diagnosis, sex, cancer stages, cancer sites, tumor histology, and treatment types are all present in the TCR. The institutional review committee of Chi Mei Medical Center approved this study (IRB: 11005-E03). Encrypted personal identification was used to prevent the possibility of an ethical violation according to the regulations of the Bureau of National Health Insurance (BNHI) in Taiwan, so informed consent was not required.

Definitions of studied subjects

Patients newly diagnosed with prostate cancer and receiving GnRH therapies from 2008 to 2015 were identified from the TCR-long form, and the detailed information is listed in Figure 1. To correspond to the aim of the completed dataset, the initial exclusion criteria for this study were patients with a history of MACCEs before cancer, incomplete medical records of cancer stage, and patients aged less than 18 years. Moreover, we defined patients who only received medical castration,

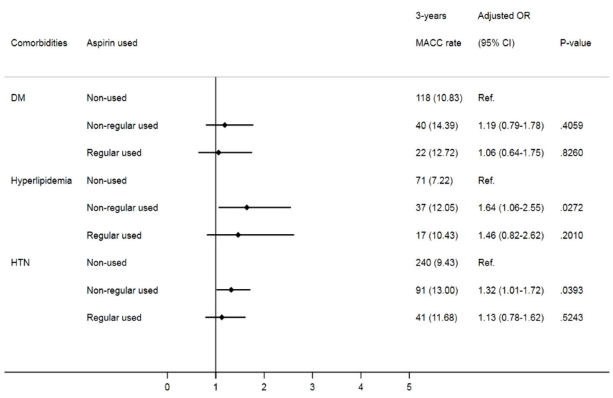

FIGURE 1
The flowchart of study design and patient selection.

including GnRH agonists/antagonists, within 2 years after the date of diagnosis of cancer as the target patients. Thus, the index date of this study was the date of prostate cancer patients receiving GnRH therapy. Patients given surgical castration or receiving both GnRH and surgical therapy, patients who received treatment before cancer diagnosis, patients receiving GnRH therapy two years after a cancer diagnosis, and MACCEs before medical castration were all excluded. Finally, patients with a history of aspirin use were assessed within one year before the diagnosis of cancer. All patients were divided into three groups: (1) patients with aspirin prescription for more than 10 months in one year were regular aspirin users, (2) otherwise patients were defined as irregular users of aspirin. Also, (3) patients without aspirin use at least one year before the diagnosis of cancer were aspirin-naïve. The dosage of aspirin was 100mg per day.

Information regarding age, clinical stage of cancer, comorbidities, and concomitant medication history within the previous 12 months among the study subjects was also considered a potential confounding factor. Age was classified into the following groups: <60, 60-69, and ≧70 years old. The clinical stage of cancer included early stages (I/II) and advanced stages (III/VI). The diagnosis codes of comorbidities and the Anatomical Therapeutic Chemical (ATC) codes of drugs are shown in Supplementary Table 1.

Study endpoint

The primary outcome was a composite endpoint of MACCEs, including new-onset acute myocardial infarction (AMI), heart failure (HF), and ischemic stroke (including transient ischemic attack [TIA]), after the index date during the study period. All patients were followed-up from the index date to death, were lost to follow-up, or were followed the whole three years. The sensitivity analysis approach was also used to verify MACCE risk. Both one-year and three-year risks of MACCEs were estimated to validate the association between MACCEs and three groups of aspirin use. Because ICD-9-CM was replaced by ICD-10-CM in 2016, both ICD-9-CM and ICD-10-CM codes were used to identify endpoints in the primary outcome during the follow-up period (Supplementary Table 1).

Statistical analysis

The baseline information of patients is presented as numbers with percentages, and the differences in proportions were evaluated using Pearson's chi-square test or Fisher's exact test. A multivariable logistic regression model was used to evaluate the risk of MACCEs among the three aspirin use groups. Patient age, clinical stage of cancer, comorbidities, and the use of drugs were included as covariates in the model to estimate the adjusted odds ratio (OR) with the 95% confidence interval (95% CI). Subgroup analyses of different age groups and cancer stages were also performed. A forest plot was used to present the risk of MACCEs between the three aspirin use groups among patients with diabetes, hyperlipidemia or hypertension. Statistical significance was considered a p-value less than 0.05. SAS 9.4 for Windows (SAS Institute Inc., Cary, NC, USA) was used for all data analyses.

Results

Demographic information of prostate cancer patients

From 2008 to 2015, we identified 7719 patients diagnosed with prostate cancer with information on aspirin use. Among

them, 6346 patients were aspirin-naïve, 952 patients were irregular aspirin users and 421 patients were regular aspirin users (Table 1). Compared with aspirin nonusers and irregular aspirin users, most patients who received regular aspirin were older and were diagnosed at an earlier cancer stage. There were more cardiovascular comorbidities, including diabetes, hypertension, hyperlipidemia, peripheral artery disease, valvular heart diseases, atrial fibrillation, and chronic kidney disease, among patients with regular aspirin use compared to that among aspirin nonusers or irregular aspirin users. Additionally, more regular aspirin users were prescribed ACEIs/ARBs and statins. Although the crude incidence of all-cause mortality was not significantly different among groups, interestingly, the one-year crude incidence of MACCEs was lowest in aspirin nonusers but highest in irregular aspirin users compared with those in regular aspirin users (2.65% vs. 4.41% vs. 2.85%, p=0.0099). The crude incidence was persistently lower in aspirin nonusers compared to those in the other two groups at the three-year follow-up.

The incidence of mortality and MACCEs between aspirin users and nonusers

After adjusting for age, comorbidities, cardiovascular medications and androgen receptor antagonists, in terms of one-year MACCEs, compared with aspirin nonusers, irregular aspirin users had a relatively higher risk of MACCEs (adjusted OR: 1.33; 95% CI: 0.93-1.90, p=0.1139), while notably, there was a trend of reducing the risk of MACCEs among those who received aspirin regularly (adjusted OR: 0.79; 95% CI: 0.44-1.42, p=0.4256) (Table 2). Additionally, other risk factors, including old age (≥70 years old) (adjusted OR: 3.31; 95% CI: 1.51-7.25, p<0.0028); advanced cancer stage (III/VI) (adjusted OR: 1.44;

TABLE 1 Demographic information of prostate cancer patient in groups of non-Aspirin use, non-regular Aspirin use and regular Aspirin use.

	Non-Aspirin use N = 6,346	Non-regularAspirin use N = 952	Regular Aspirin use N = 421	P-value
Age groups				
<60	645 (10.16)	38 (3.99)	14 (3.33)	<.0001
60-69	1849 (29.14)	238 (25.00)	92 (21.85)	
≧70	3852 (60.70)	676 (71.01)	315 (74.82)	
Clinical stage				
I, II	1764 (27.80)	296 (31.09)	136 (32.30)	0.0216
III, IV	4582 (72.20)	656 (68.91)	285 (67.70)	
Mortality	2328 (36.68)	371 (38.97)	151 (35.87)	0.3552
MACCEs				
1-years	168 (2.65)	42 (4.41)	12 (2.85)	0.0099
3-years	483 (7.61)	105 (11.03)	47 (11.16)	0.0001
Comorbidities				
PAD	54 (0.85)	19 (2.00)	10 (2.38)	0.0002
DM	1090 (17.18)	278 (29.20)	173 (41.09)	<.0001
Hyperlipidemia	983 (15.49)	307 (32.25)	163 (38.72)	<.0001
Valvular heart disease	72 (1.13)	32 (3.36)	15 (3.56)	<.0001
Asthma	200 (3.15)	33 (3.47)	14 (3.33)	0.8661
Atrial fibrillation	51 (0.80)	36 (3.78)	24 (5.70)	<.0001
CKD	465 (7.33)	101 (10.61)	40 (9.50)	0.0009
HTN	2546 (40.12)	700 (73.53)	351 (83.37)	<.0001
COPD	352 (5.55)	76 (7.98)	34 (8.08)	0.0023
Drug used				
ACEI	345 (5.44)	119 (12.50)	73 (17.34)	<.0001
Anti-coagulants: Warfarin	54 (0.85)	15 (1.58)	3 (0.71)	0.0846
ARB	1157 (18.23)	362 (38.03)	221 (52.49)	<.0001
Statin	607 (9.57)	215 (22.58)	133 (31.59)	<.0001
Cyproterone, bicalutamide and diethylstilbestrol	189 (2.98)	27 (2.84)	13 (3.09)	0.9604

P-value was from Pearson's chi-square test.
MACCEs, major adverse cardiovascular and cerebrovascular events; PAD, peripheral arterial disease; DM, diabetes mellitus; HTN, hypertension; CKD,chronic kidney disease; COPD, chronic obstructive pulmonary disease; ACEI, Angiotensin Converting Enzyme Inhibitors; ARB, Angiotensin II receptor blockers.

TABLE 2 Risks of 1-year and 3-years major adverse cardiovascular and cerebrovascular events (MACCEs) in prostate cancer patients having different treatment or comorbidities.

	1- year MACCEs				3-years MACCEs			
	Adjusted OR (95% C.I.)	P-value	Adjusted OR[a] (95% C.I.)	P-value	Adjusted OR (95% C.I.)	P-value	Adjusted OR[a](95% C.I.)	P-value
Non-used	**Ref.**		**Ref.**		**Ref.**		**Ref.**	
Non-regular aspirin used	1.33 (0.93-1.90)	0.1139	1.30 (0.91-1.85)	0.1487	1.18 (0.94-1.49)	0.1608	1.14 (0.90-1.43)	0.2824
Regular aspirin used	0.79 (0.44-1.42)	0.4256	0.77 (0.43-1.39)	0.3813	1.08 (0.78-1.51)	0.6321	1.04 (0.75-1.45)	0.7988
Age groups								
<60	Ref.		Ref.		Ref.		Ref.	
60-69	1.79 (0.78-4.09)	0.1692	1.79 (0.78-4.08)	0.1694	1.29 (0.83-2.01)	0.2532	1.29 (0.83-2.01)	0.2521
≧70	3.31 (1.51-7.25)	0.0028	3.35 (1.53-7.34)	0.0025	2.54 (1.69-3.83)	<.0001	2.61 (1.74-3.94)	<.0001
Clinical stage								
I, II	Ref.		Ref.		Ref.		Ref.	
III. IV	1.44 (1.05-1.97)	0.0256	1.46 (1.07-2.01)	0.0186	1.20 (0.99-1.44)	0.0627	1.18 (0.98-1.42)	0.0785
Comorbidities								
PAD	1.38 (0.52-3.65)	0.5158	1.36 (0.51-3.59)	0.5393	1.69 (0.92-3.10)	0.0917	1.63 (0.89-2.99)	0.1163
DM	1.65 (1.21-2.26)	0.0015	1.62 (1.18-2.20)	0.0024	1.51 (1.24-1.85)	<.0001	1.51 (1.24-1.84)	<.0001
Hyperlipidemia	0.72 (0.48-1.08)	0.1089	0.71 (0.48-1.07)	0.0995	0.82 (0.64-1.05)	0.1176	0.82 (0.64-1.05)	0.1185
Valve	1.27 (0.54-3.02)	0.5871	1.24 (0.52-2.95)	0.6275	2.05 (1.27-3.31)	0.0034	2.10 (1.31-3.37)	0.0021
Asthma	1.27 (0.65-2.45)	0.4857	1.25 (0.65-2.42)	0.5058	1.19 (0.78-1.81)	0.4296	1.27 (0.84-1.91)	0.2612
AF	0.91 (0.34-2.44)	0.8469	0.90 (0.33-2.42)	0.8313	1.21 (0.68-2.17)	0.5155	1.15 (0.64-2.06)	0.6385
CKD	1.57 (1.07-2.32)	0.0223	1.60 (1.09-2.35)	0.0161	1.34 (1.03-1.74)	0.0284	1.35 (1.04-1.74)	0.0248
HTN	1.44 (1.04-2.00)	0.0279	1.48 (1.07-2.05)	0.0169	1.27 (1.04-1.55)	0.0207	1.29 (1.06-1.58)	0.0124
COPD	1.36 (0.85-2.16)	0.1989	1.41 (0.89-2.22)	0.1432	1.24 (0.91-1.67)	0.1708	1.29 (0.96-1.73)	0.0949

[a]MACCE is the leading cause of death.
Abbreviations as listed in Table 1.

95% CI: 1.05-1.97, p<0.0256); and comorbidities, including DM (adjusted OR: 1.65; 95% CI: 1.21-2.25, p=0.0015), HTN (adjusted OR: 1.44; 95% CI: 1.04-2.00, p=0.0279) and CKD (adjusted OR: 1.57; 95% CI: 1.07-2.23, p=0.0223), were associated with the risk of MACCEs at the one-year follow-up. Given the instantaneous risk of mortality among patients with prostate cancer, we adjusted the ORs with mortality as a competing event. As MACCEs are a leading cause of death, the results also indicated a relatively higher risk of one-year MACCEs (adjusted OR: 1.30; 95% CI: 0.91-1.85, p=0.1487) in irregular users of aspirin compared to that in aspirin nonusers, while the risk was slightly reduced among those who received regular aspirin (adjusted OR: 0.77; 95% CI: 0.43-1.39, p=0.3813).

Subgroup analysis focusing on age and cancer stage among aspirin nonusers and regular and irregular users

Given that prostate cancer patients who were aspirin nonusers had fewer cardiovascular risk factors, to prevent bias, we thereafter defined the risks of aspirin nonusers as the reference and focused on the comparison between those with regular or irregular aspirin use (Table 3). As categorized by age, among patients at relatively younger ages from 60 to 69 years old, the risk of one-year MACCEs was higher in patients who took aspirin irregularly compared to patients who were aspirin nonusers (adjusted OR: 2.65; CI: 1.23-5.71, p=0.0127). Notably, among patients who received aspirin regularly, the risks decreased and became insignificant (adjusted OR: 2.28; CI: 0,68-7.64, p=0.1837). In contrast, for patients aged above 70 years, the risks of one-year MACCEs were persistently higher in both irregular aspirin users (OR: 1.41; 95% CI: 0.96-2.09, p= 0.0820) and irregular aspirin users (OR: 0.81; 95% CI: 0.41-1.61, p= 0.5459) compared to that in aspirin nonusers. To avoid competing risks of death, we adjusted the OR with mortality and found a persistently higher risk of one-year MACCEs among patients who took aspirin irregularly (adjusted OR: 2.62; 95% CI: 1.15-5.96, p=0.0221 for the 60- to 69-year-old age group) compared to those free from aspirin use, while the risk was insignificant among those who received aspirin regularly (adjusted OR: 1.99; 95% CI: 0.56-7.13, p=0.2905).

In terms of cancer stages, the use of aspirin did not show a significant impact on the risks of MACCEs in patients at a relatively earlier cancer stage (stage I/II). In contrast, among patients at an advanced cancer stage (stage III/VI), irregular aspirin use presented higher risks of MACCEs than those of

TABLE 3 Risks of 1-year and 3-years mortality and major adverse cardiovascular and cerebrovascular events (MACCEs) of Aspirin use in prostate cancer patient with different ages or cancer stages.

	1- year					3-years				
		MACC					MACC			
	Mortality (%)	Crude OR (95% C.I.)	P-value	Adjusted OR[b] (95% C.I.)	P-value	Mortality (%)	Crude OR (95% C.I.)	P-value	Adjusted OR[b] (95% C.I.)	P-value
Age groups										
60-69										
No used	60(3.24)	Ref.		Ref.		308(16.66)	Ref.		Ref.	
Non-regular aspirin used	10(4.20)	2.65 (1.23-5.71)	0.0127	2.62 (1.15-5.96)	0.0221	35(14.71)	1.93 (1.16-3.20)	0.0113	1.78(1.03-3.05)	0.0383
Regular aspirin used	5(5.43)	2.28 (0.68-7.64)	0.1837	1.99(0.56-7.13)	0.2905	8(8.70)	1.47 (0.62-3.45)	0.3812	1.30(0.53-3.20)	0.5656
70≧										
No used	306(7.94)	Ref.		Ref.		1013(26.30)	Ref.		Ref.	
Non-regular aspirin used	56(8.28)	1.41 (0.96-2.09)	0.0820	1.20(0.80-1.80)	0.3847	194(28.70)	1.32 (1.02-1.69)	0.0329	1.11(0.86-1.45)	0.4220
Regular aspirin used	21(6.67)	0.81 (0.41-1.61)	0.5459	0.63(0.31-1.27)	0.1943	82(26.03)	1.39 (0.98-1.96)	0.0626	1.07(0.74-1.54)	0.7176
Clinical stage										
I, II										
No used	35(1.98)	Ref.		Ref.		155(8.79)	Ref.		Ref.	
Non-regular aspirin used	4(1.35)	0.89 (0.38-2.12)	0.7956	0.73(0.30-1.77)	0.4822	24(8.11)	1.32 (0.85-2.06)	0.2203	1.14(0.72-1.82)	0.5834
Regular aspirin used	<3	0.97 (0.30-3.18)	0.9628	0.69(0.20-2.37)	0.5594	12(8.82)	1.57 (0.88-2.82)	0.1284	1.12(0.60-2.09)	0.7151
III. IV										
No used	351(7.66)	Ref.		Ref.		1293(28.22)	Ref.		Ref.	
Non-regular aspirin used	62(9.45)	2.02 (1.38-2.95)	0.0003	1.53(1.03-2.29)	0.0365	212(32.32)	1.59 (1.23-2.06)	0.0004	1.19(0.91-1.57)	0.2026
Regular aspirin used	25(8.77)	1.14 (0.57-2.26)	0.7184	0.78(0.39-1.60)	0.5024	79(27.72)	1.52 (1.04-2.22)	0.0296	1.06(0.71-1.57)	0.7910

[b]Adjusted for risk factor described in Table 1.

aspirin nonusers at the one-year follow-up (OR: 2.02, 95% CI: 1.38-2.95, p= 0.0003), while the risk was slightly reduced among patients with regular aspirin use (OR: 1.14, 95% CI: 0.57-2.26, p= 0.7184). Likewise, after adjusting for competing risks of mortality, the risk of one-year MACCEs remained higher in patients with irregular aspirin use (adjusted OR: 1.53; 95% CI: 1.03-2.29, p=0.03865) than in those free from aspirin use, while the risk was insignificant among those who received aspirin regularly (adjusted OR: 0.78; 95% CI: 0.39-1.60, p=0.5024).

Subgroup analysis focusing on cardiovascular risk factors among aspirin nonusers and regular and irregular users

Given that comorbidities, including diabetes, hypertension and hyperlipidemia, also contribute to MACCEs, we further analyzed the impact of aspirin use on prostate cancer patients with different cardiovascular risk factors. Despite no significant difference in MACCEs in the one-year follow-up (Figure 2), when focusing on prostate cancer patients with underlying hypertension, we found that irregular users of aspirin had a higher risk of three-year MACCEs (OR: 1.32, 95% CI: 1.01-1.72, p= 0.0393) than those who did not use aspirin. Interestingly, the increasing risk was insignificant in patients receiving aspirin regularly (OR: 1.13, 95% CI: 0.78-1.62, p= 0.5243). Likewise, among patients with coexisting hyperlipidemia, patients receiving aspirin irregularly also showed a higher risk of three-year MACCEs (OR: 1.64, 95% CI: 1.06-2.55, p= 0.0272) than those who did not use aspirin, while the risk was diminished in those with regular aspirin use (OR: 1.46, 95% CI: 0.82-2.62, p=0.2010) (Figure 3). In contrast, among patients with diabetes, the risk of MACCEs was not significantly different among the groups.

Discussion

In this nationwide cohort focusing on prostate cancer patients, we observed that, despite a higher risk of MACCEs among irregular aspirin users compared with those free from aspirin use, after adjusting for age, cancer stage and comorbidities, there was a trend of reducing the risk of MACCEs among those who received aspirin regularly. Notably, the benefit of regular aspirin use on cardiovascular risk reduction seems to be age- and cancer stage-independent. Special attention should be given to patients with underlying cardiovascular risk factors, including concomitant hypertension or hyperlipidemia, while aspirin use may be more promising in reducing the risks of MACCEs. Although Bhatia et al. raised the concept of ABCDE steps for heart and vascular wellness following a prostate cancer diagnosis, there is a missing piece in regard to evidence supporting the use of aspirin for the prevention of cardiovascular diseases in prostate cancer patients, especially those receiving GnRH therapy (8). Our findings, for the first time, indicated that regular use of aspirin may mitigate the risks of MACCEs in prostate cancer patients who underwent GnRH therapy.

Systemic review and meta-analysis studies indicated that, through achieving castration, GnRH therapy is efficient in prostate cancer control (3, 5, 17). However, as testosterone declines, adverse effects, including metabolic disorders and MACCEs, develop (4, 7). A meta-analysis study showed that

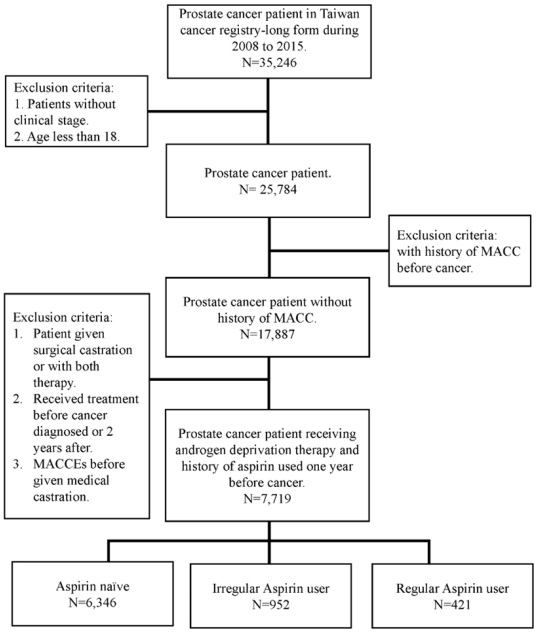

FIGURE 2
Risks of one-year MACCEs in sub-group analysis of different comorbidities. (DM, diabetes mellitus; HTN, hypertension).

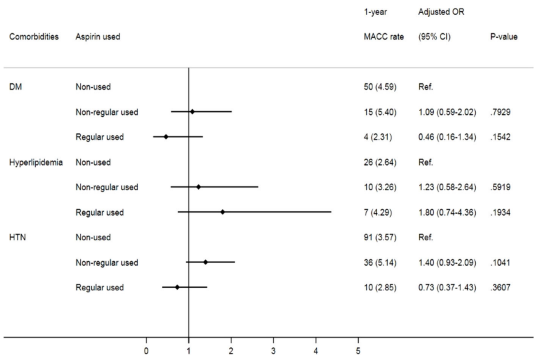

FIGURE 3
Risks of three-year MACCEs in sub-group analysis of different comorbidities. (DM, diabetes mellitus; HTN, hypertension).

low endogenous testosterone levels are associated with cardiovascular mortality (18). The Surveillance, Epidemiology and End Results (SEER)-Medicare database reported that prostate cancer itself, prostate cancer treatments, and selection mechanisms all contribute to an increased risk of thromboembolic disease (19). In terms of pathophysiology, in a murine model of orchiectomized LDLR$^{-/-}$ mice, mice fed high-fat diets developed larger atherosclerotic plaques compared to those in sham mice (20). In contrast, testosterone supplementation in the orchiectomy model significantly reduced atherosclerotic lesion size (20). Additionally, in macrophages, testosterone augmented cholesterol efflux in a dose-dependent manner, suggesting a possible mechanism by which testosterone can reduce atherosclerotic lesions (21).

Chronic inflammation is a major contributor to human cancers and exacerbates metabolic and cardiovascular disorders (22). Also, in a review article Camilli et al. highlighted the importance of the crosstalk between cancer and platelet which promotes cancer-associated inflammation, proliferation and immune (23). Aspirin is a commonly used medication with anti-platelet activity ad anti-inflammatory (9, 12, 13). Beyond its widely used application in reducing the risks of ischemic vascular diseases, there is also evidence from epidemiological and interventional studies to suggest that regular aspirin use may reduce the risk of prostate cancer development and progression (9, 12, 13). A systematic review and meta-analyses of 118 observational studies of aspirin indicated that an around 20% reduction in mortality in cancer patients receiving aspirin (24). By suppressing cyclooxygenase-2 enzyme-mediated inflammation, aspirin can modify prostate cancer biology and disease characteristics (12). Nevertheless, the evidence regarding the impact of aspirin on the risks of cancers remains controversial (9, 10, 12, 13). In a recent analysis of a large clinical database, postdiagnosis aspirin use was associated with 57% lower prostate cancer-specific mortality (25). Through large cohort studies, Cao

et al. also found that long-term aspirin use was associated with a modest but significantly reduced risk of overall cancer (26). Likewise, using the Cancer Prevention Study-II Nutrition Cohort, Jacobs et al. reported that compared with no aspirin use and neither prediagnosis nor postdiagnosis, daily aspirin use was significantly associated with the survival of prostate cancer patients (27). In a systematic review and meta-analysis, Liu et al. also demonstrated that there was no significant association between aspirin use and the risk of prostate cancer-associated mortality (28). Given the increasing risks of MACCEs in prostate cancer patients receiving GnRH therapy, the use of aspirin may further benefit cardiovascular outcomes beyond its effect on cancer survival (12, 26, 28). Therefore, there has been a precent of aspirin already used in patients with prostate cancer in order to reduce the risks associated with treating the disease (9, 25, 27, 29). However, although Li et al. showed that aspirin was associated with lower venous thrombosis and overall in-hospital mortality in older patients with cancer, there is a lack of evidence supporting the effect of aspirin use on cardiovascular risks in patients receiving GnRH therapy (29). Our findings, at least in part, provide missing evidence for the use of aspirin in reducing the risks of MACCEs in prostate cancer patients.

In a recently published cross-sectional analysis among 90,494 US veterans with prostate cancer, 54.1% had uncontrolled risk factors, but among them, 29.6% were not receiving risk-reducing medication (30). This study emphasized gaps in care and the need for interventions in this population but lacked investigations focusing on interventions for cardiovascular drugs, such as aspirin (30). To provide missing evidence, our findings highlight the importance of regular use of aspirin in reducing cardiovascular risks in prostate cancer patients receiving GnRH therapy. Notably, compared with aspirin-naïve patients, we found that those with irregular aspirin use had a higher risk of MACCEs. However, it is arbitrary jumping to the conclusion that aspirin fails to reduce cardiovascular risks given that patients who were prescribed aspirin may have increasing cardiovascular risks at baseline. In contrast, regular use of aspirin attenuated the risks of MACCEs compared with its irregular use. This underlines the issue of underassessed and undertreated cardiovascular risk factors in patients with prostate cancer, which seriously requires more attention. Especially in patients with old age, advanced cancer stage or comorbidities (such as hypertension and hyperlipidemia), the importance of regular use of aspirin is even more promising in improving cardiovascular outcomes. Although it may be premature to recommend aspirin for all patients receiving GnRH therapy, cautioning patients that irregular use may be detrimental is worth considering. Most importantly, given the ADD-aspirin trial underway, further randomized trials will benefit in illustrating the necessity of aspirin use among men diagnosed with prostate cancer.

There are some limitations to this study. First, given the retrospective study design, patients were not randomized to aspirin. Even though the study was designed under a matching method to reduce the difference between groups, there is still bias due to background cardiovascular risk factors of patients, especially those prescribed aspirin. Second, owing to database-type studies, we could not obtain full detailed information, including the integrated lifestyle-related factors of patients and the severity of MACCEs. Third, in the subgroup analysis, among patients with DM, which is also known as coronary artery disease risk equivalent, aspirin use failed to represent a beneficial effect of risk reductions. Notably, there was a significantly higher ratio of regular aspirin use than aspirin-naïve and irregular aspirin use in patients with DM. As speculated, in this population with high adherence to aspirin, the difference between irregular and regular aspirin use may be insignificant, but the importance of regular aspirin use in high-risk populations is not ignorable.

This study indicated that regular use of aspirin was with a trend of reducing risks of MACCEs in prostate cancer patients who receive GnRH therapy. However, irregular aspirin use diminished the benefits. To date, even though regular aspirin use is not yet recommended in practice guidelines, the high burden of cardiovascular diseases among prostate cancer patients requires special attention. Therefore, the major value of this study is by setting out the immediate clinical implications of aspirin use in patients with prostate cancer. Also, it is necessary for a randomized trial to illustrate the necessity of aspirin use among patients with prostate cancer. In summary, seems a valuable contribution to the literature and perhaps highlights the importance of the cardio-oncologist as cancer patients may also have elevated risks of adverse cardiovascular outcomes.

Data availability statement

The data analyzed in this study is subject to the following licenses/restrictions: The data is restrictive only to the NHIRD. Requests to access these datasets should be directed to cmcvecho3@gmail.com.

Ethics statement

The studies involving human participants were reviewed and approved by IRB: 11005-E03. Written informed consent for participation was not required for this study in accordance with the national legislation and the institutional requirements.

Author contributions

Study concept and design, W-TC. Acquisition of data, Y-CC and C-HH. Analysis and interpretation of data, Y-CC and C-HH. Drafting of the manuscript, J-YS, C-SH, K-LH, and W-TC. Critical revision of the manuscript for important intellectual content, J-YS, C-SH, K-LH, Y-CC, C-HH, J-YS, Z-CC, and W-TC. Statistical analysis, Y-CC and C-HH. Obtaining funding,

C-SH and W-TC. Supervision, W-TC. All authors contributed to the article and approved the submitted version.

Funding

This work was granted by Ministry of Science and Technology (MOST 109-2326-B-384 -001 -MY3). This study was also supported by Chi-Mei Medical Center.

Conflict of interest

The authors declare that the research was conducted in the absence of any commercial or financial relationships that could be construed as a potential conflict of interest.

Publisher's note

Supplementary material

The Supplementary Material for this article can be found online at: https://www.frontiersin.org/articles/10.3389/fonc.2022.952370/full#supplementary-material

References

1. Nyame YA, Gore JL. What goes up must come down: Identifying truth from global prostate cancer epidemiology. *Eur Urol* (2020) 77:53–4. doi: 10.1016/j.eururo.2019.09.018

2. Bechis SK, Carroll PR, Cooperberg MR. Impact of age at diagnosis on prostate cancer treatment and survival. *J Clin Oncol* (2011) 29:235–41. doi: 10.1200/JCO.2010.30.2075

3. Boccon-Gibod L, van der Meulen E, Persson BE. An update on the use of gonadotropin-releasing hormone antagonists in prostate cancer. *Ther Adv Urol* (2011) 3:127–40. doi: 10.1177/1756287211414457

4. Seong JM, Shin D, Sung JW, Cho S, Yang J, Kanget S, et al. Gonadotropin-releasing hormone agonists, anti-androgens and the risk of cardio-cerebrovascular disease in prostate cancer patients: an asian population-based observational study. *J Cancer* (2020) 11:4015–22. doi: 10.7150/jca.38237

5. Shahinian VB, Kuo YF, Freeman JL, Orihuela E, Goodwin JS. Increasing use of gonadotropin-releasing hormone agonists for the treatment of localized prostate carcinoma. *Cancer* (2005) 103:1615–24. doi: 10.1002/cncr.20955

6. Van Poppel H, Abrahamsson PA. Considerations for the use of gonadotropin-releasing hormone agonists and antagonists in patients with prostate cancer. *Int J Urol* (2020) 27:830–7. doi: 10.1111/iju.14303

7. Teoh JY, Chan SY, Chiu PK, Poon D, Cheung HY, Hou SS, et al. Risk of cardiovascular thrombotic events after surgical castration versus gonadotropin-releasing hormone agonists in Chinese men with prostate cancer. *Asian J Androl* (2015) 17:493–6. doi: 10.4103/1008-682X.143313

8. Bhatia N, Santos M, Jones LW, Beckman J, Penson D, Morgans A, et al. Cardiovascular effects of androgen deprivation therapy for the treatment of prostate cancer: ABCDE steps to reduce cardiovascular disease in patients with prostate cancer. *Circulation* (2016) 133:537–41. doi: 10.1161/CIRCULATIONAHA.115.012519

9. Barton MK. Daily aspirin may reduce mortality from prostate cancer with risk of high recurrence. *CA Cancer J Clin* (2015) 65:83–4. doi: 10.3322/caac.21263

10. Skriver C, Dehlendorff C, Borre M, Brasso K, Larsen SB, Dalton SO, et al. Use of low-dose aspirin and mortality after prostate cancer diagnosis: A nationwide cohort study. *Ann Intern Med* (2019) 170:443–52. doi: 10.7326/M17-3085

11. Pannunzio A, Coluccia M. Cyclooxygenase-1 (COX-1) and COX-1 inhibitors in cancer: A review of oncology and medicinal chemistry literature. *Pharm (Basel)* (2018) 11:101. doi: 10.3390/ph11040101

12. Joshi SN, Murphy EA, Olaniyi P, Bryant RJ. The multiple effects of aspirin in prostate cancer patients. *Cancer Treat Res Commun* (2021) 26:100267. doi: 10.1016/j.ctarc.2020.100267

13. Downer MK, Allard CB, Preston MA, Gaziano M, Stampfer M, Mucci L, et al. Regular aspirin use and the risk of lethal prostate cancer in the physicians' health study. *Eur Urol* (2017) 72:821–7. doi: 10.1016/j.eururo.2017.01.044

14. Hsieh CY, Su CC, Shao SC, Sung SF, Lin SJ, Kao Yang YH, et al. Taiwan's national health insurance research database: past and future. *Clin Epidemiol* (2019) 11:349–58. doi: 10.2147/CLEP.S196293

15. Chiang CJ, You SL, Chen CJ, Yang YW, Lo WC, Lai MS. Quality assessment and improvement of nationwide cancer registration system in Taiwan: A review. *Jpn J Clin Oncol* (2015) 45:291–6. doi: 10.1093/jjco/hyu211

16. Chiang CJ, Wang YW, Lee WC. Taiwan's nationwide cancer registry system of 40 years: Past, present, and future. *J Formos Med Assoc* (2019) 118:856–8. doi: 10.1016/j.jfma.2019.01.012

17. Sun M, Choueiri TK, Hamnvik OP, Preston M, Velasco G, Jiang W, et al. Comparison of gonadotropin-releasing hormone agonists and orchiectomy: Effects of androgen-deprivation therapy. *JAMA Oncol* (2016) 2:500–7. doi: 10.1001/jamaoncol.2015.4917

18. Araujo AB, Dixon JM, Suarez EA, Murad MH, Guey LT, Wittert GA. Clinical review: Endogenous testosterone and mortality in men: A systematic review and meta-analysis. *J Clin Endocrinol Metab* (2011) 96:3007–19. doi: 10.1210/jc.2011-1137

19. Deng Y, Bi R, Zhu Z, Li H, Xu B, Rather W, et al. A surveillance, epidemiology and end results database analysis of the prognostic value of organ-specific metastases in patients with advanced prostatic adenocarcinoma. *Oncol Lett* (2019) 18:1057–70. doi: 10.3892/ol.2019.10461

20. Hatch NW, Srodulski SJ, Chan HW, Zhang X, Tannock LR, King VL. Endogenous androgen deficiency enhances diet-induced hypercholesterolemia and atherosclerosis in low-density lipoprotein receptor-deficient mice. *Gend Med* (2012) 9:319–28. doi: 10.1016/j.genm.2012.08.003

21. Langer C, Gansz B, Goepfert C, Engel T, Uehara Y, Dehn G, et al. Testosterone up-regulates scavenger receptor BI and stimulates cholesterol efflux from macrophages. *Biochem Biophys Res Commun* (2002) 296:1051–7. doi: 10.1016/S0006-291X(02)02038-7

22. Furman D, Campisi J, Verdin E, Carrera-Bastos P, Targ S, Franceschi C, et al. Chronic inflammation in the etiology of disease across the life span. *Nat Med* (2019) 25:1822–32. doi: 10.1038/s41591-019-0675-0

23. Camilli M, Iannaccone G, La Vecchia G, Cappannoli L, Scacciavillani R, Minotti G, et al. Platelets: the point of interconnection among cancer, inflammation and cardiovascular diseases. *Expert Rev Hematol* (2021) 14:537–46. doi: 10.1080/17474086.2021.1943353

24. Elwood PC, Morgan G, Delon C, Protty M, Galante J, Pickering J, et al. Aspirin and cancer survival: A systematic review and meta-analyses of 118 observational studies of aspirin and 18 cancers. *Ecancermedicalscience* (2021) 15:1258. doi: 10.3332/ecancer.2021.1258

25. Choe KS, Cowan JE, Chan JM, Carroll PR, D'Amico AV, Liauw SL. Aspirin use and the risk of prostate cancer mortality in men treated with prostatectomy or radiotherapy. *J Clin Oncol* (2012) 30:3540–4. doi: 10.1200/JCO.2011.41.0308

26. Cao Y, Nishihara R, Wu K, Wang M, Ogino S, Willett WC, et al. Population-wide impact of long-term use of aspirin and the risk for cancer. *JAMA Oncol* (2016) 2:762–9. doi: 10.1001/jamaoncol.2015.6396

27. Jacobs EJ, Rodriguez C, Mondul AM, Connell C, Henley S, Calle E, et al. A large cohort study of aspirin and other nonsteroidal anti-inflammatory drugs and prostate cancer incidence. *J Natl Cancer Inst* (2005) 97:975–80. doi: 10.1093/jnci/dji173

28. Liu Y, Chen JQ, Xie L, Wang J, Li T, He Y, et al. Effect of aspirin and other non-steroidal anti-inflammatory drugs on prostate cancer incidence and mortality: A systematic review and meta-analysis. *BMC Med* (2014) 12:55. doi: 10.1186/1741-7015-12-55

29. Li P, Ning Y, Li M, Cai P, Siddiqui AD, Liu EY, et al. Aspirin is associated with reduced rates of venous thromboembolism in older patients with cancer. *J Cardiovasc Pharmacol Ther* (2020) 25:456–65. doi: 10.1177/1074248420925021

30. Sun L, Parikh RB, Hubbard RA, Cashy J, Takvorian SU, Vaughn DJ, et al. Assessment and management of cardiovascular risk factors among US veterans with prostate cancer. *JAMA Netw Open* (2021) 4(2):e210070. doi: 10.1001/jamanetworkopen.2021.0070

frontiers | Frontiers in Oncology

TYPE Original Research
PUBLISHED 03 October 2022
DOI 10.3389/fonc.2022.961841

OPEN ACCESS

EDITED BY
Antonella Lombardo,
Agostino Gemelli University Polyclinic, (IRCCS), Italy

REVIEWED BY
Giulia La Vecchia,
Agostino Gemelli University Polyclinic, (IRCCS), Italy
Andrea Tedeschi,
Niguarda Ca' Granda Hospital, Italy

*CORRESPONDENCE
Ying-Kun Guo
gykpanda@163.com

†These authors have contributed equally to this work and share first authorship

‡These authors have contributed equally to this work

SPECIALTY SECTION
This article was submitted to Cardio-Oncology, a section of the journal Frontiers in Oncology

RECEIVED 05 June 2022
ACCEPTED 05 September 2022
PUBLISHED 03 October 2022

CITATION
Yang M-X, Li Q-L, Wang D-Q, Ye L, Li K-M, Lin X-J, Li X-S, Fu C, Ma X-M, Liu X, Yin R-T, Yang Z-G and Guo Y-K (2022) Myocardial edema during chemotherapy for gynecologic malignancies: A cardiac magnetic resonance T2 mapping study. *Front. Oncol.* 12:961841. doi: 10.3389/fonc.2022.961841

Myocardial edema during chemotherapy for gynecologic malignancies: A cardiac magnetic resonance T2 mapping study

Meng-Xi Yang[1,2,3†], Qing-Li Li[4†], Dan-Qing Wang[4], Lu Ye[5], Ke-Min Li[4], Xiao-Juan Lin[4], Xue-Sheng Li[1], Chuan Fu[1], Xin-Mao Ma[1], Xi Liu[6], Ru-Tie Yin[4], Zhi-Gang Yang[2‡] and Ying-Kun Guo[1*‡]

[1]Department of Radiology, Key Laboratory of Obstetric & Gynecologic and Pediatric Diseases and Birth Defects of Ministry of Education, West China Second University Hospital, Sichuan University, Chengdu, China, [2]Department of Radiology, West China Hospital, Sichuan University, Chengdu, China, [3]Department of Radiology, Sichuan Cancer Hospital & Institute, Sichuan Cancer Center, School of Medicine, University of Electronic Science and Technology of China, Chengdu, China, [4]Department of Gynecology, Key Laboratory of Birth Defects and Related Diseases of Women and Children of Ministry of Education, West China Second University Hospital, Sichuan University, Chengdu, China, [5]Department of Ultrasound, Key Laboratory of Birth Defects and Related Diseases of Women and Children of Ministry of Education, West China Second University Hospital, Sichuan University, Chengdu, China, [6]Key Laboratory of Carcinogenesis and Translational Research (Ministry of Education), Department of Radiology, Peking University Cancer Hospital & Institute, Beijing, China

Objective: Myocardial edema is an early manifestation of chemotherapy-related myocardial injury. In this study, we used cardiac magnetic resonance (CMR) T2 mapping to assess myocardial edema and its changes during chemotherapy for gynecologic malignancies.

Methods: We enrolled 73 patients receiving chemotherapy for gynecologic malignancies, whose the latest cycle was within one month before the beginning of this study, and 41 healthy volunteers. All participants underwent CMR imaging. Of the 73 patients, 35 completed CMR follow-up after a median interval of 6 (3.3 to 9.6) months. The CMR sequences included cardiac cine, T2 mapping, and late gadolinium enhancement.

Results: Myocardial T2 was elevated in patients who were treated with chemotherapy compared with healthy volunteers [41ms (40ms to 43ms) vs. 41ms (39ms to 41ms), P = 0.030]. During follow-up, myocardial T2 rose further [40ms (39ms to 42ms) vs. 42.70 ± 2.92ms, P < 0.001]. Multivariate analysis showed that the number of chemotherapy cycles was associated with myocardial T2 elevation (β = 0.204, P = 0.029). After adjustment for other confounders, myocardial T2 elevation was independently associated with a decrease in left ventricular mass (β = −0.186; P = 0.024).

Conclusion: In patients with gynecologic malignancies, myocardial edema developed with chemotherapy cycles increase, and was associated with left ventricular mass decrease. T2 mapping allows the assessment of myocardial edema and monitoring of its change during chemotherapy.

KEYWORDS

gynecologic malignancies, chemotherapy, cardiac magnetic resonance (CMR), myocardial edema, T2 mapping MRI

Introduction

As survival of cancer improves, cardiovascular toxicity has become a major cancer treatment-related complication (1–5). Among several pathological changes that occur in the myocardium during chemotherapy, edema is considered an early manifestation of myocardial injury and forerunner to cardiac dysfunction and myocardial fibrosis (6–9). Cardiac magnetic resonance (CMR) T2-mapping techniques can characterize myocardial edema *in vivo* and potentially provide additional insights beyond functional assessment (3, 10, 11). Animal studies have shown that anthracycline chemotherapy causes the prolongation of the myocardial T2 derived from T2 mapping, and histological analysis has further revealed good correlation between myocardial T2 and myocardial water content (7, 8). Clinical studies in humans have also reported increase in myocardial T2 as a sensitive biomarker for myocardial involvement during chemotherapy (9).

Gynecologic malignancies remain a major cause of mortality and morbidity in women (12), and the chemotherapy regimens for those patients consist of a variety of drugs which leading to myocardial injury (13–17). Moreover, to control tumor progression, patients in advanced stages typically require long-term chemotherapy regimens, rendering them at higher risk of cardiovascular diseases. However, systematic studies focusing on cardiovascular toxicity related to chemotherapy for gynecologic malignancies are lacking. We therefore enrolled patients with gynecologic malignancies and sought to investigate changes in myocardial edema during chemotherapy using T2 mapping techniques.

Abbreviations: CMR, cardiac magnetic resonance; LGE, late gadolinium enhancement; LVEF, left ventricular eject fraction; LVEDV, left ventricular end-diastolic volume; LVESV, left ventricular end-diastolic volume; CI, coefficient interval.

Methods

Study participants

The clinical protocol adopted in this study was approved by the institutional ethics review board of our hospital and of the Chinese Clinical Trial Registry (ChiCTR-DDD-17013450). All participants provided written informed consent forms before enrollment. Patients from the Department of Tumor Radiation and Chemotherapy who were diagnosed with gynecologic malignancies were recruited. Inclusion criteria were (1) current or recent (within the preceding month) receipt of chemotherapy and (2) age between 18 and 75 years (18, 19). Exclusion criteria were (1) concomitant diagnosis of cardiovascular diseases (coronary artery disease, primary cardiomyopathy, valvular heart disease, congenital heart disease, and pericardial disease), (2) prior receipt of treatment for other diseases carrying the potential for myocardial toxicity, and (3) contraindications to CMR. Age-matched healthy female volunteers were simultaneously recruited as the control group that underwent the same imaging procedures.

Laboratory examination

We obtained venous blood samples from patients 1 hour before CMR imaging to examine serologic markers of myocardial injury, including troponin I and creatine kinase.

Image acquisition

The CMR examinations were performed using a 3.0T magnetic resonance imaging machine scanner (Magnetom Skyra, Siemens Healthcare, Inc., Erlangen, Germany). The CMR protocol consisted of cardiac cine, T2 mapping, and late gadolinium enhancement (LGE) imaging. Cine imaging used a balanced steady-state free-precession pulse sequence: echo time (TE) = 1.22 ms, temporal resolution (TR) = 39.34 ms, flip angle = 40°,

slice thickness = 8 mm, matrix = 208 × 208 pixels, and field of view (FOV) = 340 × 284 mm^2. T2 mapping images were acquired using the steady-state free-precession technique, and three single-shot images were acquired at different T2 preparation times (0 ms, 25 ms, and 55 ms). The detailed parameters were as follows: TE = 1.23 ms, TR = 38.34 ms, flip angle = 60°, slice thickness = 8 mm, matrix = 208 × 208 pixels, and FOV = 250 × 300 mm^2 (20, 21). For LGE imaging, intravenous gadolinium contrast (0.2 mL/kg) was first administered, a segmented phase-sensitive inversion recovery sequence with turbo FLASH readout at 17–19 minutes post contrast was then performed (22, 23): TR = 1.44 ms, TE = 300 ms, flip angle = 40°, slice thickness = 4 mm, matrix = 84 × 176 pixels, FOV = 153 × 106 mm. T2 mapping images were obtained in the basal, middle, apical short-axis, and four-chamber planes; cine and LGE images were obtained in the two-chamber, three-chamber and four-chamber planes, and a continuous stack of short-axis planes with full left ventricular (LV) coverage.

Image analysis

Two experienced radiologists separately conducted the image analysis using imaging postprocessing software (CVI42, Circle Cardiovascular Imaging, Calgary, Canada). The analysis of LV functional parameters was presented in previous studies (9). Myocardial T2 was measured on the basal, middle, and apical color T2 maps and then averaged as the global LV myocardial T2 (24). Local myocardial fibrosis was defined based on the acquired LGE images: After elimination of artifacts, any obvious patch of the myocardium observed on any image was accepted as local myocardial fibrosis (25). If disagreements arose, a consensus was reached by discussion between the two radiologists.

Reproducibility

To assess intraobserver variability, one radiologist randomly measured myocardial T2 in 39 subjects twice within 1 week. The other radiologist, who was blinded to the first radiologist's results, then reperformed the measurements.

Statistical analysis

Statistical analysis was performed using IBM SPSS Statistics (version 20.0; IBM Corp., Armonk, NY, USA) and GraphPad Prism (version 7.00, San Diego, CA) software applications. Categorical or enumeration parameters were presented as numbers (percentages), whereas continuous variables were expressed as the mean ± standard deviation or as medians (interquartile range), as appropriate. The chi-square test was used to compare categorical or enumeration parameters. The independent *t*-test or the rank-sum test was used to compare continuous variables between patients and healthy volunteers, as appropriate. Parameters from the two CMR examinations, performed in 35 patients who completed CMR follow-up, were compared using the paired *t*-test or rank-sum test, as appropriate. Bivariate correlation analysis was performed using the Pearson's or Spearman's method, as appropriate. To identify the factors that were independently associated with myocardial T2 and LV mass, a multivariate linear regression model was constructed. Intraobserver and interobserver variabilities of myocardial T2 measurements were assessed using intraclass correlation coefficient. All tests were two tailed; P values < 0.05 were accepted as statistically significant.

Results

Baseline characteristics

From September 2018 to December 2020, this study enrolled 73 patients treated with chemotherapy for gynecologic malignancies and 41 healthy volunteers (Figure 1). Table 1 shows the baseline characteristics of patients and volunteers, and no statistically significant differences in baseline variables were found between the two groups (all $P > 0.05$). Moreover, no cardiovascular diseases or cardiovascular risk factors were detected in any of the enrolled volunteers.

Among the 73 patients treated with chemotherapy, 6 (6/73, 8.22%) were complicated with hypertension and 3 (3/73, 4.11%) had diabetes. In addition, 6 patients (6/73, 8.22%) had a history of taking cardiac medication (Table 1). With regard to chemotherapy regimens, 64 patients (64/73, 87.67%) received a regimen consisting of paclitaxel plus platinum. The median interval between the first cycle of chemotherapy and CMR scan was 5 (2 to 12) months.

Of the 73 patients, 35 patients (35/73, 47.95%) completed the CMR follow-up. The interval between the two scans was 6 (3.3 to 9.6) months, and these patients completed 3 (2 to 5) cycles of chemotherapy during the interval.

Alteration in LV morphology during chemotherapy

For LV functional parameters (Table S1), no significant difference was observed between the two groups in LV ejection fraction (LVEF) or LV end-systolic volume (all $P > 0.05$). However, the LV mass (43.80 ± 8.61 g/m^2 vs. 46.90 ± 7.74 g/m^2, $P = 0.047$) and LV end-diastolic volume (64.44 ± 12.94 ml/m^2 vs. 69.58 ± 7.97 ml/m^2, $P = 0.038$) were slightly lower in patients compared to healthy volunteers. Among 73 patients, 17 (17/73, 23.29%) were recorded as positive for LGE, as opposed to healthy volunteers who were all negative. At CMR follow-up

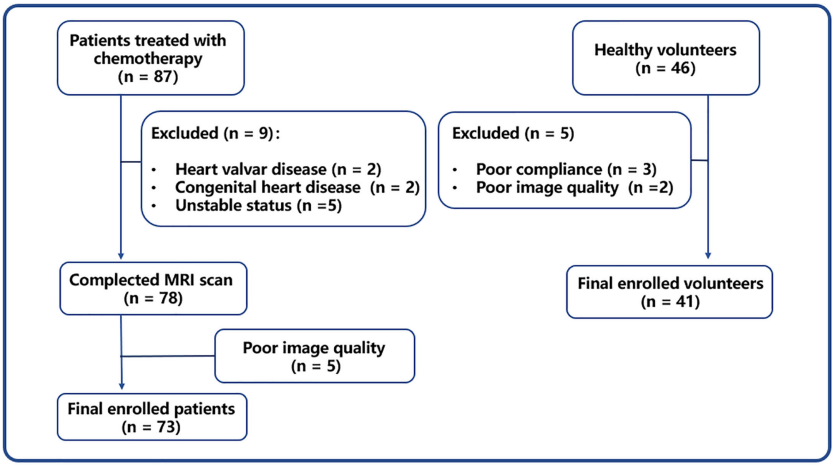

FIGURE 1
Study flowchart. CMR, cardiac magnetic resonance.

in 35 patients (Table S2), a decrease in the LV mass was observed (47.17 ± 7.73 g/m^2 vs. 44.33 ± 8.36 g/m^2, $P < 0.001$), and three patients were newly recorded as positive for LGE (8/35, 22.86% initially vs. 11/35, 31.43% at follow-up; $P = 0.250$).

Changes in myocardial T2 during chemotherapy

The global LV myocardial T2 was higher in patients than in healthy volunteers [41ms (40ms to 43ms) vs. 41ms (39ms to 41ms), P = 0.030; Figure 2A]. With regards to alterations in different slices, myocardial T2 in the apical slice was higher in patients than in healthy volunteers [42ms (40ms to 44.5ms) vs. 41ms (39.5ms to 43ms), $P = 0.013$], whereas myocardial T2 showed no difference in the middle and basal slices between the two groups (both $P > 0.05$).

As the number of chemotherapy cycles increased, an elevation in global LV myocardial T2 was noted at follow-up [40ms (39ms to 42ms) vs. 42.70 ± 2.92ms, P < 0.001, Figure 2B]. Moreover, an increase in myocardial T2 in the apical, middle, and basal slices was observed (all P < 0.05). Figure 3 presents the representative CMR images from healthy volunteers and patients.

Association of myocardial T2 with myocardial injury biomarkers

In the 35 patients who completed CMR follow-up, the myocardial injury biomarkers tended to increase from baseline to follow-up imaging: creatine kinase [39u/L (15u/L to 41u/L) vs. 78.00u/L (58.25u/L to 95.00u/L), $P < 0.001$] and troponin I [0.006ug/L (0.006ug/L to 0.006ug/L) vs. 0.006 (0.006ug/L to 0.008ug/L), $P < 0.001$].However, no correlation was observed between myocardial T2 and creatine kinase ($r = 0.152$, $P = 0.127$) or troponin I ($r = -0.046$, $P = 0.647$).

Influence of chemotherapy on myocardial T2 variation

Univariate analysis indicated that both the receipt of chemotherapy (r = 0.280, P = 0.001) and chemotherapy cycles received (r = 0.311, P < 0.001) positively correlated with myocardial T2 in all subjects. In model 1, after adjustment for chemotherapy drug types and time interval from first chemotherapy to CMR imaging, the number of chemotherapy cycles was associated with myocardial T2 (β = 0.462, P = 0.003). When Model 2 added age and clinical risk factors to the analysis, the number of chemotherapy cycles was also associated with an increase in myocardial T2 (β = 0.204, P = 0.029; Table 2).

Association between myocardial T2 and LV mass

A negative association between myocardial T2 and LV mass was observed ($r = -0.165$, $P = 0.045$). In the multivariate analysis, after adjustment for CMR parameters and clinical risk factors (including age, hypertension and diabetes

TABLE 1 Baseline characteristics of patients and normal controls.

	Normal controls (n = 41)	Patients (n = 73)	P value
Age, year	45 (35 to 59.5)	50 (45 to 56)	0.192
Female, %	41 (100%)	73 (100%)	0.999
Hypertension, %	0 (0%)	6 (8.22%)	0.059
Diabetes, %	0 (0%)	3 (4.11%)	0.188
Hyperlipidemia, %	0 (0%)	0 (0%)	0.999
Smoker, %	0 (0%)	0 (0%)	0.999
Height, cm	157.4 ± 6.02	157.5 ± 5.46	0.938
Weight, kg	59.0 (51.5 to 60.5)	58.18 ± 9.61	0.394
Body-mass index, mm2	1.53 ± 0.15	1.55 ± 0.14	0.509
Receipt of cardiac medication			
Beta-blockers	_	4 (5.48%)	_
ARB	_	2 (2.74%)	_
ACEI	_	1 (1.37%)	_
Calcium antagonist	_	5 (6.85%)	_
Diuretics	_	1 (1.37%)	_
Heparin sodium	_	5 (6.85%)	_
Cancer type			
Ovarian cancer	_	45 (61.64%)	_
Carcinoma tubae	_	9 (12.33%)	_
Cervical cancer	_	16 (21.92%)	_
Endometrial cancer	_	3 (4.11%)	_
Cancer status and treatment			
Cancer stage	_	3 (2 to 3)	_
Cancer recurrence	_	24 (32.88%)	_
Operation (n, %)	_	72 (98.63%)	_
Pelvic radiation (n, %)	_	5 (6.85%)	_
Interval between first chemo and CMR scan, mon	_	5 (2 to 12)	_
Chemotherapy number	_	6 (3 to 12)	_
Chemotherapy regimen	_	1 (1 to 2)	_
Drug type number	_	2 (2 to 3)	_
Chemotherapy drug type (n, %)			
Paclitaxel + Platinum	_	64 (87.67%)	_
Anthracycline	_	12 (16.44%)	_
Cyclophosphamide/ifosfamide	_	17 (23.29%)	_
Bevacizumab	_	12 (16.44%)	_
Others	_	6 (8.22%)	_

BMI, body index; ARB, angiotensin receptor blockers; ACEI, angiotensin converting enzyme inhibitor. *P < 0.05 vs. normal control.

mellitus), myocardial T2 remained independently associated with a reduction in LV mass (β = −0.186, $P = 0.024$; Table 3).

Reproducibility

With respect to the reproducibility of myocardial T2, the intraobserver and interobserver variability were measured at 0.955 (95% confidence interval [CI]: 0.914–0.976) and 0.904 (95% CI: 0.818–0.950), respectively.

Discussion

This study enrolled patients treated with chemotherapy for gynecologic malignancies and used CMR T2 mapping to assess myocardial edema. The main findings were the following (1): Myocardial T2 was higher in patients than in healthy volunteers and increased as the chemotherapy cycles received increase during follow-up. (2) After adjustment for chemotherapy drug types and clinical characteristics, the number of chemotherapy cycles was associated with

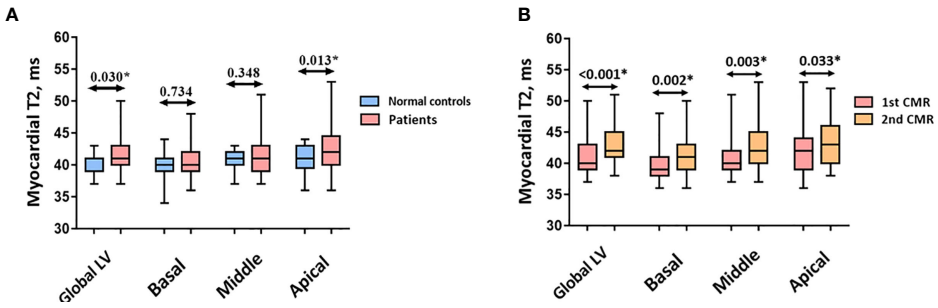

FIGURE 2
(A) Myocardial T2 between normal controls and patients. **(B)** Myocardial T2 between two CMR scans in patients. Abbreviations as in Figure 1. *p < 0.05 vs. normal control.

increased myocardial T2. (3) In the multivariate analysis including CMR and clinical risk factors, increased myocardial T2 was independently associated with lower LV mass. To the best of our knowledge, the present systematic study is the first to focus on myocardial edema associated with chemotherapy for gynecologic malignancies. Most patients included in this study underwent chemotherapy with paclitaxel plus platinum, a combination that is infrequently reported in literature. Our results showed that myocardial edema could be aggravated as chemotherapy continues and that myocardial edema is associated with a reduction in LV mass. Thus, the cardiac side effects of paclitaxel and platinum

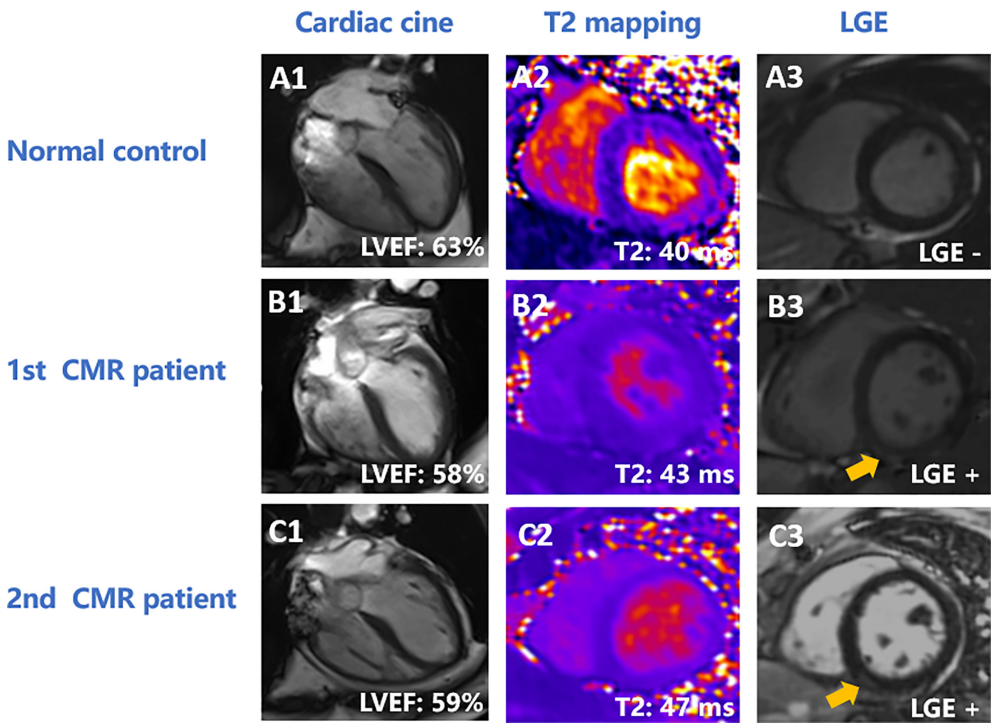

FIGURE 3
Representative CMR images of normal controls and patients. **(A)** A 58-year-old female healthy volunteer. LVEF was 63% **(A1)**, global LV myocardial T2 was 40 ms **(A2)**, and there was no enhancement on LGE **(A3)**. **(B, C)** A 44-year-old patient with ovarian cancer. The patient had undergone 12 cycles of paclitaxel plus platinum chemotherapy at the first CMR scan. LVEF was 58% **(B1)**, global LV T2 value was 43 ms **(B2)**, and had inferior enhancement (yellow arrow) on LGE **(B3)**. At 11-month follow-up, the patient had completed 15 cycles of paclitaxel plus platinum chemotherapy. LVEF was 59% **(C1)**, global LV myocardial T2 value was 47 ms **(C2)**, and had inferior enhancement (yellow arrow) **(C3)**. LVEF, left ventricular eject fraction; LGE, late gadolinium enhancement.

TABLE 2 The association between chemotherapy and myocardial T2 variation.

Univariate analysis	R	P value
Chemotherapy	0.280	0.001*
Numbers of chemotherapy	0.311	<0.001*
Multivariate analysis	**β**	**P value**
Model 1: adjusting for time interval between first chemotherapy and CMR, and chemotherapy drugs (time interval, anthracycline, bevacizumab, and cyclophosphamide/ifosfamide)		
Chemotherapy	0.013	0.939
Numbers of chemotherapy	0.462	0.003*
Model 2: adjusting for clinical risk factors (age, hypertension, and diabetes)		
Chemotherapy	0.186	0.048*
Numbers of chemotherapy	0.204	0.029*

CMR, cardiac magnetic resonance. *P < 0.05.

TABLE 3 The risk factors of indexed LV mass by univariable and multivariable analysis.

	Univariable Analysis		Multivariable Analysis	
	R	P value	β	P value
Age	-0.159	0.053	-0.206	0.014*
Hypertension	-0.065	0.430	-0.033	0.697
Diabetes mellitus	0.156	0.058	0.253	0.002*
LVEF	-0.045	0.586	-0.027	0.734
Myocardial T2	-0.165	0.045*	-0.186	0.024*
LGE present	-0.083	0.317	0.005	0.953

LVEF, left ventricular eject fraction; LGE, late gadolinium enhancement. *P < 0.05.

chemotherapy require clinical attention. Using CMR T2 mapping, clinicians can assess myocardial injury and track changes of myocardial edema during chemotherapy.

Chemotherapy-related cardiotoxicity develops because of a variety of physiological changes, and myocardial edema is an early manifestation (6–9). Quantitative assessment of myocardial edema through T2 mapping allows for the early detection of myocardial injury. In a rat model of anthracycline-induced myocardial edema, the prolongation of myocardial T2 was associated with an increase in myocardial water content, which appeared earlier than hemodynamic deterioration, LVEF decrease, and fibrous collagen deposition (7). In addition, Galán-Arriola observed the same change in large-animal models (8). In patients received with anthracyclines, Lustberg et al. demonstrated that myocardial T2 increased after the first cycle of chemotherapy, but LVEF and circumferential strain declined several months later (9). Similar to previous studies, our study found that myocardial T2 was higher in patients treated with chemotherapy for gynecological malignancies than in healthy volunteers, although no difference in LVEF was observed between the two groups. Moreover, in this study, the troponin I values of patients were within normal range and showed no correlation with myocardial T2, suggesting that the myocardial injury was in early stage, and troponin I was not significantly elevated. These results supported the advantage of T2 mapping for the early detection of myocardial injury during chemotherapy.

Additionally, our study revealed that the increase in myocardial T2 of patients was more pronounced in the apical slice than in the middle and basal slices. Although similar data haven't been reported about the regional distribution of myocardial T2, published literatures have demonstrated the greatest motion impairments at heart apex in patients treated with chemotherapy (26, 27). Taken together, we speculated that apical myocardium is more vulnerable to chemotherapy. The potential causes might be the increased exposure of terminal circulation regions to chemotherapy drugs or the differential local activation of signal transduction (26), but the exact mechanism needs further exploration.

As reported in the previous studies, myocardial T2 varies with the individual, and is potentially influenced by factors such as age and sex (28–30). Longitudinal assessment of myocardial T2 during chemotherapy is helpful for recognizing change in myocardial edema, obviating the effects of other factors. In our patients, who completed the CMR follow-up, myocardial T2 tended to increase with the continuation of chemotherapy. Multivariate analysis demonstrated that the number of chemotherapy cycles was independently associated with an increase in myocardial T2. These results suggest that myocardial edema could be aggravated

with an increase in chemotherapy cycles. Thus, patients treated with long-term chemotherapy are at an increased cardiac risk and require more attention. A study by Lustberg et al. supports our hypothesis, because those authors also observed a continuous increase in myocardial T2 during chemotherapy (9). On the other hand, myocardial edema subsides as chemotherapy ends or myocardial fibrosis develops. One study found a reduction in myocardial T2 at 12 months after the last chemotherapy cycle (25), and no difference was observed in myocardial T2 between cancer survivors after long-term chemotherapy and healthy individuals (31). The physiologic process of myocardial edema in patients undergoing chemotherapy for gynecologic malignancies requires further investigation with a longer follow-up period.

To date, clinical studies have focused mostly on the cardiotoxicity caused by anthracyclines and/or trastuzumab (7–9, 32–34); few studies have focused on cardiotoxicity caused by other chemotherapy drugs. Our study provides relevant data for other chemotherapy drugs used in gynecologic malignancies. Our patients received with various chemotherapy drugs, with the largest proportion receiving paclitaxel plus platinum regimens. Previous studies has reported that the cardiac implications of paclitaxel mostly manifest as myocardial ischemia or arrhythmia (35, 36), whereas platinum can lead to cardiac motion dysfunction (37). Our results suggest that paclitaxel plus platinum could potentially cause myocardial edema. Although the myocardial edema observed during chemotherapy was mild, myocardial injury could be aggravated as chemotherapy cycles increase. Paclitaxel and platinum are first-line drugs in a variety of tumors (38), more attention and further exploration of their cardiotoxicity is needed.

During chemotherapy for cancer, the left ventricle can undergo a series of morphological changes, and those changes have prognostic significance (3–5). Several studies reported that the receipt of chemotherapy was associated with a reduction in LV mass (39–42), which predicts for adverse cardiovascular events (41, 42). After adjustment for CMR and clinical risk factors, we found that myocardial T2 was independently associated with a reduction in LV mass, suggesting that myocardial edema potentially contributed to LV remodeling during chemotherapy.

This study has several limitations. (1) This single-center study had a relatively small sample size. Nevertheless, the findings demonstrated that T2 mapping can be used to assess myocardial injury in patients undergoing chemotherapy for gynecologic malignancies. Future studies with larger populations are needed to strengthen our findings. (2) Most enrolled patients were at critical condition, meaning that they had to start chemotherapy as soon as possible. Consequently, a baseline CMR examination before chemotherapy was not performed. Given that situation, we recruited healthy volunteers to act as a control group. (3) Because the experiment was conducted during the COVID-19 outbreak, some patients contracted the virus, and thus, the rate of follow-up in the study was low. Future studies with larger cohorts are required to investigate whether myocardial T2 can predict a reduction in LVEF. (4) Our patient cohort received several different chemotherapy regimens. Although the effect of chemotherapy on myocardial edema was adjusted for drug types, the individual effects of the various drugs require further elucidation. (5) This study didn't measure N-terminal pro-B type natriuretic peptide in patients, the association between N-terminal pro-B type natriuretic peptide and myocardial T2 needs further study with longer follow-up.

Conclusion

In patients receiving chemotherapy for gynecologic malignancies, myocardial edema develops with the increase of chemotherapy cycles received. The myocardial edema is associated with a reduction in LV mass. T2 mapping allows the assessment of myocardial injury and the monitoring of myocardial edema during chemotherapy.

Data availability statement

The original contributions presented in the study are included in the article/supplementary material. Further inquiries can be directed to the corresponding author.

Ethics statement

The clinical protocol of this study was approved by the institutional ethics review board of West China Second Hospital and Chinese Clinical Trial Registry (ChiCTR-DDD-17013450). The patients/participants provided their written informed consent to participate in this study.

Author contributions

Conceptualization, Y-KG and Z-GY; methodology and formal analysis, M-XY, XL, and LY; data curation and investigation, Q-LL, D-QW, and K-ML; supervision, R-TY and X-JL; original draft, M-XY and XL; review and editing, X-SL, CF, and X-MM; guarantor, Y-KG. All authors contributed to the article and approved the submitted version.

Funding

This work was supported by National Natural Science Foundation of China (82071874, 81971586, 81771897, 81901712,

81771887,82202094, 82102022, 82120108015); Sichuan Science and Technology Program (2020YFS0050, 2020YJ0029, 2017TD0005, 21ZDYF1967; 2022NSFSC1600,2019YFS0430); Fundamental Research Funds for the Central University (SCU2020D4132); Clinical Research Finding of Chinese Society of Cardiovascular Disease of 2019 (HFCSC2019B01) and 1·3·5 project for disciplines of excellence, West China Hospital, Sichuan University (ZYGD18013, ZYGD18019).

Conflict of interest

The authors declare that the research was conducted in the absence of any commercial or financial relationships that could be construed as a potential conflict of interest.

Publisher's note

Supplementary material

The Supplementary Material for this article can be found online at: https://www.frontiersin.org/articles/10.3389/fonc.2022.961841/full#supplementary-material

References

1. Okwuosa TM, Barac A. Burgeoning cardio-oncology programs: Challenges and opportunities for early career Cardiologists/Faculty directors. *J Am Coll Cardiol* (2015) 66(10):1193–7. doi: 10.1016/j.jacc.2015.07.033

2. Lenneman CG, Sawyer DB. Cardio-oncology: An update on cardiotoxicity of cancer-related treatment. *Circ Res* (2016) 118(6):1008–20. doi: 10.1161/CIRCRESAHA.115.303633

3. Thavendiranathan P, Wintersperger BJ, Flamm SD, Marwick TH. Cardiac MRI in the assessment of cardiac injury and toxicity from cancer chemotherapy: a systematic review. *Circ Cardiovasc Imaging.* (2013) 6(6):1080–91. doi: 10.1161/CIRCIMAGING.113.000899

4. Plana JC, Thavendiranathan P, Bucciarelli-Ducci C, Lancellotti P. Multi-modality imaging in the assessment of cardiovascular toxicity in the cancer patient. *JACC Cardiovasc Imaging.* (2018) 11(8):1173–86. doi: 10.1016/j.jcmg.2018.06.003

5. Jeong D, Gladish G, Chitiboi T, Fradley MG, Gage KL, Schiebler ML. MRI In cardio-oncology: A review of cardiac complications in oncologic care. *J Magn Reson Imaging.* (2019) 50(5):1349–66. doi: 10.1002/jmri.26895

6. Yu AF, Chan AT, Steingart RM. Cardiac magnetic resonance and cardio-oncology: Does T2 signal the end of anthracycline cardiotoxicity? *J Am Coll Cardiol* (2019) 73(7):792–4. doi: 10.1016/j.jacc.2018.11.045

7. Farhad H, Staziaki PV, Addison D, Coelho-Filho OR, Shah RV, Mitchell RN, et al. Characterization of the changes in cardiac structure and function in mice treated with anthracyclines using serial cardiac magnetic resonance imaging.*Circ Cardiovasc Imaging.* (2016) 9(12):e003584. doi: 10.1161/CIRCIMAGING.115.003584

8. Galán-Arriola C, Lobo M, Vílchez-Tschischke JP, López GJ, de Molina-Iracheta A, Pérez-Martínez C, et al. Serial magnetic resonance imaging to identify early stages of anthracycline-induced cardiotoxicity. *J Am Coll Cardiol* (2019) 73 (7):779–91. doi: 10.1016/j.jacc.2018.11.046

9. Lustberg MB, Reinbolt R, Addison D, Ruppert AS, Moore S, Carothers S, et al. Early detection of anthracycline-induced cardiotoxicity in breast cancer survivors with T2 cardiac magnetic resonance. *Circ Cardiovasc Imaging.* (2019) 12 (5):e0087707. doi: 10.1161/CIRCIMAGING.118.008777

10. Ferreira VM, Schulz-Menger J, Holmvang G, Kramer CM, Carbone I, Sechtem U, et al. Cardiovascular magnetic resonance in nonischemic myocardial inflammation: Expert recommendations. *J Am Coll Cardiol* (2018) 72(24):3158–76. doi: 10.1016/j.jacc.2018.09.072

11. Lota AS, Gatehouse PD, Mohiaddin RH. T2 mapping and T2* imaging in heart failure. *Heart Fail Rev* (2017) 22(4):431–40. doi: 10.1007/s10741-017-9616-5

12. Siegel RL, Miller KD, Jemal A. Cancer statistics, 2020. *CA Cancer J Clin* (2020) 70(1):7–30. doi: 10.3322/caac.21590

13. Gottdiener JS, Appelbaum FR, Ferrans VJ, Deisseroth A, Ziegler J. Cardiotoxicity associated with high-dose cyclophosphamide therapy. *Arch Intern Med* (1981) 141(6):758–63. doi: 10.1001/archinte.1981.00340060066015

14. Pai VB, Nahata MC. Cardiotoxicity of chemotherapeutic agents: incidence, treatment and prevention. *Drug Saf.* (2000) 22(4):263–302. doi: 10.2165/00002018-200022040-00002

15. Goldberg MA, Antin JH, Guinan EC, Rappeport JM. Cyclophosphamide cardiotoxicity: an analysis of dosing as a risk factor. *Blood* (1986) 68(5):1114–8. doi: 10.1182/blood.V68.5.1114.1114

16. Quezado ZM, Wilson WH, Cunnion RE, Parker MM, Reda D, Bryant G, et al. High-dose ifosfamide is associated with severe, reversible cardiac dysfunction. *Ann Intern Med* (1993) 118(1):31–6. doi: 10.7326/0003-4819-118-1-199301010-00006

17. Zhang C, Chen B, Guo A, Zhu Y, Miller JD, Gao S, et al. Microtubule-mediated defects in junctophilin-2 trafficking contribute to myocyte transverse-tubule remodeling and Ca2+ handling dysfunction in heart failure. *Circulation* (2014) 129(17):1742–50. doi: 10.1161/CIRCULATIONAHA.113.008452

18. Suerken CK, D'Agostino RBJr, Jordan JH, Meléndez GC, Vasu S, Lamar ZS, et al. Simultaneous left ventricular volume and strain changes during chemotherapy associate with 2-year postchemotherapy measures of left ventricular ejection fraction. *J Am Heart Assoc* (2020) 9(2):e015400. doi: 10.1161/JAHA.119.015400

19. Jolly MP, Jordan JH, Meléndez GC, McNeal GR, D'Agostino RBJr, Hundley WG. Automated assessments of circumferential strain from cine CMR correlate with LVEF declines in cancer patients early after receipt of cardio-toxic chemotherapy. *J Cardiovasc Magn Reson* (2017) 19(1):59. doi: 10.1186/s12968-017-0373-3

20. McAlindon EJ, Pufulete M, Harris JM, Lawton CB, Moon JC, Manghat N, et al. Measurement of myocardium at risk with cardiovascular MR: comparison of techniques for edema imaging. *Radiology* (2015) 275(1):61–70. doi: 10.1148/radiol.14131980

21. Bulluck H, White SK, Rosmini S, Bhuva A, Treibel TA, Fontana M, et al. T1 mapping and T2 mapping at 3T for quantifying the area-at-risk in reperfused STEMI patients. *J Cardiovasc Magn Reson* (2015) 17(1):73. doi: 10.1186/s12968-015-0173-6

22. Bojer AS, Sørensen MH, Vejlstrup N, Goetze JP, Gæde P, Madsen PL. Distinct non-ischemic myocardial late gadolinium enhancement lesions in patients with type 2 diabetes. *Cardiovasc Diabetol* (2020) 19(1):184. doi: 10.1186/s12933-020-01160-y

23. Martini N, Aimo A, Barison A, Della Latta D, Vergaro G, Aquaro GD, et al. Deep learning to diagnose cardiac amyloidosis from cardiovascular magnetic resonance. *J Cardiovasc Magn Reson* (2020) 22(1):84. doi: 10.1186/s12968-020-00690-4

24. Altaha MA, Nolan M, Marwick TH, Somerset E, Houbois C, Amir E, et al. Can quantitative CMR tissue characterization adequately identify cardiotoxicity during chemotherapy?: impact of temporal and observer variability. *JACC Cardiovasc Imaging.* (2020) 13(4):951–62. doi: 10.1016/j.jcmg.2019.10.016

25. Haslbauer JD, Lindner S, Valbuena-Lopez S, Zainal H, Zhou H, D'Angelo T, et al. CMR imaging biosignature of cardiac involvement due to cancer-related treatment by T1 and T2 mapping. *Int J Cardiol* (2019) 275:179–86. doi: 10.1016/j.ijcard.2018.10.023

26. Zito C, Manganaro R, Cusmà Piccione M, Madonna R, Monte I, Novo G, et al. Anthracyclines and regional myocardial damage in breast cancer patients. a multicentre study from the working group on drug cardiotoxicity and cardioprotection, Italian society of cardiology (SIC). *Eur Heart J Cardiovasc Imaging.* (2021) 22(4):406–15. doi: 10.1093/ehjci/jeaa339

27. Astuti A, Erwinanto E, Akbar MR, Martanto E, Badudu DF. Global and regional longitudinal strain reduction in breast cancer patients after first chemotherapy cycle with fluorouracil, adriamycin, and cyclophosphamide regimen. *Cardiol Res* (2021) 12(4):238–43. doi: 10.14740/cr1229

28. von Knobelsdorff-Brenkenhoff F, Prothmann M, Dieringer MA, Wassmuth R, Greiser A, Schwenke C, et al. Myocardial T1 and T2 mapping at 3 T: reference values, influencing factors and implications. *J Cardiovasc Magn Reson* (2013) 15 (1):53. doi: 10.1186/1532-429X-15-53

29. Bönner F, Janzarik N, Jacoby C, Spieker M, Schnackenburg B, Range F, et al. Myocardial T2 mapping reveals age- and sex-related differences in volunteers. *J Cardiovasc Magn Reson* (2015) 17(1):9. doi: 10.1186/s12968-015-0118-0

30. Roy C, Slimani A, de Meester C, Amzulescu M, Pasquet A, Vancraeynest D, et al. Age and sex corrected normal reference values of T1, T2 T2* and ECV in healthy subjects at 3T CMR. *J Cardiovasc Magn Reson* (2017) 19(1):72. doi: 10.1186/s12968-017-0371-5

31. Tong X, Li VW, Liu AP, So EK, Chan Q, Ho KK, et al. Cardiac magnetic resonance T1 mapping in adolescent and young adult survivors of childhood cancers. *Circ Cardiovasc Imaging.* (2019) 12(4):e008453. doi: 10.1161/CIRCIMAGING.118.008453

32. Fallah-Rad N, Walker JR, Wassef A, Lytwyn M, Bohonis S, Fang T, et al. The utility of cardiac biomarkers, tissue velocity and strain imaging, and cardiac magnetic resonance imaging in predicting early left ventricular dysfunction in patients with human epidermal growth factor receptor II-positive breast cancer treated with adjuvant trastuzumab therapy. *J Am Coll Cardiol* (2011) 57(22):2263–70. doi: 10.1016/j.jacc.2010.11.063

33. Guglin M, Krischer J, Tamura R, Fink A, Bello-Matricaria L, McCaskill-Stevens W, et al. Randomized trial of lisinopril versus carvedilol to prevent trastuzumab cardiotoxicity in patients with breast cancer. *J Am Coll Cardiol* (2019) 73(22):2859–68. doi: 10.1016/j.jacc.2019.03.495

34. Bowles EJ, Wellman R, Feigelson HS, Onitilo AA, Freedman AN, Delate T, et al. Pharmacovigilance study team. risk of heart failure in breast cancer patients after anthracycline and trastuzumab treatment: a retrospective cohort study. *J Natl Cancer Inst* (2012) 104:1293–305. doi: 10.1093/jnci/djs317

35. Rowinsky EK, McGuire WP, Guarnieri T, Fisherman JS, Christian MC, Donehower RC. Cardiac disturbances during the administration of taxol. *J Clin Oncol* (1991) 9(9):1704–12. doi: 10.1200/JCO.1991.9.9.1704

36. McGuire WP, Rowinsky EK, Rosenshein NB, Grumbine FC, Ettinger DS, Armstrong DK, et al. Taxol: a unique antineoplastic agent with significant activity in advanced ovarian epithelial neoplasms. *Ann Intern Med* (1989) 111(4):273–9. doi: 10.7326/0003-4819-111-4-273

37. Anjo A, Dantchev D, Mathé G. Notes on the cardiotoxicity of platinum complexes (except 1- OHP) in ultrastructural study. *BioMed Pharmacother.* (1989) 43(4):265–6. doi: 10.1016/0753-3322(89)90006-1

38. Zamorano JL, Lancellotti P, Rodriguez Muñoz D, Aboyans V, Asteggiano R, Galderisi M, et al. ESC Position paper on cancer treatments and cardiovascular toxicity developed under the auspices of the ESC committee for practice guidelines: The task force for cancer treatments and cardiovascular toxicity of the European society of cardiology (ESC). *Eur Heart J* (2016) 37(36):2768–801. doi: 10.1093/eurheartj/ehw211

39. Ferreira de Souza T, Quinaglia AC, Silva T, Osorio Costa F, Shah R, Neilan TG, et al. Anthracycline therapy is associated with cardiomyocyte atrophy and preclinical manifestations of heart disease. *JACC Cardiovasc Imaging.* (2018) 11 (8):1045–55. doi: 10.1016/j.jcmg.2018.05.012

40. Lipshultz SE, Lipsitz SR, Sallan SE, Dalton VM, Mone SM, Gelber RD, et al. Chronic progressive cardiac dysfunction years after doxorubicin therapy for childhood acute lymphoblastic leukemia. *J Clin Oncol* (2005) 23(12):2629–36. doi: 10.1016/j.amjcard.2012.07.040

41. Neilan TG, Coelho-Filho OR, Pena-Herrera D, Shah RV, Jerosch-Herold M, Francis SA, et al. Left ventricular mass in patients with a cardiomyopathy after treatment with anthracyclines. *Am J Cardiol* (2012) 110(11):1679–86. doi: 10.1161/CIRCHEARTFAILURE.117.004560

42. Jordan JH, Castellino SM, Meléndez GC, Klepin HD, Ellis LR, Lamar Z, et al. Left ventricular mass change after anthracycline chemotherapy. *Circ Heart Fail* (2018) 11(7):e004560. doi: 10.1200/JCO.2005.12.121

frontiers | Frontiers in Cardiovascular Medicine

TYPE Original Research
PUBLISHED 13 October 2022
DOI 10.3389/fcvm.2022.951940

OPEN ACCESS

EDITED BY
Rod Skinner,
Newcastle University, United Kingdom

REVIEWED BY
Yongqiang Zheng,
Sun Yat-sen University Cancer Center (SYSUCC), China
Sakima A. Smith,
The Ohio State University,
United States

*CORRESPONDENCE
Jun Liu
liujunheliyun@163.com
Juyu Tang
tangjuyu@csu.edu.cn

SPECIALTY SECTION
This article was submitted to Cardio-Oncology, a section of the journal Frontiers in Cardiovascular Medicine

RECEIVED 24 May 2022
ACCEPTED 26 September 2022
PUBLISHED 13 October 2022

CITATION
Chen B, Zhao X, Li X, Liu J and Tang J (2022) Fatal heart disease in patients with bone and soft tissue sarcoma. *Front. Cardiovasc. Med.* 9:951940. doi: 10.3389/fcvm.2022.951940

Fatal heart disease in patients with bone and soft tissue sarcoma

Bei Chen[1,2,3], Xin Zhao[2], Xiying Li[2], Jun Liu[2]* and Juyu Tang[1,3]*

[1]Department of Orthopaedics, Xiangya Hospital, Central South University, Changsha, China, [2]Department of Musculoskeletal Oncology, Chenzhou No. 1 People's Hospital, Chenzhou, China, [3]Department of Hand and Microsurgery, Xiangya Hospital, Central South University, Changsha, China

Background/purpose: With improved cancer survivorship, non-cancer events, especially heart disease (HD), have become the underlying cause of death in cancer patients, but the risk of HD mortality in sarcoma patients remains poorly characterized. Therefore, our purpose was to: (1) identify sarcoma patients at the highest risk of fatal HD compared with the general population, (2) identify patients and sarcoma characteristics associated with a higher risk of HD death, and (3) determine if chemotherapy increased the risk of HD death in sarcoma patients.

Methods: From 1975 to 2016, we identified patients diagnosed with bone and soft tissue sarcoma from the Surveillance, Epidemiology, and End Results (SEER) database in the US. Standardized mortality ratios (SMRs) were evaluated using mortality data from the general population collected by the National Center for Health Statistics. This was the largest retrospective cohort study of fatal HD in individuals with sarcoma.

Results: In 80,905 sarcoma patients observed for 530,290 person-years, 3,350 deaths from HD were identified with a mortality of 631.7/100,000 person-years. The SMR of death from HD was 1.38 (95% CI: 1.33–1.42). The highest risks of death from HD were observed in patients with Ewing sarcoma (SMR = 5.44; 95% CI: 3.38–8.75) and osteosarcoma (SMR = 1.92; 95% CI: 1.55–2.38). Patients diagnosed at < 19 years old had the highest SMR in all age subgroups, and a higher risk of fatal HD relative to the general population was observed in sarcoma survivors diagnosed at < 85 years old. In patients diagnosed at < 19 years old, HD plurality occurred in those with Ewing sarcoma (29.4%) and osteosarcoma (32.4%) and at > 35 years old, HD plurality occurred in those diagnosed with liposarcoma (19.0%) and malignant fibro histiocytoma (MFH) (23.6%). For sarcoma survivors, HD mortality risks were highest within the first year after diagnosis (SMR = 1.31; 95% CI: 1.21–1.41), and this risk remained elevated throughout follow-up compared with the general population. Subgroup analyses indicated that chemotherapy significantly increased the risk of fatal HD in patients with localized osteosarcoma (Hazard ratio (HR) = 3.18; 95% CI: 1.24–8.13; P = 0.016), but not in patients with other histological sarcoma subtypes and clinical stages.

Conclusion: The risk of death from HD mainly varied in patients with different histological sarcoma subtypes and clinical stages. Chemotherapy increased the risk of fatal HD in patients with localized osteosarcoma. To lower the risk of fatal HD in patients with sarcoma, we call for enhanced multidisciplinary cooperation, including cardiologists and orthopedic surgeons.

KEYWORDS

sarcoma, chemotherapy, osteosarcoma, heart diseases, standardized mortality ratio

Introduction

Over several decades, heart diseases (HD) have become the first leading cause of death globally, and in 2019, killed approximately nine million individuals, accounting for 9% of all deaths (1). Cancer and HD may occur separately in patients, or cancer may cause HD via non-bacterial thrombotic endocarditis and chemoradiation therapy (2–4). As survival rate of cancer patients improve, medical officers have gradually realized that the risk of death from other non-cancer diseases in cancer patients was higher when compared with the general population (5–7), furthermore, HD as the first leading cause of non-cancer death among cancer patients have attracted more and more attention from clinicians (7–9).

Bone and soft tissue sarcoma comprise several rare malignant tumors which arise from mesenchymal tissue (10), they are responsible for more deaths than testicular cancer, Hodgkin's disease, and thyroid cancer combined due to their more recurrent and metastatic nature (11). The standard therapy for patients with sarcoma is neoadjuvant chemotherapy, surgical resection, and adjuvant chemotherapy (12). Anthracyclines are commonly used chemotherapy drugs, but may cause HD, reduce the quality of life in patients, and increase mortality in sarcoma patients (3). Previous studies reporting the risk of HD in sarcoma patients were limited by small sample sizes and data collected primarily at single institutions (13–16). Currently, limited guidelines are available on fatal HD prevention, identification, or management, specifically in sarcoma patients. One strategy aimed at preventing fatal HD in this group is to identify and target subgroups at greatest HD risk, therefore, retrospective cohort studies such as ours could be used by clinicians to generate survivorship programs and mitigate HD risks in these patients.

In our study, we had the following objectives: (1) to identify sarcoma patients at highest risk of fatal HD compared with the general population, (2) to identify patients and sarcoma characteristics associated with a higher risk of HD death, and (3) to determine if chemotherapy increased the risk of HD death in sarcoma patients.

Materials and methods

In this retrospective cohort study, we used the Surveillance, Epidemiology, and End Results (SEER) database at the National Cancer Institute, which comprised 18 registries and covered approximately 28% of the US general population (17). Given that anthracyclines or cisplatin were discovered in the 1980s, we included patients diagnosed with sarcoma between 1975 and 2016 (18). As a comparison, general population mortality data, spanning 1969–2016 from the National Center for Health Statistics, were used (5, 17, 19). Using exclusion criteria (**Figure 1**), we identified the final study cohort. Patients whose information was obtained solely from death certificates or autopsies were excluded due to no survival time data (<1.5% of patients). Patients diagnosed with bone and soft tissue sarcoma without a definite socioeconomic status were also excluded (11). Sarcomas were classified into ten histological subtypes according to the International Classification of Disease for Oncology third revision (ICD-O-3), and included chondrosarcoma, osteosarcoma, Ewing sarcoma, liposarcoma, malignant fibro histiocytoma (MFH), leiomyosarcoma, fibrosarcoma, synovial sarcoma, Malignant Peripheral Nerve Sheath Tumor (MPNST), and others (ICD-O-3 codes are shown in **Table 1**) (11).

We extracted demographic data, including age at diagnosis, sex (female, male), race (white, black, and others), calendar year of diagnosis (1975–2016), marital status at diagnosis (married, unmarried, and unknown), insurance status (insured, Medicaid, uninsured, unknown), and socioeconomic indicators (income and educational status). Income (median family income) and educational level (percentage of individuals > 25 years of age with at least a high school degree) from county-level data were calculated by referring to 2000 US census data and categorizing data into tertiles (high, median, low). Tumor-related characteristics included histological subtype, grade (I–IV), clinical sarcoma stage (localized, regional, distant, and unknown), and treatment information (chemotherapy, radiotherapy, and surgery status). Time of follow-up and cause of death were also available and collected. Patients were considered to have committed HD death if the cause of death variable was coded as "Diseases of Heart (50060)."

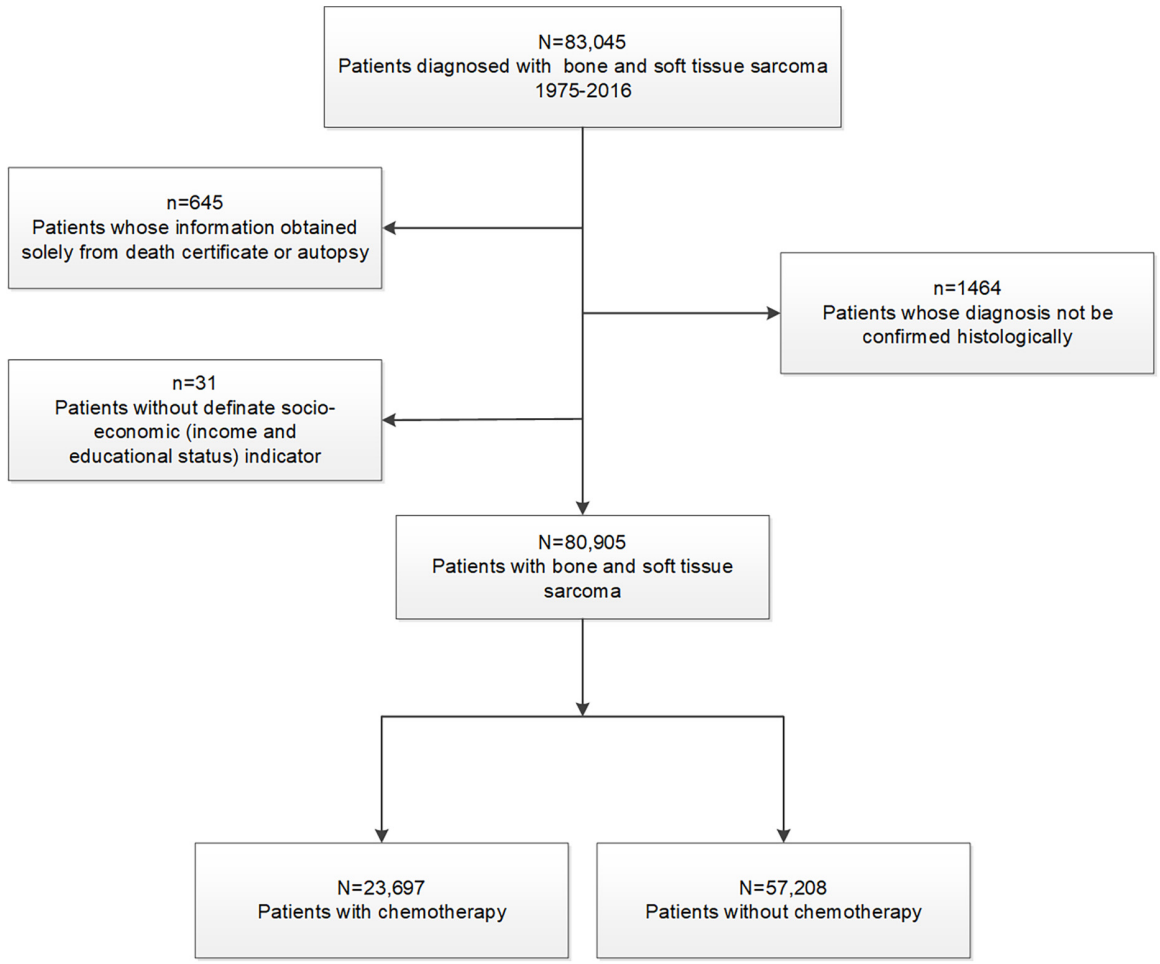

FIGURE 1
Flowchart describing initial dataset and exclusions leading to final study cohorts.

For objective 1, we calculated standardized mortality ratios (SMRs), which provided the relative risk of HD death for sarcoma patients when compared with all US residents, stratified by histological subgroup. SMRs and 95% confidence intervals (CIs) were calculated as previously described (19, 20). Briefly, SMRs were estimated as the ratio of observed to expected numbers of deaths. The observed number of HD deaths represented the total number of deaths from heart events in sarcoma patients during the follow-up period; the expected number of deaths represented the number of deaths from heart events in the general population with a similar age at diagnosis, sex, race, and calendar year distribution. Five-year age categories and three-year calendar categories were used for standardization (21). Mortality from fatal HD was calculated as the number of deaths from HD divided by person-years at risk (20).

For objective 2, considering other competitive risk events, we plotted cumulative incidence curves and compared them using the Gray test. Furthermore, we constructed logistic regression and multivariate Cox proportional hazards models to identify risk factors associated with a higher risk of HD death in sarcoma patients.

For objective 3, we conducted subgroup analysis by histological subtype and clinical stage to determine if chemotherapy increased the risk of fatal HD in sarcoma patients. The survival time was from sarcoma diagnosis until fatal HD; values recorded as 0 months in the SEER database were converted to one-half of a month according to accepted epidemiological practices (19). Statistical significance was accepted at $P < 0.05$ (two-sided). Analyses were performed using SEER*Stat software version 8.3.6 and R version 3.51 statistical software.

Results

In total, 3,350 HD deaths were identified in 80,905 patients with bone and soft tissue sarcoma over 530,291

TABLE 1 Death from HD among patients with bone and soft tissue sarcomas by demographic and tumor characteristics.

Characteristic	Patients with cancer in SEER		HD death		Person-years accrued	Mortality[1]	SMR[2]	95% CI
	No.	%	No.	%				
Sex								
Female	36283	45	1353	40	247636	546.4	1.45	1.37–1.53
Male	44622	55	1997	60	282655	706.5	1.33	1.28–1.39
Race[3]								
White	65618	81	2876	84	433078	664.1	1.35	1.30–1.40
Black	8530	11	303	9	54297	558.0	1.48	1.32–1.66
Other	6757	8	171	5	42915	398.5	1.70	1.47–1.98
American Indian/Alaska Native	553	1	12	1	3762	318.9	2.13	1.21–3.75
Asian or Pacific Islander	5430	7	149	4	33934	439.1	1.70	1.45–2.00
Unknown	774	1	10	1	5218	191.6	1.42	0.77–2.64
Year of diagnosis								
1975–1977	1667	2	194	6	22941	845.6	1.75	1.52–2.02
1978–1980	1797	2	183	5	25057	730.3	1.86	1.61–2.15
1981–1983	1879	2	184	5	25039	734.8	2.00	1.73–2.31
1984–1986	1986	2	180	5	25146	715.8	1.73	1.50–2.00
1987–1989	2055	3	180	5	26061	690.7	1.61	1.39–1.86
1990–1992	2683	3	206	6	31502	653.9	1.65	1.44–1.89
1993–1995	3593	4	237	7	38861	609.9	1.43	1.26–1.62
1996–1998	3984	5	251	7	40156	625.1	1.37	1.21–1.55
1999–2001	7253	9	376	11	63231	594.6	1.37	1.24–1.52
2002–2004	9463	12	372	11	71767	518.3	1.09	0.98–1.20
2005–2007	9997	12	347	10	60811	570.6	1.14	1.03–1.27
2008–2011	14594	18	387	12	64184	603.0	1.19	1.08–1.32
2012–2016	19954	25	253	8	35529	712.1	1.29	1.14–1.46
Marital status								
Married	38650	48	1690	50	257737	655.7	1.24	1.18–1.30
Unknown	4312	5	233	7	26155	890.8	1.57	1.38–1.78
Unmarried	37943	47	1427	43	246397	579.1	1.54	1.47–1.63
Education[4]								
High	26221	32	888	27	137715	644.8	1.39	1.30–1.49
Median	27786	34	1227	37	190351	644.6	1.38	1.30–1.45
Low	26898	33	1235	37	202224	610.7	1.37	1.29–1.44
Income[4]								
High	26657	33	1159	35	191456	605.4	1.32	1.24–1.39
Median	23844	29	910	27	156387	581.9	1.28	1.20–1.37
Low	30404	38	1281	38	182447	702.1	1.52	1.44–1.61
Insurance								
Uninsured	1259	2	13	1	3741	347.5	2.25	1.31–3.88
Any Medicaid	5668	7	73	2	15481	471.5	2.13	1.69–2.68
Insured	29498	36	621	19	95223	652.1	1.13	1.04–1.22
Unknown	44480	55	2643	78	415844	635.6	1.44	1.38–1.49
Histology[5]								
Ewing sarcoma	3055	4	17	1	21430	79.3	5.44	3.38–8.75
Osteosarcoma	6504	8	83	2	46552	178.3	1.92	1.55–2.38
Synovial sarcoma	3171	4	42	1	23181	181.2	1.55	1.14–2.10

(Continued)

TABLE 1 (Continued)

Characteristic	Patients with cancer in SEER		HD death		Person-years accrued	Mortality[1]	SMR[2]	95% CI
	No.	%	No.	%				
MPNST	2116	3	64	2	11374	562.7	1.57	1.23–2.00
Chondrosarcoma	5941	7	232	7	50229	461.9	1.37	1.20–1.55
MFH	8492	10	775	23	66089	1172.7	1.34	1.25–1.44
Fibrosarcoma	4102	5	185	6	29838	620.0	1.27	1.10–1.47
Liposarcoma	10819	13	623	19	81894	760.7	1.26	1.16–1.36
Leiomyosarcoma	7532	9	338	10	41938	805.9	1.18	1.06–1.31
Chordoma	1605	2	55	2	10147	542.0	1.05	0.81–1.37
Others	27568	34	936	28	147614	634.1	1.59	1.49–1.69
Grade at presentation[6]								
Grade I	9595	12	485	14	84323	575.2	1.22	1.11–1.33
Grade II	10074	12	438	13	80079	547.0	1.23	1.12–1.35
Grade III	11701	14	429	13	58801	729.6	1.39	1.27–1.53
Grade IV	17159	21	559	17	76839	727.5	1.34	1.24–1.46
Unknown	32376	40	1439	43	230247	625.0	1.51	1.43–1.59
Stage at presentation								
Localized	42042	52	2152	64	332076	648.0	1.33	1.27–1.38
Regional	19671	24	706	21	126953	556.1	1.32	1.23–1.42
Distant	12414	15	199	6	30812	645.8	2.11	1.84–2.42
Unknown	6778	8	293	9	40448	724.4	1.60	1.42–1.79
Chemotherapy								
No/Unknown	57208	71	3059	91	395330	773.8	1.35	1.31–1.40
Yes	23697	29	291	9	134960	215.6	1.69	1.51–1.90
Radiotherapy								
No/Unknown	52386	65	2314	69	355007	651.8	1.49	1.43–1.56
Yes	28519	35	1036	31	175283	591.0	1.17	1.10–1.25
Surgery								
None	14481	18	427	13	40693	1049.3	2.16	1.96–2.37
Yes	64412	80	2826	84	476861	592.6	1.29	1.24–1.34
Unknown	2012	2	97	3	12736	761.6	2.04	1.67–2.49
All sarcoma patients	80905	100	3350	100	530290	631.7	1.38	1.33–1.42

HD, heart diseases; SEER, Surveillance, Epidemiology, and End Results; SMR, standardized mortality ratio; MFH, malignant fibrohistiocytoma; MPNST, Malignant Peripheral Nerve Sheath Tumor; NOS, not of specific.

[1]Per 100,000 person-years.

[2]SMRs were estimated as the ratios of observed to expected number of deaths. Observed number of HD death represent the total number of deaths from HD among patients with sarcoma recorded during the study period. Expected death represent the number of individuals who died of HD in the general population with a similar distribution of age at diagnosis (5-year intervals), sex, race (white, black, and other), and calendar year of diagnosis (3-year intervals). The calculation for SMRs were adjusted to the age, sex, race/ethnicity, and calendar year distributions between sarcoma patients and the general population.

[3]Others included American Indian/AK Native, Asian/Pacific Islander and unknown race.

[4]Education status and income level were categorized into tertiles.

[5]ICD-O-3: Chondrosarcoma, 9220–9243; Osteosarcoma, 9180–9200; Ewing sarcoma, 9260; Liposarcoma, 8850–8858; MFH, 8830; Leiomyosarcoma, 8890–8891 and 8896; Synovial sarcoma, 9040–9044; MPNST, 9540 and 9561; Chordoma, 9370–9372.

[6]Grade I: Well differentiated; Grade II: Moderately differentiated; Grade III: Poorly differentiated; Grade IV: Undifferentiated; anaplastic.

person-years, and provided an age-, sex-, race-, and year-adjusted HD mortality of 631.7/100,000 person-years. The corresponding HD mortality in the general US population was 16.7/100,000 person-years. This generated an SMR = 1.38 (95% CI: 1.33–1.42). The survival time range was 0–39.25 years, with a mean survival time of 7.34 years for sarcoma patients dying from HD.

Sarcoma patient risk of fatal heart disease versus the general population

The characteristics of sarcoma patients and those who died of HD vs. all cancer patients are shown (Table 1). Higher SMRs for fatal HD in patients with sarcoma were associated with the female sex (546.4/100,000 person-years;

TABLE 2 Risk of fatal HD among patients with sarcoma by age at diagnosis.

Age at diagnosis (years)	Mortality in general population[1]	Mortality in patients with sarcoma[2]	Person-years accrued	No. of deaths	SMR[3]	95% CI
00–19	2.6	32.7	103,970	34	9.46	6.76–13.24
20–29	4.5	42.7	56,215	24	7.24	4.86–10.81
30–34	7.7	76.9	31,216	24	5.59	3.75–8.34
35–39	14.5	113.7	35,173	40	4.11	3.01–5.60
40–44	29.2	170.1	37,626	64	3.09	2.42–3.95
45–49	58.8	217.6	40,893	89	2.17	1.77–2.68
50–54	109.5	330.0	41,213	136	1.96	1.65–2.32
55–59	188.7	481.2	39,694	191	1.71	1.49–1.97
60–64	310.4	709.5	36,925	262	1.60	1.41–1.80
65–69	508.0	1,050.7	33,121	348	1.55	1.40–1.72
70–74	804.0	1,501.6	27,903	419	1.37	1.24–1.51
75–79	1308.2	2,303.0	22,535	519	1.31	1.20–1.43
80–84	2133.1	3,636.1	14,658	533	1.22	1.12–1.33
85+	3586.2	7,295.3	9,142	667	1.04	0.96–1.12

HD, heart diseases; SMR, standardized mortality ratio.
[1]Per 100,000 person-years. Reference population: general US population, 1969–2016.
[2]Among persons with sarcoma in the populations served by the SEER program.
[3]Adjusted to the race and sex distributions between patients and the general population.

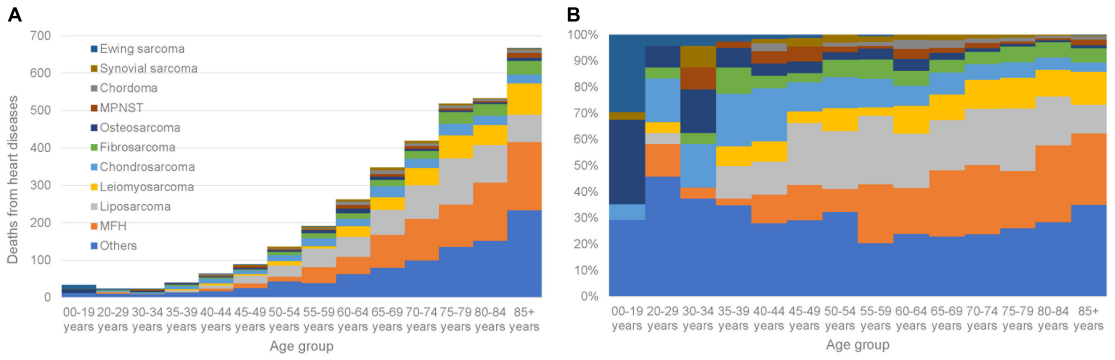

FIGURE 2
Fatal HD among sarcoma patients as a function of age group. **(A)** The *y*-axis depicts the absolute number of HD deaths and the *x*-axis depicts the age group at time of diagnosis. The colors depict the histological subtypes of sarcoma. **(B)** The *y*-axis depicts the relative number of HD deaths and the *x*-axis depicts the age group at time of diagnosis. The colors depict the histological subtypes of sarcoma.

SMR = 1.45; 95% CI: 1.37–1.53), the American Indian/Alaskan Native race (318.9/100,000 person-years; SMR = 2.13; 95% CI: 1.21–3.75), and an unmarried status (579.1/100,000 person-years; SMR = 1.54; 95% CI: 1.47–1.63). For patients as a whole, the risk of fatal HD was higher when compared with the general population over the 40 years covered in the SEER data, except for those diagnosed between 2002 and 2004 (518.3/100,000 person-years; SMR = 1.09; 95% CI: 0.98–1.20). Patients with high and low educational levels were equal likely to die from HD: 32% vs. 33%. Patients with low income levels (SMR = 1.52; 95% CI: 1.44–1.61) and an uninsured status (SMR = 2.25; 95% CI: 1.31–3.88) had a higher SMR for fatal HD when compared with those with a high income level (SMR = 1.32; 95% CI: 1.24–1.39) and an insured status (SMR = 1.13; 95% CI: 1.04–1.22). Patients diagnosed at a younger age had a higher SMR for HD, and SMRs gradually declined as patients were diagnosed at later ages (Table 2); patients < 19 years old had an SMR = 9.46 (95% CI: 6.76–13.24, 32.7/100,000 person-years) vs. >85 years old who had an SMR = 1.04 (95% CI: 0.96–1.12, 7,295.3/100,000 person-years). Fatal HD in sarcoma patients as a function of age group is shown (Figure 2). In patients diagnosed at <19 years old, HD plurality occurred in those with Ewing sarcoma (29.4%) and osteosarcoma (32.4%). In contrast, in patients diagnosed at >35 years old, HD plurality occurred in those diagnosed with liposarcoma (19.0%) and MFH (23.6%).

Histological sarcoma subtype is associated with a higher risk of fatal heart disease

The risk of fatal HD in patients with most sarcoma subtypes was higher when compared with the general US population, except for chordoma (542.0/100,000 person-years; SMR = 1.05; 95% CI: 0.81–1.37) (Table 1). The highest SMR was observed in patients with Ewing sarcoma (79.3/100,000 person-years; SMR = 5.44; 95% CI: 3.38–5.75), followed by osteosarcoma (178.3/100,000 person-years; SMR = 1.92; 95% CI: 1.55–2.38), MPNST (562.7/100,000 person-years; SMR = 1.57; 95% CI: 1.23–2.00), and synovial sarcoma (181.2/100,000 person-years; SMR = 1.55; 95% CI: 1.14–2.10). Also, patients with MFH had the highest mortality for fatal HD across all patients (1172.7/100,000 person-years; SMR = 1.34; 95% CI: 1.25–1.44). In patients with Ewing sarcoma, osteosarcoma, MPNST, and MFH with chemotherapy a higher relative risk of fatal HD was observed when compared with the general population (Table 3). However, patients with synovial sarcoma (SMR = 1.69; 95% CI: 0.88–3.52), chondrosarcoma (SMR = 1.10; 95% CI: 0.52–2.30), fibrosarcoma (SMR = 1.28; 95% CI: 0.64–2.56), liposarcoma (SMR = 1.25; 95% CI: 0.83–1.88), leiomyosarcoma (SMR = 1.30; 95% CI: 0.87–1.94), and chordoma (SMR = 0.66; 95% CI: 0.09–4.67), and receiving chemotherapy had an equal risk when compared with the general population.

Risk of heart disease death over time after diagnosis

For all sarcoma subtypes, the risk of death from HD was higher relative to the general population in the first year after a diagnosis, but decreased gradually from 1–5 years, but then increased after this (Table 4). The relative risk of fatal HD in sarcoma patients when compared with the general population was highest in the 10 years after a sarcoma diagnosis (SMR = 2.85; 95% CI: 2.68–3.04). For most sarcoma types, the risk of death from HD was equal to the general population in the first year of diagnosis. For patients with osteosarcoma, the relative risk was higher when compared with the general population in the first year after a sarcoma diagnosis (SMR = 1.73; 95% CI: 1.12–2.69) and after 10 years (SMR = 4.75; 95% CI: 3.43–6.59).

Characteristics associated with a higher risk of fatal heart disease

From multivariable logistic regression (Table 5) of sarcoma patients, older age at diagnosis [odds ratio (OR) = 1.06; 95% CI: 1.05–1.07; $P < 0.001$], male sex (OR = 1.44; 95% CI: 1.33–1.56; $P < 0.001$), black race (OR = 1.28; 95% CI: 1.12–1.45;

TABLE 3 Standardized mortality ratios (SMRs) of fatal HD among patients with sarcoma by histology and chemotherapy status.

Histology	Patients without chemotherapy					Patients with chemotherapy				
	No. of deaths	No. of patients	Person-years	Mortality[1]	SMR (95% CI)	No. of deaths	No. of patients	Person-years	Mortality[1]	SMR (95% CI)
Ewing sarcoma	3	241	1,796	167.0	5.12 (1.65–15.87)	14	2,814	19,634	71.3	5.52 (3.27–9.31)
Osteosarcoma	45	1,683	11,899	378.2	1.49 (1.11–1.99)	38	4,821	34,654	109.7	2.93 (2.13–4.02)
Synovial sarcoma	33	1,797	14,677	224.8	1.51 (1.08–2.13)	9	1,374	8,504	105.8	1.69 (0.88–3.25)
MPNST	57	1,591	9,338	610.4	1.47 (1.33–1.90)	7	525	2,037	343.7	3.59 (1.71–7.52)
Chondrosarcoma	225	5,352	47,285	475.8	1.38 (1.21–1.57)	7	589	2,944	237.8	1.10 (0.52–2.30)
MFH	716	6,973	56,245	1,273.0	1.33 (1.24–1.43)	59	1,519	9,845	599.3	1.41 (1.09–1.82)
Fibrosarcoma	177	3,613	27,338	647.4	1.27 (1.10–1.48)	8	489	2,500	320.0	1.28 (0.64–2.56)
Liposarcoma	600	9,735	75,766	791.9	1.26 (1.16–1.36)	23	1,084	6,129	375.3	1.25 (0.83–1.88)
Leiomyosarcoma	314	5,997	36,725	855.0	1.17 (1.05–1.31)	24	1,535	5,214	460.3	1.30 (0.87–1.94)
Chordoma	54	1,532	9,782	552.0	1.06 (0.81–1.39)	1	73	366	273.3	0.66 (0.09–4.67)
Others	835	18,694	104,478	799.2	1.56 (1.46–1.67)	101	8,874	43,136	234.1	1.80 (1.48–2.18)

SMR, standardized mortality ratio; HD, heart diseases; MFH, Malignant fibrohistiocytoma; MPNST, Malignant Peripheral Nerve Sheath Tumor.
[1]Per 100,000 person-years.

TABLE 4 Fatal HD among patients with sarcoma by histological subtypes and years since diagnosis.

Histology	Time since diagnosis			
	0–1 Year	1–5 Years	5–10 Years	>10 Years
All				
No. of deaths	675	1016	720	939
Person-years	69,322	181,220	130,829	154,069
SMR[1]	1.31	0.94	1.32	2.85
95%CI	1.21–1.41	0.89–1.00	1.22–1.42	2.68–3.04
Chondrosarcoma				
No. of deaths	27	73	38	94
Person-years	5,388	16,056	12,997	16,202
SMR	0.9	1.05	0.92	2.98
95%CI	0.62–1.31	0.84–1.33	0.67–1.27	2.44–3.65
Chordoma				
No. of deaths	9	16	17	13
Person-years	1,458	4,184	2,643	1,973
SMR	0.84	0.61	1.48	2.77
95%CI	0.44–1.62	0.37–0.99	0.92–2.38	1.61–4.78
Ewing sarcoma				
No. of deaths	1	4	3	9
Person-years	2,804	7,044	4,947	6,844
SMR	1.28	3.42	4.81	15.16
95%CI	0.18–9.09	1.28–9.11	1.55–14.91	7.89–29.13
Fibrosarcoma				
No. of deaths	33	62	38	52
Person-years	3,685	10,331	7,218	8,885
SMR	1.1	0.91	1.17	3.12
95%CI	0.78–1.54	0.71–1.17	0.85–1.61	2.38–4.1
Leiomyosarcoma				
No. of deaths	72	115	77	74
Person-years	6,450	16,327	10,387	9,252
SMR	1.13	0.86	1.25	2.33
95%CI	0.89–1.42	0.72–1.03	1.00–1.57	1.86–2.93
Liposarcoma				
No. of deaths	72	153	162	236
Person-years	9,812	28,926	21,418	22,498
SMR	0.88	0.73	1.28	2.89
95%CI	0.70–1.11	0.62–0.85	1.10–1.49	2.54–3.28
MFH				
No. of deaths	120	250	184	221
Person-years	7,472	20,681	16,734	21,766
SMR	1.06	0.99	1.35	2.60
95%CI	0.89–1.27	0.87–1.12	1.17–1.56	2.28–2.97
MPNST				
No. of deaths	14	19	12	19
Person-years	1,805	4,148	2,872	2,677
SMR	1.62	1.02	1.32	3.8
95%CI	0.96–2.74	0.65–1.60	0.75–2.32	2.43–5.96
Osteosarcoma				
No. of deaths	20	15	12	36
Person-years	5,743	14,378	10,884	15,972

(Continued)

TABLE 4 (Continued)

Histology	Time since diagnosis			
	0–1 Year	1–5 Years	5–10 Years	>10 Years
SMR	1.73	0.96	1.33	4.75
95%CI	1.12–2.69	0.58–1.59	0.76–2.35	3.43–6.59
Synovial sarcoma				
No. of deaths	8	10	7	17
Person-years	2,872	7,842	5,681	7,005
SMR	1.46	0.93	1.12	3.35
95%CI	0.73–2.91	0.50–1.74	0.53–2.35	2.08–5.39
Others				
No. of deaths	299	299	170	168
Person-years	21,827	51,298	35,044	40,989
SMR	1.87	1.12	1.51	2.82
95%CI	1.67–2.09	1.00–1.25	1.30–1.76	2.43–3.28

SMR, standardized mortality ratio; MFH, Malignant fibrohistiocytoma; MPNST, Malignant Peripheral Nerve Sheath Tumor; NOS, not of specific.
[1]Reference population: general US population, 1969 to 2016. Adjusted to the age, sex and race distributions between patients and the general population.

$P < 0.001$), unmarried status (OR = 1.22; 95% CI: 1.13–1.33; $P < 0.001$), and a low income (OR = 1.16; 95% CI: 1.05–1.29; $P = 0.004$) were associated with significantly greater odds of dying from HD. Neither educational level nor insurance status were associated with a risk of dying from HD in the multivariable model. Moreover, sarcoma patients with distant metastases of sarcoma had a lower OR of fatal HD than patients with localized sarcoma (OR = 0.36; 95% CI: 0.3–0.43; $P < 0.001$). Receiving chemotherapy was associated with marginally lower odds of fatal HD (vs. without chemotherapy; OR = 0.77; 95% CI: 0.67–0.88; $P < 0.001$). As shown (**Table 5** – Cox proportional hazards model in the right panel), the HRs of patients who died of HD are stratified by subgroup. In the Cox regression model, receiving radiotherapy (vs. without radiotherapy; HR = 0.80; 95% CI: 0.74–0.87; $P < 0.001$) and surgery (vs. without surgery; HR = 0.56; 95% CI: 0.50–0.63; $P < 0.001$) was still associated with a lower odds of fatal HD.

Subgroup analysis of the risk of fatal heart disease

We conducted subgroup analysis of the study cohort based on histological sarcoma subtypes. Cumulative incidence curves are shown (**Figure 3**). Survival analysis indicated that all patients with sarcoma benefited from chemotherapy except those with chordoma ($P = 0.280$) and Ewing sarcoma ($P = 0.555$). To further determine if chemotherapy increased the risk of fatal HD in patients with sarcoma, we conducted subgroup analysis by clinical stage. In the subgroup analysis, chemotherapy could protect patients with regional Ewing sarcoma from dying from HD (**Table 6**). Moreover, we found that chemotherapy could increase significantly the risk of fatal HD among patients with localized osteosarcoma (HR = 3.18; 95% CI: 1.24–8.13; $P = 0.016$), but not those with regional (HR = 0.63; 95% CI: 0.28–1.40; $P = 0.259$) or advanced osteosarcoma (HR = 0.25; 95% CI: 0.06–1.03; $P = 0.055$). For other subgroups with sarcoma at different clinical stages, chemotherapy did not have any effect on the risk of fatal HD.

Discussion

With the development of multimodality therapy, including advances in imaging techniques and neoadjuvant chemotherapy, sarcoma patient survival has improved significantly (22). In addition to prolonging survival rates, clinicians are now increasingly concerned about complications caused by sarcoma therapy (20, 23). Several small sample or single-center clinical cohort studies reported that antineoplastic agents such as anthracyclines increased the risk of dying from HD in sarcoma patients (14, 15). However, due to low sarcoma incidence rates and limitations with small sample or single center studies, no robust data are available to inform clinical practice. To address this, and to our knowledge, ours is the largest retrospective cohort study on the risk of fatal HD in patients with bone and soft tissue sarcoma.

We performed a contemporary analysis of the risk of fatal HD in >80,000 sarcoma patients and showed that HD risk varied as a function of age, histological subtype, clinical stage, and time after diagnosis. Earlier studies reported that cancers were associated with a high risk of death from HD (4, 6, 7). We first reported that sarcoma patients had a higher risk of fatal HD when compared with the general US population, which was potentially attributed to antineoplastic agents such as anthracycline (24). Anthracyclines are antibiotics discovered

TABLE 5 Odds ratios and hazard ratios of fatal HD among sarcoma patients.

	Logistic regression model			Cox proportional hazards model		
	Odds ratio	**95% CI**	***P*-value**	**Hazard ratio**	**95% CI**	***P*-value**
Age at diagnosis[1]	1.06	1.05–1.07	<0.001	1.10	1.09–1.12	<0.001
Sex						
Female	Reference			Reference		
Male	1.44	1.33–1.56	<0.001	1.63	1.51–1.75	<0.001
Race						
White	Reference			Reference		
Black	1.27	1.11–1.45	<0.001	1.33	1.18–1.50	<0.001
Other	0.83	0.70–0.97	0.025	0.79	0.68–0.93	0.003
Year of diagnosis[1]	0.94	0.92–0.95	<0.001	0.97	0.96–0.98	<0.001
Marital status						
Married	Reference			Reference		
Unmarried	1.22	1.13–1.33	<0.001	1.48	1.37–1.60	<0.001
Unknown	1.33	1.14–1.55	<0.001	1.27	1.11–1.47	0.001
Income						
High	Reference			Reference		
Medium	1.00	0.91–1.09	0.922	1.02	0.94–1.12	0.592
Low	1.16	1.05–1.29	0.004	1.22	1.11–1.34	<0.001
Education						
High	Reference			Reference		
Medium	0.96	0.86–1.07	0.428	0.97	0.88–1.07	0.542
Low	0.99	0.88–1.11	0.829	0.99	0.89–1.11	0.894
Insurance						
Uninsured	Reference			Reference		
Any Medicaid	1.03	0.58–1.96	0.923	0.94	0.70–2.14	0.831
Insured	0.85	0.51–1.56	0.566	0.59	0.34–1.02	0.060
Unknown	1.27	0.76–2.34	0.399	0.59	0.34–1.03	0.062
Grade at presentation						
Grade I	Reference			Reference		
Grade II	0.90	0.78–1.03	0.127	1.07	0.94–1.22	0.312
Grade III	0.83	0.72–0.96	0.010	1.41	1.23–1.61	<0.001
Grade IV	0.78	0.68–0.89	<0.001	1.35	1.19–1.54	<0.001
Other	0.84	0.75–0.94	0.003	1.21	1.09–1.35	<0.001
Stage at presentation						
Localized	Reference			Reference		
Regional	0.76	0.69–0.84	<0.001	1.02	0.94–1.12	0.589
Distant	0.36	0.31–0.43	<0.001	1.31	1.12–1.53	<0.001
Unknown	0.70	0.61–0.81	<0.001	0.91	0.80–1.04	0.156
Radiotherapy						
No/Unknown	Reference			Reference		
Yes	0.84	0.77–0.91	<0.001	0.80	0.74–0.87	<0.001
Chemotherapy						
No/Unknown	Reference			Reference		
Yes	0.77	0.67–0.88	<0.001	0.97	0.85–1.11	0.659
Surgery						
None	Reference			Reference		
Yes	1.18	1.04–1.33	0.009	0.56	0.50–0.63	<0.001
Unknown	0.53	0.41–0.67	<0.001	0.86	0.63–1.00	0.050

HD, heart diseases; NOS, not of specific.
[1]Increase 1 year.

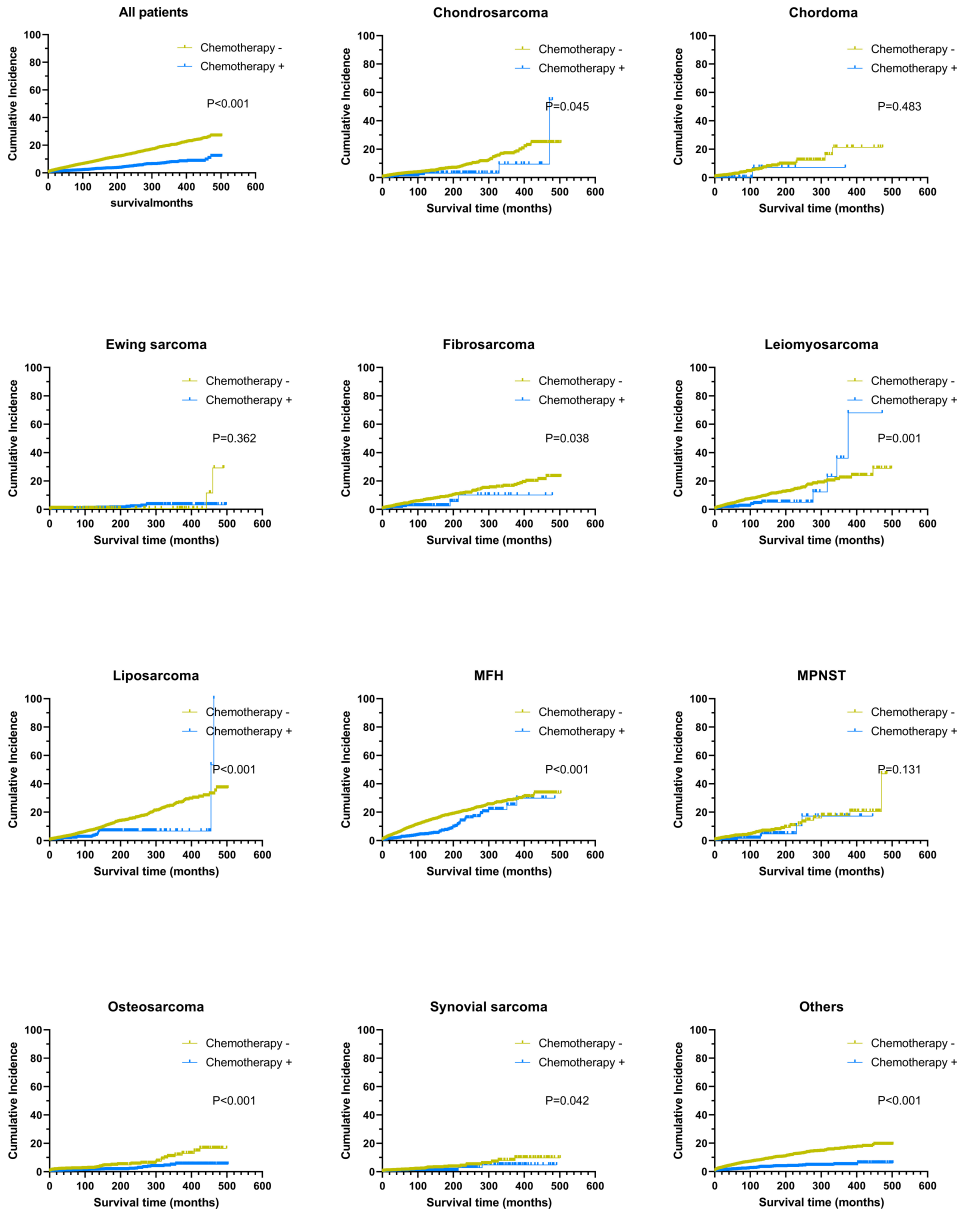

FIGURE 3
Subgroup analysis: the graph showed cumulative incidence curves of death resulting from heart events. MFH, malignant fibro histiocytoma; MPNST, malignant peripheral nerve sheath tumors.

approximately 50 years ago, are used as antineoplastic agents, and are the most successful anticancer therapies ever developed for sarcoma (3). However, a worrisome adverse side effect is ventricular dysfunction and heart failure (25). Due to low sarcoma incidence rates, previous cardio-toxicity studies in sarcoma patients receiving chemotherapy were conducted in small sample or at single centers (13–15). In a recent comparative study of 95 patients with sarcoma, approximately 17% developed cardio-toxicity after receiving doxorubicin (26). Indeed, the death rate due to HD in patients receiving chemotherapy was seriously underreported due to inaccurate statistics about cause of death.

The systematic and standardized data collection procedures are used to ensure that the causes of death recoded in SEER are accurate (27); therefore, we believe our study presents a reliable picture of death rates from HD in patients with sarcoma in the US. Using the SEER database, we showed that the incidence rate of fatal HD in sarcoma patients was 631.7/100,000 person-years. In subgroup analyses, chemotherapy for sarcoma only increased the risk of fatal HD in patients with localized osteosarcoma, but not for other subtypes. These subgroups results may be

TABLE 6 Subgroup analysis of fatal HD among patients with sarcoma by histology and clinical stage.

Histology	Clinical stage	HR[1]	95% CI	*P*-value
Ewing sarcoma				
	All	0.97	0.85–1.11	0.659
	Localized	Inf	0.00 – Inf	0.999
	Regional	0.04	0.01–0.29	0.001
	Distant	0.00	0.00 – Inf	1.000
Osteosarcoma				
	All	0.97	0.85–1.11	0.659
	Localized	3.18	1.24–8.13	0.016
	Regional	0.63	0.28–1.40	0.259
	Distant	0.25	0.06–1.03	0.055
Synovial sarcoma				
	All	0.97	0.85–1.11	0.659
	Localized	0.40	0.06–2.86	0.363
	Regional	3.06	0.85–11.11	0.088
	Distant	Inf	0.00–Inf	1.000
MPNST				
	All	0.97	0.85–1.11	0.659
	Localized	4.59	0.85–24.67	0.076
	Regional	0.71	0.05–10.57	0.804
	Distant	0.87	0.18–4.24	0.867
Chondrosarcoma				
	All	0.97	0.85–1.11	0.659
	Localized	0.44	0.10–1.87	0.268
	Regional	1.05	0.30–3.60	0.949
	Distant	0.52	0.10–2.81	0.449
MFH				
	All	0.97	0.85–1.11	0.659
	Localized	1.17	0.83–1.65	0.375
	Regional	0.89	0.51–1.53	0.667
	Distant	0.28	0.07–1.16	0.079
Fibrosarcoma				
	All	0.97	0.85–1.11	0.659
	Localized	0.94	0.36–2.47	0.902
	Regional	1.76	0.38–8.23	0.474
	Distant	1.06	0.06–18.89	0.968
Liposarcoma				
	All	0.97	0.85–1.11	0.659
	Localized	0.84	0.48–1.45	0.523
	Regional	1.33	0.54–3.23	0.534
	Distant	0.49	0.06–3.94	0.504
Leiomyosarcoma				
	All	0.97	0.85–1.11	0.659
	Localized	0.83	0.39–1.77	0.635
	Regional	1.31	0.57–2.97	0.524
	Distant	0.44	0.14–1.39	0.162
Chordoma				
	All	0.97	0.85–1.11	0.659
	Localized	1.66	0.16–17.36	0.673
	Regional	0.00	0.00 – Inf	0.998
	Distant	0.00	0.00 – Inf	1.000
Others				
	All	0.97	0.85–1.11	0.659
	Localized	0.97	0.70–1.34	0.848
	Regional	0.76	0.46–1.24	0.273
	Distant	0.47	0.29–0.77	0.003

HD, heart diseases; HR, hazard ratio; MFH, malignant fibrohistiocytoma; MPNST, Malignant Peripheral Nerve Sheath Tumor.

[1]We performed a survival analysis using a Cox proportional hazards model to calculate hazard ratios (HRs), adjusting for demographics: age, sex, race, year of diagnosis, socioeconomic status, insurance status and tumor characteristics: clinical stage, grade at presentation, radiotherapy and surgery status.

attributed to the low incidence rates of Ewing sarcoma in the SEER database.

Apart from chemotherapy, surgery is the main treatment method for sarcoma as it aims to remove all sarcoma traces from patients (22). In 2005, an estimated 18,000 patients underwent amputation due to bone and soft tissue sarcoma, which was the third leading cause of amputation in the US (28). We showed that 79% of patients underwent sarcoma surgery in the study cohort. These patients typically lost a certain degree of physical activity, which is a known risk factor for cardiovascular events (24, 29). Moreover, earlier reports indicated that sarcoma patients presented a certain degree of anxiety and depression which were related to functional and appearance changes (30, 31). Physical inactivity and demoralization are risk factors for HD (32). In our study, the higher relative risk of fatal HD in sarcoma patients to general population in the first year was possibly attributed to chemotherapy, and the relative risk of fatal HD was highest during follow-up after 10 years, which was possibly attributed to combined physical inactivity and demoralization effects. Therefore, clinicians should orchestrate specific rehabilitation care strategies to help long-term sarcoma survivors improve their exercise regimens. Also, evidence now suggests that exercise may inhibit both early and late doxorubicin-induced cardiotoxicity (33). Likewise, psychological assessments such as the Hamilton Depression and Hamilton Anxiety Scales are necessary for long-term sarcoma survivors (20), and can help orthopedic surgeons identify psychological disorders in patients and allow psychologists commence interventions as early as possible.

Cardiovascular events have typically been regarded as age-related disorders, but in our study, younger patients with sarcoma had a higher relative risk of fatal HD when compared with older patients. In the general population aged < 19 years old, HD mortality was very low, at only 2.6/100,000 person-years. But in similar-aged sarcoma patients, this mortality was 32.7/100,000 person-years due to sarcoma and chemotherapy.

Given the high risk of fatal HD among younger patients with sarcoma, clinicians should closely monitor cardiac functions in these younger patients.

Our study had several limitations, most of which were related to the SEER database. Firstly, the database program was limited in terms of detailed information on chemoradiotherapy such as doses and cycles. In a phase III ANNOUNCE trial evaluating cardiotoxicity in patients with soft-tissue sarcoma given doxorubicin, cardiac dysfunction occurred in 2% of patients receiving doses of <450 mg/m^2, 3% at 450 – <600 mg/m^2, and 1.1% at ≥ 600 mg/m^2 (14). Considering the dose-dependent cardiotoxicity of doxorubicin (34, 35), direct associations must be assessed between chemotherapy dose or cycles and the risk of HD death in sarcoma patients. Future analyses can be augmented by the SEER-Medicare data set, which may elucidate direct relationships with chemotherapy doses and cycles. Secondly, in subgroup analyses, we observed no chemotherapy effects on the risk of fatal HD in other subgroups, such as patients with Ewing sarcoma, inconsistent with previous studies (14, 33, 36). A possible explanation could be the relatively low number of deaths due to cardiovascular events which in turn may have reduced the statistical power of our subgroup analyses, therefore, this requires further investigation. Despite these limitations, ours is the first large sample and population-based study with the longest follow-up times, to explore the risk of HD death in sarcoma patients. Our results are reliable and robust and may be used to guide clinical practice.

Conclusion

This is the first large population-based study on the risk of fatal HD in sarcoma patients, which up to now were rarely reported. Our results suggest that the risk of fatal HD in sarcoma patients is higher than that of the general population, and increases with longer follow-up times. The relative risk of HD to the general population varied in patients with different histological sarcoma subtypes and clinical stage. Subgroup analyses indicated that chemotherapy increased the risk of fatal HD in patients with localized osteosarcoma. To mitigate the risk of fatal HD in sarcoma patients, enhanced multidisciplinary cooperation is warranted, including cardiologists and orthopedic surgeons.

Data availability statement

The original contributions presented in this study are included in the article/supplementary material, further inquiries can be directed to the corresponding authors.

Ethics statement

Ethical review and approval was not required for this study in accordance with the local legislation and institutional requirements. Written informed consent from the participants was not required for this study in accordance with the local legislation and institutional requirements.

Author contributions

BC and JT: conception and design of study. BC and XZ: acquisition of data. BC, XZ, XL, JL, and JT: analysis and/or interpretation of data. BC, XL, JL, and JT: drafting the manuscript. All authors contributed to the article and approved the submitted version.

Funding

This work was supported by the National Natural Science Foundation of China (81871577 by JT) and the Natural Science Foundation of Hunan Province China (2022JJ30001 by JL).

Conflict of interest

The authors declare that the research was conducted in the absence of any commercial or financial relationships that could be construed as a potential conflict of interest.

Publisher's note

All claims expressed in this article are solely those of the authors and do not necessarily represent those of their affiliated organizations, or those of the publisher, the editors and the reviewers. Any product that may be evaluated in this article, or claim that may be made by its manufacturer, is not guaranteed or endorsed by the publisher.

References

1. World Health Organization [WHO]. *The Top 10 Causes of Death*. (2020). Available online at: https://www.who.int/news-room/fact-sheets/detail/the-top-10-causes-of-death (accessed December 9, 2020).

2. Raposeiras Roubín S, Cordero A. The two-way relationship between cancer and atherosclerosis. *Revista Española de Cardiol.* (2019) 72:487–94.

3. Mazevet M, Moulin M, Llach-Martinez A, Chargari C, Deutsch É, Gomez A-M, et al. Complications of chemotherapy, a basic science update. *Presse Med.* (2013) 42(9 Pt 2.):e352–61.

4. Navi BB, Howard G, Howard VJ, Zhao H, Judd SE, Elkind MSV, et al. New diagnosis of cancer and the risk of subsequent cerebrovascular events. *Neurology.* (2018) 90:e2025–33.

5. Misono S, Weiss NS, Fann JR, Redman M, Yueh B. Incidence of suicide in persons with cancer. *J Clin Oncol.* (2008) 26:4731–8.

6. Sturgeon KM, Deng L, Bluethmann SM, Zhou S, Trifiletti DM, Jiang C, et al. A population-based study of cardiovascular disease mortality risk in US cancer patients. *Eur Heart J.* (2019) 40:3889–97.

7. Zaorsky NG, Zhang Y, Tchelebi LT, Mackley HB, Chinchilli VM, Zacharia BE. Stroke among cancer patients. *Nat Commun.* (2019) 10:5172.

8. Smith GL, Smith BD, Buchholz TA, Giordano SH, Garden AS, Woodward WA, et al. Cerebrovascular disease risk in older head and neck cancer patients after radiotherapy. *J Clin Oncol.* (2008) 26:5119–25.

9. Henson KE, Reulen RC, Winter DL, Bright CJ, Fidler MM, Frobisher C, et al. Cardiac mortality among 200000 five-year survivors of cancer diagnosed at 15 to 39 years of age: the teenage and young adult cancer survivor study. *Circulation.* (2016) 134:1519–31. doi: 10.1161/CIRCULATIONAHA.116.022514

10. Smith GM, Johnson GD, Grimer RJ, Wilson S. Trends in presentation of bone and soft tissue sarcomas over 25 years: little evidence of earlier diagnosis. *Ann R Coll Surg Engl.* (2011) 93:542–7. doi: 10.1308/147870811X13137608455055

11. Yu K, Chen Y, Song K, Xiong F, Tian Y, Guan H, et al. Impact of limb salvage on prognosis of patients diagnosed with extremity bone and soft tissue sarcomas. *Front Oncol.* (2022) 12:873323. doi: 10.3389/fonc.2022.873323

12. Argenziano M, Tortora C, Pota E, Di Paola A, Di Martino M, Di Leva C, et al. Osteosarcoma in children: not only chemotherapy. *Pharmaceuticals.* (2021) 14:923.

13. Van Tine BA, Agulnik M, Olson RD, Walsh GM, Klausner A, Frank NE, et al. A phase II clinical study of 13-deoxy, 5-iminodoxorubicin (GPX-150) with metastatic and unresectable soft tissue sarcoma. *Cancer Med.* (2019) 8:2994–3003. doi: 10.1002/cam4.2136

14. Jones RL, Wagner AJ, Kawai A, Tamura K, Shahir A, Van Tine BA, et al. Prospective evaluation of doxorubicin cardiotoxicity in patients with advanced soft-tissue sarcoma treated in the announce phase III randomized trial. *Clin Cancer Res.* (2021) 27:3861–6. doi: 10.1158/1078-0432.CCR-20-4592

15. Van Tine BA, Hirbe AC, Oppelt P, Frith AE, Rathore R, Mitchell JD, et al. Interim analysis of the phase II study: noninferiority study of doxorubicin with upfront dexrazoxane plus olaratumab for advanced or metastatic soft-tissue sarcoma. *Clin Cancer Res.* (2021) 27:3854–60.

16. Vos M, Sleijfer S, Litiere S, Touati N, Duffand F, van der Graaf WT, et al. Association of pazopanib-induced toxicities with outcome of patients with advanced soft tissue sarcoma; a retrospective analysis based on the European Organisation for Research and Treatment of Cancer (EORTC) 62043 and 62072 clinical trials. *Acta Oncol.* (2019) 58:872–9.

17. NIH National Cancer Institute. *Overview of the SEER Program*. (2018). Available online at: http://seer.cancer.gov/about/overview.html (accessed July 8, 2016).

18. Fung C, Fossa SD, Milano MT, Sahasrabudhe DM, Peterson DR, Travis LB. Cardiovascular disease mortality after chemotherapy or surgery for testicular nonseminoma: a population-based study. *J Clin Oncol.* (2015) 33:3105–15.

19. Koepsell TD, Weiss NS. *Epidemiologic Methods: Studying the Occurrence of Illness*. New York, NY: Oxford University Press (2003).

20. Yu K, Wu B, Chen Y, Kang H, Song K, Dong Y, et al. Suicide and accidental deaths among patients with primary malignant bone tumors. *J Bone Oncol.* (2021) 27:100353. doi: 10.1016/j.jbo.2021.100353

21. Chen Y, Yu K, Xiong J, Zhang J, Zhou S, Dai J, et al. Suicide and accidental death among women with primary ovarian cancer: a population-based study. *Front Med.* (2022) 9:833965. doi: 10.3389/fmed.2022.833965

22. Nagarajan R, Neglia JP, Clohisy DR, Robison LL. Limb salvage and amputation in survivors of pediatric lower-extremity bone tumors: what are the long-term implications? *J Clin Oncol.* (2002) 20:4493–501. doi: 10.1200/JCO.2002.09.006

23. Yu K, Chen Y, Tian Y, Kang H, Song K, Dong Y, et al. Characteristics, incidence, and risk factors for death from fatal pneumonia among patients with primary malignant bone tumors: a SEER-based observational study. *Transl. Cancer Res.* (2021) 10:3659–70. doi: 10.21037/tcr-21-306

24. Seixas AA, Vallon J, Barnes-Grant A, Butler M, Langford AT, Grandner MA, et al. Mediating effects of body mass index, physical activity, and emotional distress on the relationship between short sleep and cardiovascular disease. *Medicine.* (2018) 97:e11939. doi: 10.1097/MD.0000000000011939

25. Oikonomou EK, Kokkinidis DG, Kampaktsis PN, Amir EA, Marwick TH, Gupta D, et al. Assessment of prognostic value of left ventricular global longitudinal strain for early prediction of chemotherapy-induced cardiotoxicity: a systematic review and meta-analysis. *JAMA Cardiol.* (2019) 4:1007–18. doi: 10.1001/jamacardio.2019.2952

26. Lee S-H, Cho I, You S-C, Cha M-J, Chang J-S, Kim WD, et al. Cancer therapy-related cardiac dysfunction in patients treated with a combination of an immune checkpoint inhibitor and doxorubicin. *Cancers.* (2022) 14:2320. doi: 10.3390/cancers14092320

27. Park HS, Lloyd S, Decker RH, Wilson LD, Yu JB. Overview of the surveillance, epidemiology, and end results database: evolution, data variables, and quality assurance. *Curr Probl Cancer.* (2012) 36:183–90. doi: 10.1016/j.currproblcancer.2012.03.007

28. Ziegler-Graham K, MacKenzie EJ, Ephraim PL, Travison TG, Brookmeyer R. Estimating the prevalence of limb loss in the United States: 2005 to 2050. *Arch Phys Med Rehabil.* (2008) 89:422–9.

29. Mioc M-L, Prejbeanu R, Vermesan D, Haragus H, Niculescu M, Pop DL, et al. Deep vein thrombosis following the treatment of lower limb pathologic bone fractures - a comparative study. *BMC Musculoskelet Disord.* (2018) 19:213. doi: 10.1186/s12891-018-2141-4

30. Paredes T, Canavarro MC, Simões MR. Anxiety and depression in sarcoma patients: emotional adjustment and its determinants in the different phases of disease. *Eur J Oncol Nurs.* (2011) 15:73–9. doi: 10.1016/j.ejon.2010.06.004

31. Wiener L, Battles H, Bernstein D, Long L, Derdak J, Mackall CL, et al. Persistent psychological distress in long-term survivors of pediatric sarcoma: the experience at a single institution. *Psychooncology.* (2006) 15:898–910. doi: 10.1002/pon.1024

32. Raiè M. Depression and heart diseases: leading health problems. *Psychiatr Danub.* (2017) 29(Suppl 4.):770–7.

33. Wang F, Chandra J, Kleinerman ES. Exercise intervention decreases acute and late doxorubicin-induced cardiotoxicity. *Cancer Med.* (2021) 10:7572–84. doi: 10.1002/cam4.4283

34. Zhang H, Weng J, Sun S, Zhou J, Yang Q, Huang X, et al. Ononin alleviates endoplasmic reticulum stress in doxorubicin-induced cardiotoxicity by activating SIRT3. *Toxicol Appl Pharmacol.* (2022) 452:116179. doi: 10.1016/j.taap.2022.116179

35. Kim SW, Ahn B-Y, Tran TTV, Pyun J-H, Kang J-S, Leem Y-E. PRMT1 suppresses doxorubicin-induced cardiotoxicity by inhibiting endoplasmic reticulum stress. *Cell Signal.* (2022) 98:110412. doi: 10.1016/j.cellsig.2022.110412

36. Vitfell-Rasmussen J, Krarup-Hansen A, Vaage-Nilsen M, Kümler T, Zerahn B. Real-life incidence of cardiotoxicity and associated risk factors in sarcoma patients receiving doxorubicin. *Acta Oncol.* (2022) 61:801–8. doi: 10.1080/0284186X.2022.2082884

frontiers | Frontiers in Cardiovascular Medicine

TYPE Original Research
PUBLISHED 01 December 2022
DOI 10.3389/fcvm.2022.1062858

OPEN ACCESS

EDITED BY
Antonella Lombardo,
Agostino Gemelli University Polyclinic (IRCCS), Italy

REVIEWED BY
Chiara Lestuzzi,
Santa Maria degli Angeli Hospital, Italy
Federico Quaini,
University of Parma, Italy

*CORRESPONDENCE
María Torrente
maria.torrente@salud.madrid.org

†These authors have contributed equally to this work

SPECIALTY SECTION
This article was submitted to Cardio-Oncology, a section of the journal Frontiers in Cardiovascular Medicine

RECEIVED 06 October 2022
ACCEPTED 08 November 2022
PUBLISHED 01 December 2022

CITATION
Torrente M, Blanco M, Franco F, Garitaonaindia Y, Calvo V, Collazo-Lorduy A, Gutiérrez L, Sánchez JC, González-del-Alba A, Hernández R, Méndez M, Cantos B, Núñez B, Sousa PAC and Provencio M (2022) Assessing the risk of cardiovascular events in patients receiving immune checkpoint inhibitors.
Front. Cardiovasc. Med. 9:1062858.
doi: 10.3389/fcvm.2022.1062858

Assessing the risk of cardiovascular events in patients receiving immune checkpoint inhibitors

María Torrente[1,2*†], Mariola Blanco[1†], Fabio Franco[1], Yago Garitaonaindia[1], Virginia Calvo[1], Ana Collazo-Lorduy[1], Lourdes Gutiérrez[1], Juan Cristóbal Sánchez[1], Aranzazu González-del-Alba[1], Roberto Hernández[1], Miriam Méndez[1], Blanca Cantos[1], Beatriz Núñez[1], Pedro A. C. Sousa[3] and Mariano Provencio[1]

[1]Department of Medical Oncology, Puerta de Hierro Majadahonda University Hospital, Madrid, Spain, [2]Faculty of Health Sciences, Francisco de Vitoria University, Madrid, Spain, [3]Department of Electrical Engineering, NOVA School of Science and Technology, Universidade Nova de Lisboa, Lisbon, Portugal

Background: Immune checkpoint inhibitors (ICIs) have revolutionized cancer treatment. However, despite their excellent therapeutic effect, these medications typically result in a broad spectrum of toxicity reactions. Immune-related cardiotoxicity is uncommon but can be potentially fatal, and its true incidence is underestimated in clinical trials. The aim of this study is to assess the incidence and identify risk factors for developing a cardiac event in patients treated with ICIs.

Methods: We conducted a single-institution retrospective study, including patients treated with ICIs in our center. The main outcomes were cardiac events (CE) and cardiovascular death.

Results: A total of 378 patients were analyzed. The incidence of CE was 16.7%, during a median follow-up of 50.5 months. The multivariable analysis showed that age, a history of arrhythmia or ischemic heart disease, and prior immune-related adverse events were significantly associated with CE.

Conclusion: CE during ICI treatment are more common than currently appreciated. A complete initial cardiovascular evaluation is recommended, especially in high-risk patients, being necessary a multidisciplinary approach of a specialized cardio-oncology team.

KEYWORDS

cardiovascular event, immune checkpoint inhibitors, myocarditis, cardiotoxicity, risk factors

Introduction

The hallmark of many cancers is their ability to avoid the host immune response, allowing cell proliferation and metastasis (1). Cytotoxic T lymphocyte-associated antigen-4 (CTLA-4) and programmed cell death protein (PD-1) are co-inhibitory T-cell surface molecules, which downregulate the immune response by attenuating T-cell activation, proliferation, and cytokine production (2, 3). The immune system employs these inhibitory pathways to maintain T-cell tolerance and prevent autoimmunity (4). Numerous cancer cells overexpress the programmed cell death ligand 1 (PD-L1) on their surface, which contributes to their immune evasion by enhancing their immune escape ability, resulting in a poor prognosis for the patient (5). Based on these inhibitory molecules, several monoclonal antibodies targeting these immune checkpoint pathways have been developed in the last decade.

Immune checkpoint inhibitors (ICIs) have revolutionized the therapeutic landscape of many hematological and solid tumors. Since the introduction of the first ICI, ipilimumab (human IgG1 k anti-CTLA-4 monoclonal antibody) in 2011, six additional ICIs have been approved for cancer therapy by regulatory agencies (6), becoming a mainstay in the treatment of several neoplasms, including non-small cell lung cancer (NSCLC) and malignant melanoma. ICIs have shown high and durable response rates, either alone or in combination with other therapies, improving the survival of patients with advanced-stage malignancies, historically endowed with a poor prognosis (7, 8).

However, these agents also produce a wide spectrum of immune-related adverse events (irAEs), mainly due to aberrant autoreactive T-cell activation (9). These immune-mediated toxicities may affect any organ or tissue, with the most frequently reported being the skin, gastrointestinal system, and endocrine system (10). The incidence of irAEs varies between CTLA-4 inhibitors and PD-1 inhibitors, being high-grade adverse events more common with the combination ICI therapy (11).

Immune-related cardiotoxicity is a potentially fatal irAE. Since the first specific case of ICI-associated cardiotoxicity was reported in 2014 (12), cardiotoxicity during ICI treatment has been increasingly reported (13–15). The current evidence available arises from pharmacovigilance databases, case reports, and retrospective series (16), but no randomized controlled trials have assessed the potential cardiotoxic role of ICIs. Among the various forms of ICI cardiotoxicities, myocarditis is the most frequently reported due to its high morbidity and mortality. Retrospective evaluation literature has estimated that the incidence of ICI-related myocarditis ranges from 0.09 to 1.14% (17, 18). Nevertheless, the true incidence of other cardiovascular effects of immunotherapy is uncertain. Immune-related cardiotoxicity involves almost all parts of the heart, being the myocardium the most sensitive to ICIs toxicity. The potential mechanism of ICI-mediated cardiac toxicity is not fully understood, but histological analysis has revealed that the infiltration of CD4+/CD8+ T-cells and macrophages in the heart tissue may play a key role in the pathogenesis (19). ICI-related cardiotoxicity can be inflammatory, including conditions such as pericarditis, myocarditis, and perimyocarditis, or non-inflammatory, including left ventricular dysfunction without myocarditis, Takotsubo-like syndrome, coronary vasospasm, arrhythmias, and myocardial infarction (20). Various reports have revealed that immune-related cardiotoxicity may occur early after exposure to an ICI, suggesting a potential predisposition to cardiotoxicity that is possibly associated with pre-existing cardiovascular risk factors (CVRF) (21). Likewise, as reported with other irAEs, a combined ICI therapy with anti-CTLA4 and anti-PD-1/PD-L1, significantly increases the risk of developing an immune-related CE (22), as well as previous administration of other cardiotoxic cancer therapies, such as anthracyclines, trastuzumab, thoracic radiotherapy, or antiangiogenic therapy.

In order to gain a more robust understanding of immune-related cardiotoxicity, we reviewed the incidence of CE developed during ICI treatment in our institution. In addition, we tried to assess the role of CVRF and other cancer therapies in the development of cardiac toxicity.

Materials and methods

Study population

We conducted a single-institution retrospective study at the Puerta de Hierro-Majadahonda University Hospital in Madrid, Spain. Oncologic patients treated in our center with immune checkpoint inhibitors, either in monotherapy or in combination with chemotherapy or other therapies, were included from March 2014 to November 2020.

Clinical history from electronic health records was retrieved, and specific data were collected regarding demographics, previous CVRF, and oncological features such as specific tumor, histology, AJCC/UICC stage, treatments received (including type of chemotherapy and targeted therapies, with an emphasis on those with cardiotoxic effects), treatment-related toxicity, and outcomes (overall survival).

Cardiac events identified during or after immune checkpoint inhibition were electrocardiographic alterations (such as long QT syndrome, any grade bundle branch or atrioventricular blockades or atrial fibrillation), congestive heart failure, pulmonary embolism, acute coronary syndrome, pericarditis, and myocarditis. Treatment interruptions, hospitalizations due to cardiologic issues, and cardiac-related deaths were also identified.

The aim of the study was to determine the incidence of cardiac events in patients exposed to immune checkpoint

inhibitors and to identify clinical factors for predicting the onset of these events.

Statistical analysis

Qualitative variables are expressed as an absolute value and percentage. Quantitative variables are expressed as the median and interquartile range (IQR). To test for clinical data categorical associations with cardiac event development, we performed a Chi-square test in variables such as sex, known CVRF (hypertension, diabetes, valve disease, chronic kidney disease, ischemic heart disease, previous history of arrhythmia, smoking habit, tumor location, previous potentially cardiotoxic drug exposure, previous chest radiotherapy, and tumor objective response). T-student test was used for age. To identify risk factors increasing the probability of CE, Cox models were constructed. Risk factors with a *P*-value lower than 0.05 in the univariable analysis were developed into multivariable models. Odds ratios (ORs) and 95% confidence intervals (CIs) were provided for the multivariable model. In line with recommendations, the cumulative incidence was designed up to the 95 percentile of follow-up duration.

Based on the results obtained in the multivariable analysis, as well as clinically important variables, we developed a predictive score for the risk of developing a cardiac event after immunotherapy exposure. The score calibration was assessed using the Hosmer–Lemeshow goodness-of-fit test as well as the discrimination through the area under the receiver operating characteristic curve.

All statistical analyses were performed using Stata version 23 software.

Ethics

Ethical approval was granted by the Puerta de Hierro-Majadahonda University Hospital Clinical Research Ethics Committee. The study was carried out in accordance with the requirements expressed in the Declaration of Helsinki, as well as with the current legislation in Spain on conducting observational studies (Ministerial Order SAS/3470/2009).

Results

Baseline characteristics of the full cohort

Between March 2014 and November 2020, a total of 378 patients receiving ICIs treatment in our institution were analyzed. Of those, 134 were females (35.5%) and 244 were males (64.6%). The median age was 61 years old (p25–p75: 55–68).

Table 1 lists the main baseline characteristics of our cohort of patients. The most frequent comorbidities were hypertension (40.7%), dyslipidemia (30.4%), and type 2 diabetes (13.2%); 29.9% of patients were current smokers at the time of the analysis, and 51.3% were former smokers. Regarding other more specific CVRF, the most prevalent was peripheral vascular disease (17.2%), followed by history of coronary heart disease (5.0%), heart valve disease (5.0%), chronic renal failure (4.5%), and congestive HF (0.5%); 24 patients (6.4%) had history of arrhythmia being the most frequent atrial fibrillation (83.4%). In addition, 10.9% of the patients were receiving anticoagulants and 11.9% antiplatelet treatment. Only 41 (10.8%) patients had a family history of cardiovascular disease. In the cardiologic evaluation prior to the start of ICI treatment, 20 patients (5.3%) presented with alterations in cardiac contractility, and 25 (6.6%) had left ventricular hypertrophy in the echocardiographic assessment. Only 2 patients had evaluable cardiomegaly in chest X-ray.

Regarding tumor characteristics, most of the patients receiving ICI treatment were lung cancer patients (62.3%), followed by melanoma (12.7%), renal cell carcinoma (5.0%), urothelial carcinoma (4.8%), and head-and-neck tumors (4.2%). The predominant histology was adenocarcinoma (42.9%) followed by squamous cell carcinoma (20.6%) and melanoma (12.7%). Most of the patients were at stage IV of the disease (82.2%). 34.4% of patients received ICI in the first-line setting, in monotherapy, or in combination with other therapies. Regarding the type of ICI treatment administered, most of the patients received anti-PD1 drugs (64.8%), followed by anti-PDL1 drugs (9%) and anti-CTLA4 drugs (1.6% in monotherapy and 9.5% in combination with anti-PD1), with a median of 6 cycles per patient. Details on ICI treatment are listed in **Table 2**. When we evaluated the best response to ICIs by radiologic assessment, 32.3% of patients had a partial response, 13% stable disease, and 9.2% complete response. Nevertheless, most of the patients had progressive disease at first evaluation (43.1%). At the time of the analysis, 335 patients (88.6%) had interrupted the ICI therapy, most of them due to disease progression (51.6%) or death (10.6%), end of treatment after 2 years completion (14.2%) and only 37 (9.8%) due to immune-related toxicity. The most frequent irAE was gastrointestinal (18.9%), followed by skin disorders (16.5%) and pneumonitis (16.5%). 45 patients experienced grade 3 adverse events (11.9%). Of note, only one patient interrupted ICI treatment due to SARS-CoV-2 infection.

As abovementioned, most patients presented advance stage of the disease upon ICIs initiation, and had progressed to several lines of treatment, including potentially cardiotoxic drugs. Specifically, 3.4% of patients had previously received anthracyclines, 23.0% cisplatin, 29.1% antimicrotubule agents, 13% antiangiogenic therapy, and only 0.5% (2 patients) anti-HER2 therapy. Regarding radiotherapy, 95 patients (25.1%) had received thoracic radiotherapy (including lung/mediastinum in 80%), most of them with radical/curative intention (median

10.3389/fcvm.2022.1062858

TABLE 1 Baseline characteristics of patients at the time of initial administration of immune checkpoint inhibitors.

Variable	*N* = 378 patients (%)
Sex	Male: 244 (64.6%) Female: 134 (35.5%)
Age (median)	61.0 (p25–p75: 55–68)
Hypertension	154 (40.7%)
Diabetes	50 (13.2%)
Hypercholesterolemia	115 (30.4%)
Current or prior smoking	307 (81.2%)
Coronary syndrome	19 (5.0%)
Heart failure	2 (0.5%)
Chronic renal failure	17 (4.5%)
Valvular disease	19 (5.0%)
Arrhythmia	24 (6.4%)
Peripheral arterial disease	65 (17.2%)
Type of tumor	Lung cancer: 236 (62.3%) Melanoma: 48 (12.7%) Renal cell carcinoma: 19 (5.0%) Bladder cancer: 18 (4.8%) Head and neck tumors: 16 (4.2%) Hepatocellular carcinoma: 9 (2.4%) Lymphoma: 8 (2.1%) Colorectal cancer: 5 (1.3%) Gastric cancer: 5 (1.3%) Gynecological tumors: 3 (0.8%) Breast cancer: 3 (0.8%) Thymoma: 2 (0.5%) Cholangiocarcinoma: 1 (0.3%) Esophagus tumors: 1 (0.3%)
Tumor stage when ICI was started	I: 4 (1.0%) II: 8 (2.1%) III: 52 (14.0%) IV: 313 (82.8%)
Previous cardiotoxic treatments	Anthracyclines: 13 (3.4%) Cisplatin: 87 (23.0%) Antimicrotubule: 110 (29.1%) Antiangiogenic therapy: 49 (13.0%) HER2 targeted therapy: 2 (0.5%) Thoracic radiotherapy: 95 (25.1%)

ICI, immune checkpoint inhibitors.

TABLE 2 Type of ICI treatment received.

ICI-treatment	
○ ICI-monotherapy	Anti-PD1: 245 (64.8%) Anti-PDL1: 34 (9.0%) Anti-CTLA4: 6 (1.6%)
○ ICI-combinations	Anti-CTLA4 + anti-PD1: 36 (9.5%) ICI + chemotherapy: 49 (13.0%) ICI + VEGF inhibitors: 7 (1.8%) ICI + tyrosine kinase inhibitors: 1 (0.3%)

ICI, immune checkpoint inhibitors; VEGF, vascular endothelial growth factor.

dose of 60 Gy). Only 54 patients received concomitant chemotherapy (55% platinum-based chemotherapy).

Incidence of cardiac events in the full cohort

Focusing on the CE, 63 patients (16.7%) presented a CE during ICI treatment in our study (with some patients presenting more than one CE). The median time to CE onset from the initiation of ICI therapy was 4.3 months (p25: 1.5–p75: 11.1). Table 3 summarizes the incidence of each CE. Considering non-cardiac death as a competing event, the cumulative incidence rates for a CE were 10.2% at 6 months, 13.8% at 12 months, 16% at 18 months, 17.7% at 24 months, 18.8% at 6 months, and 19.8% at 48 months (Figure 1). The most prevalent event was an electrocardiographic alteration (69.8% of all CE), being atrial fibrillation the most frequently reported. Among the 44 patients who developed some type of arrhythmia during immunotherapy, 42 were newly onset and only 4 had history of atrial fibrillation. Congestive HF accounted for 19.0% of all CE; of important note, we found that all of these patients had previous CVRF, which could have predisposed to the subsequent HF event during ICIs. However, none of these patients had a history of HF or echocardiographic abnormalities prior to ICI therapy. Pulmonary embolism represented 10.8% of all CE, having all of them predisposing factors such as recent surgery, immobilization, or disease progression. None required fibrinolysis or ICU admission, and 3 patients (4.6% of all CE) developed an ACS, of whom, two had a previous history of coronary heart disease and were under cardiologic follow-up.

Regarding the "inflammatory" cardiotoxicity, two patients were diagnosed with pericarditis and two with myocarditis. These patients required hospital admission and close cardiologic monitoring, as well as high-dose corticosteroids, and, in the case of myocarditis, immunosuppressive treatment. Three of these four patients diagnosed with peri- or myocarditis presented other concomitant irAE, such as myasthenia gravis, polyarthritis, or Guillain–Barre syndrome. As previously stated, 37 patients (9.8%) had to interrupt treatment because of an irAE, but only 2 patients (0.5%) due to specific cardiac toxicity. During a median follow-up of 50.5 months (95% CI 45.5–57.7), 202 patients (53.4%) died, of whom 3 (0.8%) the cause of death was due to a CE: 2 fatal events associated to myocarditis and 1 to congestive HF.

The cumulative incidence function (CIF) represents the incidence rates of cardiac events in our cohort of patients, considering non-cardiac deaths as a competing event. Probably, the incidence of CE might be underestimated due to the high mortality rates observed in cancer patients.

Risk factors for cardiac events

Univariable and multivariable Cox regression analyses are presented in Table 4. Older patients and those with history of heart valve disease, ischemic heart disease, or arrhythmia were prone to develop a CE in the univariable analysis. However, only age (OR 1.03; 95% CI 0.99–1.06; $p = 0.05$),

10.3389/fcvm.2022.1062858

TABLE 3 Global incidence of cardiovascular events during ICI treatment.

Cardiac event	Incidence
Electrocardiographic alterations	12.2%
Pulmonary embolism	1.9%
Mace	
• Heart failure	3.4%
• Acute coronary syndrome	0.8%
Myocarditis	0.5%
Pericardial disease	0.5%
Mortality	
• Global mortality	53.4%
• Cardiovascular mortality	0.8%

MACE, major adverse cardiovascular events.

a history of ischemic heart disease (OR 3.25; 95% CI 1.16–9.14; p = 0.025), or arrhythmia (OR 4.11; 95% CI 1.66–10.22; p = 0.002), remained significantly associated with CE in the multivariable analysis. Likewise, those patients who had developed another irAE (31.7%) were also at increased risk (OR 2.08; 95% CI 1.11–3.94; p = 0.023). By contrast, other known CVRF such as hypertension, diabetes, dyslipidemia, chronic kidney failure, or smoking habit, did not increase the risk for cardiac toxicity in our study, nor did the type of tumor, stage, or response to treatment. Regarding ICI therapy, there were no differences between combination regimens (with other ICI, antiangiogenic therapy, or chemotherapy) and monotherapy (p = 0.87). Similarly, patients who had received other cardiotoxic therapies (anthracyclines, cisplatin, antimicrotubule agents, antiangiogenic therapy, anti-HER2 therapy, or thoracic radiotherapy), were not at increased risk for cardiac toxicity.

Discussion

This study provides real-world observational data on the risk of CE associated with ICI treatment, which can extend beyond myocarditis. Their detection is currently challenging due to the lack of consistency of its clinical manifestation, and, consequently, their incidence is probably underestimated in clinical trials. Thus, prospective or retrospective studies with larger cohorts are essential for capturing the true incidence of CE in daily practice. A pharmacovigilance study using VigiBase, the WHO's global database of individual case safety reports, reported significantly higher, but still very low incidences of myocarditis and pericarditis, with an incidence of 0.39 and 0.30%, respectively (23). A Danish nationwide study evaluated the risk of CE in ICI-treated patients, reporting an absolute risk at 1 year of 9.7% in 743 patients with lung cancer and 6.6% in 145 patients with melanoma. They concluded that the hazard rates of CE were higher in patients with vs. without ICI treatment (24).

The most prevalent CE reported in our study were arrhythmias, of which, atrial fibrillation was the most prevalent one. ICI-mediated arrhythmias and conduction diseases, in the absence of generalized myocarditis, are emerging as a more frequent and potentially serious cause of ICI-mediated sudden death (21). The mechanisms underlying the arrhythmias are unknown, but might include inflammation of the His–Purkinje conduction system, increased systemic inflammatory state, myocarditis with inflammation and fibrosis, and other causes of arrhythmias in cancer patients (QT-interval prolonging drugs, electrolyte imbalances, myocardial metastases) (20). Other relevant CE reported in our study were HF and ACS, which can be considered MACE. Although other well-known CVRF, such as hypertension, diabetes, or dyslipidemia, are major risk factors for developing a MACE, and immunotherapy seems to play an important role in the pathogenesis of these events. Preclinical models have shown that cardiomyocyte PD-L1 expression is upregulated in cardiac stress, including ischemia reperfusion and left ventricular hypertrophy, and might have cardioprotective actions by suppressing excessive myocardial inflammation (25). Likewise, it is known that atherosclerosis is characterized by low-grade chronic inflammation, and that acute or chronic inflammatory conditions can accelerate plaque rupture (26). Thus, ICIs could induce acceleration or decompensation of pre-existing HF and ACS in susceptible individuals. In line with this, in a matched cohort study of 5,684 patients, a threefold higher risk of atherosclerotic CE (myocardial infarction, coronary revascularization, and ischemic stroke) was observed after starting ICI therapy (27). Additionally, HF is not a marginal issue in this study and requires a better understanding of the systemic perturbation induced by immune checkpoints and its impact on cardiac function. Patients with dilated cardiomyopathy can have heterogeneous etiology such as genetic, viral, immunological, and environmental factors. Despite several animal studies that indicate that PD-1 may be an important factor contributing to the prevention of autoimmune diseases (28, 29), the involvement of an immune mechanism in patients with dilated cardiomyopathy is still controversial.

Regarding pulmonary embolisms, the evidence is scarce. Some reports suggest that these events may be associated with ICI therapy (30); however, this should be viewed as speculative and requires further investigation. In our cohort, the incidence of myocarditis and pericardial diseases was 0.5. Our rate is similar to that previously reported in other studies, although there has been a substantial increase in reporting incidence over time (31), probably due to an increased use of ICIs, along with heightened recognition of this new clinical entity. With a fatality rate of 27–46%, ICI- related myocarditis is the most lethal form of irAE (32), requiring high-dose corticosteroids and, in most cases, immunosuppressive treatment. The pathophysiology

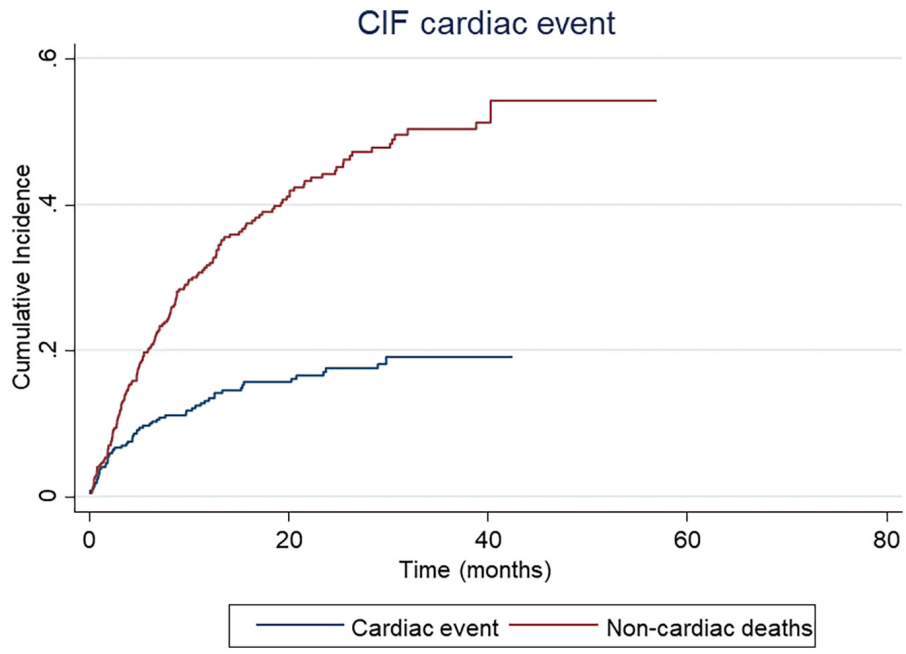

FIGURE 1
Cumulative Incidence Function (CIF) of cardiac events.

of ICI-induced myocarditis is incompletely understood. Post-mortem evaluations have observed inflammatory T-cell (CD4+ and CD8+) and macrophage infiltrate, as well as loss of cardiomyocytes, which, as mentioned before, might also employ the PD-1/PD-L1 pathway to prevent T-cell hyperactivation in the heart in physiological conditions (17). These findings are consistent with the mechanism of ICI action and can be considered an on-target toxicity.

The presence of pre-existent CVRF was common in our study population (46.6%), similar to that reported in the literature (33). Little is known about predisposing risk factors for ICI-related cardiotoxicity. Mahmood et al. reported that diabetes mellitus may predispose to immune-related myocarditis, but no such association has yet been found for other CVRF (18). In a recent retrospective match-cohort study of 672 patients treated with ICIs, only age, history of HF, and heart valve disease were independently associated with MACE (34). In our study, the multivariable analysis showed that older patients, those with history of ischemic heart disease or arrhythmias, and those who developed an irAE are at increased risk of developing a CE during ICI treatment. Other non-cardiac irAEs are frequent, occurring in approximately half of the patients with ICI-mediated myocarditis (18). Myositis is one of the most prevalent (23–25%) (21, 31), and this association might reflect a shared antigen profile and immune phenotype between cardiac and skeletal muscle.

A combination of ICI therapy seems to be a clear risk factor for developing a CE according to the literature. Johnson et al. reported a higher incidence (0.27 vs. 0.06%) and severity (60 vs. 10%) of myocarditis in patients receiving a combination of nivolumab and ipilimumab compared to nivolumab alone (17). Similarly, combined immunotherapy and other cardiotoxic cancer therapy (such as anti-VEGF-tyrosine kinase inhibitors, platinum-based chemotherapy, or radiotherapy) seem to increase the vulnerability for developing a CE (35). However, our study was unable to demonstrate those associations; possibly, a larger study sample might have exposed a statistical difference. On the other hand, many patients with metastatic disease have received multiple treatments before initiating ICIs treatment, some of which might have been cardiotoxic. By inducing myocardium damage, these treatments can lead to the exposure of cardiac antigens developing immune responses that can be amplified upon the initiation of ICIs (36). In our cohort, previous treatment with cardiotoxic therapy was common (58.9%), but no association was observed with the development of CE in the multivariable analysis.

Our real-world data support a baseline and protocoled cardio-oncology follow-up of high-risk patients, such as elderly patients and those with pre-existing cardiovascular comorbidities, especially history of ischemic heart disease and arrhythmias. In addition, patients who develop another irAE should be included in this high-risk group. Based on these results, we have designed a predictive risk-score, which could potentially assess the probability of developing a CE based on the presence or absence of these specific risk factors

10.3389/fcvm.2022.1062858

TABLE 4 Univariable and multivariable Cox regression analysis.

	No cardiac event (n = 313)	Cardiac event (n = 65)	Univariable analysis, P-value	Multivariable analysis OR (95% CI), P-value
Sex				
• Male	204 (65.2%)	40 (61.5%)	0.557	
• Female	109 (34.8%)	25 (38.5%)		
Clinical factors:				
• Age	59.68 (58.4–61.0)	64.82 (62.5–67.1)	0.001*	**OR 1.03, 95% CI 0.99–1.06 p = 0.05***
• Hypertension	125 (39.9%)	29 (44.6%)	0.485	
• Dyslipidemia	89 (28.4%)	26 (40.0%)	0.065	
• Diabetes mellitus	40 (12.8%)	10 (15.4%)	0.074	
• Valve heart disease	11 (3.5%)	8 (12.3%)	0.003*	OR 1.51, 95% CI 0.48–4.76 p = 0.480
• Chronic kidney disease	13 (4.2%)	4 (6.2%)	0.479	
• Ischemic heart disease	12 (3.8%)	7 (10.8%)	0.020*	**OR 3.25, 95% CI 1.16–9.14 p = 0.025***
• Arrhythmia	13 (4.2%)	11 (16.9%)	0.000*	**OR 4.11, 95% CI 1.66–10.22 p = 0.002***
Type of tumor			0.060	
Stage			0.394	
Previous therapies				
• Anthracycline	10 (3.2%)	3 (4.6%)	0.567	
• Cisplatin	74 (23.6%)	13 (20.0%)	0.526	
• Antimicrotubule	92 (29.4%)	18 (27.7%)	0.784	
• Antiangiogenic	43 (13.7%)	6 (9.2%)	0.325	
• AntiHer2	1 (0.3%)	1 (1.5%)	0.218	
• Thoracic radiotherapy	74 (24.0%)	20 (30.8%)	0.250	
Best response			0.345	
Other irAE	58 (18.5%)	20 (30.8%)	0.027*	**OR 1.08, 95% CI 1.11–3.94 p = 0.023***

ORs and 95% CIs were derived from adjusted Cox proportional hazards model. irAEs, immune-related adverse events; OR, odds ratio; CI, confidence interval. *Statistically significant ($p < 0.05$). Bold values represent the statistically significant results ($p < 0.05$).

(Figure 2). This predictive risk score is based on four different variables associated with the development of a CE in our study. Depending on the presence or absence of each variable, the patient gets a score which might predict the probability of developing a cardiac event.

No evidence-based algorithm yet exists for the management of these patients, mainly due to the absence of prospective trials. Two risk scores in the setting of breast cancer, specifically in early-stage HER2-positive breast cancer patients treated with trastuzumab have been reported. In 2012, Romond et al. used 7-year follow-up data from the National Surgical Adjuvant Breast and Bowel Project B-31 adjuvant trastuzumab study to derive a prediction tool for cardiotoxicity (37). A second prediction tool was derived by Ezaz et al., who used data from the U.S. Surveillance, Epidemiology, and End Results database in 1,664 women with previous exposure to trastuzumab (38). Moreover, the CHEMO—RADIAT study validated a predictive model for risk of major cardiovascular events after the diagnosis of breast cancer based on both conventional cardiovascular risk factors and breast cancer treatment—related cardiovascular risk factors, showing a good performance but only valid for breast cancer and again, based only on CVRF. The main limitation of these cardiotoxicity scores is that they focus on CVRF but do not incorporate damage cardiac biomarkers such as BNP or troponins, nor novel echocardiography parameters such as global longitudinal strain (GLS), used in clinical practice for early detection of changes in myocardial contractile function (39, 40).

In this sense, our score has two advantages: one, it is valid for any type of cancer, and two, that it includes cardiac biomarkers determination and echocardiography exams. Nevertheless, it needs to be validated in the different pathologies in a larger sample. Thus, a thorough cardiovascular evaluation is essential before starting ICI treatment, necessary for the multidisciplinary assessment of a cardio-oncology team.

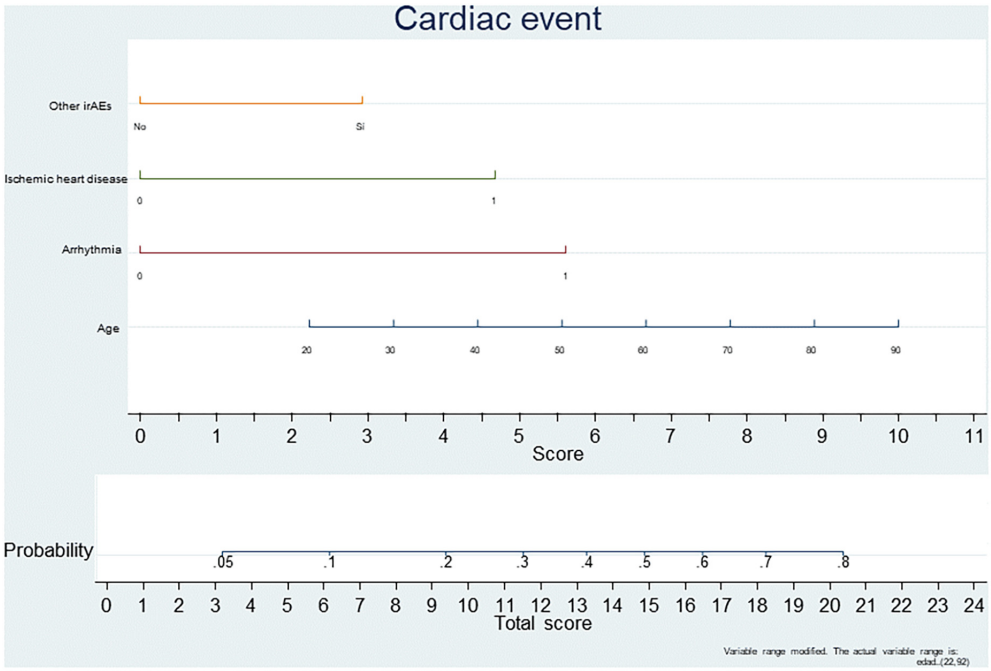

FIGURE 2
Predictive risk score for developing a cardiac event during ICI treatment.

The American Society of Clinical Oncology (ASCO) recommends a baseline cardiac workup before initiating potential cardiotoxic therapy, and, in case of symptoms, an extended cardiology workup including echocardiography, chest x-ray, and cardiac biomarkers, such as cardiac troponin and brain natriuretic peptide (BNP) (41). On the other hand, other studies have also suggested a surveillance strategy for high-risk patients who are receiving ICI treatment (20). The baseline cardiac assessment pre-ICI should include a complete clinical history and risk factor assessment, electrocardiogram (ECG), cardiac troponin, BNP, and echocardiogram. In high-risk patients, a closer monitoring is recommended, with ECG and cardiac biomarkers determination before ICI initiation and dose-adjustment. These specific tests are proposed because ICI-related CE has been characterized consistently by BNP elevation or conduction disease. Measurement of cardiac troponin should also be considered because it is more specific for myocarditis, the most important ICI-triggered cardiotoxic effect. Given the heterogeneity in the risk of cardiotoxic effects, a personalized strategy based on the patient´s baseline risk assessment may be relevant. Upon cardiotoxicity suspicion, it is recommended to immediately interrupt ICI therapy, repeat all cardiovascular exams, and refer the patient to a cardio-oncology specialist (20). In case of major cardiovascular complications, management should be in accordance with the current European Society of Cardiology (ESC) and American Heart Association (AHA) guidelines.

The main limitation of this study is its retrospective, descriptive nature, based on the activity conducted in a single center, Puerta de Hierro-Majadahonda University Hospital. Consequently, the incidence of CE might have been underestimated due to the lack of information in the medical records.

Conclusion

The real incidence of immune-related cardiotoxicity in real-world practice is higher than that reported in clinical trials. Cardiovascular history, older age, and prior irAEs are potential risk-factors, making patients more susceptible to these events. A thorough cardiovascular evaluation is strongly recommended before ICI treatment and, in high-risk patients, a closer follow-up and prompt referral to a cardio-oncology specialist as soon as cardiotoxicity is suspected. Risk stratification using a risk scoring system may improve the cardiovascular outcomes of patients treated with ICIs by identifying the patients at risk for cardiovascular events. Incorporation of clinical biomarkers and imaging parameters should be incorporated into these scores in order to improve the accuracy of prediction. Future studies with larger samples are needed in order to validate risk scores and develop standardized follow-up strategies for these patients.

Data availability statement

The raw data supporting the conclusions of this article will be made available by the authors upon reasonable request.

Ethics statement

The studies involving human participants were reviewed and approved by the Comité de Ética de Investigación con Medicamentos del Hospital Universitario Puerta de Hierro Majadahonda. The patients/participants provided their written informed consent to participate in this study.

Author contributions

MT, MB, FF, and MP drafted and designed the study. MM, BC, LG, MB, RH, AC-L, VC, JS, AG-d-A, and BN performed patients' inclusion. MT, MB, PS, and MP drafted the manuscript. All authors reviewed and approved the manuscript and read and agreed to the published version of the manuscript.

Funding

This article is part of the CLARIFY project, supported by the European Union Horizon 2020 Research and Innovation Program under grant agreement number 875160.

Conflict of interest

The authors declare that the research was conducted in the absence of any commercial or financial relationships that could be construed as a potential conflict of interest.

Publisher's note

All claims expressed in this article are solely those of the authors and do not necessarily represent those of their affiliated organizations, or those of the publisher, the editors and the reviewers. Any product that may be evaluated in this article, or claim that may be made by its manufacturer, is not guaranteed or endorsed by the publisher.

References

1. Zhou YW, Zhu YJ, Wang MN, Xie Y, Chen CY, Zhang T, et al. Immune checkpoint inhibitor-associated cardiotoxicity: current understanding on its mechanism, diagnosis and management. *Front Pharmacol.* (2019) 10:1350. doi: 10.3389/fphar.2019.01350

2. Swaika A, Hammond WA, Joseph RW. Current state of anti-PD-L1 and anti-PD-1 agents in cancer therapy. *Mol Immunol.* (2015) 67(2 Pt A):4–17.

3. Walker LS, Sansom DM. The emerging role of CTLA4 as a cell-extrinsic regulator of T cell responses. *Nat Rev Immunol.* (2011) 11:852–63. doi: 10.1038/nri3108

4. Boussiotis VA. Molecular and biochemical aspects of the PD-1 checkpoint pathway. *N Engl J Med.* (2016) 375:1767–78. doi: 10.1056/NEJMra1514296

5. Hino R, Kabashima K, Kato Y, Yagi H, Nakamura M, Honjo T, et al. Tumor cell expression of programmed cell death-1 ligand 1 is a prognostic factor for malignant melanoma. *Cancer.* (2010) 116:1757–66.

6. Vaddepally RK, Kharel P, Pandey R, Garje R, Chandra AB. Review of indications of FDA-approved immune checkpoint inhibitors per NCCN guidelines with the level of evidence. *Cancers.* (2020) 12:738. doi: 10.3390/cancers12030738

7. Reck M, Rodríguez-Abreu D, Robinson AG, Hui R, Csőszi T, Fülöp A, et al. Pembrolizumab versus chemotherapy for PD-L1-positive non-small-cell lung cancer. *N Engl J Med.* (2016) 375:1823–33.

8. Hodi FS, O'Day SJ, McDermott DF, Weber RW, Sosman JA, Haanen JB, et al. Improved survival with ipilimumab in patients with metastatic melanoma. *N Engl J Med.* (2010) 363:711–23.

9. Postow MA, Sidlow R, Hellmann MD. Immune-related adverse events associated with immune checkpoint blockade. *N Engl J Med.* (2018) 378:158–68.

10. Michot JM, Bigenwald C, Champiat S, Collins M, Carbonnel F, Postel-Vinay S, et al. Immune-related adverse events with immune checkpoint blockade: a comprehensive review. *Eur J Cancer.* (2016) 54:139–48.

11. Wolchok JD, Chiarion-Sileni V, Gonzalez R, Rutkowski P, Grob JJ, Cowey CL, et al. Overall survival with combined nivolumab and ipilimumab in advanced melanoma. *N Engl J Med.* (2017) 377:1345–56.

12. Heery CR, O'Sullivan Coyne GH, Madan RA, Schlom J, von Heydebreck A, Cuillerot JM, et al. Phase I, open-label, multi-ascending dose trial of avelumab (MSB0010718C), an anti-PD-L1 monoclonal antibody, in Japanese patients with advanced solid tumors. *J Clin Oncol.* (2015) 33(15_suppl.):3023–3023.

13. Geisler BP, Raad RA, Esaian D, Sharon E, Schwartz DR. Apical ballooning and cardiomyopathy in a melanoma patient treated with ipilimumab: a case of takotsubo-like syndrome. *J Immunother Cancer.* (2015) 3:4. doi: 10.1186/s40425-015-0048-2

14. Läubli H, Balmelli C, Bossard M, Pfister O, Glatz K, Zippelius A. Acute heart failure due to autoimmune myocarditis under pembrolizumab treatment for metastatic melanoma. *J Immunother Cancer.* (2015) 3:11. doi: 10.1186/s40425-015-0057-1

15. Norwood TG, Westbrook BC, Johnson DB, Litovsky SH, Terry NL, McKee SB, et al. Smoldering myocarditis following immune checkpoint blockade. *J Immunother Cancer.* (2017) 5:91.

16. Choueiri TK, Larkin J, Oya M, Thistlethwaite F, Martignoni M, Nathan P, et al. Preliminary results for avelumab plus axitinib as first-line therapy in patients with advanced clear-cell renal-cell carcinoma (JAVELIN Renal 100): an open-label, dose-finding and dose-expansion, phase 1b trial. *Lancet Oncol.* (2018) 19:451–60.

17. Johnson DB, Balko JM, Compton ML, Chalkias S, Gorham J, Xu Y, et al. Fulminant myocarditis with combination immune checkpoint blockade. *N Engl J Med.* (2016) 375:1749–55.

18. Mahmood SS, Fradley MG, Cohen JV, Nohria A, Reynolds KL, Heinzerling LM, et al. Myocarditis in patients treated with immune checkpoint inhibitors. *J Am Coll Cardiol.* (2018) 71:1755–64.

19. Ji C, Roy MD, Golas J, Vitsky A, Ram S, Kumpf SW, et al. Myocarditis in cynomolgus monkeys following treatment with immune checkpoint inhibitors. *Clin Cancer Res.* (2019) 25:4735–48. doi: 10.1158/1078-0432.CCR-18-4083

20. Lyon AR, Yousaf N, Battisti NML, Moslehi J, Larkin J. Immune checkpoint inhibitors and cardiovascular toxicity. *Lancet Oncol.* (2018) 19:e447–58.

21. Escudier M, Cautela J, Malissen N, Ancedy Y, Orabona M, Pinto J, et al. Clinical features, management, and outcomes of immune checkpoint inhibitor-related cardiotoxicity. *Circulation.* (2017) 136:2085–7.

22. Larkin J, Chiarion-Sileni V, Gonzalez R, Grob JJ, Cowey CL, Lao CD, et al. Combined nivolumab and ipilimumab or monotherapy in untreated melanoma. *N Engl J Med.* (2015) 373:23–34.

23. Salem JE, Manouchehri A, Moey M, Lebrun-Vignes B, Bastarache L, Pariente A, et al. Cardiovascular toxicities associated with immune checkpoint inhibitors: an observational, retrospective, pharmacovigilance study. *Lancet Oncol.* (2018) 19:1579–89. doi: 10.1016/S1470-2045(18)30608-9

24. D'Souza M, Nielsen D, Svane IM, Iversen K, Rasmussen PV, Madelaire C, et al. The risk of cardiac events in patients receiving immune checkpoint inhibitors: a nationwide Danish study. *Eur Heart J.* (2021) 42:1621–31. doi: 10.1093/eurheartj/ehaa884

25. Baban B, Liu JY, Qin X, Weintraub NL, Mozaffari MS. Upregulation of programmed death-1 and its ligand in cardiac injury models: interaction with GADD153. *PLoS One.* (2015) 10:e0124059. doi: 10.1371/journal.pone.0124059

26. JBS3 Board. Joint British Societies' consensus recommendations for the prevention of cardiovascular disease (JBS3). *Heart.* (2014) 100(Suppl 2.):ii1–67.

27. Drobni ZD, Alvi RM, Taron J, Zafar A, Murphy SP, Rambarat PK, et al. Association between immune checkpoint inhibitors with cardiovascular events and atherosclerotic plaque. *Circulation.* (2020) 142:2299–311.

28. Nishimura H, Okazaki T, Tanaka Y, Nakatani K, Hara M, Matsumori A, et al. Autoimmune dilated cardiomyopathy in PD-1 receptor-deficient mice. *Science.* (2001) 291:319–22. doi: 10.1126/science.291.5502.319

29. Okazaki T, Tanaka Y, Nishio R, Mitsuiye T, Mizoguchi A, Wang J, et al. Autoantibodies against cardiac troponin I are responsible for dilated cardiomyopathy in PD-1-deficient mice. *Nat Med.* (2003) 9:1477–83. doi: 10.1038/nm955

30. Bazaz R, Marriott HM, Francis SE, Dockrell DH. Mechanistic links between acute respiratory tract infections and acute coronary syndromes. *J Infect.* (2013) 66:1–17. doi: 10.1016/j.jinf.2012.09.009

31. Moslehi JJ, Salem JE, Sosman JA, Lebrun-Vignes B, Johnson DB. Increased reporting of fatal immune checkpoint inhibitor-associated myocarditis. *Lancet.* (2018) 391:933.

32. Wang DY, Salem JE, Cohen JV, Chandra S, Menzer C, Ye F, et al. Fatal toxic effects associated with immune checkpoint inhibitors: a systematic review and meta-analysis. *JAMA Oncol.* (2018) 4:1721–8.

33. Rubio-Infante N, Ramírez-Flores YA, Castillo EC, Lozano O, García-Rivas G, Torre-Amione G. Cardiotoxicity associated with immune checkpoint inhibitor therapy: a meta-analysis. *Eur J Heart Fail.* (2021) 23:1739–47.

34. Laenens D, Yu Y, Santens B, Jacobs J, Beuselinck B, Bechter O, et al. Incidence of cardiovascular events in patients treated with immune checkpoint inhibitors. *J Clin Oncol.* (2022) 40:3430–8.

35. Du S, Zhou L, Alexander GS, Park K, Yang L, Wang N, et al. PD-1 modulates radiation-induced cardiac toxicity through cytotoxic T lymphocytes. *J Thorac Oncol.* (2018) 13:510–20. doi: 10.1016/j.jtho.2017.12.002

36. Cihakova D, Rose NR. Pathogenesis of myocarditis and dilated cardiomyopathy. *Adv Immunol.* (2008) 99:95–114.

37. Romond EH, Jeong JH, Rastogi P, Swain SM, Geyer CE Jr, Ewer MS, et al. Seven-year follow-up assessment of cardiac function in NSABP B-31, a randomized trial comparing doxorubicin and cyclophosphamide followed by paclitaxel (ACP) with ACP plus trastuzumab as adjuvant therapy for patients with node-positive, human epidermal growth factor receptor 2-positive breast cancer. *J Clin Oncol.* (2012) 30:3792–9. doi: 10.1200/JCO.2011.40.0010

38. Ezaz G, Long JB, Gross CP, Chen J. Risk prediction model for heart failure and cardiomyopathy after adjuvant trastuzumab therapy for breast cancer. *J Am Heart Assoc.* (2014) 3:e000472. doi: 10.1161/JAHA.113.000472

39. Kim DY, Park MS, Youn JC, Lee S, Choi JH, Jung MH, et al. Development and validation of a risk score model for predicting the cardiovascular outcomes after breast cancer therapy: the CHEMO-RADIAT score. *J Am Heart Assoc.* (2021) 10:e021931. doi: 10.1161/JAHA.121.021931

40. Oikonomou EK, Kokkinidis DG, Kampaktsis PN, Amir EA, Marwick TH, Gupta D, et al. Assessment of prognostic value of left ventricular global longitudinal strain for early prediction of chemotherapy-induced cardiotoxicity: a systematic review and meta-analysis. *JAMA Cardiol.* (2019) 4:1007–18. doi: 10.1001/jamacardio.2019.2952

41. Armenian SH, Lacchetti C, Barac A, Carver J, Constine LS, Denduluri N, et al. Prevention and monitoring of cardiac dysfunction in survivors of adult cancers: American society of clinical oncology clinical practice guideline. *J Clin Oncol.* (2017) 35:893–911.

frontiers | Frontiers in Cardiovascular Medicine

TYPE Original Research
PUBLISHED 11 January 2023
DOI 10.3389/fcvm.2022.996809

OPEN ACCESS

EDITED BY
Antonella Lombardo,
Agostino Gemelli University Polyclinic (IRCCS), Italy

REVIEWED BY
Mahboobeh Ghasemzadeh Rahbardar,
Mashhad University of Medical Sciences, Iran
Giulia Russo,
University Health Organization Giuliano Isontina (ASU GI), Italy

*CORRESPONDENCE
Weizhong Zhu
✉ Zhuwz@ntu.edu.cn

SPECIALTY SECTION
This article was submitted to Cardio-Oncology, a section of the journal Frontiers in Cardiovascular Medicine

RECEIVED 18 July 2022
ACCEPTED 19 December 2022
PUBLISHED 11 January 2023

CITATION
Qian H, Qian Y, Liu Y, Cao J, Wang Y, Yang A, Zhao W, Lu Y, Liu H and Zhu W (2023) Identification of novel biomarkers involved in doxorubicin-induced acute and chronic cardiotoxicity, respectively, by integrated bioinformatics.
Front. Cardiovasc. Med. 9:996809.
doi: 10.3389/fcvm.2022.996809

Identification of novel biomarkers involved in doxorubicin-induced acute and chronic cardiotoxicity, respectively, by integrated bioinformatics

Hongyan Qian[1,2], Yi Qian[1], Yi Liu[1], Jiaxin Cao[1], Yuhang Wang[1], Aihua Yang[1], Wenjing Zhao[1], Yingnan Lu[3], Huanxin Liu[4] and Weizhong Zhu[1*]

[1]Department of Pharmacology, School of Medicine and School of Pharmacy Nantong University, Nantong, China, [2]Cancer Research Center Nantong, Nantong Tumor Hospital and Tumor Hospital Affiliated to Nantong University, Nantong, China, [3]School of Overseas Education, Changzhou University, Changzhou, China, [4]Shanghai Labway Medical Laboratory, Shanghai, China

Background: The mechanisms of doxorubicin (DOX) cardiotoxicity were complex and controversial, with various contradictions between experimental and clinical data. Understanding the differences in the molecular mechanism between DOX-induced acute and chronic cardiotoxicity may be an ideal entry point to solve this dilemma.

Methods: Mice were injected intraperitoneally with DOX [(20 mg/kg, once) or (5 mg/kg/week, three times)] to construct acute and chronic cardiotoxicity models, respectively. Survival record and ultrasound monitored the cardiac function. The corresponding left ventricular (LV) myocardium tissues were analyzed by RNA-seq to identify differentially expressed genes (DEGs). Gene Ontology (GO), Kyoto Encyclopedia of Gene and Genome (KEGG), and Gene Set Enrichment Analysis (GSEA) found the key biological processes and signaling pathways. DOX cardiotoxicity datasets from the Gene expression omnibus (GEO) database were combined with RNA-seq to identify the common genes. Cytoscape analyzed the hub genes, which were validated by quantitative real-time PCR. ImmuCo and ImmGen databases analyzed the correlations between hub genes and immunity-relative markers in immune cells. Cibersort analyzed the immune infiltration and correlations between the hub genes and the immune cells. Logistic regression, receiver operator characteristic curve, and artificial neural network analysis evaluated the diagnosis ability of hub genes for clinical data in the GEO dataset.

Results: The survival curves and ultrasound monitoring demonstrated that cardiotoxicity models were constructed successfully. In the acute model, 788 DEGs were enriched in the activated metabolism and the suppressed

10.3389/fcvm.2022.996809

immunity-associated signaling pathways. Three hub genes (Alas1, Atp5g1, and Ptgds) were upregulated and were negatively correlated with a colony of immune-activating cells. However, in the chronic model, 281 DEGs showed that G protein-coupled receptor (GPCR)-related signaling pathways were the critical events. Three hub genes (Hsph1, Abcb1a, and Vegfa) were increased in the chronic model. Furthermore, Hsph1 combined with Vegfa was positively correlated with dilated cardiomyopathy (DCM)-induced heart failure (HF) and had high accuracy in the diagnosis of DCM-induced HF (AUC = 0.898, P = 0.000).

Conclusion: Alas1, Atp5g1, and Ptgds were ideal biomarkers in DOX acute cardiotoxicity. However, Hsph1 and Vegfa were potential biomarkers in the myocardium in the chronic model. Our research, first, provided bioinformatics and clinical evidence for the discovery of the differences in mechanism and potential biomarkers of DOX-induced acute and chronic cardiotoxicity to find a therapeutic strategy precisely.

KEYWORDS

doxorubicin, cardiotoxicity, RNA-seq, biomarkers, mice

Introduction

Cardiovascular disease and cancer rank as the two leading premature causes of death worldwide (1). In the last decade, the survival of patients with cancer has greatly improved due to the improvement of comprehensive treatment, especially the tremendous development and application of anticancer drugs (2). However, the following problem is that due to prolonged survival, complications caused by various cancer therapies appear, especially the toxicity of anticancer drugs to the heart (3). In fact, there are very few interventions available to address the problem. Therefore, it is particularly important to discover the mechanisms involved in the cardiotoxicity induced by these anticancer drugs and to find potential biomarkers.

Doxorubicin (DOX), as the first-line chemotherapy drug for various cancers, has limited availability since its cardiotoxicity was first reported in 1979 (4). Its cardiotoxicity is divided into three categories based on the time of onset. The first is acute cardiotoxicity, which occurs within 2 weeks after a single chemotherapy regimen. The second is early-onset chronic cardiotoxicity, which occurs within 1 year after stopping the treatment, usually manifesting as heart failure (HF) caused by dilated cardiomyopathy (DCM). The third is late-stage chronic cardiotoxicity, which develops years or even decades after the end of chemotherapy (5). The incidence rate of acute cardiotoxicity and chronic one is 11–21 and 1.7%, respectively (6, 7). Their pathophysiological changes are complex, with both similarities and differences. Though the underlying mechanisms such as oxidative stress, lipid peroxidation, topoisomerase II inhibition, DNA binding and alkylation, dysregulation of the cardiomyocyte-specific genes, inflammatory cytokines, necroptosis, autophagy, direct membrane damage, dysfunction of adrenergic receptors, and misregulation of calcium handling have been found for DOX-induced cardiotoxicity (8–10), the prevailing paradigm holds that oxidative stress is the key mechanism that is associated with mitochondrial dysfunction and cardiomyocyte death in both models (11). Acute cardiotoxicity includes myocardial rupture, cardiomyocyte atrophy, and vacuolar pro-apoptotic cells. The chronic model can lead to left ventricular (LV) dysfunction and typical DCM, which can affect the ventricles and atria, dilate the heart muscles and chamber, and eventually lead to HF (7, 12, 13). In fact, the potential differences are far more than these, and there is a lack of biomarkers for their respective classifications. Therefore, comprehensively understanding these differences and finding the appropriate biomarkers will have a profound impact on clinical management and prognosis.

The rapid development of microarray and sequencing technologies has revolutionized the depth of research and the complexity of collecting and examining molecular data in current biomedical research (14). Gene expression omnibus (GEO) database provides flexible mining tools that enable users to easily query and download data in the context of their specific interests (15, 16). For example, by using the GEO database *via* GEO2R, Qin et al. (17) have revealed the potential roles of HMOX1 in DOX-induced cardiotoxicity. However, the study has only focused on acute cardiotoxicity.

Herein, we established the acute and chronic mouse models, respectively, and used RNA-seq data as the training

group to identify differentially expressed genes (DEGs) for further analysis. The molecular mechanisms were addressed by the Gene Ontology (GO) function, Kyoto Encyclopedia of Gene and Genome (KEGG) pathways, Gene Set Enrichment Analysis (GSEA), protein–protein interaction (PPI) network, and Cytoscape analysis. RNA expression datasets for DOX-induced cardiotoxicity were downloaded from the GEO databases as the testing group to acquire common DEGs with our RNA-seq. We further identified the hub genes and validated the experiments. Finally, we analyzed the correlations between hub genes and immune cells. The clinical database from the GEO database as the validation group verified the predictive effect of the hub genes. Our findings provided further insights into the mechanisms underlying the progression of DOX-induced acute and chronic cardiotoxicity and suggested that hub genes are potential diagnostic biomarkers in the myocardium.

Materials and methods

Mouse models of DOX-induced acute and chronic cardiotoxicity

Animal studies were approved by the Institutional Animal Care and Use Committee of Nantong University. In the acute model, 6–8-week-old male C57BL/6 mice were injected intraperitoneally with 20 mg/kg of DOX once (n = 23) or saline solution (n = 10), based on a previous study (18). Mice were euthanized on day 4 after the first injection, and the LV tissues were stored in liquid nitrogen. In the chronic model, mice (n = 15) were injected intraperitoneally with 5 mg/kg of DOX weekly for 3 continuous weeks, with reference to a previous report (19). Then, the mice were euthanized and the LV tissues were stored in liquid nitrogen for 6 weeks after the first injection. The same protocols for each model were reproductive for survival analysis.

Cardiac function evaluation by echocardiography

The LV function was evaluated with transthoracic echocardiography before the mice were euthanized. Blind tests were performed on the treatment and control groups using echocardiography. With a high-resolution ultrasound frequency-imaging platform (Vevo 2100 System), echocardiography was performed 10 min after initiation of sedation to limit anesthesia-induced impairment of cardiac function. The percentages of LV ejection fraction (EF) and fractional shortening (FS) were calculated from the echocardiography data, as previously described (20).

RNA sequencing data

Nine LV tissues of each group (NC group, acute DOX group, and chronic DOX group) were divided into triplicates randomly. Total RNA was extracted by Trizol reagent (Invitrogen, USA), and the purity was evaluated with an Agilent 2100 Bioanalyzer. Subsequently, the library constructions were made using 1 μg of total RNA with RIN > 6.5. Next-generation sequencing library preparations were constructed according to the manufacturer's protocol. The prepared libraries were then subsequently multiplexed and loaded on an Illumina HiSeq instrument. Sequencing was carried out using a paired-end configuration. Image analysis and base calling were conducted by the HiSeq instrument. To remove the technical element, Cutadpt (V1.9.1) was used to process pass-filter data in FASTQ format, converting it into high-quality, clean data. Differential expression analysis employed the DESeq2 Bioconductor package, and regularized logarithm was used as the standardized method. The | fold change| (| FC|) > 2 and Benjamini-Hochberg-adjusted p-value of genes were set at < 0.05 to detect DEGs.

GEO data download

The keywords "anthracycline cardiotoxicity," "DOX cardiotoxicity," or "cardiotoxicity" were used to search for the GEO Datasets. The "GEO query" package in R software was used to download expression profiling by microarray datasets of DOX-induced cardiotoxicity (GSE59672, GSE23598, GSE2965, and GSE120895) from the GEO database. The microarray datasets GSE59672[1] and GSE23598[2] presented the acute model, whose DEGs were screened by | FC| > 1.5 and P < 0.05. In GSE59672 (3 model samples vs. 3 control samples), the whole hearts of mice were selected for RNA extraction and hybridization on Affymetrix microarrays at day 5 after a single intraperitoneal injection of 15 mg/kg DOX (or saline solution). In GSE23598 (2 model samples vs. 2 control samples), the model construction method was the same as GSE59672, except that the heart tissues were collected on day 4. The GSE2965[3] showed chronic models (2 model samples vs. 2 control samples), where mice were injected with 3 mg/kg DOX weekly for 12 weeks and their hearts were harvested at 12 and 18 weeks after the first injection. The DEGs of

1 https://www.ncbi.nlm.nih.gov/geo/query/acc.cgi?acc=GSE59672
2 https://www.ncbi.nlm.nih.gov/geo/query/acc.cgi?acc=GSE23598
3 https://www.ncbi.nlm.nih.gov/geo/query/acc.cgi?acc=GSE2965

GSE2965 were screened by | FC| > 1.5. The GSE120895[4] showed human endomyocardial biopsies (47 DCM patients showing HF symptoms vs. eight individuals with normal LVEF), which was profiled to identify possible biomarkers sensitive to HF.

Establishment of DOX-treated primary cardiomyocytes of the adult rat model

Rat cardiomyocytes were isolated as previously described (21). Adult rat cardiomyocytes were isolated by Langendorff perfusion and Type II collagenase digestion and cultured in the serum-free Medium199 for 4 h before DOX treatment. After culturing these cardiomyocytes in Medium199 with 2 μM DOX for 24 h, the cells were harvested for further analysis.

Quantitative real-time PCR (qPCR)

RNA was isolated from heart tissues or cardiomyocytes by using Trizol. Reverse transcription and quantitative PCR were carried out by using a two-step PrimeScriptTM RT reagent kit (TAKARA), and a QuantStudio3 Real-Time PCR System (Applied Biosystems, Thermo Fisher Scientific, United States) was used for qPCR. Primers for the genes were synthesized and obtained from Thermo Fisher Scientific. The primer sequences are presented in **Supplementary Table 1**.

Bioinformatics analysis

The Limma software package in R[5] was employed to screen DEGs of GEO data. The GO and KEGG analyses were performed using the cluster profiler package in R (22). A *P*-value of < 0.05 was set as the cut-off criterion for significance. The GSEA was used to associate genes with possible pathways. A false discovery rate (FDR) of < 0.5 and $P < 0.05$ were used as the criteria for judging statistical significance. Interactive relationships and PPI networks of the DEGs were evaluated using the STRING database. The Cytoscape software 3.2.2 was used to construct and visualize a biological network of key DEGs. The Clustering Coefficient and DMNT method in the CytoHubba were used to find the hub genes. Tabula Muris database[6] analyzed the location of hub genes in the normal mouse heart based on single-cell transcriptome data. ImmuCo database[7] and ImmGen database[8] analyzed the gene co-expression and correlation in immune cells. Cibersort analyzed immune infiltration.

A receiver operating characteristic curve analysis

The receiver operating characteristic curve was used to analyze diagnostic values of hub genes, including the area under the curve (AUC) and significance obtained from the GSE120895 dataset.

Artificial neural network analysis

Artificial neural networks are complex computational models that can implement machine learning and pattern recognition. The key pretreatment variables identified as having diagnostic significance by ROC and logistic regression were chosen as input variables for our ANN. These variables were VEGFA, HSPH1, and VEGFA combined with HSPH1. The multilayer perceptron analysis (MLP) used the normalized and log2 transformed gene expression data. The complete procedure for MLP analysis was performed with reference to a previous report (23). All models were trained with a randomly selected subset of 70% of the patients, while the other 30% was used to test each model. A minimum number of one up to a maximum of 50 iterations was established for each network. There was only one hidden layer with two units using hyperbolic tangent activation functions. The output layer used softmax activation functions. This analysis was performed in IBM SPSS Statistics Version 17.

Statistical analysis

Limma package, ClusterProfiler package, and Cytoscape V3.8.2 software were used to analyze RNA-seq or GEO data. SPSS V17 and GraphPad V8.0.2 software were used for the statistical analysis of experimental or clinical data. Unpaired Student's *t*-test or one-way ANOVA test was used to compare the difference between two or three groups. Correlations were determined by Pearson analysis. The logistic regression analyzed the relationship between the hub genes and DCM. The difference was considered statistically significant if $^{*}P < 0.05$, $^{**}P < 0.01$, and $^{***}P < 0.001$.

4 https://www.ncbi.nlm.nih.gov/geo/query/acc.cgi?acc=GSE120895
5 https://bioconductor.org/packages/release/bioc/html/limma.html
6 https://tabula-muris.ds.czbiohub.org/
7 http://immuco.bjmu.edu.cn/
8 http://rstats.immgen.org/DataPage/

Results

Assessment of DOX-induced cardiotoxicity models

The workflow of this research was shown in **Figure 1**. To explore the different mechanisms of DOX-induced acute and chronic cardiotoxicity, mouse models were constructed and assessed. The Kaplan–Meier survival analysis showed that mice began to die 3 days after injection, and four mice (4/23) barely survived on day 7 in the acute model (vs. normal control, $P < 0.0001$), whereas only one mouse (1/15) died after 35 days post the first injection in the chronic model (**Figures 2A,B**). However, echocardiographic data displayed that the EF and FS of the living mice before sacrifice in the acute model sharply declined by about 20% (42.36 vs. 62.14% in the normal control) and by about 15% (20.18 vs. 35.91% in the normal control), respectively. While EF and FS of the mice before sacrifice in the chronic model decreased by about 15% (46.35 vs. 62.14% in the normal control) and 13% (22.85 vs. 35.91% in the normal control), respectively (**Figures 2C–E**). These results illustrated that cardiotoxicity was presented in both models, evidenced by EF < 50% or a 10% decrease from baseline. However, the acute model mice appeared to have much more severe cardiotoxicity in a shorter time and higher mortality than the chronic one.

Identification of the key biological processes and signaling pathways in DOX-induced cardiotoxicity

RNA-seq was carried out to understand the distinct mechanisms behind the two models. In comparison with normal control, 788 DEGs (212 down, 576 up) in the acute group and 281 DEGs (113 down, 168 up) in the chronic group were found. A total of 713 DEGs (220 down, 493 up) were displayed by comparing the acute group with the chronic group (**Figures 3A,C,E**). Then, principal component analysis (PCA) demonstrated that samples from the three groups were significantly separated from each other and clustered well (**Figures 3B,D,F**). Furthermore, GO analysis for BP in the acute model showed TOP10 terms (297 DEGs) that focused on the generation of precursor metabolites and energy, carboxylic acid metabolic process, adaptive immune response, leukocyte differentiation, innate immune response, etc. Noticeably, metabolism-associated DEGs were about 50% (146/297) and immune-regulation-associated DEGs were about 30% (87/297) (**Figure 4A** and **Supplementary Table 2**). The GO analysis for the chronic model showed that the TOP10 terms (135 DEGs) focused on the cell-cycle process and negative regulation of signal transduction, which was about 40% (48/135) and 13% (18/135), respectively (**Figure 4B** and **Supplementary Table 2**). Furthermore, metabolic processes, such as the oxoacid metabolic process, carboxylic acid metabolic process, and oxidation–reduction process, were more highlighted in the acute model than in the chronic model (**Figure 4C**).

In fact, KEGG further validated our findings. KEGG analysis exhibited that metabolism and immunity-associated signaling pathways were the most relevant pathways in the acute model (**Figure 5A** and **Table 1**). However, G protein-coupled receptor (GPCR) related signals, such as cAMP and cGMP-PKG signaling pathways, platelet activation, and vascular smooth muscle contraction were the hub signaling pathways in the chronic model (**Figure 6A** and **Table 1**). Further analysis revealed that metabolic pathways, such as 2-oxocarboxylic acid metabolism and carbon metabolism, were activated, while immunity-associated signaling pathways, such as the B-cell receptor signaling pathway and T-cell receptor signaling pathway, were suppressed in the acute model (**Figure 5B**). However, GPCR-related signaling pathways and vascular smooth muscle contraction were suppressed in the chronic model (**Figure 6B**). In addition to these, GSEA also validated metabolic pathways (NES = 2.1918, $P = 0.0019$) and oxidative phosphorylation (NES = 1.7981, $P = 0.0115$) that were upregulated, while T cell receptor signaling pathway (NES = −2.1862, $P = 0.0021$) was inhibited in the acute model (**Figures 5C–E**). These results collectively reminded us that activated metabolism and suppressed immunity regulation were the key signaling pathways in acute cardiotoxicity, while GPCR-related signaling pathways were the critical events in the chronic model.

Mining the hub genes in DOX-induced acute and chronic cardiotoxicity

As the signaling pathways referred to lots of DEGs, we got the DEGs from the TOP10 signaling pathways of KEGG (**Table 1**) and systematically analyzed the relationships between them by STRING database and visualized the data using Cytoscape (**Figures 6C**, **7A**). To identify the hub genes, two methods—clustering coefficient and density of maximum neighborhood component (DMNC), of the CytoHubba package in Cytoscape were used to get TOP20 hub genes in the acute model and TOP10 hub genes in the chronic model (**Figures 6D,E**, **7B,C**).

To certify our findings, GEO data were analyzed to further validate the above results. As shown in **Figures 8A,G**, 39 DEGs were identified as common to GSE23589, GSE59672, and RNA-seq data in the acute model, which contained some proven genes, such as Klf15 and Neat1. Meanwhile, 25 DEGs were identified as common to GSE2965 and RNA-seq data in the chronic model, where Ckm had been reported (**Figures 8B,H**). Furthermore, we analyzed the intersection of the common DEGs and above TOP20 or TOP10 hub genes in our RNA-seq data. Ultimately, we found 3 hub genes (Alas1, Atp5g1, and

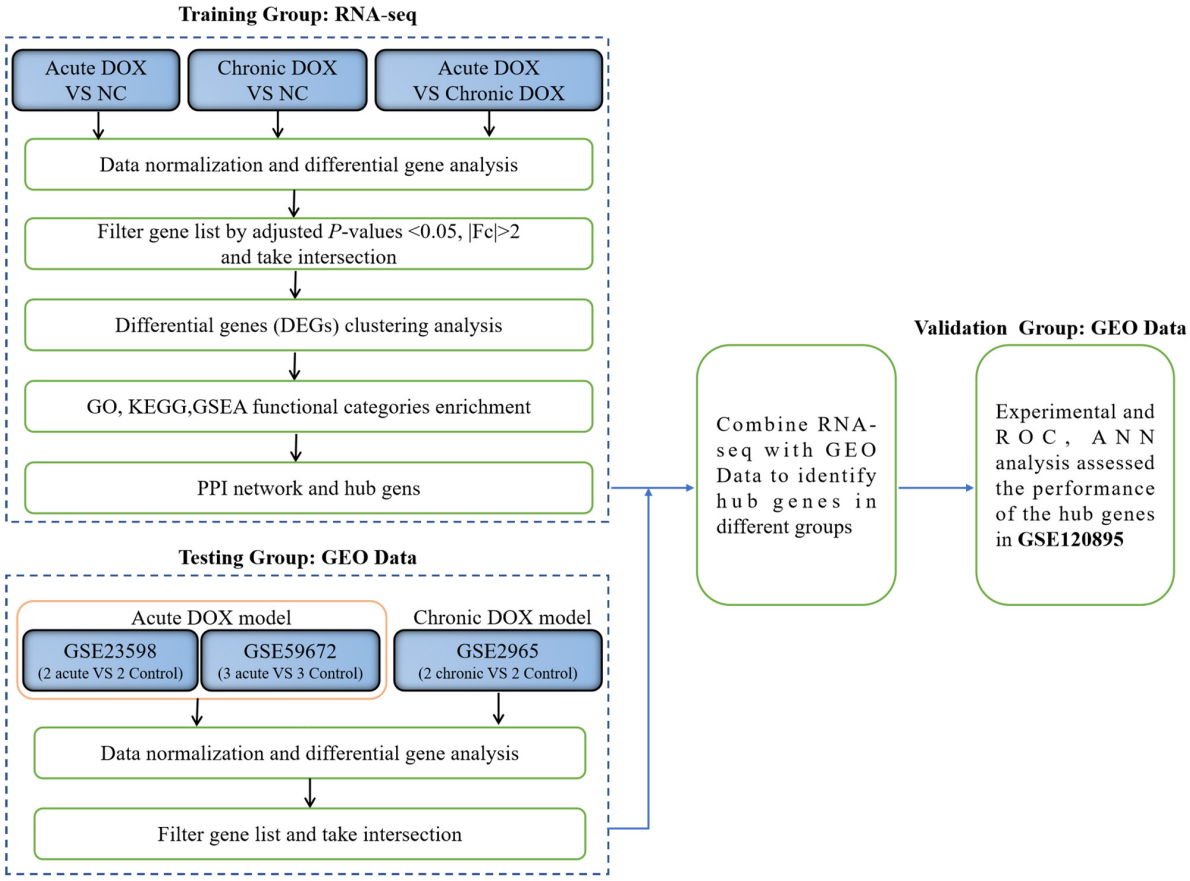

FIGURE 1
Flow chart of the study.

Ptgds) in the acute model and three hub genes (Hsph1, Abcb1a, and Vegfa) in the chronic model (Figures 8B,H). Furthermore, based on the gene expression matrix, gene correlation coefficient analysis showed that the hub genes had a high correlation in each model (Figures 8C,I).

Identifying candidate biomarkers in DOX-induced acute cardiotoxicity

To further verify the accuracy of these hub genes, qPCR detected that Alas1, Atp5g1, and Ptgds displayed upregulated tendency in the LV tissues of the acute model, which were consistent with the RNA-seq (Figures 3A, 8D–F). Furthermore, single-cell transcriptome data of the heart from the normal mouse on the Tabula Muris database reminds us that except Abcb1a, the rest of the hub genes is mainly located in cardiac muscle cells (Supplementary Figures 1A–F). Hence, we established the DOX-treated adult rat cardiomyocytes model to examine the findings. qPCR showed that Atp5g1, Alas1, and Ptgds had the same tendency in the cardiomyocytes as one in the tissues (Supplementary Figures 1G–I). In addition to these, we found that Atp5g1, Alas1, and Ptgds also appeared in immune cells, such as leukocyte cells. Now that both GO and KEGG showed that metabolism and immunity were core mechanisms in the acute model, we guessed whether the 3 hub genes were involved in core mechanisms. KEGG database showed that Alas1 is a 5-aminolevulinate synthase located in the mitochondrion and it participated in glycine, serine, and threonine metabolism. Atp5g1 was focused on oxidative phosphorylation, metabolic pathways, ROS, and diabetic cardiomyopathy. Ptgds took part in arachidonic acid metabolism and lipid transport (Supplementary Figures 2–4).

We took out the classic immune cell markers involved in our RNA-seq data (Cd3d, Rasgrp1, Lck, Cd19, and Gata3) and analyzed the relationship between the hub genes and these markers. ImmuCo database showed that in normal mouse, the expression of Alas1 was negative with Cd3d in CD8 + T cell ($R = -0.22$, $P = 0.001$), with Cd19 in B cell ($R = -0.39$, $P = 0.000$), and with Gata3 in splenocyte cell ($R = -0.47$, $P = 0.000$). Atp5g1 was negative with Lck in CD8 + T cell ($R = -0.17$, $P = 0.007$), Cd19 in B cell ($R = -0.44$, $P = 0.000$),

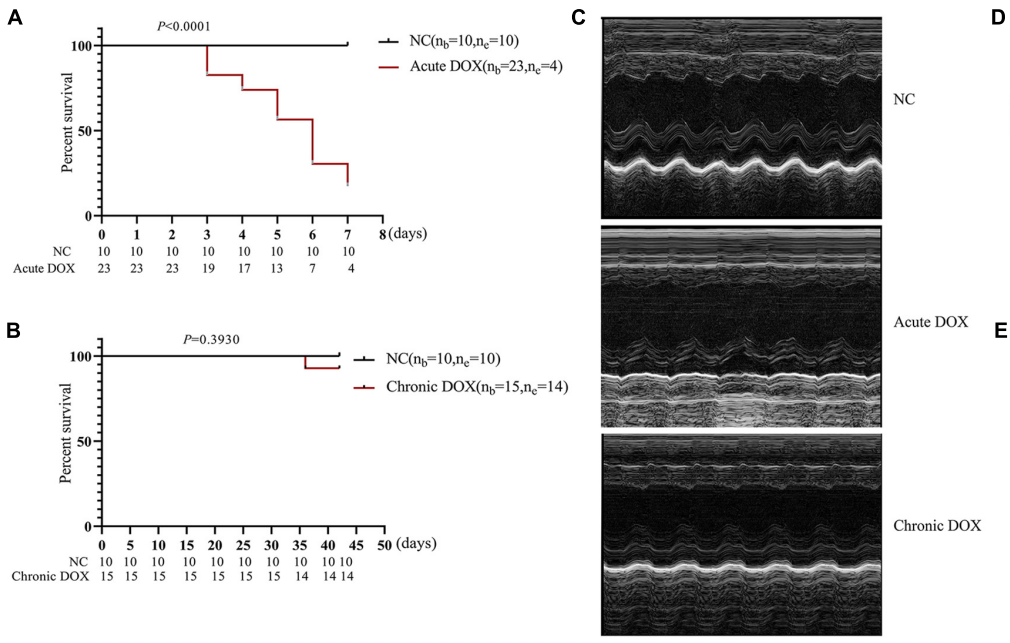

FIGURE 2
Detecting DOX-induced acute and chronic cardiotoxicity of mouse model. **(A)** Survival analysis of the acute model. **(B)** Survival analysis of the chronic model. **(C)** Representative echocardiography images of the normal control (NC), DOX-induced acute cardiotoxicity group (acute DOX), DOX-induced chronic cardiotoxicity group (chronic DOX). **(D,E)** The percentages of EF and FS were calculated from the echocardiography data. ***$P < 0.001$, as calculated by one-way ANOVA.

and Gata3 in splenocyte cell ($R = -0.40$, $P = 0.000$). Ptgds was negative with Gata3 in the splenocyte cell ($R = -0.03$, $P = 0.720$) and Rasgrpl in DC cell ($R = -0.04$, $P = 0.421$) (**Supplementary Figure 5**). To confirm this finding, the ImmGen database further declared that three hub genes were downregulated while these immune markers had a contrary tendency in the CD8 + T cell, CD4 + T cell, B cell, and DC cell of a normal mouse, reminding us that the three hub genes may negatively regulate immune activation (**Figure 9A**). Importantly, in the RNA-seq data of the acute model, the three hub genes were upregulated while the five immune markers were downregulated (**Figure 9B**). Expression matrix correlation analysis also showed that Alas1 was negatively correlated with Gata3, Lck, Cd19, and Cd3d significantly (correlation coefficient = −1, −log10 (*P*-value) = 16), while Atp5g1 and Ptgds were negatively correlated with Rasgrp1 (correlation coefficient = −1, −log10 (*P*-value) = 16) (**Figures 9C,D**). These results demonstrated that the elevated expression of the three hub genes inhibited the activation of some immunocytes in the acute model.

Moreover, Cibersort analysis for 22 mouse immune cells illustrated that the proportion of monocyte, Th1 cell, and activated NK cell were slightly improved from 8.1 to 12%, 0 to 0.9%, and 2.9 to 3.9%, respectively. This suggested that inflammation appeared to be involved in acute cardiotoxicity, which was generally consistent with the previous report (24, 25). Notably, M0 macrophages were slightly improved from 12.7 to 14.6% but the M1 macrophage remained unchanged. However, M2 macrophage obviously increased about 2 times—from 3.6 to 9.6%—and the plasma cell sharply decreased from 10.2% to about 0. In addition, the B cells naive, Treg cells, and CD4 memory T Cells were all decreased more or less, revealing immunosuppression appeared in the acute model (**Figures 10A,B**). These results declared that the immunosuppressive feature was more obvious than inflammation in the acute model. In addition to these, the correlation between the three hub genes with immunity cells showed that Alas1 was negatively correlated with activated NK cell, Gamma delta T cell, CD4 memory T cell, and M0 macrophage. Both Ptgds and Atp5g1 were negative with M1 macrophage, B cells naive, plasma cell, and CD8 memory T cell (**Figure 10C**). All of the results strongly demonstrated that Alas1, Atp5g1, and Ptgds were candidate biomarkers for DOX-induced acute cardiotoxicity as they dominated metabolism and immunity simultaneously.

Testing potential biomarkers for DOX-induced chronic cardiotoxicity

Analogously, qPCR showed the hub genes Hsph1, Vegfa, and Abcb1a were increased in the LV tissues of the chronic model, whose trends were consistent with RNA-seq data (**Figures 3C, 8J–L**). While qPCR detected that only Hsph1

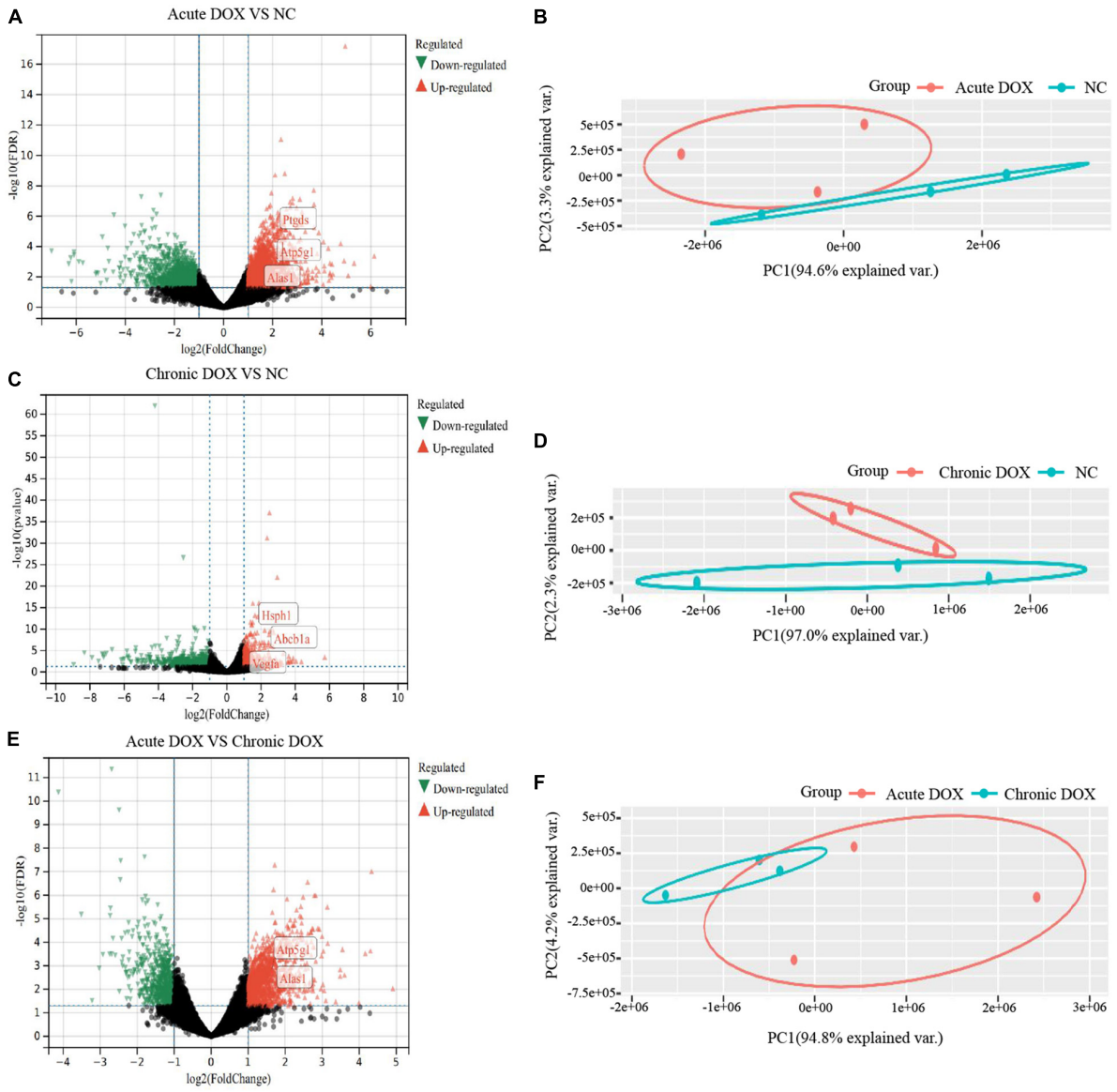

FIGURE 3
Identification of differently expressed genes in RNA-seq. **(A,C,E)** Volcano plots of differently expressed genes (DEGs) in RNA-seq. Green: down-regulated genes; Gray: no DEGs; Red: up-regulated genes. **(B,D,F)** Principle component analysis (PCA). Total RNA was extracted and subjected to RNA sequencing analysis. PCA shows distinct patterns among groups. *n* = 3 of each group.

was elevated significantly in the DOX-treated cardiomyocytes (**Supplementary Figures 1J–L**), we considered that though Vegfa mainly came from the cardiac muscle cell, it was a secreted protein that led to the detection of no significant changes in the cell. In addition, Abcb1a mainly came from endothelial cells, so it was understandable that no significant changes were detected in cardiomyocytes with DOX treatment. To explore whether these hub genes were the potential biomarkers in the chronic model, we took patients with DCM-induced HF data (GSE120895) as the validation group. The GSE120895 dataset was chosen for two reasons (1) DCM was a typical pathological alteration in DOX-induced chronic cardiotoxicity (5, 7, 12, 13). Liang et al. (2) There was so little clinical data or limited sample capacity of DOX-induced chronic cardiotoxicity in the GEO database that we had to employ DCM GEO data for validation. Logistic regression analysis reminded us that HSPH1 combined with VEGFA (HR = 4.904, P = 0.004) was positively associated with chronic DCM-induced HF (**Figure 11A**). Based on logistic regression analysis, ROC analysis demonstrated that HSPH1 (AUC = 0.814, P = 0.005) and VEGFA (AUC = 0.814, P = 0.005) had high accuracy in diagnosing chronic DCM-induced HF,

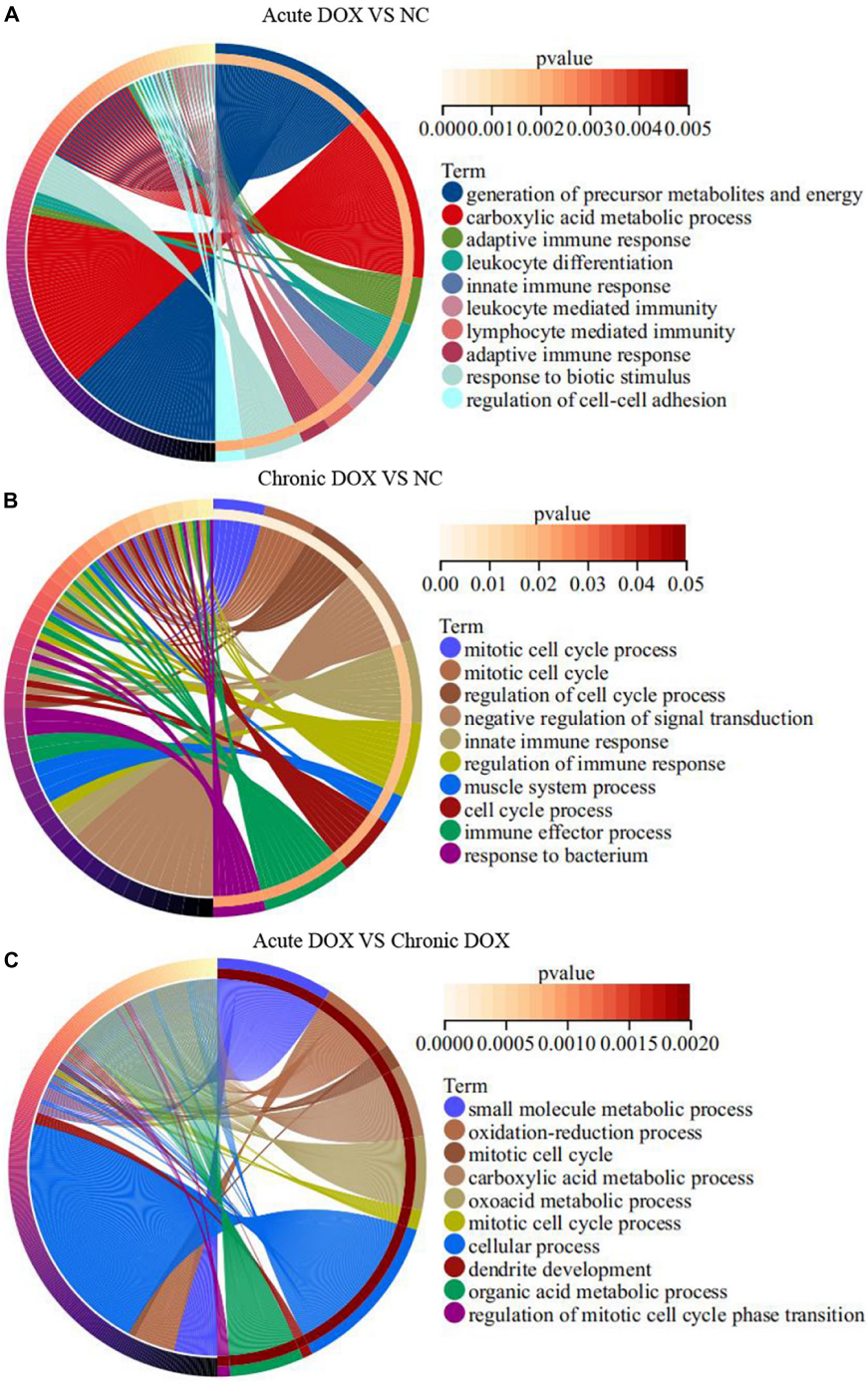

FIGURE 4
GO enrichment analyses of DEGs in TOP10 biological process. **(A)** Acute DOX vs. NC. **(B)** Chronic DOX vs. NC. **(C)** Acute DOX vs. Chronic DOX.

especially HSPH1 combined with VEGFA (AUC = 0.898, P = 0.000) (Figures 11B–D). Furthermore, ANN analysis confirmed that HSPH1 combined with VEGFA took a significant proportion in monitoring chronic DCM-induced HF (Figures 11E,F). In fact, we did not find the expression of ABCB1a in this database. It was speculated that ABCB1a is a membrane-associated protein, whose level was too low to be detected.

In addition, we analyzed 713 DEGs by comparing the acute model with the chronic one. KEGG further proved that metabolism was dramatically activated in the acute model. Venn analysis showed overlapping between the TOP20 hub genes

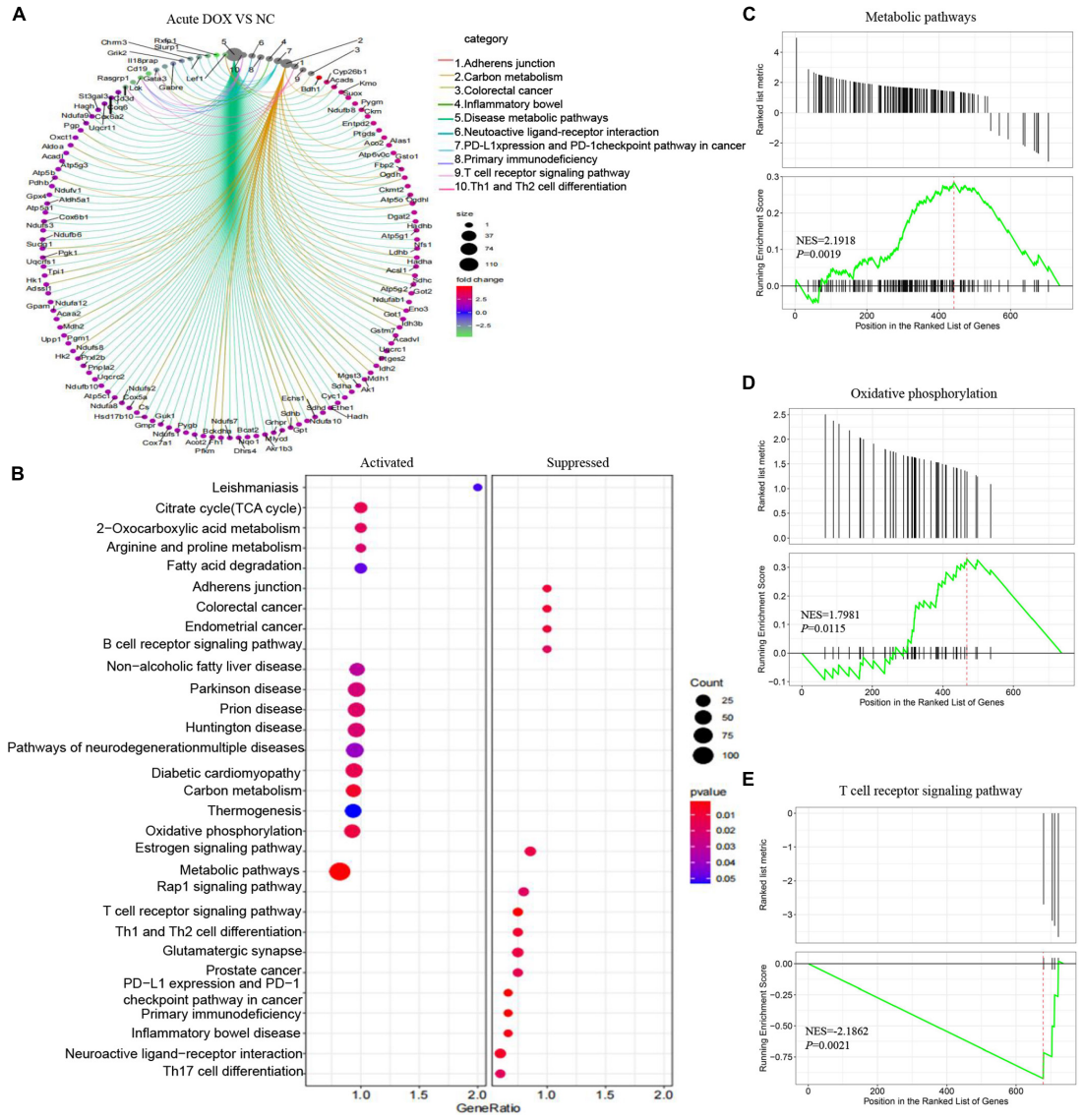

FIGURE 5
Kyoto Encyclopedia of Gene and Genome and Gene Set Enrichment analyses of DEGs in the acute model. **(A)** The circle graph shows the DEGs enriched in the TOP10 KEGG signaling pathways. **(B)** KEGG analysis showed the activated and suppressed signaling pathways. **(C–E)** GSEA analysis showed various signaling pathways associated with DOX-induced acute cardiotoxicity.

from the acute vs. the chronic model and TOP20 hub genes from the acute model. All of the 13 common genes were located in metabolism, including Alas1 and Atp5g1 (**Supplementary Figure 6**). All these results strongly declared that activation of metabolism was the distinctive feature in DOX-induced acute cardiotoxicity. Furthermore, we tested these five biomarkers in the blood (leukocyte) from 11 patients with cancer by qPCR, who were undergoing anthracyclines treatment and had no underlying cardiovascular disease before this therapy. Among these samples, five patients appeared to have abnormal ECG or myocardial enzymes (positive group), while six patients did not show these clinical manifestations (negative group). Exciting results showed ALAS1 and PTGDS were greatly elevated in the positive group (**Figures 8M,N**), which was highly consistent with our acute model. Indeed, more cases need to be analyzed for further verification.

Discussion

Both DOX-induced acute and chronic cardiotoxicity can lead to decreased cardiac function and diverse pathologic changes, while the underlying difference in molecular mechanism is still unclear. Exploring the molecular

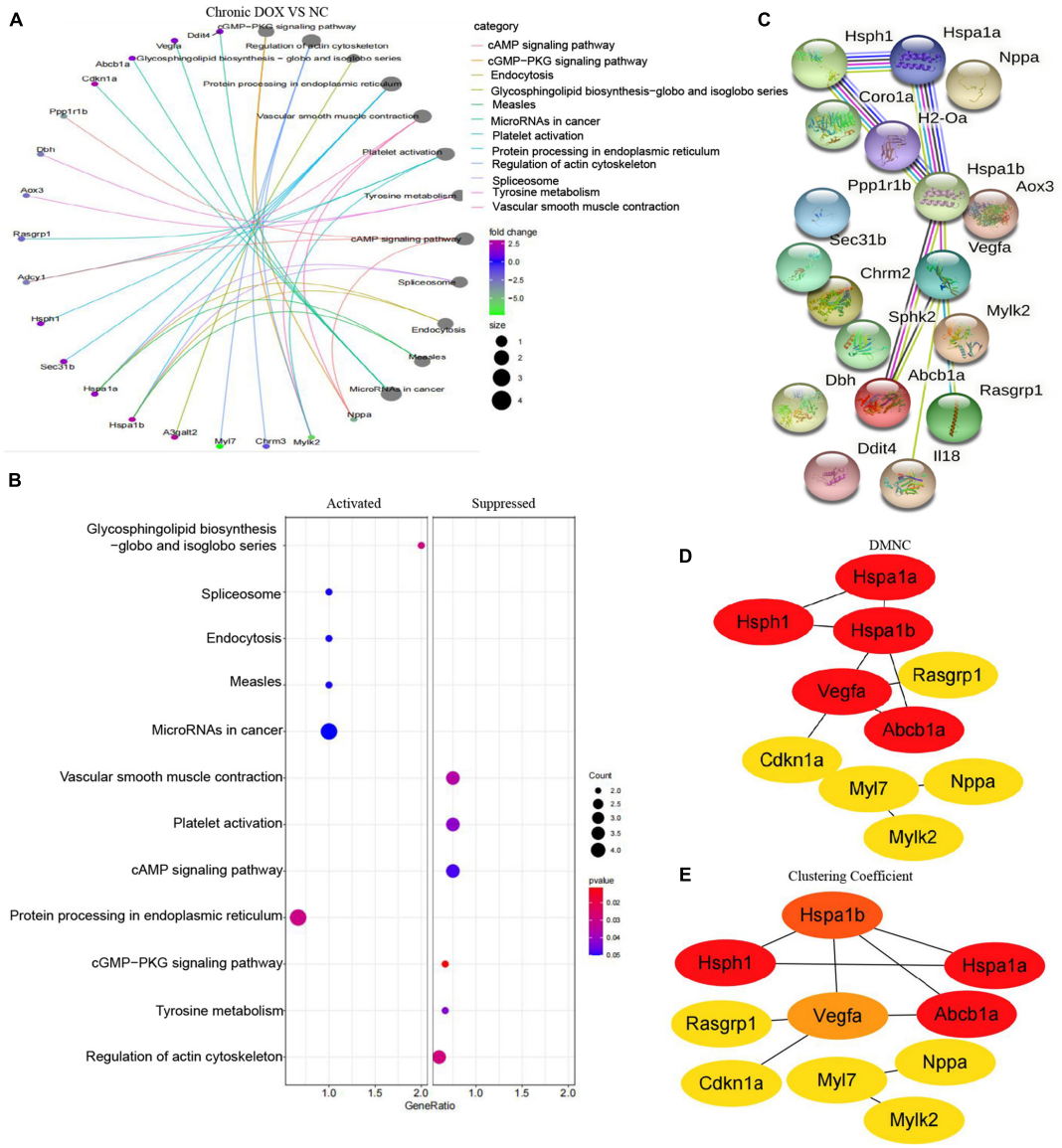

FIGURE 6
Kyoto Encyclopedia of Gene and Genome and protein–protein interaction network analyses of DEGs in chronic model. **(A)** The circle graph shows the DEGs enriched in the TOP10 KEGG signaling pathways. **(B)** KEGG analysis showed the activated and suppressed signaling pathways. **(C)** STRING database analysis of the DEGs in chronic model. **(D,E)** TOP10 hub genes were screened from the PPI network using the Clustering Coefficient and DMNC methods of the CytoHubba.

mechanism difference may be an ideal entry point to find their respective biomarkers.

Activated metabolism and suppressed immunity regulation were the core events in DOX-induced acute cardiotoxicity

The GO and KEGG analysis for the acute model powerfully indicated that the abnormality of metabolic pathways and immunity regulation were the core events. In line with our results, Tan et al. (26) and Ni et al. (27) highlighted several metabolites as potential biomarkers for DOX-induced acute cardiotoxicity. In fact, metabolic disturbances, such as heme metabolism (28), carbon metabolism (29), and oxidative phosphorylation were closely linked to oxidative stress and ROS, which acted as key factors of HF (30). This was also confirmed by our GSEA analysis. Furthermore, the difference between DOX acute and chronic cardiotoxicity was still focused on metabolism. This reminded us again that in addition

TABLE 1 TOP10 KEGG terms of the DEGs in the acute and chronic model, respectively.

ID	Description	Enrichment score	NES	*P-value*	Group
mmu01100	Metabolic pathways	0.284	2.1918	0.0019	Acute
mmu04660	T cell receptor signaling pathway	−0.925	−2.1862	0.0021	Acute
mmu05235	PD-L1 expression and PD-1 checkpoint pathway in cancer	−0.9578	−1.9732	0.0021	Acute
mmu05340	Primary immunodeficiency	−0.9578	−1.9732	0.0021	Acute
mmu05321	Inflammatory bowel disease	−0.8978	−1.8497	0.0042	Acute
mmu04080	Neuroactive ligand-receptor interaction	−0.5771	−2.0047	0.0064	Acute
mmu01200	Carbon metabolism	0.398	2.0649	0.0074	Acute
mmu04658	Th1 and Th2 cell differentiation	−0.779	−1.8412	0.0083	Acute
mmu04520	Adherens junction	−0.9483	−1.6527	0.0101	Acute
mmu05210	Colorectal cancer	−0.9483	−1.6527	0.0101	Acute
mmu04022	cGMP-PKG signaling pathway	−0.8626	−1.5821	0.0118	Chronic
mmu04810	Regulation of actin cytoskeleton	−0.7195	−1.558	0.0289	Chronic
mmu00603	Glycosphingolipid biosynthesis—globo and isoglobo series	0.9811	1.327	0.0292	Chronic
mmu04141	Protein processing in endoplasmic reticulum	0.6189	1.7133	0.0304	Chronic
mmu04270	Vascular smooth muscle contraction	−0.7594	−1.5185	0.0358	Chronic
mmu04611	Platelet activation	−0.751	−1.5015	0.042	Chronic
mmu00350	Tyrosine metabolism	−0.7901	−1.4491	0.0438	Chronic
mmu04024	cAMP signaling pathway	−0.7447	−1.4889	0.0482	Chronic
mmu03040	Spliceosome	0.8555	1.4909	0.0498	Chronic
mmu04144	Endocytosis	0.8555	1.4909	0.0498	Chronic

to addressing oxidative stress and ROS, the importance of metabolism should not be neglected, especially in DOX acute cardiotoxicity.

The DOX-induced immune abnormalities had significant effects on the progression of cardiovascular damage, particularly in the acute phase (31, 32). In the acute model, a seemingly contradictory result showed the coexistence of inflammation and immunosuppression. In fact, the relationship between them is complex, especially in a severe trauma or stressful situations (33, 34). On the one hand, when the inflammatory response persists, it releases both pro- and anti-inflammatory factors to restore the balance. However, the inappropriate expression of these immunosuppressive molecules can aggravate immune suppression (35). On the other hand, patients with severe trauma have a decline in immune function, which makes it difficult to clear the infectious pathogen. This induces the continuous release of pathogen-related molecular patterns or antigens, which in turn act on immune cell pattern recognition receptors or induce adaptive immune activation, leading to persistent inflammatory responses. Thus, the coexistence of inflammation and immunosuppression was not contradictory but a character of serious illness (36). Indeed, in the acute model, we did find that immunosuppressive relative cells were raised substantially, such as M2 macrophage, and a proportion of immune-activating associated cells were sharply decreased, such as Plasma cells and B cells naive. However, Th1 cells, activated NK, and immature DC were increased slightly, which kept the inflammation activation in one of the levels. All these collectively suggested that suppressed immunity regulation is the principal character in DOX acute cardiotoxicity.

Alas1, Atp5g1, and Ptgds were potential biomarkers in DOX-induced acute cardiotoxicity

Investigating progression-associated gene expression profiles could enrich our understanding of the mechanisms. qPCR verified that three hub genes (Alas1, Atp5g1, and Ptgds), as metabolism-related enzymes, were upregulated in LV tissues of the acute model and DOX-treated cardiomyocytes. Alas1, as a rate-limiting enzyme for heme biosynthesis in the mitochondrial matrix, was associated with coronary artery disease (37). It has been highlighted that elevated heme causes oxidant damage and ROS, which thicks filament proteins to cardiomyocytes contractile dysfunction, breaks DNA strands, and mediates DNA mutations (38, 39). Alas1 was increased when the H9c2 cardiomyocyte was exposed to DOX (40). Hence, we speculated that DOX-induced elevation of Alas1

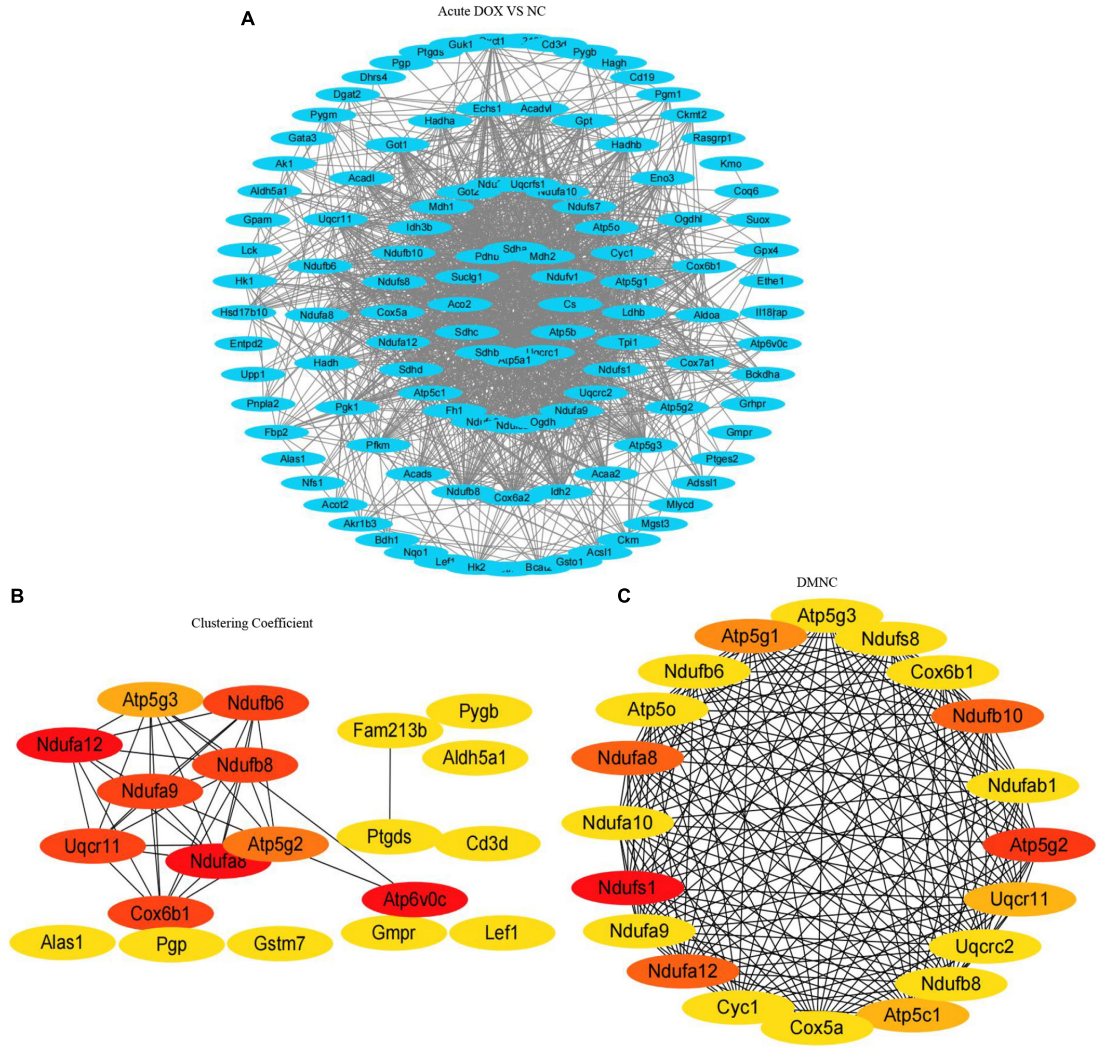

FIGURE 7
Protein–protein interaction network and hub clustering modules. **(A)** STRING database analysis of the DEGs in acute model. **(B,C)** TOP20 hub genes were screened from the PPI network using the Clustering Coefficient and DMNC methods of the CytoHubba.

promoted heme biosynthesis to induce oxidative stress, which destroyed mitochondria and led to mitochondrial DNA damage (39, 41, 42). Atp5g1, as the ATP synthase membrane subunit c locus 1, regulated the mitochondrial permeability transition pore complex (PTPC) (43), and its mutation aggravated PTPC-mediated hypoxia/reoxygenation damages in cardiomyocytes (44). In addition, Atp5g1 is co-localized with the mitochondrial marker HSP60, which is associated with ROS, increased fibrosis, mitochondrial damage, and autophagosomes during HF (45, 46). DOX stimulated calcium release from the mitochondrial matrix through induction of the PTPC, which led to oxidative stress, contributing to mitochondrial bioenergetic failure and cell death (47). Based on our results and from the literature, we guessed elevated Atp5g1 promoted PTPC-induced oxidative stress mediating mitochondrial damage and cell death. Prostaglandin-D2-synthase (Ptgds) was expressed in the atherosclerotic intima and accumulated in the atherosclerotic plaque of coronary arteries with severe stenosis (48).

Intricate relationships between metabolism and immunity were immanent, especially in the mitochondria (49). The abnormal metabolism of immune cells can mediate immune and inflammatory response disorders, where insufficient ATP production aggravates immunosuppression (50, 51). The immune disorder can in turn induce metabolic disorders (52). In line with these reports, we found three hub genes were negatively correlated with Gata3 (53, 54), Lck (55, 56), Cd19 (57), Cd3d (58, 59), and Rasgrp1 (60, 61), which were known markers of immune cells activation in the heart and were decreased DEGs in our RNA-seq.

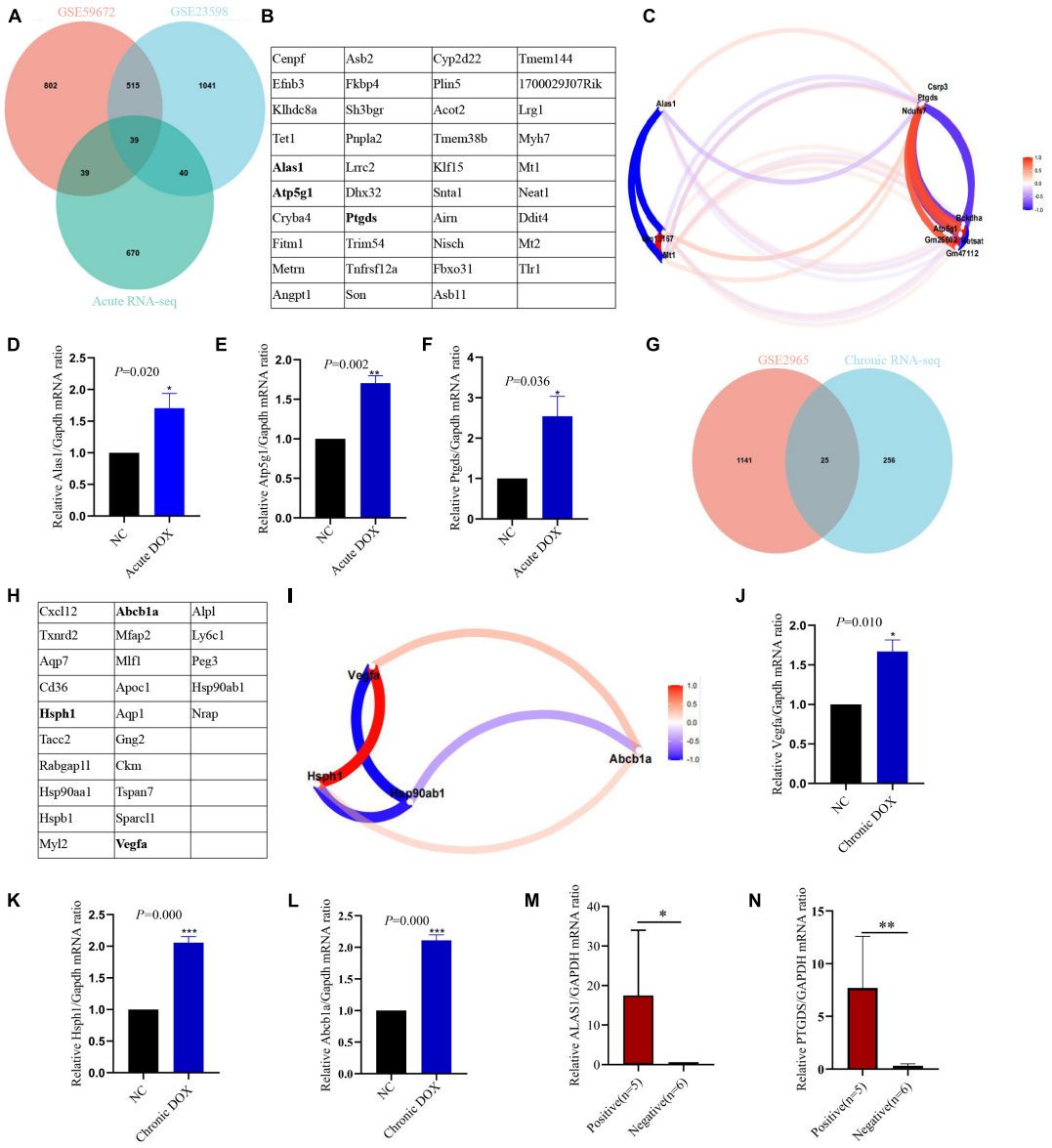

Cenpf	Asb2	Cyp2d22	Tmem144
Efnb3	Fkbp4	Plin5	1700029J07Rik
Klhdc8a	Sh3bgr	Acot2	Lrg1
Tet1	Pnpla2	Tmem38b	Myh7
Alas1	Lrrc2	Klf15	Mt1
Atp5g1	Dhx32	Snta1	Neat1
Cryba4	**Ptgds**	Airn	Ddit4
Fitm1	Trim54	Nisch	Mt2
Metrn	Tnfrsf12a	Fbxo31	Tlr1
Angpt1	Son	Asb11	

Cxcl12	**Abcb1a**	Alpl
Txnrd2	Mfap2	Ly6c1
Aqp7	Mlf1	Peg3
Cd36	Apoc1	Hsp90ab1
Hsph1	Aqp1	Nrap
Tacc2	Gng2	
Rabgap1l	Ckm	
Hsp90aa1	Tspan7	
Hspb1	Sparcl1	
Myl2	**Vegfa**	

FIGURE 8
Validation of hub genes in acute and chronic model. An intersection analysis of RNA-seq and GEO databases of acute model **(A)** and chronic model **(G)**. 39 common DEGs of acute model **(B)** and 25 common DEGs of chronic model **(H)** were listed in the table. The genes marked in bold were the hub genes. Gene correlation coefficient diagram showed the relationship between hub genes and DEGs in the acute **(C)** and chronic **(I)** models. qPCR detected the expression of the hub genes in LV tissues of the acute model **(D–F)** and chronic model **(J–L)**. **(M,N)** qPCR detected the expression of the hub genes in the blood (leukocyte) of patients who were undergoing anthracyclines treatment. NC, normal control; positive, anthracyclines -induced cardiac injury patients; negative: normal cardiac function patients; $^{*}P < 0.05$; $^{**}P < 0.01$; $^{***}P < 0.001$; $n = 3$.

Furthermore, Alas1 was negatively correlated with activated NK, Gamma delta T cell, etc., and both Ptgds and Atp5g1 were negatively correlated with M1 macrophage, B cells naive, plasma cell, etc., suggesting that the three hub genes suppressed the immune cell activation. Remarkably, these results collectively suggested that Alas1, Atp5g1, and Ptgds might be desirable markers as they broadly influenced metabolism and immunity simultaneously in DOX-induced acute cardiotoxicity.

GPCRs pathway, platelet activation, and vascular smooth muscle contraction were involved as the core events in DOX-induced chronic cardiotoxicity

In the chronic model, cAMP and cGMP-PKG signaling pathways, platelet activation, and vascular smooth muscle

10.3389/fcvm.2022.996809

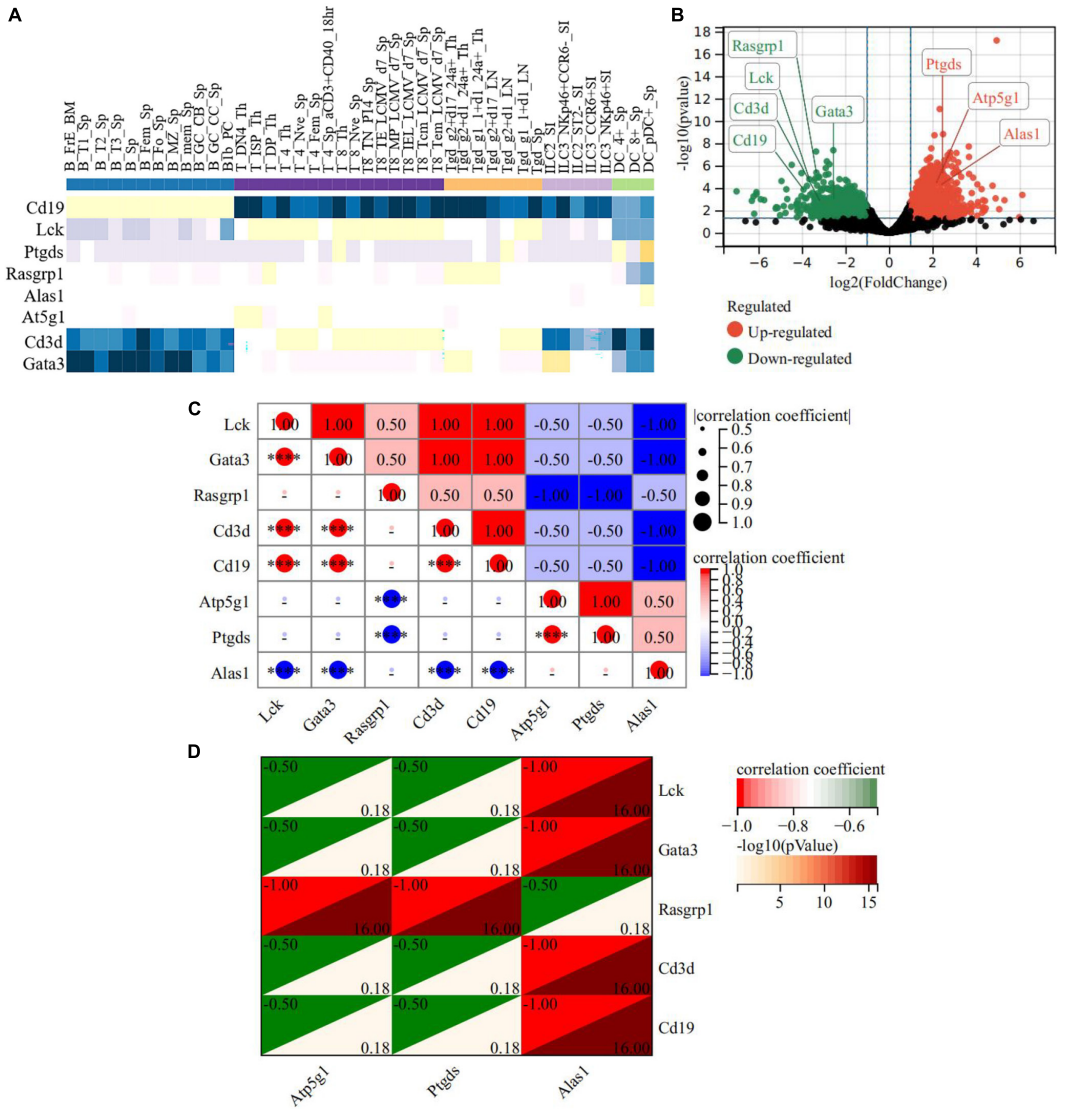

FIGURE 9
A heat map of the correlation between hub genes and immune-related DEGs in the acute model. **(A)** ImmGen database showed correlation between hub genes and immune-related genes in the immune cell of normal mice. **(B)** The expression of the 3 hub genes and the five immune-related DEGs in RNA-seq of the acute model. **(C,D)** The relationship between Atp5g1 and five immune-related DEGs in the acute model. The horizontal and vertical coordinates represent genes, and different colors represent correlation coefficients. ****$P < 0.0001$.

contraction were the hub signaling pathways that were suppressed. We and others have demonstrated that cAMP or cGMP, as the important elements of GPCRs, were widely involved in the regulation of cardiac function: both β_1AR- and β_2AR-mediated augmentation in cAMP led to the activation of PKA, resulting in positive inotropic and relaxant effects (62, 63). In line with our results, Can Ciric Zdravkovic et al. (29) found that DOX inhibited the cAMP/PKA/SIRT1 pathway, which could be attenuated by a Meteorin-like protein. In fact, we have discovered that Gs biased β_2AR agonist can reduce DOX-induced chronic cardiotoxicity (data not shown here). The cGMP-PKG signaling protects various myocardial properties, including cell growth and survival, endothelial permeability, cardiac contractility, and cardiovascular remodeling (64). Additionally, platelet activation and the coagulation cascade raise thrombosis, which is the most feared complication of cardiovascular diseases. However, DOX did not induce platelet activation but resulted in apoptosis, which might contribute to thrombocytopenia (65), and vascular smooth muscle sensitivity decreases and uncouples in HF. Patients with HF have augmented vascular tone, which increases cardiac workload, impairs ventricular output, and promotes further myocardial dysfunction. These results suggested that DOX stimulation persistently resulted in abnormal GPCRs signal, coagulation disorders, and impairing ventricular output, which led to cardiac remodeling. Once

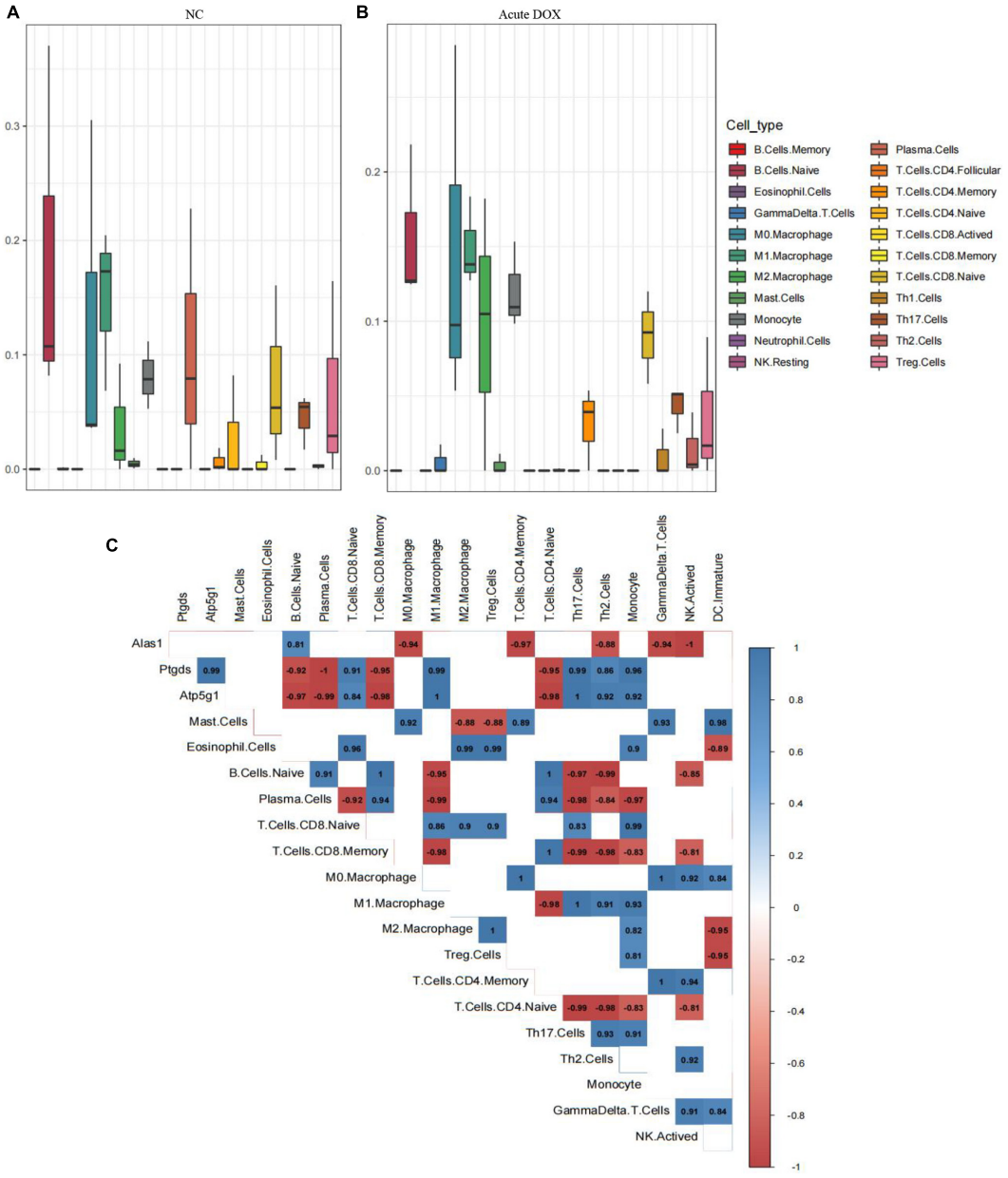

FIGURE 10
Cibersort analysis for the associations between hub genes and immune cells. **(A)** 22 immune cells infiltration in normal control. **(B)** 22 immune cells infiltration in the acute model. **(C)** The relationship between 3 hub genes with immune cells in the acute model.

cardiac remodeling occurs, even drug withdrawal cannot stop this irreversible damage.

Vegfa and Hsph1 were potential biomarkers in diagnosing DOX chronic cardiotoxicity

Vegfa and Hsph1 were dug out by hub gene analysis, and qPCR proved that they were increased in LV tissues of the chronic model. Consistent with our results, Vegfa was upregulated in myocardial injury-associated ventricular remodeling (66), and it was reported that VEGFA is a biomarker in risk factors that mediated coronary heart disease (67). However, an inconsistent report showed that miR-526b-3p mediates DOX-induced cardiotoxicity by targeting STAT3 to inactivate VEGFA (68). For the inconsistent result, we carefully traced the original literature and found that the inconsistency was generated mainly for two reasons: the mice were treated as DOX-induced acute model and they studied the mechanism

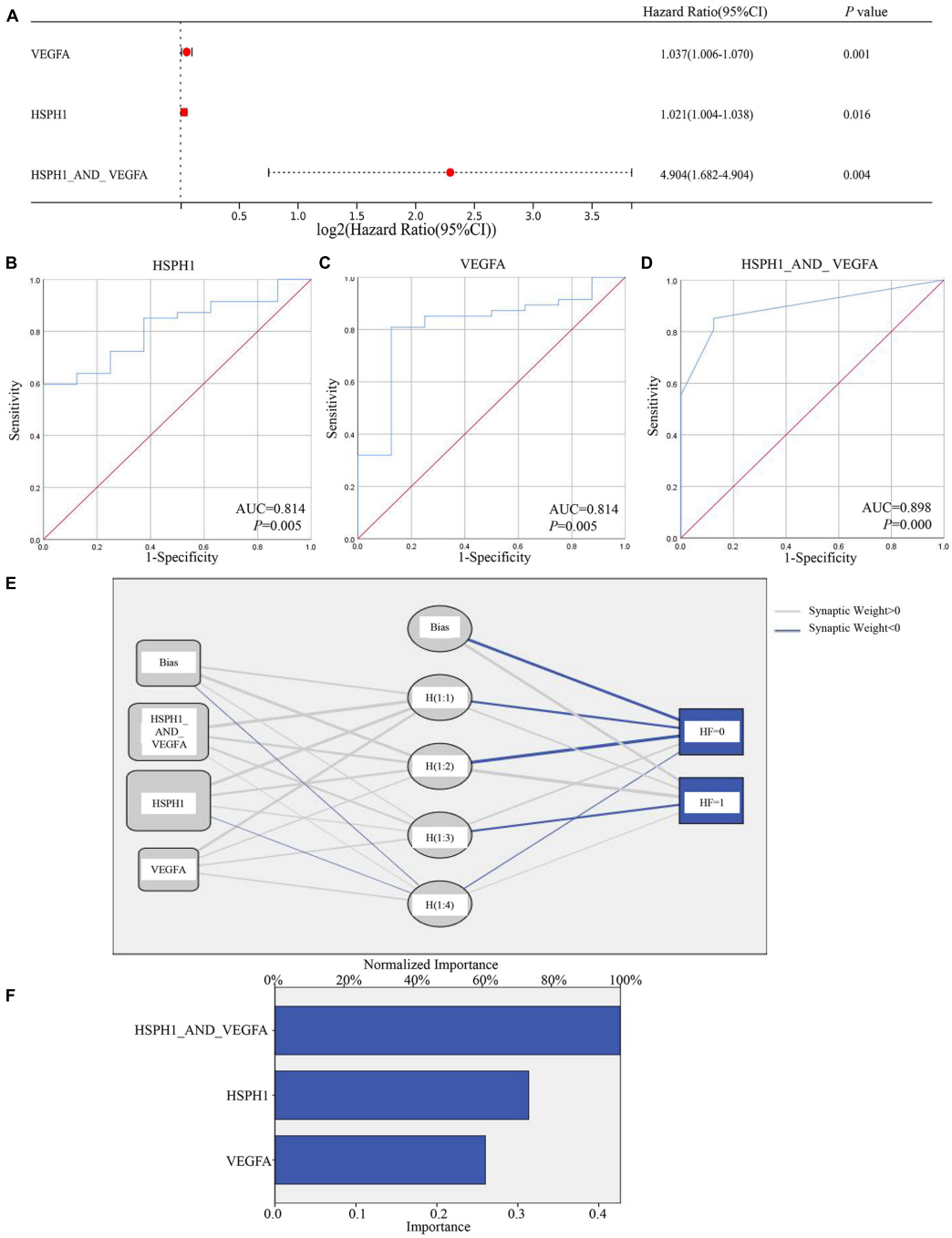

FIGURE 11
Testing the hub genes of the chronic models by GSE120895. **(A)** Logist regression analysis of factors associated with DCM-induced HF. **(B–D)** ROC curve analysis showed HSPH1 and VEGFA as biomarkers that predicted DCM-induced HF. **(E,F)** ANN analysis of the important role of HSPH1 and VEGFA in predicting DCM-induced HF.

based on the endothelial cells, which focused on angiogenesis. In fact, besides its role in angiogenesis, VEGFA is also involved in many other aspects: in a mouse DCM model, Vegfa mRNA and protein levels were strikingly upregulated, whereas there was no increase in capillary density (69). Also, Vegfa overexpression in the context of cardiac injury enabled ectopic cardio-myogenesis but inhibited regeneration at the site of the injury in zebrafish (70). Since DOX-induced chronic cardiotoxicity involved DCM (12) and ventricular remodeling (71), we speculated that DOX elevated Vegfa, which promoted DCM-induced HF. Heat shock protein family H member 1 (HSPH1), as a molecular chaperone, was associated with lipid droplets and was upregulated in

atherosclerosis (72). Analogously, we found both VEGFA and HSPH1 were increased in patients with DCM, which was an important pathologic change in DOX-induced chronic cardiotoxicity, and VEGFA combined with HSPH1 showed high accuracy in diagnosing DCM-induced HF.

This study has some limitations. At present, DOX-induced chronic cardiotoxicity gene expression data in the publicly available datasets are relatively deficient. Hence, we took DCM GEO data to replace DOX chronic cardiotoxicity data, though DCM was the typical pathological characteristic. In the future, more DOX-induced chronic cardiotoxicity gene expression data will be needed for further analysis. We used the human database to validate the finding from the mouse model, so there may be species differences here. We validated the hub genes at the transcription level, and the potential mechanism should be further explored.

Conclusion

In the present study, it is concluded that (1) activated metabolism and suppressed immunity regulation were the core events in DOX acute cardiotoxicity; (2) Alas1, Atp5g1, and Ptgds were potential biomarkers for DOX acute cardiotoxicity, as they contributed to metabolism and immunity-regulation simultaneously; (3) the inhibition of GPCR signaling pathway, platelet activation, and vascular smooth muscle contraction was the key mechanisms in DOX chronic cardiotoxicity; and (4) Vegfa and Hsph1 were potential biomarkers for DOX chronic cardiotoxicity. The study provided bioinformatics and clinical evidence for the discovery of the mechanism difference and potential biomarkers of DOX-induced acute and chronic cardiotoxicity in the myocardium so as to find a more precise therapeutic strategy.

Data availability statement

Publicly available datasets were analyzed in this study. This data can be found here: GSE23598 (https://www.ncbi.nlm.nih.gov/geo/query/acc.cgi?acc=GSE23598), GSE59672 (https://www.ncbi.nlm.nih.gov/geo/query/acc.cgi?acc=GSE59672), GSE2965 (https://www.ncbi.nlm.nih.gov/geo/query/acc.cgi?acc=GSE2965), and GSE120895 (https://www.ncbi.nlm.nih.gov/geo/query/acc.cgi?acc=GSE120895).

Ethics statement

The studies involving human participants were reviewed and approved by the Research Ethics Board of the Tumor Hospital Affiliated to Nantong University. The patients/participants provided their written informed consent to participate in this study. The animal study was reviewed and approved by Animal Care and Use Committee of the Nantong University.

Author contributions

WZhu: conception and design, financial support, and final approval of the manuscript. HQ, YQ, YLi, JC, and YW: manuscript writing. HQ, JC, YQ, AY, and WZha: experiment research. HQ, YLu, and HL: statistical analysis. All authors contributed to the article and approved the submitted version.

Funding

This work was supported by the National Natural Science Foundation of China (Grant nos. 81770400 and 81370345), the Foundation of Nantong Science and Technology Bureau (Grant no. JC2020025), the Health Committee of Nantong (Grant no. MB2020021), and the Clinical Medicine Special Program from Nantong University (Grant no. 2019JY017).

Acknowledgments

We gratefully acknowledge the data provided by patients and researchers participating in GEO. We thank Henry Xie at Nantong University, Nantong Institute of Bioinformatics for the critical reading of the manuscript.

Conflict of interest

The authors declare that the research was conducted in the absence of any commercial or financial relationships that could be construed as a potential conflict of interest.

Publisher's note

Supplementary material

The Supplementary Material for this article can be found online at: https://www.frontiersin.org/articles/10.3389/fcvm.2022.996809/full#supplementary-material

References

1. Bray F, Laversanne M, Cao B, Varghese C, Mikkelsen B, Weiderpass E, et al. Comparing cancer and cardiovascular disease trends in 20 middle- or high-income countries 2000-19: a pointer to national trajectories towards achieving sustainable development goal target 3.4. *Cancer Treat Rev.* (2021) 100:102290.

2. Liang Z, He Y, Hu X. Cardio-oncology: mechanisms, drug combinations, and reverse cardio-oncology. *Int J Mol Sci.* (2022) 23:10617. doi: 10.3390/ijms231810617

3. Wang Y, Wang Y, Han X, Sun J, Li C, Adhikari B, et al. Cardio-oncology: a myriad of relationships between cardiovascular disease and cancer. *Front Cardiovasc Med.* (2022) 9:727487. doi: 10.3389/fcvm.2022.727487

4. Curigliano G, Cardinale D, Dent S, Criscitiello C, Aseyev O, Lenihan D, et al. Cardiotoxicity of anticancer treatments: epidemiology, detection, and management. *CA Cancer J Clin.* (2016) 66:309–25.

5. Wenningmann N, Knapp M, Ande A, Vaidya T, Ait-Oudhia S. Insights into doxorubicin-induced cardiotoxicity: molecular mechanisms, preventive strategies, and early monitoring. *Mol Pharmacol.* (2019) 96:219–32. doi: 10.1124/mol.119.115725

6. Willis M, Parry T, Brown D, Mota R, Huang W, Beak J, et al. Doxorubicin exposure causes subacute cardiac atrophy dependent on the striated muscle-specific ubiquitin ligase MuRF1. *Circ Heart Fail.* (2019) 12:e005234. doi: 10.1161/CIRCHEARTFAILURE.118.005234

7. Ma Z, Kong C, Wu H, Song P, Zhang X, Yuan Y, et al. Toll-like receptor 5 deficiency diminishes doxorubicin-induced acute cardiotoxicity in mice. *Theranostics.* (2020) 10:11013–25. doi: 10.7150/thno.47516

8. Rahbardar M, Eisvand F, Rameshrad M, Razavi B, Hosseinzadeh H. In vivo and in vitro protective effects of rosmarinic acid against doxorubicin-induced cardiotoxicity. *Nutr Cancer.* (2022) 74:747–60. doi: 10.1080/01635581.2021.1931362

9. Eisvand F, Imenshahidi M, Ghasemzadeh Rahbardar M, Tabatabaei Yazdi S, Rameshrad M, Razavi B, et al. Cardioprotective effects of alpha-mangostin on doxorubicin-induced cardiotoxicity in rats. *Phytother Res.* (2022) 36:506–24. doi: 10.1002/ptr.7356

10. Sangweni N, Gabuza K, Huisamen B, Mabasa L, van Vuuren D, Johnson R. Molecular insights into the pathophysiology of doxorubicin-induced cardiotoxicity: a graphical representation. *Arch Toxicol.* (2022) 96:1541–50. doi: 10.1007/s00204-022-03262-w

11. Octavia Y, Tocchetti C, Gabrielson K, Janssens S, Crijns H, Moens A. Doxorubicin-induced cardiomyopathy: from molecular mechanisms to therapeutic strategies. *J Mol Cell Cardiol.* (2012) 52:1213–25.

12. Kankeu C, Clarke K, Passante E, Huber H. Doxorubicin-induced chronic dilated cardiomyopathy-the apoptosis hypothesis revisited. *J Mol Med (Berl).* (2017) 95:239–48. doi: 10.1007/s00109-016-1494-0

13. Wang P, Lan R, Guo Z, Cai S, Wang J, Wang Q, et al. Histone demethylase JMJD3 mediated doxorubicin-induced cardiomyopathy by suppressing SESN2 expression. *Front Cell Dev Biol.* (2020) 8:548605. doi: 10.3389/fcell.2020.548605

14. Oshi M, Angarita F, Tokumaru Y, Yan L, Matsuyama R, Endo I, et al. High expression of NRF2 is associated with increased tumor-infiltrating lymphocytes and cancer immunity in ER-positive/HER2-negative breast cancer. *Cancers (Basel).* (2020) 12:3856. doi: 10.3390/cancers12123856

15. Hunt G, Grassi L, Henkin R, Smeraldi F, Spargo T, Kabiljo R, et al. GEOexplorer: a webserver for gene expression analysis and visualisation. *Nucleic Acids Res.* (2022) 50:W367–74. doi: 10.1093/nar/gkac364

16. Barrett T, Troup D, Wilhite S, Ledoux P, Rudnev D, Evangelista C, et al. NCBI GEO: mining tens of millions of expression profiles–database and tools update. *Nucleic Acids Res.* (2007) 35:D760–5. doi: 10.1093/nar/gkl887

17. Qin D, Yue R, Deng P, Wang X, Zheng Z, Lv M, et al. 8-Formylophiopogonanone B antagonizes doxorubicin-induced cardiotoxicity by suppressing heme oxygenase-1-dependent myocardial inflammation and fibrosis. *Biomed Pharmacother.* (2021) 140:111779. doi: 10.1016/j.biopha.2021.111779

18. Zhang W, Zheng Y, Wu Y. Protective effects of oroxylin A against doxorubicin-induced cardiotoxicity via the activation of Sirt1 in mice. *Oxid Med Cell Longev.* (2021) 2021:6610543. doi: 10.1155/2021/6610543

19. Ye S, Su L, Shan P, Ye B, Wu S, Liang G, et al. LCZ696 attenuated doxorubicin-induced chronic cardiomyopathy through the TLR2-MyD88 complex formation. *Front Cell Dev Biol.* (2021) 9:654051. doi: 10.3389/fcell.2021.654051

20. An L, Hu X, Zhang S, Hu X, Song Z, Naz A, et al. UVRAG deficiency exacerbates doxorubicin-induced cardiotoxicity. *Sci Rep.* (2017) 7:43251. doi: 10.1038/srep43251

21. Nippert, F, Schreckenberg R, Schluter K. Isolation and cultivation of adult rat cardiomyocytes. *J Vis Exp.* (2017) 128:56634.

22. Li N, Li L, Wu M, Li Y, Yang J, Wu Y, et al. Integrated bioinformatics and validation reveal potential biomarkers associated with progression of primary Sjogren's syndrome. *Front Immunol.* (2021) 12:697157. doi: 10.3389/fimmu.2021.697157

23. Carreras J, Hiraiwa S, Kikuti Y, Miyaoka M, Tomita S, Ikoma H, et al. Artificial neural networks predicted the overall survival and molecular subtypes of diffuse large B-cell lymphoma using a pancancer immune-oncology panel. *Cancers (Basel).* (2021) 13:6384. doi: 10.3390/cancers13246384

24. Zhang W, Lai X, Guo X. Activation of Nrf2 by miR-152 inhibits doxorubicin-induced cardiotoxicity via attenuation of oxidative stress, inflammation, and apoptosis. *Oxid Med Cell Longev.* (2021) 2021:8860883. doi: 10.1155/2021/8860883

25. Qi J, Yang Y, Jiang C, Zhao Y, Wu Y, Han X, et al. Exploring the mechanism of danshensu in the treatment of doxorubicin-induced cardiotoxicity based on network pharmacology and experimental evaluation. *Front Cardiovasc Med.* (2022) 9:827975. doi: 10.3389/fcvm.2022.827975

26. Tan G, Lou Z, Liao W, Zhu Z, Dong X, Zhang W, et al. Potential biomarkers in mouse myocardium of doxorubicin-induced cardiomyopathy: a metabonomic method and its application. *PLoS One.* (2011) 6:e27683. doi: 10.1371/journal.pone.0027683

27. Ni C, Ma P, Wang R, Lou X, Liu X, Qin Y, et al. Doxorubicin-induced cardiotoxicity involves IFNgamma-mediated metabolic reprogramming in cardiomyocytes. *J Pathol.* (2019) 247:320–32. doi: 10.1002/path.5192

28. Bostick B, Aroor A, Habibi J, Durante W, Ma L, DeMarco V, et al. Daily exercise prevents diastolic dysfunction and oxidative stress in a female mouse model of western diet induced obesity by maintaining cardiac heme oxygenase-1 levels. *Metabolism.* (2017) 66:14–22. doi: 10.1016/j.metabol.2016.09.005

29. Ciric Zdravkovic S, Kostic T, Marcetic Z, Sulovic L, Nedeljkovic B, Preljevic A, et al. Melatonin modulates acute cardiac muscle damage induced by carbon tetrachloride - involvement of oxidative damage, glutathione, and arginine and nitric oxide metabolism. *Can J Physiol Pharmacol.* (2021) 99:360–7. doi: 10.1139/cjpp-2020-0201

30. Paulus W. Unfolding discoveries in heart failure. *N Engl J Med.* (2020) 382:679–82.

31. Syukri A, Budu, Hatta M, Amir M, Rohman M, Mappangara I, et al. Doxorubicin induced immune abnormalities and inflammatory responses via HMGB1, HIF1-alpha and VEGF pathway in progressive of cardiovascular damage. *Ann Med Surg (Lond).* (2022) 76:103501. doi: 10.1016/j.amsu.2022.103501

32. Yu L, Cao Z, Makhoul I, Daniels J, Klimberg S, Wei J, et al. Immune response proteins as predictive biomarkers of doxorubicin-induced cardiotoxicity in breast cancer patients. *Exp Biol Med (Maywood).* (2018) 243:248–55.

33. Horiguchi H, Loftus T, Hawkins R, Raymond S, Stortz J, Hollen M, et al. Innate immunity in the persistent inflammation, immunosuppression, and catabolism syndrome and its implications for therapy. *Front Immunol.* (2018) 9:595. doi: 10.3389/fimmu.2018.00595

34. Hawkins R, Raymond S, Stortz J, Horiguchi H, Brakenridge S, Gardner A, et al. Chronic critical illness and the persistent inflammation, immunosuppression, and catabolism syndrome. *Front Immunol.* (2018) 9:1511. doi: 10.3389/fimmu.2018.01511

35. Fattahi F, Ward P. Understanding immunosuppression after sepsis. *Immunity.* (2017) 47:3–5.

36. Torgersen C, Moser P, Luckner G, Mayr V, Jochberger S, Hasibeder W, et al. Macroscopic postmortem findings in 235 surgical intensive care patients with sepsis. *Anesth Analg.* (2009) 108:1841–7. doi: 10.1213/ane.0b013e318195e11d

37. Steidle-Kloc E, Schonfelder M, Muller E, Sixt S, Schuler G, Patsch W, et al. Does exercise training impact clock genes in patients with coronary artery disease and type 2 diabetes mellitus? *Eur J Prev Cardiol.* (2016) 23:1375–82. doi: 10.1177/2047487316639682

38. Ucar B, Ucar G, Saha S, Buttari B, Profumo E, Saso L. Pharmacological protection against ischemia-reperfusion injury by regulating the Nrf2-Keap1-ARE signaling pathway. *Antioxidants (Basel).* (2021) 10:823.

39. Liang F, Godley B. Oxidative stress-induced mitochondrial DNA damage in human retinal pigment epithelial cells: a possible mechanism for RPE aging and age-related macular degeneration. *Exp Eye Res.* (2003) 76:397–403. doi: 10.1016/s0014-4835(03)00023-x

40. Wang Z, Gao J, Teng H, Peng J. Effects of doxorubicin on heme biosynthesis and metabolism in cardiomyocyte. *Arq Bras Cardiol.* (2021) 116:315–22.

41. Brito V, Nascimento L, Nunes R, Moura D, Lago P, Saffi J. Exercise during pregnancy decreases doxorubicin-induced cardiotoxic effects on neonatal hearts. *Toxicology.* (2016) 368-369:46–57. doi: 10.1016/j.tox.2016.08.017

42. Ishikawa K, Takenaga K, Akimoto M, Koshikawa N, Yamaguchi A, Imanishi H, et al. ROS-generating mitochondrial DNA mutations can regulate tumor cell metastasis. *Science.* (2008) 320:661–4.

43. Bonora M, Bononi A, De Marchi E, Giorgi C, Lebiedzinska M, Marchi S, et al. Role of the c subunit of the FO ATP synthase in mitochondrial permeability transition. *Cell Cycle.* (2013) 12:674–83. doi: 10.4161/cc.23599

44. Morciano G, Pedriali G, Bonora M, Pavasini R, Mikus E, Calvi S, et al. A naturally occurring mutation in ATP synthase subunit c is associated with increased damage following hypoxia/reoxygenation in STEMI patients. *Cell Rep.* (2021) 35:108983. doi: 10.1016/j.celrep.2021.108983

45. Enomoto H, Mittal N, Inomata T, Arimura T, Izumi T, Kimura A, et al. Dilated cardiomyopathy-linked heat shock protein family D member 1 mutations cause up-regulation of reactive oxygen species and autophagy through mitochondrial dysfunction. *Cardiovasc Res.* (2021) 117:1118–31. doi: 10.1093/cvr/cvaa158

46. Krishnan-Sivadoss I, Mijares-Rojas I, Villarreal-Leal R, Torre-Amione G, Knowlton A, Guerrero-Beltran C. Heat shock protein 60 and cardiovascular diseases: an intricate love-hate story. *Med Res Rev.* (2021) 41:29–71. doi: 10.1002/med.21723

47. Ascensao A, Lumini-Oliveira J, Machado N, Ferreira R, Goncalves I, Moreira A, et al. Acute exercise protects against calcium-induced cardiac mitochondrial permeability transition pore opening in doxorubicin-treated rats. *Clin Sci (Lond).* (2011) 120:37–49. doi: 10.1042/CS20100254

48. Hirawa N, Uehara Y, Yamakado M, Toya Y, Gomi T, Ikeda T, et al. Lipocalin-type prostaglandin d synthase in essential hypertension. *Hypertension.* (2002) 39(2 Pt 2):449–54. doi: 10.1161/hy0202.102835

49. Zhu L, Luo X, Fu N, Chen L. Mitochondrial unfolded protein response: a novel pathway in metabolism and immunity. *Pharmacol Res.* (2021) 168:105603.

50. Cheng S, Scicluna B, Arts R, Gresnigt M, Lachmandas E, Giamarellos-Bourboulis E, et al. Broad defects in the energy metabolism of leukocytes underlie immunoparalysis in sepsis. *Nat Immunol.* (2016) 17:406–13. doi: 10.1038/ni.3398

51. Kau A, Ahern P, Griffin N, Goodman A, Gordon J. Human nutrition, the gut microbiome and the immune system. *Nature.* (2011) 474:327–36.

52. Bieghs V, Trautwein C. The innate immune response during liver inflammation and metabolic disease. *Trends Immunol.* (2013) 34:446–52.

53. Yu K, Chen Z, Khatri I, Gorczynski R. CCR4 dependent migration of Foxp3+ Treg cells to skin grafts and draining lymph nodes is implicated in enhanced graft survival in CD200tg recipients. *Immunol Lett.* (2011) 141:116–22. doi: 10.1016/j.imlet.2011.09.002

54. Raid R, Krinka D, Bakhoff L, Abdelwahid E, Jokinen E, Karner M, et al. Lack of Gata3 results in conotruncal heart anomalies in mouse. *Mech Dev.* (2009) 126:80–9. doi: 10.1016/j.mod.2008.10.001

55. Katayama M, Vieira R, Andrade V, Roela R, Lima L, Kerr L, et al. Stromal cell signature associated with response to neoadjuvant chemotherapy in locally advanced breast cancer. *Cells.* (2019) 8:1566. doi: 10.3390/cells8121566

56. Kolur V, Vastrad B, Vastrad C, Kottursheti S, Tengli A. Identification of candidate biomarkers and therapeutic agents for heart failure by bioinformatics analysis. *BMC Cardiovasc Disord.* (2021) 21:329. doi: 10.1186/s12872-021-02146-8

57. Goldman A, Maor E, Bomze D, Liu J, Herrmann J, Fein J, et al. Adverse cardiovascular and pulmonary events associated with chimeric antigen receptor T-cell therapy. *J Am Coll Cardiol.* (2021) 78:1800–13. doi: 10.1016/j.jacc.2021.08.044

58. Gao Y, Sun B, Hu J, Ren H, Zhou H, Chen L, et al. Identification of gene modules associated with survival of diffuse large B-cell lymphoma treated with CHOP-based chemotherapy. *Pharmacogenomics J.* (2020) 20:705–16. doi: 10.1038/s41397-020-0161-6

59. Noutsias M, Rohde M, Goldner K, Block A, Blunert K, Hemaidan L, et al. Expression of functional T-cell markers and T-cell receptor Vbeta repertoire in endomyocardial biopsies from patients presenting with acute myocarditis and dilated cardiomyopathy. *Eur J Heart Fail.* (2011) 13:611–8. doi: 10.1093/eurjhf/hfr014

60. Li L, Fan D, Wang C, Wang J, Cui X, Wu D, et al. Angiotensin II increases periostin expression via Ras/p38 MAPK/CREB and ERK1/2/TGF-beta1 pathways in cardiac fibroblasts. *Cardiovasc Res.* (2011) 91:80–9. doi: 10.1093/cvr/cvr067

61. Tian X, Cai J, Ma S, Fang Y, Huang H, Lin T, et al. BRD2 induces drug resistance through activation of the RasGRP1/Ras/ERK signaling pathway in adult T-cell lymphoblastic lymphoma. *Cancer Commun (Lond).* (2020) 40:245–59. doi: 10.1002/cac2.12039

62. Zheng M, Zhu W, Han Q, Xiao R. Emerging concepts and therapeutic implications of beta-adrenergic receptor subtype signaling. *Pharmacol Ther.* (2005) 108:257–68. doi: 10.1016/j.pharmthera.2005.04.006

63. Woo A, Song Y, Xiao R, Zhu W. Biased beta2-adrenoceptor signalling in heart failure: pathophysiology and drug discovery. *Br J Pharmacol.* (2015) 172:5444–56. doi: 10.1111/bph.12965

64. Huang Y, Zhang K, Liu M, Su J, Qin X, Wang X, et al. An herbal preparation ameliorates heart failure with preserved ejection fraction by alleviating microvascular endothelial inflammation and activating NO-cGMP-PKG pathway. *Phytomedicine.* (2021) 91:153633. doi: 10.1016/j.phymed.2021.153633

65. Wang Z, Wang J, Xie R, Liu R, Lu Y. Mitochondria-derived reactive oxygen species play an important role in doxorubicin-induced platelet apoptosis. *Int J Mol Sci.* (2015) 16:11087–100. doi: 10.3390/ijms160511087

66. Zhu J, Zhou H, Li C, He Y, Pan Y, Shou Q, et al. Guanxinshutong capsule ameliorates cardiac function and architecture following myocardial injury by modulating ventricular remodeling in rats. *Biomed Pharmacother.* (2020) 130:110527. doi: 10.1016/j.biopha.2020.110527

67. V A, Nayar P, Murugesan R, S S, Krishnan J, Ahmed S. A systems biology and proteomics-based approach identifies SRC and VEGFA as biomarkers in risk factor mediated coronary heart disease. *Mol Biosyst.* (2016) 12:2594–604. doi: 10.1039/c6mb00264a

68. Zhang L, Liu L, Li X. MiR-526b-3p mediates doxorubicin-induced cardiotoxicity by targeting STAT3 to inactivate VEGFA. *Biomed Pharmacother.* (2020) 123:109751. doi: 10.1016/j.biopha.2019.109751

69. Tham E, Wang J, Piehl F, Weber G. Upregulation of VEGF-a without angiogenesis in a mouse model of dilated cardiomyopathy caused by mitochondrial dysfunction. *J Histochem Cytochem.* (2002) 50:935–44. doi: 10.1177/002215540205000707

70. Karra R, Foglia M, Choi W, Belliveau C, DeBenedittis P, Poss K. Vegfaa instructs cardiac muscle hyperplasia in adult zebrafish. *Proc Natl Acad Sci USA.* (2018) 115:8805–10. doi: 10.1073/pnas.1722594115

71. Milano G, Raucci A, Scopece A, Daniele R, Guerrini U, Sironi L, et al. Doxorubicin and trastuzumab regimen induces biventricular failure in mice. *J Am Soc Echocardiogr.* (2014) 27:568–79. doi: 10.1016/j.echo.2014.01.014

72. Robichaud S, Fairman G, Vijithakumar V, Mak E, Cook D, Pelletier A, et al. Identification of novel lipid droplet factors that regulate lipophagy and cholesterol efflux in macrophage foam cells. *Autophagy.* (2021) 17:3671–89. doi: 10.1080/15548627.2021.1886839

frontiers | Frontiers in Cardiovascular Medicine

TYPE Mini Review
PUBLISHED 21 February 2023
DOI 10.3389/fcvm.2023.1090103

OPEN ACCESS

EDITED BY
June-Wha Rhee,
City of Hope Medical Center, United States

REVIEWED BY
Caitlin Bell,
Stanford University, United States

*CORRESPONDENCE
Massimiliano Camilli
massimiliano.camilli91@gmail.com

SPECIALTY SECTION
This article was submitted to Cardio-Oncology, a section of the journal Frontiers in Cardiovascular Medicine

RECEIVED 04 November 2022
ACCEPTED 06 February 2023
PUBLISHED 21 February 2023

CITATION
Camilli M, Maggio L, Tinti L, Lamendola P, Lanza GA, Crea F and Lombardo A (2023) Chimeric antigen receptor-T cell therapy-related cardiotoxicity in adults and children cancer patients: A clinical appraisal.
Front. Cardiovasc. Med. 10:1090103.
doi: 10.3389/fcvm.2023.1090103

Chimeric antigen receptor-T cell therapy-related cardiotoxicity in adults and children cancer patients: A clinical appraisal

Massimiliano Camilli[1,2]*, Luca Maggio[1], Lorenzo Tinti[1], Priscilla Lamendola[2], Gaetano Antonio Lanza[1,2], Filippo Crea[1,2] and Antonella Lombardo[1,2]

[1]Department of Cardiovascular and Pulmonary Sciences, Catholic University of the Sacred Heart, Rome, Italy, [2]Department of Cardiovascular Medicine, Fondazione Policlinico Universitario A. Gemelli IRCCS, Rome, Italy

Chimeric antigen receptor-T (CAR-T) cells therapies represent an innovative immunological treatment for patients suffering from advanced and refractory onco-hematological malignancies. The infusion of engineered T-cells, exposing chimeric receptors on the cell surface, leads to an immune response against the tumor cells. However, data from clinical trials and observational studies showed the occurrence of a constellation of adverse events related to CAR-T cells infusion, ranging from mild effects to life-threatening organ-specific complications. In particular, CAR-T cell-related cardiovascular toxicities represent an emerging group of adverse events observed in these patients, correlated with increased morbidity and mortality. Mechanisms involved are still under investigation, although the aberrant inflammatory activation observed in cytokine release syndrome (CRS) seems to play a pivotal role. The most frequently reported cardiac events, observed both in adults and in the pediatric population, are represented by hypotension, arrhythmias and left ventricular systolic dysfunction, sometimes associated with overt heart failure. Therefore, there is an increasing need to understand the pathophysiological basis of cardiotoxicity and risk factors related to its development, in order to identify most vulnerable patients requiring a close cardiological monitoring and long-term follow-up. This review aims at highlighting CAR-T cell-related cardiovascular complications and clarifying the pathogenetic mechanisms coming at play. Moreover, we will shed light on surveillance strategies and cardiotoxicity management protocols, as well as on future research perspectives in this expanding field.

KEYWORDS

chimeric antigen receptor T-cell therapy, cardiotoxicity, heart failure, cardio-oncology, cardio-immunology

1. Introduction

In the recent years, immune-related therapies have revolutionized the field of onco-hematology, gaining a primary role in the treatment of solid and liquid cancers associated with poor prognosis (1).

Chimeric antigen receptor T (CAR-T) cells administration represents a novel paradigm of cancer management, consisting in the infusion of "engineered" immune cells able to elicit a response against the tumor (2). The biological foundations of this treatment are layed on the development of *in vitro* mature T-cell receptor (TCR)-lymphocytes, created to recognize tumor cells antigens (3). These chimeric receptors are composed by four domains: the extracellular antigen-binding portion, tailored to recognize the specific tumor target, an hinge point, the transmembrane domain and the signaling domain, responsible for signal transduction into the cell and linked with different other co-stimulatory molecules (4). The antigen-binding domain, constituted by an antibody-specific fragment obtained from monoclonal antibodies, leads to the recognition of the target tumor antigen, subsequently resulting in a major histocompatibility complex (MHC)-independent activation of the engineered T cells antitumor function (5, 6). In order to enhance the efficacy of CAR-T cells, a chemotherapeutic scheme containing fludarabine/cyclophosphamide is generally co-administrated. This conditioning regimen determines different biological effects, such as lymphodepletion, eradication of immunosuppressive cells (regulatory T cells and myeloid-derived suppressor cells), modulation of tumor microenvironment and increased expansion and persistence of CAR-T cells (7–10).

Over the years, numerous studies have been carried out with the aim of improving T cells clonal expansion and cytokine secretion. The first CAR-T cell therapy to be approved in 2017 was Axicabtagene Ciloleucel, developed to treat adults with relapsed or refractory (R-R) large B-cell lymphoma expressing membrane antigen cluster domain (CD)19 (11). Approvement came after the ZUMA-1 trial, a multicenter phase 2 study, that reported in the 101 patients finally treated, an objective response rate of 82 and 54% of complete remission rate (12). Tisagenlecleucel was instead, distributed after the results of the ELIANA trial, which reported an overall remission in 81% of the 75 patients enrolled within 3 months (13, 14). The non-CD19 cell therapy firstly approved was Idecabtagene Vicleucel, created against B-cell maturation antigen (BCMA): this demonstrated an encouraging response rate of 73% in a phase II study in patients with R-R multiple myeloma (15).

Thanks to the success obtained in B-cell malignancies, new trials have been launched with the aim of replicating the same results in other tumors, such as non-Hodgkin lymphoma (NCT02315612) and chronic lymphocytic leukemia (NCT02194374), or otherwise solid neoplasms like hepatocellular carcinoma (NCT02541370), breast cancer (NCT00673829) or pancreatic cancer (NCT02706782) (5).

Similarly to other oncological targeted therapies, CAR-T cells demonstrated in clinical trials to be associated with several adverse events, sometimes fatal. In particular, available evidences, including prospective and retrospective reports, highlighted a correlation between CAR-T cell therapy and cardiovascular (CV) adverse complications, both in children and adults, significantly affecting morbidity and mortality (12, 13, 15–24). Given the increasing number of patients who will benefit from this therapy in the near future, it is expected that CAR-T cell therapy-related cardiotoxicity will become a clinical problem not uncommon to cardiologists. Therefore, the aim of this review is to provide a general picture of CAR-T cell therapy CV effects, briefly describing their pathophysiological mechanisms and clinical implications. We will make a distinction between adult and pediatric population, provide practical management/surveillance advises and shed light on future research perspectives in this field.

2. Pathogenesis of CAR-T cell therapy CV toxicity

The spread of CAR-T cell therapy in the hemato-oncological population has led to the identification of novel forms of toxicity, both systemic and organ-specific (25). The most common manifestation of CAR-T cell-related toxicity is the cytokine release syndrome (CRS), characterized by a proinflammatory cytokine "storm," subsequent to the infusion of cells and their interaction with the tumor microenvironment (26). In the 2018 American Society for Transplantation and Cellular Therapy (ASTCT) consensus, CRS is defined as a supraphysiologic response following any immune therapy that results in the activation or engagement of endogenous or infused T cells and/or other immune effector cells. In CRS clinical presentation, symptoms can be progressive and may include fever (mostly present at onset), hypotension, hypoxia, capillary leak syndrome and life-threatening organ dysfunctions (27).

In Lee et al. (28) proposed a revised grading system of CRS: in grade 1 symptoms are not life threatening (fever, nausea, fatigue, headache, myalgias) and require symptomatic treatment only; in grade 2 symptoms require and respond to moderate intervention, such as hypotension responsive to fluids or low dose of one vasopressor or Grade 2 organ toxicity, with oxygen requirement $< 40\%$ FiO2. Grade 3 symptoms require an aggressive intervention, such as hypotension requiring high dose or multiple vasopressors, Grade 3 organ toxicity or grade 4 transaminitis, with oxygen requirement $> 40\%$ FiO2. In Grade 4, symptoms are life-threatening, with requirement for ventilator support or Grade 4 organ toxicity (excluding transaminitis); lastly, grade 5 relates instead to death (28, 29).

The basis of these manifestations is complex: Morris et al. (30) proposed a five phases process of CRS pathophysiology. The first relates to the interaction between CAR-T cells and tumor site, with the recognition of antigen-expressing target cells; gradually the proliferation of CAR-T cells and *in situ* cytokine production by both CAR-T cells and cellular components of the tumor microenvironment occur. The proliferation of CAR-T cells, together with increased cytokine levels, leads to a systemic inflammatory response, associated with endothelial injury and tissue capillary leakage. Progressively, the transmigration of cytokines, CAR-T cells and immune system cellular effectors into the central nervous system, causes a breakdown of the blood–brain barrier. At last, the eradication of the tumor and the inactivation of the immune response, results in decreased cytokine levels and systemic inflammatory response. Therefore, the interaction

between CAR-T cells and tumor microenvironment, and the associated up-regulation of proinflammatory cytokine secretion into the bloodstream, represent a crucial phase in the genesis of CRS (31).

Different studies on murine models highlighted the main role of *in situ* monocyte/macrophage cells in the secretion of pro-inflammatory cytokines, such as interleukin (IL)-6 and IL-1, and the correlation between their blood levels and CRS mortality (32, 33). In these reports, the blockade of IL-6 and IL-1 signaling pathways in humanized murine models caused downregulation of proinflammatory cytokine secretion and resolution of most CRS clinical manifestations. As a result, various consecutive clinical studies demonstrated the role of anti-IL-6 monoclonal antibody tocilizumab as first-line therapy in CRS management; ongoing clinical trials on IL-1 antagonist Anakinra aim to prove its role as an emergent therapeutic option (NCT04148430) (32, 34, 35).

Other pro-inflammatory soluble effectors revealed to play a pivotal role in the CRS pathogenesis, such as Granulocyte-Macrophage Colony Stimulating Factor (GM CSF) and Tumor Necrosis Factor (TNF)-alpha The blockade of their signaling pathways on murine models has also been shown to be associated with reduced IL-6 levels and CRS manifestations, without interfering with the antitumor effects of CAR-T cells (36, 37).

That said, although mechanisms involved in the pathogenesis of CV toxicity may be numerous and are still under investigation, the abnormal proinflammatory cytokine release related to the occurrence of CRS is one of the most recognized mediators so far.

The resemblance of CAR-T cell related cardiac dysfunction with cardiomyopathies observed during sepsis, has suggested the recognition of the elevated levels of IL-6 as a common substrate of myocardial depression (38). Actually, in sepsis-related cardiomyopathy, the elevated levels of proinflammatory cytokines leads to microvascular dysfunction with capillary permeability, mitochondrial dysfunction and altered intracellular calcium metabolism, that are responsible for myocardial inflammation and impaired perfusion (39). As exposed afterward, alterations in myocardial performance, observed in patients undergoing CAR-T cell infusion, are most commonly related to higher grades of CRS, highlighting the close relationship between cardiomyocyte damage and inflammatory response.

Another peculiar mechanism of CV toxicity was observed by Linette et al. (40), that firstly described two cases of fatal myocarditis and cardiogenic shock occurred as a result of cross-reactivity of engineered T cells expressing an affinity-enhanced receptor against MAGE-A3 (melanoma-associated antigen-3), which cross-reacted with titin, a myocardial protein. Of note, these manifestations were observed with an old generation of engineered T-cells therapy, and to date, there are no reports of cardiac toxicity through cross-reactivity with the new approved CAR-T cells, although research in this field is needed.

In these pathogenetic considerations, it should be acknowledged that patients undergoing CAR-T cell administration have been already exposed to numerous potentially cardiotoxic chemotherapy lines, influencing the susceptibility to myocardial dysfunction (41).

Table 1 summarizes available studies in the adult and pediatric population.

3. CAR-T cell therapy cardiotoxicity in adult patients

Although patients with recent or previous cardiovascular events were excluded from main clinical trials leading to the approval of CAR-T cell therapies, in real-world observational data a high percentage of subjects undergoing this therapy experienced CV side effects, that have been associated with significant morbidity and mortality (41). Increasing pharmacovigilance data about patients treated with CAR-T cell therapies are now available.

A wide variety of cardiac adverse events has been reported in adults, including hypotension (in some cases life-threatening requiring vasopressor support), arrhythmias, left ventricular systolic dysfunction, myocardial injury, ST-segment changes on the electrocardiogram (ECG) and rarely cardiac death (42). Most of cardiac manifestations reported, in particular hypotension and reflex tachycardia, can arise as cardiovascular issues or mostly as consequences of CRS (43), so it may result difficult to regard them as pure cardiotoxic events.

Goldman et al. (19) reported data on 2,657 patients exposed to CAR-T cell therapy (65% treated with Axicabtagene and 35% with Tisagenlecleucel). The treatment was associated with hypotension (10.8%), tachyarrhythmias (2.8%, among which atrial fibrillation was the most frequent), cardiomyopathy (2.6%), cardiogenic shock (1.8%) and pericardial disease (0.4%).

When comparing CAR-T products, Axicabtagene was associated with higher reporting of CRS (59% vs 47%), tachyarrhythmias (3.4% vs 1.7%), and VTE (1.6% vs 0.7%). Any grade CRS was reported in 55% of studied population and the authors further focused on the overlap between CRS and cardiovascular events. Concurrent CRS was reported in 78% of hypotension cases, 79% of tachyarrhythmia, 65% of cardiogenic shocks, 51% of cardiomyopathy cases and with 64% of pericardial manifestations (19).

Analogously, Salem et al. (20) described the treatment effects on 1,921 subjects, among which 13.3% documented similar cardiac events, all of which occurred in association with grade $\geq$ 2 CRS. Among patients suffering from cardiac events, 57% were treated with Axicabtagene and 43% were treated with Tisagenlecleucel (20).

As far as clinical trials on CAR-T cell therapies are concerned, in ZUMA-1, JULIET, ZUMA-2 and NCT03361748, hypotension of any grade was described in 16–59% of the analyzed population, with up to 22% of these requiring vasopressor support. Another cardiac adverse event frequently reported was tachycardia (11–39%). As well, in ZUMA-1 trial, a case of cardiac arrest occurred in a patient with grade 5 CRS (12, 15, 22, 44). Nevertheless, the 2-year follow-up data of the same trial showed development of hypertension in 16% of patients (45).

In depth, Neelapu et al. (12) and Wang et al. (22) reported data about the correlation between CRS and cardiovascular events: in ZUMA-1 trial, 54% of tachycardia cases, 68% of any grade hypotension and 64% of $\geq$3 grade hypotension were associated with CRS, while in ZUMA-2 all cases of hypotension and 76% of tachycardia occurred in the context of CRS.

Smaller phase I clinical trials reported grade $\geq$ 3 hypotension in 20–37% and left ventricular dysfunction in 10% of treated patients (46–49).

TABLE 1 Summary of cardiovascular adverse events reported in studies enrolling adult and pediatric patients.

Study	Disease and patient population in safety analysis	Grade ≥ 3 CRS	Hypotension requiring vasopressor support or shock	Reduced EF	Tachycardia	Cardiac arrest	Other cardiac adverse events
Adult population							
Neelapu et al. (12) (ZUMA-1) phase II clinical trial	LBCL (n = 101)	13 (12.9%) (Lee criteria) (28)	14 (13.9%)	–	39 (39.4%)	1 (<1%)	Cardiac death: 1 (<1%)
Schuster et al. (44) (JULIET) phase II clinical trial	LBCL (n = 111)	24 (21.6%) (Penn criteria) (60)	10 (9%)	–	12 (10.8%)	–	–
Wang et al. (22) (ZUMA-2) phase II clinical trial	MCL (n = 68)	10 (14.7%) (Lee criteria) (28)	15 (22.1%)	–	21 (30.9%)	–	–
Alvi et al. (21) retrospective	NHL, MM (n = 137)	6 (4.4%) (Lee criteria) (28)	–	8/29 (27.6%)*,¥	–	3 (2.2%)	Cardiac death: 6 (4.4%) HF: 6 (4.4%) arrhythmia: 5 (3.6%) elevated troponin: 29/53 (54.7%)°
Ganatra et al. (50) retrospective	NHL, B-ALL, PML (n = 187)	10 (5.3%) (Lee criteria) (28)	14 (7.5%)	12/116 (10.3%)^, ¥	–	–	Cardiac death: 3 (1.6%)
Lefebvre et al. (17) retrospective	NHL, B-ALL, CLL (n = 145)	–	33 (22.7%)	–	–	1 (0.7%)	Cardiac death: 2 (1.4%) HF: 21 (14.5%) Arrhythmia: 13 (8.9%) ACS: 2 (1.3%)
Munshi et al. (15) (NCT03361748) phase II clinical trial	MM (n = 128)	7 (5.5%) (Lee criteria) (28)	1 (<1%)	–	–	–	–
Goldman et al. (19) retrospective	Various (n = 2657)	–	–	69 (2.6%)°°	–	–	Arrhythmia: 74 (2.8%) pericardial disease: 11 (0.4%) VTE: 28 (1.6%) cardiogenic shock: 49 (1.8%)
Pediatric and young adult population							
Maude et al. (52) phase I-IIa clinical trial	B-ALL (n = 30)^^	8 (27%)	8 (27%)	–	–	–	Severe coagulopathy: 3 (10%)
Lee et al. (51) phase I clinical trial	B-ALL (n = 25)	6 (32%) (Lee criteria) (51)	4 (22%)	1 (5%)¬	–	1 (5%)	QT prolongation: 1 (5%)
Fitzgerald et al. (18) retrospective	B-ALL (n = 39)	18 (46%) (Porter criteria) (61)	13 (33%)	1 (2%)∞	–	–	–
Maude et al. (13) (ELIANA) phase II clinical trial	B-ALL (n = 75)	25 (46%) (Penn criteria) (60)	13 (17%)	3 (4%)**	3 (4%)	3 (4%)	HF: 2 (2.7%)
Burstein et al. (54) retrospective	B-ALL, NHL, T-ALL, APL (n = 98)	24 (24%) (Penn criteria) (60)	24 (24%)	10 (10%)±	–	0	ST segment changes: 6 (6%)
Shalabi et al. (23) retrospective	B-ALL, NHL (n = 52)	9 (17%) (Lee criteria) (27, 28)	9 (24.3%)	6 (11.5%)⊥	36 (69.2%)	1 (2.7%)	

APL, acute promyelocytic leukemia; B-ALL, B-cell acute lymphoblastic leukemia; ACS, acute coronary syndrome; CLL, chronic lymphocytic leukemia; CRS, cytokine release syndrome; EF, ejection fraction; HF, hearth failure; LBCL, large B-cell lymphoma; MCL, mantle cell lymphoma; MM, multiple myeloma; NHL, non-Hodgkin lymphoma; PML, primary mediastinal large B-cell lymphoma; T-ALL, T cell-acute lymphoblastic leukemia; VTE, venous thromboembolic events.

*Considered only patients with echocardiographic data pre- and post-CAR-T.

°Considered only patients with post-CAR-T troponin level assessment.

^Considered only patients with serial echocardiogram.

^^Considered a sample size of 25 children and 5 adults.

¥Reduced EF: reduction in LVEF > 10% from baseline to <50%.

°°Left ventricular systolic dysfunction according to MedDRA version 22.1 (62).

±Reduced EF: decrease of ≥10% in ejection fraction or ≥5% in shortening fraction compared with baseline or ejection fraction < 55% or shortening fraction < 28% in those with previously normal systolic function (54).

⊥Reduced EF: decrease of >10% absolute decrease in LVEF compared with baseline or new-onset LVEF < 50% (23).

¬LV systolic dysfunction according to Common Terminology Criteria for Adverse Events v4.02 (63).

∞LV systolic dysfunction according to Goldstein et al. (64).

**LV systolic dysfunction according to Common Terminology Criteria for Adverse Events v4.03 (63).

10.3389/fcvm.2023.1090103

As mentioned, all reported clinical trials excluded subjects with significant pre-existing cardiovascular disease (e.g., heart failure) (12, 15, 22, 44) and they did not focus on the correlation between cardiovascular risk factors and safety endpoints.

Besides clinical trials, real-world, observational studies included, even if marginally, patients with baseline significant cardiac disease (17, 21), and made an attempt to evaluate the role of pre-existing CV risk factors and cardiac biomarkers to predict the occurrence of cardiotoxicity. In a retrospective study of 137 patients treated with CAR-T therapy, Alvi et al. (21) described 17 cases of cardiovascular complications (12%), including 6 cases of cardiovascular death, 6 cases of HF and 5 cases of supraventricular arrhythmia. Of interest, all these events occurred in patients developing high-grade CRS (≥2), and among this population, 69% were treated with Axicabtagene and 31% with other investigational CAR-T.

Furthermore, in this study, the authors evaluated the potential role of troponin in predicting cardiotoxicity. Post-CAR-T cell infusion troponin levels were measured, witnessing that CV event rate for patients with elevated troponin was 55%, compared to 4% in patients without elevation.

As for cardiovascular events, also troponin elevation was closely related to CRS grading (reported in 77% of patients with ≥2 CRS grade vs 22% of patients with lower grade CRS). Among subjects with troponin release, 45% were treated with Axicabtagene and 55% with investigational CAR-T.

When pre- and post-CAR-T cell therapy left ventricular ejection fraction (LVEF) assessment was available, a significant reduction in LVEF was observed in 28% of cases. As mentioned, all these patients had also elevated troponin levels at blood samples (21).

Another retrospective study conducted by Lefebvre et al. (17) evaluated the correlation between major adverse cardiac events (MACE) and population baseline characteristics. In 145 patients, it was reported a total of 41 MACEs. Some pre-CAR-T cell therapy features, as the use of statins, insulin and aspirin, as well as higher baseline creatinine levels, were each associated with MACE, likely reflecting patients with high cardiovascular risk profile and pre-existing comorbidities. The grade of CRS (27) was also defined as an independent predictor of MACE. Baseline LVEF was not associated with MACE in this population, unlike some diastolic parameters, such as elevated E/e' ratio and left atrial volume could represent valuable predictors (17).

Ganatra et al. (50) otherwise focused on development of cardiomyopathy following CAR-T cell therapy in a sample size of 116 patients who underwent serial echocardiograms. Their results demonstrated that 12 patients (about 10% of the population) developed new-onset or worsening cardiomyopathy, nearly always (11/12) in association with grade ≥ 2 CRS. Again, baseline features such as hyperlipidemia or older age, history of coronary artery disease and use of beta blockers and renin-angiotensin inhibitors therapy, appeared to increase the risk of developing cardiomyopathy. Among those patients (n = 12) with cardiomyopathy, 6 had a complete recovery of LVEF, 3 had a partial recovery and 3 died (50). In this report, Axicabtagene was the main treatment investigated (used in 94% of the patients) and it was associated with the majority of cases of new-onset or worsening cardiomyopathy (92% vs 8% associated with Tisagenlecleucel).

Overall, in retrospective studies, the timing from CAR-T infusion to reported cardiac events ranged from a median of 5–21 days (42). This suggests that in adult patients, cardiotoxicity could be closely related to high grade CRS onset and subsequent resolution.

Data regarding the CV effects of CAR-T cell therapy in adults are illustrated in **Table 1**.

4. CAR-T cell therapy cardiotoxicity in the pediatric and young adults population

Thanks to the available data, we are now more aware of the prevalence and impact on morbidity and mortality of CAR-T cell-related CV toxicity in the pediatric and young adult population.

In depth, Lee et al. (51) led a phase I trial enrolling children and young adults with R-R acute lymphoblastic leukemia or non-Hodgkin lymphoma; in a cohort of 21 subjects, 4 (22%) developed severe hypotension requiring vasopressor support, 1 had QT prolongation and 1 hypertension. Furthermore, one patient was successfully resuscitated after cardiac arrest during a severe CRS, associated with a drop in his cardiac ejection fraction from a baseline of 65% to less than 25% (51). In a comparable limited cohort of 30 children and adults with relapsed acute lymphoblastic leukemia (ALL), 27% required vasopressor support for hypotension and 3 subjects presented bleeding due to severe coagulopathy (52).

The ELIANA and ENSIGN phase-2 clinical trials enrolled CD19 + relapsed or refractory B-cell ALL patients, exposed to Tisagenlecleucel, an anti-CD19 CAR T-cell therapy (13, 53). In the face of impressive clinical benefits and hematological disease response, they demonstrated that CV complications were predominantly seen in the first 8 weeks post-infusion, especially during CRS, and were mostly reversible. A pooled analysis from these trials (ELIANA: n = 79; ENSIGN: n = 58) reported that in a total analyzed population of 137 patients, 31% presented cardiac complications, 7% of grade 3 or 4. The most common events were arrhythmias (29%); five patients (4%) developed left ventricular cardiac dysfunction during CRS, which regressed in all but 2 patients, who died due to disease progression. Hypotension occurred in 24% of the patients, 19% of grade 3 or 4 requiring intervention or vasopressor support; interestingly, hypotension was always related with CRS (53). In the ELIANA cohort, 3 (4%) subjects developed LV dysfunction, 2 patients presenting with symptomatic heart failure, and all had cardiac arrest (13).

As regards to retrospective studies, data seem more homogeneous. Fitzgerald et al. (18) reported, in 39 patients receiving CAR-T cells infusion for R-R ALL, that 36% showed CV complications, 13 with fluid refractory shock requiring the infusion of α-agonist, 10 necessitating more than one vasopressor due to catecholamine resistance and 1 supported with milrinone because of the development of diminished left ventricular systolic function (18). CV complications generally occurred within the 5 days after cell infusion, hypotension was always preceded by fever and 96% of the patients with CV complications also had CRS, with 18% CRS grade 3 and 28% CRS grade 4 (18).

Shalabi et al. (23) retrospectively revised the cases of 52 pediatric patients affected by hematological malignancies; nine of

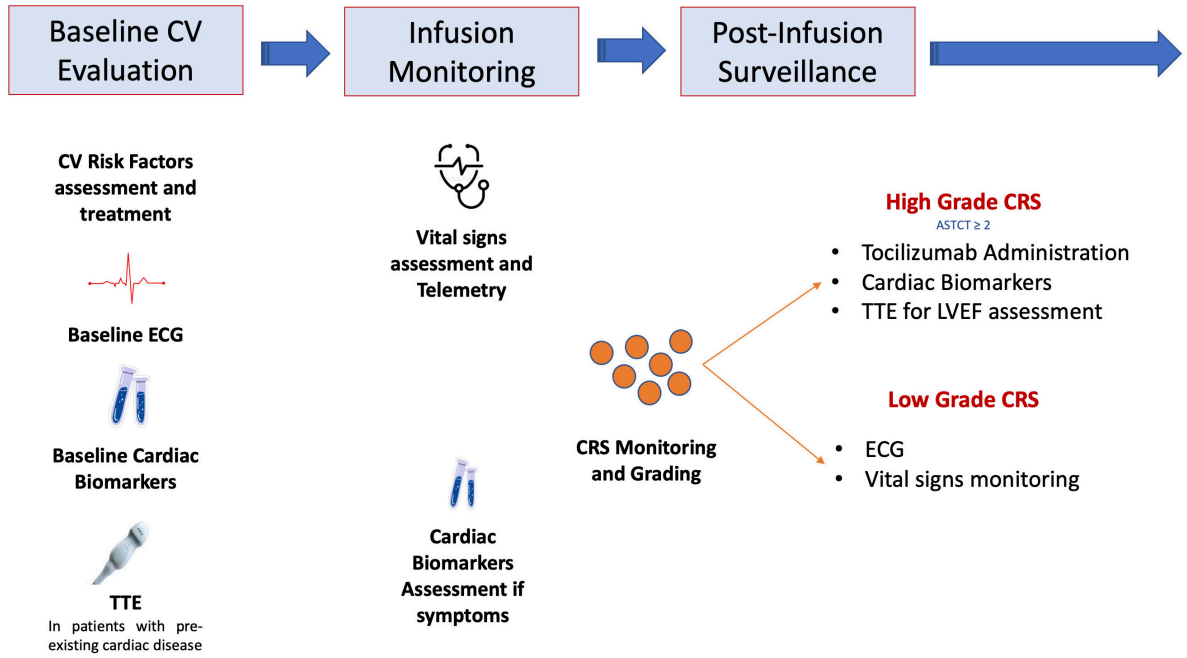

FIGURE 1
Proposed diagnostic work-up and management strategy in patients undergoing chimeric antigen receptor (CAR)-T cell treatment and with suspected cardiovascular toxicity. ASTCT, American Society for Transplantation and Cellular Therapy; CRS, cytokine release syndrome; CV, cardiovascular; ECG, electrocardiogram; TTE, transthoracic echocardiography.

them (17%) developed hypotension requiring vasopressor support. Of the 37 patients with CRS, 6 (16%) presented a post-infusion echocardiogram showing cardiac dysfunction, among whom 4 had grade 3–4 CRS. Of importance, all cases with cardiac dysfunction and HF recovered within 3 months. Moreover, it was noted a higher likelihood of reduced cardiac performance in patients with early and severe CRS, as well as in those receiving tocilizumab. As acknowledged, none of the cases without CRS experienced CV toxicity (23).

In another report including 98 subjects and aimed at identifying predictors of CV toxicity (in particular of hypotension requiring vasopressor support), 24 experienced shock and 10 (41%) of them concomitantly developed cardiac dysfunction. Five subjects with cardiac dysfunction required inotropic support with milrinone and 6 of these needed pharmacological escalation. In accordance with data from other published retrospective studies, all patients affected by CV toxicity had grade 3–4 CRS and those with impaired systolic function recovered by 6 months of follow-up; nevertheless, none of the cardiac events contributed to mortality (54).

In summary, from all the studies available, it seems that cardiac toxicity associated with CAR-T in the pediatric and young adult population is closely associated with CRS and is largely self-limited, with most patients recovering cardiac function back to pre-treatment baseline values within few weeks from exposition (23, 54).

Nevertheless, the majority of data on determinants of cardiotoxicity come from retrospective studies. In pediatric and young adult patients, the risk of developing severe hypotension requiring vasopressor support appears to be associated with high disease burden (>25% of blast on bone marrow biopsy), pre-treatment cardiac dysfunction (lower baseline ejection fraction, lower GLS or diastolic dysfunction), high-grade CRS (3-4), and delays in the administration of tocilizumab for CRS. Pre-existing cardiomyopathy and higher anthracycline dose did not appear to be associated with hypotension-requiring inotropic support in previous reports (42, 54).

There is still little knowledge regarding the predictive role of cardiac biomarkers, such as ultra-sensitive troponins and Brain Natriuretic Peptides (BNP) or N-terminal pro-BNP (NTpro-BNP). In the Shalabi et al. (23) cohort, 13 patients underwent troponin levels dosage during CRS: 4 cases resulted with abnormal troponin values, all of them associated with cardiac dysfunction quantified by decreased LVEF; NTpro-BNP was assessed only in 7 patients and proved to be elevated during CRS, with the highest values observed in two patients with cardiac impairment developed during CRS (23). Because of the scarceness of investigations, it is not possible to establish a precise role for cardiac biomarkers in patients undergoing CAR-T cell therapy, including their usefulness for patients' surveillance.

5. Monitoring and management of CV complications in patients undergoing CAR-T cell therapy

Considering the burden of CV complications occurring during CAR-T cells infusions, the latest 2022 ESC cardio-oncology guidelines recommend to perform a baseline cardiological evaluation, including electrocardiogram, natriuretic peptides, troponins and transthoracic echocardiogram, in particular in subjects with pre-existing CV conditions (41). However, it should

be acknowledged, due to the patient heterogeneity and small sample sizes of available studies, that these recommendations only rely on expert consensus and not on high-quality evidences.

During infusion, frequent vital signs assessment and arrhythmias monitoring through telemetry should be performed. Volume resuscitation with intravenous fluid represents the first-line therapy for hypotension and shock related to CRS (42). For resistant cases, vasopressors (e.g., adrenaline, noradrenaline, vasopressin) should be considered (26, 55, 56). However, other causes of hypotension and shock, such as severe infections, cardiac tamponade, pulmonary embolism or acute cardiac dysfunction, should be ruled out.

The occurrence of signs of high-grade CRS should be promptly followed by complete cardiac evaluation, including electrocardiogram, biomarkers and echocardiogram (57).

Tocilizumab is an anti-IL-6-receptor antagonist that is approved to manage severe CRS and may also mitigate CV toxicity of CAR T-cells (58, 59). Tocilizumab should hence be used in subjects with CRS grade 2 or higher and with high suspicion of CV complications: troponin elevation may help identifying candidates experiencing CRS for early tocilizumab administration (21). Nevertheless, prospective investigations are needed to define the optimal management strategy for CAR T-cell related cardiotoxicity.

Figure 1 shows a proposed diagnostic work-up and management strategy of CV complications in patients exposed to CAR-T cell therapy.

6. Future perspectives

Mechanisms underlying CV events in patients undergoing CAR-T cell infusion are poorly understood; basic mechanistic studies are therefore needed in order to investigate possible myocardial damage pathways, which may occur regardless of cytokine release and CRS. For example, measurement of soluble cardio-depressant factors, commonly found in patients with septic cardiomyopathy, could help identifying novel mechanisms of cardiac failure. On the other hand, prospective imaging studies, using non-invasive advanced metrics of myocardial function (e.g., strain imaging with speckle tracking) are also necessary. At last, a multidisciplinary approach to the management of patients on CAR-T cells is needed to optimize outcomes and to ensure a comprehensive care of these patients.

7. Conclusion

Chimeric antigen receptor T-cell immunotherapy has recently changed the scenario of cancer treatment, with expanding indications also for solid tumors. Therefore, the awareness of its possible complications is of utmost importance, in order to early identify and treat these manifestations. However, at this point in time, preventive measures, pharmacological management and surveillance strategies remain poorly understood and data available rely on retrospective reports. Dedicated prospective clinical studies, including large cohorts of patients, are hence warranted in order to clarify the CV involvement pathogenesis, the use of imaging and serum biomarkers in events identification and treatment opportunities.

Author contributions

MC, LM, and LT wrote the manuscript, prepared the figure and table, and edited the manuscript. MC, PL, GL, FC, and AL critically reviewed the manuscript. All authors contributed to the article and approved the submitted version.

Conflict of interest

The authors declare that the research was conducted in the absence of any commercial or financial relationships that could be construed as a potential conflict of interest.

Publisher's note

References

1. Zhang Y, Zhang Z. The history and advances in cancer immunotherapy: understanding the characteristics of tumor-infiltrating immune cells and their therapeutic implications. *Cell Mol Immunol.* (2020) 17:807–21. doi: 10.1038/s41423-020-0488-6

2. Nair R, Westin J. CAR T-cells. *Adv Exp Med Biol.* (2020) 1244:215–33. doi: 10.1007/978-3-030-41008-7_10

3. Alabanza L, Pegues M, Geldres C, Shi V, Wiltzius JJW, Sievers SA, et al. Function of novel anti-CD19 chimeric antigen receptors with human variable regions is affected by hinge and transmembrane domains. *Mol Ther.* (2017) 25:2452–65. doi: 10.1016/j.ymthe.2017.07.013

4. Sterner RC, Sterner RM. CAR-T cell therapy: current limitations and potential strategies. *Blood Cancer J.* (2021) 11:1–11. doi: 10.1038/s41408-021-00459-7

5. Mohanty R, Chowdhury CR, Arega S, Sen P, Ganguly P, Ganguly N. CAR T cell therapy: a new era for cancer treatment (review). *Oncol Rep.* (2019) 42:2183–95. doi: 10.3892/or.2019.7335

6. Dai H, Wang Y, Lu X, Han W. Chimeric antigen receptors modified T-cells for cancer therapy. *JNCI J Natl Cancer Inst.* (2016) 108:439. doi: 10.1093/jnci/djv439

7. Ninomiya S, Narala N, Huye L, Yagyu S, Savoldo B, Dotti G, et al. Tumor indoleamine 2,3-dioxygenase (IDO) inhibits CD19-CAR T cells and is downregulated by lymphodepleting drugs. *Blood.* (2015) 125:3905–16. doi: 10.1182/blood-2015-01-621474

8. Gattinoni L, Finkelstein SE, Klebanoff CA, Antony PA, Palmer DC, Spiess PJ, et al. Removal of homeostatic cytokine sinks by lymphodepletion enhances the efficacy of

adoptively transferred tumor-specific CD8+ T cells. *J Exp Med.* (2005) 202:907–12. doi: 10.1084/jem.20050732

9. Muranski P, Boni A, Wrzesinski C, Citrin DE, Rosenberg SA, Childs R, et al. Increased intensity lymphodepletion and adoptive immunotherapy—how far can we go? *Nat Clin Pract Oncol.* (2006) 3:668. doi: 10.1038/ncponc0666

10. Neelapu SS. CAR-T efficacy: is conditioning the key? *Blood.* (2019) 133:1799–800. doi: 10.1182/blood-2019-03-900928

11. Australian Prescriber. Axicabtagene ciloleucel for B-cell lymphoma. *Aust Prescr.* (2021) 44:207. doi: 10.18773/austprescr.2021.058

12. Neelapu SS, Locke FL, Bartlett NL, Lekakis LJ, Miklos DB, Jacobson CA, et al. Axicabtagene ciloleucel CAR T-cell therapy in refractory large B-cell lymphoma. *N Engl J Med.* (2017) 377:2531–44. doi: 10.1056/NEJMoa1707447

13. Maude SL, Laetsch TW, Buechner J, Rives S, Boyer M, Bittencourt H, et al. Tisagenlecleucel in children and young adults with B-cell lymphoblastic leukemia. *N Engl J Med.* (2018) 378:439–48.

14. Australian Prescriber. Tisagenlecleucel for B-cell cancers. *Aust Prescr.* (2020) 43:30. doi: 10.18773/austprescr.2019.077

15. Munshi NC, Anderson LD, Shah N, Madduri D, Berdeja J, Lonial S, et al. Idecabtagene vicleucel in relapsed and refractory multiple myeloma. *N Engl J Med.* (2021) 384:705–16. doi: 10.1056/NEJMoa2024850

16. Park JH, Rivière I, Gonen M, Wang X, Sénéchal B, Curran KJ, et al. Long-term follow-up of CD19 CAR therapy in acute lymphoblastic leukemia. *N Engl J Med.* (2018) 378:449–59. doi: 10.1056/NEJMoa1709919

17. Lefebvre B, Kang Y, Smith AM, Frey N, Carver JR, Scherrer-Crosbie M. Cardiovascular effects of CAR T cell therapy: a retrospective study. *JACC Cardio Oncol.* (2020) 2:193–203. doi: 10.1016/j.jaccao.2020.04.012

18. Fitzgerald JC, Weiss SL, Maude SL, Barrett DM, Lacey SF, Melenhorst JJ, et al. Cytokine release syndrome after chimeric antigen receptor T cell therapy for acute lymphoblastic leukemia. *Crit Care Med.* (2017) 45:e124–5. doi: 10.1097/CCM.0000000000002053

19. Goldman A, Maor E, Bomze D, Liu JE, Herrmann J, Fein J, et al. Adverse cardiovascular and pulmonary events associated with chimeric antigen receptor T-cell therapy. *J Am Coll Cardiol.* (2021) 78:1800–13. doi: 10.1016/j.jacc.2021.08.044

20. Salem JE, Ederhy S, Lebrun-Vignes B, Moslehi JJ. Cardiac events associated with chimeric antigen receptor T-cells (CAR-T): a vigibase perspective. *J Am Coll Cardiol.* (2020) 75:2521–3. doi: 10.1016/j.jacc.2020.02.070

21. Alvi RM, Frigault MJ, Fradley MG, Jain MD, Mahmood SS, Awadalla M, et al. Cardiovascular events among adults treated with chimeric antigen receptor T-cells (CAR-T). *J Am Coll Cardiol.* (2019) 74:3099–108. doi: 10.1016/j.jacc.2019.10.038

22. Wang M, Munoz J, Goy A, Locke FL, Jacobson CA, Hill BT, et al. KTE-X19 CAR T-cell therapy in relapsed or refractory mantle-cell lymphoma. *N Engl J Med.* (2020) 382:1331–42. doi: 10.1056/NEJMoa1914347

23. Shalabi H, Sachdev V, Kulshreshtha A, Cohen JW, Yates B, Rosing DR, et al. Impact of cytokine release syndrome on cardiac function following CD19 CAR-T cell therapy in children and young adults with hematological malignancies. *J Immunother Cancer.* (2020) 8:e001159. doi: 10.1136/jitc-2020-001159

24. Camilli M, Skinner R, Iannaccone G, Vecchia G, Montone RA, Lanza GA, et al. Cardiac imaging in childhood cancer survivors: a state-of-the-art review. *Curr Probl Cardiol.* (2022) 2022:101544. doi: 10.1016/j.cpcardiol.2022.101544

25. Wallet F, Sesques P, Devic P, Levrard M, Ader F, Friggeri A, et al. CAR-T cell: toxicities issues: mechanisms and clinical management. *Bull Cancer.* (2021) 108:S117–27. doi: 10.1016/j.bulcan.2021.05.003

26. Cobb DA, Lee DW. Cytokine release syndrome biology and management. *Cancer J.* (2021) 27:119–25. doi: 10.1097/PPO.0000000000000515

27. Lee DW, Santomasso BD, Locke FL, Ghobadi A, Turtle CJ, Brudno JN, et al. ASTCT consensus grading for cytokine release syndrome and neurologic toxicity associated with immune effector cells. *Biol Blood Marrow Transpl.* (2019) 25:625–38. doi: 10.1016/j.bbmt.2018.12.758

28. Lee DW, Gardner R, Porter DL, Louis CU, Ahmed N, Jensen M, et al. Current concepts in the diagnosis and management of cytokine release syndrome. *Blood.* (2014) 124:188–95. doi: 10.1182/blood-2014-05-552729

29. Pennisi M, Jain T, Santomasso BD, Mead E, Wudhikarn K, Silverberg ML, et al. Comparing CAR T-cell toxicity grading systems: application of the ASTCT grading system and implications for management. *Blood Adv.* (2020) 4:676–86. doi: 10.1182/bloodadvances.2019000952

30. Morris EC, Neelapu SS, Giavridis T, Sadelain M. Cytokine release syndrome and associated neurotoxicity in cancer immunotherapy. *Nat Rev Immunol.* (2021) 22:85–96. doi: 10.1038/s41577-021-00547-6

31. Shimabukuro-Vornhagen A, Gödel P, Subklewe M, Stemmler HJ, Schlößer HA, Schlaak M, et al. Cytokine release syndrome. *J Immunother Cancer.* (2018) 6:56. doi: 10.1186/s40425-018-0343-9

32. Norelli M, Camisa B, Barbiera G, Falcone L, Purevdorj A, Genua M, et al. Monocyte-derived IL-1 and IL-6 are differentially required for cytokine-release syndrome and neurotoxicity due to CAR T cells. *Nat Med.* (2018) 24:739–48. doi: 10.1038/s41591-018-0036-4

33. Giavridis T, van der Stegen SJC, Eyquem J, Hamieh M, Piersigilli A, Sadelain M. CAR T cell–induced cytokine release syndrome is mediated by macrophages and abated by IL-1 blockade. *Nature Med.* (2018) 24:731–8. doi: 10.1038/s41591-018-0041-7

34. Le RQ, Li L, Yuan W, Shord SS, Nie L, Habtemariam BA, et al. FDA approval summary: tocilizumab for treatment of chimeric antigen receptor T cell-induced severe or life-threatening cytokine release syndrome. *Oncologist.* (2018) 23:943–7. doi: 10.1634/theoncologist.2018-0028

35. Camilli M, Viscovo M, Hohaus S, Lamendola P, Verrecchia E, Gerardino L, et al. Incessant pericarditis successfully treated with anakinra in a patient on active treatment for mediastinal lymphoma: a case report. *Can J Cardiol.* (2022). doi: 10.1016/j.cjca.2022.10.027 [Epub ahead of print].

36. Li Y, He Y, Butler W, Xu L, Chang Y, Lei K, et al. Targeting cellular heterogeneity with CXCR2 blockade for the treatment of therapy-resistant prostate cancer. *Sci Transl Med.* (2019) 11:521. doi: 10.1126/scitranslmed.aax0428

37. Sterner RM, Sakemura R, Cox MJ, Yang N, Khadka RH, Forsman CL, et al. GM-CSF inhibition reduces cytokine release syndrome and neuroinflammation but enhances CAR-T cell function in xenografts. *Blood.* (2019) 133:697–709. doi: 10.1182/blood-2018-10-881722

38. Pathan N, Hemingway CA, Alizadeh AA, Stephens AC, Boldrick JC, Oragui EE, et al. Role of interleukin 6 in myocardial dysfunction of meningococcal septic shock. *Lancet.* (2004) 363:203–9.

39. Hollenberg SM, Singer M. Pathophysiology of sepsis-induced cardiomyopathy. *Nat Rev Cardiol.* (2021) 18:424–34. doi: 10.1038/s41569-020-00492-2

40. Linette GP, Stadtmauer EA, Maus M, Rapoport AP, Levine BL, Emery L, et al. Cardiovascular toxicity and titin cross-reactivity of affinity-enhanced T cells in myeloma and melanoma. *Blood.* (2013) 122:863–71. doi: 10.1182/blood-2013-03-490565

41. Lyon AR, López-Fernández T, Couch LS, Asteggiano R, Aznar MC, Bergler-Klein J, et al. 2022 ESC Guidelines on cardio-oncology developed in collaboration with the European Hematology Association (EHA), the European Society for Therapeutic Radiology and Oncology (ESTRO) and the International Cardio-Oncology Society (IC-OS). *Eur Heart J.* (2022) 43:4229–361.

42. Burns EA, Gentille C, Trachtenberg B, Pingali SR, Anand K. Cardiotoxicity associated with anti-CD19 chimeric antigen receptor T-cell (CAR-T) therapy: recognition, risk factors, and management. *Diseases.* (2021) 9:20. doi: 10.3390/diseases9010020

43. Baik AH, Oluwole OO, Johnson DB, Shah N, Salem JE, Tsai KK, et al. Mechanisms of cardiovascular toxicities associated with immunotherapies. *Circ Res.* (2021) 128:1780–801. doi: 10.1161/CIRCRESAHA.120.315894

44. Schuster SJ, Bishop MR, Tam CS, Waller EK, Borchmann P, McGuirk JP, et al. Tisagenlecleucel in adult relapsed or refractory diffuse large B-cell lymphoma. *N Engl J Med.* (2019) 380:45–56. doi: 10.1056/NEJMoa1804980

45. Locke FL, Ghobadi A, Jacobson CA, Miklos DB, Lekakis LJ, Oluwole OO, et al. Long-term safety and activity of axicabtagene ciloleucel in refractory large B-cell lymphoma (ZUMA-1): a single-arm, multicentre, phase 1–2 trial. *Lancet Oncol.* (2019) 20:31–42. doi: 10.1016/S1470-2045(18)30864-7

46. Kochenderfer JN, Dudley ME, Carpenter RO, Kassim SH, Rose JJ, Telford WG, et al. Donor-derived CD19-targeted T cells cause regression of malignancy persisting after allogeneic hematopoietic stem cell transplantation Key Points. *Blood.* (2013) 122:4129–39. doi: 10.1182/blood-2013-08-519413

47. Davila ML, Riviere I, Wang X, Bartido S, Park J, Curran K, et al. Efficacy and toxicity management of 19-28z CAR T cell therapy in B cell acute lymphoblastic leukemia. *Sci Transl Med.* (2014) 6:224. doi: 10.1126/scitranslmed.3008226

48. Kochenderfer JN, Dudley ME, Kassim SH, Somerville RPT, Carpenter RO, Maryalice SS, et al. Chemotherapy-refractory diffuse large B-cell lymphoma and indolent B-cell malignancies can be effectively treated with autologous T cells expressing an anti-CD19 chimeric antigen receptor. *J Clin Oncol.* (2015) 33:540–9. doi: 10.1200/JCO.2014.56.2025

49. Brudno JN, Somerville RPT, Shi V, Rose JJ, Halverson DC, Fowler DH, et al. Allogeneic T cells that express an anti-CD19 chimeric antigen receptor induce remissions of B-cell malignancies that progress after allogeneic hematopoietic stem-cell transplantation without causing graft-versus-host disease. *J Clin Oncol.* (2016) 34:1112–21. doi: 10.1200/JCO.2015.64.5929

50. Ganatra S, Redd R, Hayek SS, Parikh R, Azam T, Yanik GA, et al. Chimeric antigen receptor T-cell therapy-associated cardiomyopathy in patients with refractory or relapsed non-hodgkin lymphoma. *Circulation.* (2020) 142:1687–90. doi: 10.1161/CIRCULATIONAHA.120.048100

51. Lee DW, Kochenderfer JN, Stetler-Stevenson M, Cui YK, Delbrook C, Feldman SA, et al. T cells expressing CD19 chimeric antigen receptors for acute lymphoblastic leukaemia in children and young adults: a phase 1 dose-escalation trial. *Lancet.* (2015) 385:517–28. doi: 10.1016/S0140-6736(14)61403-3

52. Maude SL, Frey N, Shaw PA, Aplenc R, Barrett DM, Bunin NJ, et al. Chimeric antigen receptor T cells for sustained remissions in leukemia. *N Engl J Med.* (2014) 371:1507–17. doi: 10.1056/NEJMoa1407222

53. Levine JE, Grupp SA, Pulsipher MA, DIetz AC, Rives S, Myers GD, et al. Pooled safety analysis of tisagenlecleucel in children and young adults with B cell acute lymphoblastic leukemia. *J Immunother Cancer.* (2021) 9:e002287. doi: 10.1136/jitc-2020-002287

54. Burstein DS, Maude S, Grupp S, Griffis H, Rossano J, Lin K. Cardiac profile of chimeric antigen receptor T cell therapy in children: a single-institution experience. *Biol Blood Marrow Transpl.* (2018) 24:1590–5. doi: 10.1016/j.bbmt.2018.05.014

55. Ganatra S, Carver JR, Hayek SS, Ky B, Leja MJ, Lenihan DJ, et al. Chimeric antigen receptor T-cell therapy for cancer and heart: JACC council perspectives. *J Am Coll Cardiol.* (2019) 74:3153. doi: 10.1016/j.jacc.2019.10.049

56. Freyer CW, Porter DL. Cytokine release syndrome and neurotoxicity following CAR T-cell therapy for hematologic malignancies. *J Allergy Clin Immunol.* (2020) 146:940–8. doi: 10.1016/j.jaci.2020.07.025

57. Asnani A. Cardiotoxicity of immunotherapy: incidence, diagnosis, and management. *Curr Oncol Rep.* (2018) 20:44. doi: 10.1007/s11912-018-0690-1

58. Pathan N, Hemingway CA, Alizadeh AA, Stephens AC, Boldrick JC. Role of interleukin 6 in myocardial dysfunction of meningococcal septic shock. *Lancet.* (2004) 363:203–9. doi: 10.1016/S0140-6736(03)15326-3

59. June CH, Sadelain M. Chimeric antigen receptor therapy. *N Engl J Med.* (2018) 379:64–73. doi: 10.1056/NEJMra1706169

60. Porter D, Frey N, Wood PA, Weng Y, Grupp SA. Grading of cytokine release syndrome associated with the CAR T cell therapy tisagenlecleucel. *J Hematol Oncol.* (2018) 11:35. doi: 10.1186/s13045-018-0571-y

61. Porter DL, Hwang WT, Frey N, Lacey SF, Shaw PA, Loren AW, et al. Chimeric antigen receptor T cells persist and induce sustained remissions in relapsed refractory chronic lymphocytic leukemia. *Sci Transl Med.* (2015) 7:303ra139. doi: 10.1126/scitranslmed.aac5415

62. MedDRA. *Introductory Guide MedDRA Version 22.1. Notice to Reader MedDRA Introductory Guide Notice to Reader*. (2019). Available online at: https://www.meddra.org/sites/default/files/guidance/file/intguide_23_0_english.pdf (accessed March 10, 2020).

63. National Cancer Institute. *Common Terminology Criteria for Adverse Events (CTCAE) Version 4.0*. Bethesda, MD: National Cancer Institute (2009).

64. Goldstein B, Giroir B, Randolph A. International pediatric sepsis consensus conference: Definitions for sepsis and organ dysfunction in pediatrics. *Pediatr Crit Care Med.* (2005) 6:2–8. doi: 10.1097/01.PCC.0000149131.72248.E6

frontiers | Frontiers in Cardiovascular Medicine

TYPE Original Research
PUBLISHED 29 March 2023
DOI 10.3389/fcvm.2023.1085737

OPEN ACCESS

EDITED BY
Antonella Lombardo,
Agostino Gemelli University Polyclinic (IRCCS), Italy

REVIEWED BY
Giulia La Vecchia,
Agostino Gemelli University Polyclinic (IRCCS), Italy
Mariacarla Valli,
Oncology Institute of Southern Switzerland (IOSI), Switzerland
Thiago Quinaglia A. C. Silva,
Massachusetts General Hospital, United States

*CORRESPONDENCE
Cuiyan Wang
✉ wcyzhang@163.com

†These authors have contributed equally to this work and share first authorship

SPECIALTY SECTION
This article was submitted to Cardio-Oncology, a section of the journal Frontiers in Cardiovascular Medicine

RECEIVED 31 October 2022
ACCEPTED 13 March 2023
PUBLISHED 29 March 2023

CITATION
Tian Y, Wang T, Tian L, Yang Y, Xue C, Sheng W and Wang C (2023) Early detection and serial monitoring during chemotherapy-radiation therapy: Using T1 and T2 mapping cardiac magnetic resonance imaging.
Front. Cardiovasc. Med. 10:1085737.
doi: 10.3389/fcvm.2023.1085737

Early detection and serial monitoring during chemotherapy-radiation therapy: Using T1 and T2 mapping cardiac magnetic resonance imaging

Yaotian Tian[1†], Teng Wang[1†], Liwen Tian[1], Yucheng Yang[2], Chen Xue[3], Wei Sheng[4] and Cuiyan Wang[1*]

[1]Department of Radiology, Shandong Provincial Hospital, Shandong University, Jinan, China, [2]Department of Radiology, Shandong Provincial Hospital Affiliated to Shandong First Medical University, Jinan, China, [3]Department of Radiology, Shandong Provincial Hospital, Binzhou Medical University, Jinan, China, [4]Department of Oncology, Shandong Provincial Hospital Affiliated to Shandong First Medical University, Jinan, China

Purpose: To confirm the ability of native T1 and T2 values in detecting and monitoring early myocardial injuries of chest radiotherapy in neoplasm patients.
Materials and methods: Fifteen participants received non-anthracycline chemotherapy and chest radiotherapy, and 30 age/gender-matched controls were enrolled in this prospective study. Cardiac magnetic resonance scans were performed within 2 days, 3 months, and 6 months after chest radiotherapy. Myocardial native T1 and T2 values were measured in irradiated and nonirradiated areas. Meanwhile, the parameters of left ventricular function and left ventricular myocardial strain were obtained.
Results: There were no significant differences in left ventricular function, native T1, T2, and strain between patients and controls before chest radiotherapy. In 15 participants who were followed up for 6 months, there was a significant change only in left ventricular ejection fraction (LVEF) among baseline and the first follow-up ($P = 0.021$), while the adjusted P-value was higher than 0.05 after Bonferroni correction, as well as other parameters. Native T1 values were elevated at 3 and 6 months in irradiated areas compared with baseline (1,288.72 ± 66.59 ms vs. 1,212.51 ± 45.41 ms; 1,348.01 ± 54.16 ms vs. 1,212.51 ± 45.41 ms; $P < 0.001$ for both). However, T2 values only changed at 3 months in irradiated areas compared with baseline (44.21 ± 3.35 ms vs. 39.14 ± 1.44 ms; $P = 0.006$). Neither the native T1 nor T2 values changed in nonirradiated areas during the follow-up period (all $P > 0.05$). There were no significant differences in strain changes during the follow-up period (all $P > 0.05$).
Conclusion: Native T1 and T2 values elevated at 3 months after chest radiotherapy, whereas LVEF showed no significant change during the 6-month follow-up.

KEYWORDS

chemotherapy–radiation therapy, magnetic resonance, cardiac toxicity, mapping techniques, heart

Abbreviations
CMR, cardiac magnetic resonance; LVEF, left ventricular ejection fraction; IMRT, intensity-modulated radiation therapy; IA, irradiated areas; NIA, nonirradiated areas; GLS, global longitudinal strain; GCS, global circumferential strain; GRS, global radial strain; ROI, regions of interest; NA, not applicable; BMI, body mass index; HR, heart rate; FU, follow-up; PTV, planning target volume; ECV, extracellular volume; LGE, late gadolinium enhancement.

Introduction

The incidence of cancer is increasing and the age of onset is getting younger, but due to advances in medical care, patients are surviving significantly longer (1, 2). Chest malignancies, including lung, esophageal, and breast cancers, as well as lymphomas, usually include radiation therapy as part of their treatment regimen (3–5). The scope of radiation therapy for chest malignancies usually includes the heart. However, radiation can increase cancer survivors' long-term risk of cardiac death (6–10). Although radiation was previously thought to not affect the heart, recent studies have found that the relative risk of heart disease and major cardiac events may be 4%–16% per Gray (Gy) of the average cardiac radiation dose without a defined safe dose (11–13). Therefore, it is significant to early detect and carefully monitor cardiac changes in patients treated with radiation for chest malignancies.

T1 and T2 mapping is an emerging quantitative MRI technique that allows dynamic analysis of changes in myocardial tissue components by measuring T1 and T2 values, directly reflecting their pathophysiological statuses such as edema, fibrosis, and iron deposition without the use of contrast agents (14), and providing a more accurate diagnosis and assessment of disease outcome, bringing cardiology to a new frontier. Unlike existing semiquantitative techniques [T1WI, T2WI, late gadolinium enhancement (LGE), etc.], these quantitative methods do not require normal myocardial tissue as a control and therefore can assess not only focal myocardial lesions but also early microscopic lesions and diffuse myocardial lesions, which are already widely used in many diseases of the heart, such as various types of myocardial involvement disease, heart failure, and unexplained troponin elevation in patients (15–22). Although left ventricular ejection fraction (LVEF) is the most commonly used parameter in clinical practice and represents a global systolic function, irreversible myocardial damage has occurred when LVEF is reduced (23). There is growing evidence that myocardial strain can be detected as impaired systolic function in normal LVEF, thus allowing early detection of functional impairment due to radiotherapy and early intervention (24, 25). Several animal studies have shown that changes in myocardial edema, fibrosis, and endothelial injury precede changes in cardiac function (26–28). Therefore, myocardial native T1 and T2 values may precede the changes in global left ventricular (LV) function after radiotherapy.

Previous studies (29–32) have exploited the benefits of T1 and T2 mapping techniques to explore cancer radiotherapy-associated cardiotoxicity, but the time points of follow-up have varied and the results have been controversial. Some studies (29, 30) have indicated that changes in native T1 and T2 values predate LVEF, but others (31) have not found significant changes in them during follow-ups. Also, most studies were limited to a single disease. Therefore, the purpose of our study was to explore the value of native T1 and T2 mapping in the early detection of radiotherapy-associated cardiotoxicity in cancer under real-world conditions.

Materials and methods

Study design and participants

All patients who received chest radiotherapy at our institution from March 2019 to September 2020 were included in this prospective study. Exclusion criteria included younger than 18 years old and older than 75 years, inappropriate irradiation field (whole heart exposed to radiation field or not exposed to radiation field), receiving anthracycline chemotherapy, and having known cardiac symptoms or diseases (organic heart disease, hypertension, coronary artery disease, etc.). Finally, our prospective observational study included 15 consecutive patients who received non-anthracycline chemotherapy and chest radiotherapy and 30 healthy controls with matched age and gender. To evaluate the changes in myocardial tissue, four cardiac MRI examinations were performed in patient groups before radiotherapy (baseline), as well as within 2 days, 3 months, and 6 months after chest radiotherapy. The healthy controls underwent cardiac MRI only once. **Figure 1** shows the flowchart of patient selection.

This study was approved by the Ethical Committee of Shandong Provincial Hospital Affiliated to Shandong First Medical University, and all patients signed informed consent to participate in this study.

Chemotherapy–radiation therapy

All patients were receiving standard treatment according to Chinese guidelines at the time of inclusion, and they were treated with intensity-modulated radiation therapy (IMRT), in which multiple beams of uneven intensity are aimed at the tumor, which also improves the consistency of treatment and reduces the dose to normal tissue. Meanwhile, the hearts of all patients in this study were partly exposed to the radiation field. Thus, the heart could be divided into two parts, the irradiated areas (IA) and nonirradiated areas (NIA), see **Figure 1**. Then calculate their radiation doses separately.

MRI acquisition protocol

All MRI examinations were performed using a 3.0 T Siemens Skyra scanner (Siemens Medical Systems, Erlangen, Germany) with a 32-channel matrix coil. The cardiac magnetic resonance (CMR) imaging protocols included cine MRI, Native T1 map, and T2 map in four-chamber, three-chamber, two-chamber, and short-axis views. Steady-state free precession (SSFP) cine images were obtained with the following imaging parameters: TR/TE = 39.2/1.4 ms; FA = 80°, FOV = 300 × 225 mm^2, acquisition matrix = 192 × 140, and voxel size = 1.6 × 1.6 × 6.0 mm^3. Native T1 map was acquired with a 3 s(3 s)5 s modified Look-Locker inversion recovery (MOLLI) sequence with the following parameters: TR/TE = 2.4/1.1 ms, FA = 35°, FOV = 300 × 225 mm^2, acquisition

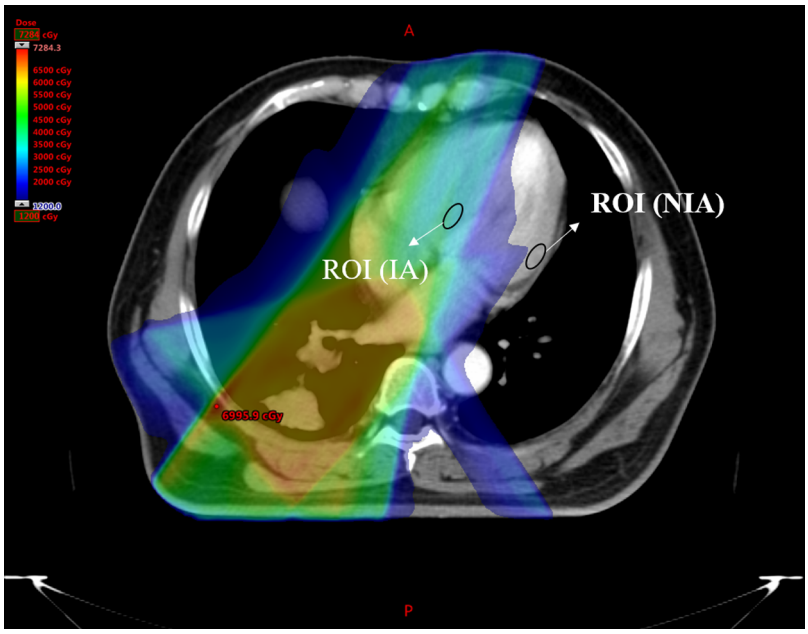

FIGURE 1
Zone map of IA and NIA. IA, irradiated areas; NIA, nonirradiated areas.

matrix = 256 × 192, and voxel size = 1.2 × 1.2 × 8.0 mm^3. The T2 map was obtained using the SSFP sequence with three different T2 preparation times. Parameters were as follows: TE = 0 ms, 25 ms, 55 ms; TR = 3 × RR; FA = 50°; FOV = 300 × 225 mm^2; acquisition matrix = 256 × 192, and voxel size = 1.2 × 1.2 × 8.0 mm^3.

Image analysis

All analyses were using commercial software (CVI[42], circle cardiovascular imaging, Inc., Calgary, Canada). The contour of the myocardial endocardium and epicardium were drawn by the semiautomatic method provided by CVI[42] to obtain global T1 values, global T2 values, and parameters about LV function and strain. To avoid blood pool and epicardial fat contamination, a 10% automated contour adjustment was applied to move both contours toward each other to eliminate potential in-plane partial volume effects. The global longitudinal strain (GLS) was measured as an average of peak diastolic longitudinal strain from all three long-axis views using a tissue tracking method. The global T1 values, global T2 values, global circumferential strain (GCS), and global radial strain (GRS) were calculated based on all short axis from bottom to apex.

Two experienced radiologists, blinded to the clinical characteristics of and each other's data, delineated the regions of interest (ROI) of irradiated and nonirradiated areas in the native T1 map and T2 map independently to assess intra- and interrater reliability and to get regional T1 and T2 values. ROI was greater than 1.0 cm^2 and placed on the mid-myocardial layers to minimize partial volume effects from adjacent blood pool or extra-myocardial tissues. The irradiated areas were defined as the myocardial areas with maximum radiation dose, and the nonirradiated areas were defined as the myocardial areas with minimum radiation dose at the same slice. To make sure the ROIs were same in all T1 and T2 mapping images, the copy-and-paste function was used, see **Figure 1**. If the ROI was questioned, it would be re-delineated until achieving mutual agreements.

Statistical analysis

All statistical analyses were performed by using SPSS (version 21.0; IBM, Armonk, NY, United States). Two-sided $P < 0.05$ was considered statistically significant. All discrete variables were reported as numbers of participants with percentages in parentheses. All continuous variables with a normal distribution (Shapiro–Wilk test, $P > 0.05$) were reported as mean ± SD, and those without were reported as median with an interquartile range in parentheses. Intraclass correlation coefficient (ICC) and Bland–Altman analyses were used for evaluating the agreement of ROI measurements. Differences in count variables of demographic data were tested by using the χ^2 test. The differences between baseline and controls were compared with the Student's *t*-test or Mann–Whitney *U* test to eliminate the interference of chemotherapy partly. The differences in variables between IA and NIA were compared with paired sample *t*-test. Data were compared among baseline and follow-ups by using the Friedman rank test with *post-hoc test* with Bonferroni correction. Since adjusted *P*-values of the Friedman rank test were not reported when there were no significances in SPSS, it would be

reported as not applicable (NA). For correlations between regional radiation dose and percent change of T1 and T2 values in the IA, Pearson correlation coefficients were computed.

Results

Patient characteristics

Of all 362 patients who would receive chest radiotherapy between March 2019 and September 2020 in our institution, 296 were excluded because of the reasons listed in Figure 2. Thirty-eight patients consented and 15 of them (9 men and 6 women) completed all three follow-ups. The reasons for drop-out were as follows: four were due to contraindications of CMR examination, six were due to unqualified data, four denied to conduct, two needed additional therapy, two were due to noncardiac adverse reactions, and five were due to other reasons. None of the patients had adverse cardiac events during the follow-ups. In addition, 30 healthy controls (15 men and 15 women) with matched age and gender were enrolled in this study. The characteristics of all participants are summarized and compared in Table 1. The heart rate (HR) in patients was significantly higher than that in healthy controls at baseline ($P < 0.01$); however, there was no significant difference between the follow-up groups (see Supplementary material Table 1). The body mass index (BMI) had significantly lower values in patients compared with healthy controls (24.7, range 20.2–25.26, vs. 27.1, range 22.7–27.7, $P = 0.037$). There were no statistical differences between the two groups in terms of other variables.

Chemotherapy–radiation therapy

In terms of the oncological diagnosis of patients enrolled, six were squamous cell lung carcinoma, three were lung adenocarcinoma, two were small-cell lung carcinoma, and four were esophageal cancer, see Table 2. All patients in this study accepted sequential chemotherapy–radiation therapy. The details of the chemotherapy approach are shown in Table 2. The mean duration of the three follow-up periods was within approximately 2 days, 117.7 days, and 206.1 days after the end of radiotherapy, respectively. The follow-up intervals were slightly longer than expected due to the patient's physical condition, treatment plan, and holidays. The planning target volume (PTV) of tumors received 62.22 ± 4.46 Gy (mean ± SD). However, the mean radiation dose in IA was 35.98 ± 6.29 Gy, which was significantly higher than that in NIA (3.08 ± 1.83 Gy, $P < 0.001$), shown in Table 2.

Global native T1, T2 values, LV function, and strain

The average values of mentioned parameters among controls, baseline, and follow-ups are shown in Table 3. No statistical differences were found between controls and patients at baseline for all parameters demonstrated in Table 3, and they all had normal LV functions. It indicated that there was a significant change only in LVEF among baseline and the first follow-up ($P = 0.021$), but the adjusted P-value was higher than 0.05 after the Bonferroni correction. There were no statistically significant changes in other LV function parameters, global native T1 and T2 values, GRS, GCS, and GLS at all follow-ups compared with baseline.

Native T1 and T2 values in different radiation areas after IMRT

Native T1, T2 values, and their temporal percent changes are summarized in Table 4. The ICC and Bland–Altman analyses demonstrated good intra- and interobserver reproducibility of the native T1 and T2 values in different radiation areas (see Supplementary material Table 4). At baseline, there were no significant differences in native T1 and T2 values between NIA and IA (native T1: 1,212.51 ± 45.41 vs. 1,200.99 ± 35.32, $P = 0.144$; T2: 39.14 ± 1.44 vs. 38.61 ± 1.62, $P = 0.248$) and between those of NIA at each time point. Native T1 values in IA were significantly elevated compared with that in NIA at all follow-ups (1,226.52 ± 53.09 vs. 1,201.60 ± 40.37, $P = 0.02$; 1,288.72 ± 66.59 vs. 1,211.13 ± 43.27, $P < 0.001$; 1,348.01 ± 54.16 vs. 1,210.12 ± 27.73, $P < 0.001$, respectively). Although T2 values of IA at all time points were higher than that in NIA, only the second follow-up demonstrated a statistically significant difference (44.21 ± 3.35 vs. 39.70 ± 2.42, $P = 0.004$).

The native T1 values gradually increased since the first follow-up in IA but only showed significant differences since the second follow-up compared with baseline ($P = 0.006$, $P < 0.001$, separately). As for T2 values in IA, they increased slightly at the first follow-up, elevated sharply and peaked at the second follow-up, and then decreased at the last follow-up, but only showed statistical difference at the second follow-up compared with baseline ($P = 0.006$). As for NIA, no significant changes were found in native T1 and T2 values at all follow-ups compared with baseline. The longitudinal trend of native T1 and T2 values in different radiation fields is shown in Figure 3.

To eliminate the interference of regional measurements, a percentage change was calculated. The percentage change of native T1 and T2 values in IA at the first follow-up was not significantly changed compared to NIA. At the second follow-up, the percentage change in native T1 and T2 values was significantly higher in IA than in NIA ($P = 0.001$, $P = 0.004$, respectively), but at the third follow-up, only the change in native T1 values was statistically significant (11.24 ± 4.36 vs. 0.79 ± 1.99, $P < 0.001$). Furthermore, the correlation of the percent change of native T1 and T2 values with radiation dose in IA was evaluated and no statistical significance was found (see Supplementary material Table 2).

Discussion

Our study prospectively assessed changes in myocardial tissue characteristics, global left ventricular function, and strain in the

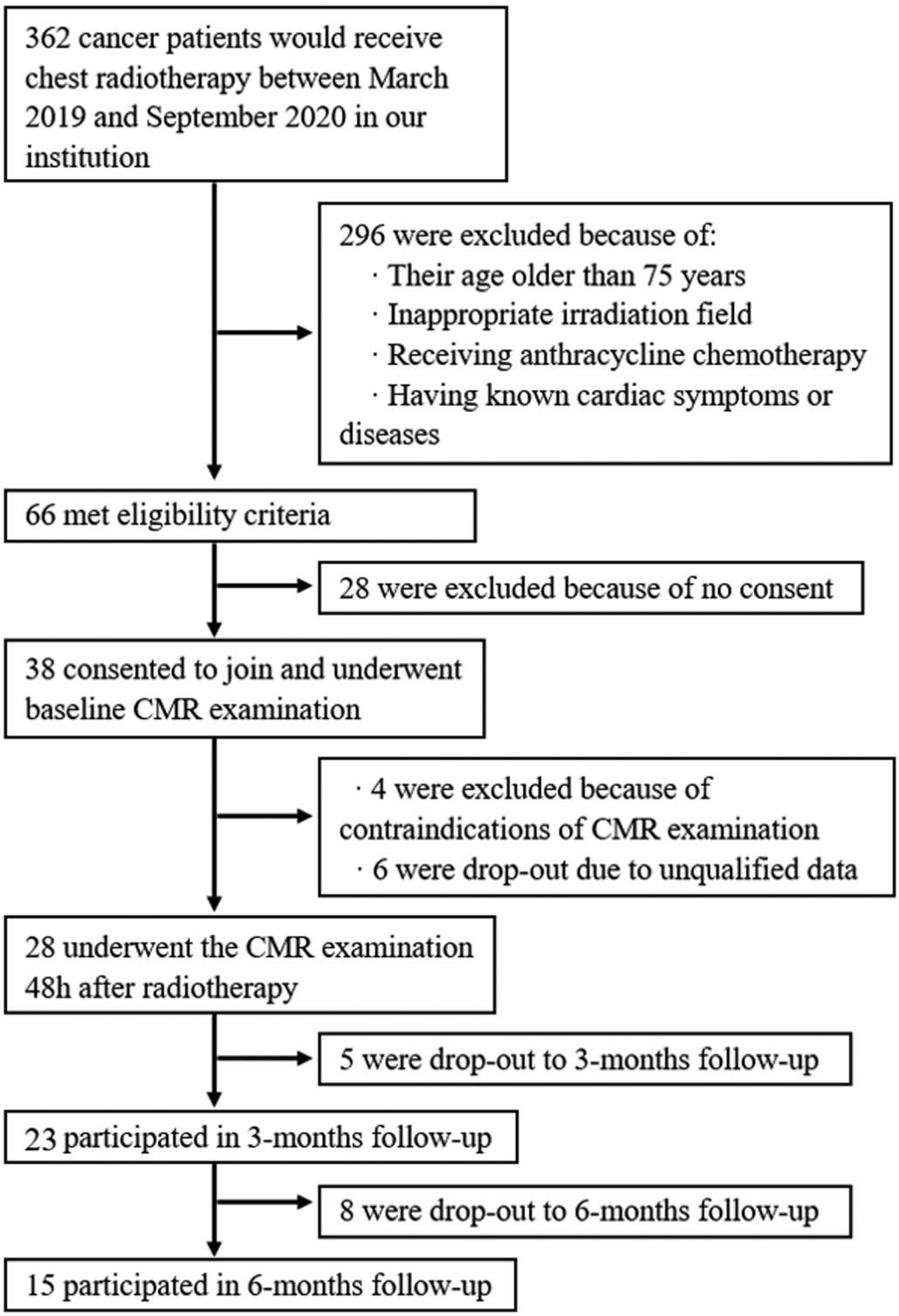

FIGURE 2
STROBE flow diagram.

early post-radiotherapy period. Our main findings were as follows: native T1 in the IA region was consistently elevated during all follow-ups and was significantly elevated both at 3 and 6 months; T2 values in the IA region were elevated significantly at 3 months and then decreased close to baseline at 6 months after radiotherapy, and no significant changes in tissue characteristics were observed in the NIA region at all follow-ups. Finally, the ejection fraction and global myocardial strain of the left ventricle at all follow-ups were not significantly different from those at baseline. These findings suggest that natural T1 and T2 values

TABLE 1 Clinical characteristics of participants at baseline and healthy controls.

Variables	Controls ($n = 30$)	Patients ($n = 15$)	*P*-values
Age[a] (years)	59.8 ± 5.8	60.2 ± 8.2	0.89
Men	15 (50)	9 (60)	0.53
Heart rate[b] (beats/min)	62.5 (62–73)	83.5 (66–86)	<0.01
BMI[b] (kg/m^2)	27.1 (22.7–27.7)	24.7 (20.2–25.26)	0.04
Risk factors			
Current or ex-smoker	13 (43)	9 (60)	0.35
Hypertension	7 (23)	5 (33)	0.50
Diabetes	0 (0)	0 (0)	NA
Hyperlipidemia	0 (0)	1 (7)	NA

BMI, body mass index; NA, not applicable.
Unless otherwise specified, data are numbers of participants, with percentages in parentheses. Data were compared by using Student's *t*-tests or Mann–Whitney *U* test.
[a]Data are mean ± SD.
[b]Data are medians, and data in parentheses are the interquartile range.

TABLE 2 Tumor entity and characteristics of cancer therapy within the study sample.

Tumor entity, chemotherapy, and radiotherapy	Values
Squamous cell lung carcinoma	
Nedaplatin + paclitaxel	6 (40)
Lung adenocarcinoma	
Nedaplatin + pemetrexed	3 (20)
Small-cell lung carcinoma	
Nedaplatin + etoposide	2 (13)
Esophageal cancer	
Nedaplatin + paclitaxel	4 (27)
Mean interval of FU1 (days)	<2
Mean interval of FU2[a] (days)	117.7 ± 15.4
Mean interval of FU3[a] (days)	206.1 ± 24.0
PTV of tumor[a] (Gy)	62.22 ± 4.46
Mean dose of IA[a] (Gy)	35.98 ± 6.29
Mean dose of NIA[a] (Gy)	3.08 ± 1.83

FU, follow-up; PTV, planning target volume; IA, irradiated areas; NIA, nonirradiated areas; FU1, 2 days post radiotherapy; FU2, 3 months post radiotherapy; FU3, 6 months post radiotherapy.
Unless otherwise specified, data are numbers of participants, with percentages in parentheses.
[a]Data are mean ± SD.

altered earlier than LVEF after radiotherapy, and it can be detected as early as 3 months after radiotherapy. Although the same situation occurs in strain, the global strain value may mask the regional myocardial changes, so further studies are needed to explore the application value of the global strain parameter in regional myocardial injury.

To observe the heart injury by radiotherapy, we compared the MRI findings both of IA and NIA before and after radiotherapy. However, some studies (33) have indicated that abnormal T1 values are associated with the cancer process before radiotherapy and we found that nearly all patients received chemotherapy before radiotherapy. So, we compared the MRI findings of healthy volunteers and patients at baseline to assess the effect of cancer and chemotherapy on the heart before radiotherapy. While anthracyclines have been shown to cause early myocardial injury and a decrease in global strain (31, 34–36), patients who used anthracyclines were excluded from this study. Our study showed that there was no significant difference between all the MR parameters of patients at baseline and those of volunteers, which implied that it can be ignored about the damage result from cancer and chemotherapy expected for anthracyclines. We found there was a difference in heart rate between the control and radiotherapy groups at baseline, and there were no significant differences among the various follow-up time points (see **Supplementary material Table 1**). There might have been selection bias due to the better habits and fitness of the healthy controls, and the pre-chemotherapy of the patients might also cause the heart rate a little higher than the healthy controls, but no significant difference was found in the T1 values between the healthy controls and the patients at baseline in our study. As a result, we supposed that the effect of the heart rate on T1 values could be ignored in our groups, although some scholars declared that the heart rate could affect the T1 values (37, 38).

Past studies have suggested that the acute phase of the radiation response may manifest as time-dependent inflammatory changes, decreased microvascular density, and activation of fibrotic pathways with preserved LV function and subsequent reduction in ejection fraction (39–42). Both cellular edema induced by early inflammation and secondary myocardial fibrosis could lead to an increase in natural T1 values (43, 44), which could explain the increase in natural T1 values in the IA region. Cellular edema can also lead to an increase in T2 values in the IA region (31, 32, 45), while the decrease in T2 values may be associated with the resolution of edema as well as secondary myocardial fibrosis. Then, in our study, within 3 months after radiotherapy, both T1 and T2 values' increase implied that cellular edema may be the main process during this period; and then T2 values decreased since T1 values increased continually, which showed us that myocardial fibrosis may be dominant instead after 3 months. However, as edema is reversible and fibrosis is irreversible, our study provides a reference point for the period in which cardioprotective drugs should be applied.

It was the first time to find myocardium T1 and T2 values changes at 3 months after radiotherapy. Takagi et al. (29) reported that native T1 could detect early changes in myocardial tissue; however, they started follow-up just from 6 months and much later than us. In the study by Kvernby et al. (30) on radiotherapy for breast cancer, it was found that at the 6-month follow-up, T1 increased and T2 decreased significantly compared to the earlier follow-ups. The T1 values changed similarly to this study, but the T2 values were different, perhaps due to the different tumor types they used (breast cancer), the different chemotherapy (anthracyclines), and the small amount of data. In another study (31) in patients treated with radiotherapy for breast cancer, no significant changes in myocardium native T1 and T2 values were found within 1-year follow-up, probably because their follow-up time point was different from ours. So, the long-term changes in these parameters may need more investigation in the future. Recently, an animal study (46) found significant changes in T2 values at 8 weeks, which just was similar to our findings.

TABLE 3 CMR measurements compared among controls, baseline, and follow-ups.

Parameters	Controls	FU0	FU1	FU2	FU3
LVEF (%)[a]	61.95 ± 5.25	62.25 ± 4.55	57.30 ± 3.20	60.97 ± 3.44	62.70 ± 4.78
LVEDV (mL)	129.71 ± 20.79	134.49 ± 24.90	127.27 ± 21.15	125.80 ± 21.63	120.45 ± 19.85
LVESV (mL)	49.44 ± 10.83	51.22 ± 11.09	55.37 ± 10.77	50.98 ± 11.73	48.43 ± 8.91
LVEDVI (mL/m^2)	73.28 ± 11.19	77.69 ± 10.27	74.13 ± 8.98	73.11 ± 11.07	71.09 ± 7.81
LVESVI (mL/m^2)	27.99 ± 6.21	29.62 ± 5.40	32.39 ± 5.95	29.29 ± 6.17	27.69 ± 3.67
LV mass (g)	82.13 ± 15.63	79.71 ± 18.77	78.56 ± 16.19	76.91 ± 14.45	75.98 ± 13.34
GLS (%)	−15.29 ± 2.22	−15.53 ± 1.68	−14.13 ± 1.58	−14.83 ± 1.40	−15.05 ± 1.57
GRS (%)	34.10 ± 6.23	34.18 ± 4.84	30.71 ± 5.19	32.52 ± 3.64	33.49 ± 5.96
GCS (%)	−19.40 ± 2.20	−19.49 ± 1.69	−18.23 ± 1.88	−18.73 ± 1.30	−19.18 ± 1.87
Global T1 value	1,201.51 ± 37.92	1,212.86 ± 26.59	1,224.61 ± 39.13	1,243.47 ± 40.43	1,241.37 ± 26.02
Global T2 value	40.65 ± 2.38	39.85 ± 1.95	39.64 ± 1.98	41.13 ± 2.64	39.54 ± 1.70

CMR, cardiac magnetic resonance; LV, left ventricular; LVEF, left ventricle ejection fraction; LVEDV, left ventricular end-diastolic volume; LVESV, left ventricular end-systolic volume; LVEDVI, left ventricular end-diastolic volume index; LVESVI, left ventricular end-systolic volume index; GLS, global longitudinal strain; GCS, global circumferential strain; GRS, global radial strain; FU0, baseline; FU1, 2 days post radiotherapy; FU2, 3 months post radiotherapy; FU3, 6 months post radiotherapy.
Unless otherwise specified, data are mean ± SD. Data were compared among baseline and follow-ups by using the Friedman rank test with *post-hoc test* with Bonferroni correction. Data were compared between controls and baseline by using Student's *t*-tests or Mann–Whitney *U* test.
After using a *post-hoc test* with Bonferroni correction, none of those parameters had a significant difference among baseline and follow-ups.
[a]$P < 0.05$ using Friedman rank test compared with baseline.

TABLE 4 Native T1 values, T2 values, and their temporal percent changes at baseline and follow-ups.

Variables	Native T1 values			T2 values		
	NIA[a]	IA	*P*-values	NIA[a]	IA	*P*-values
FU0	1,200.99 ± 35.32	1,212.51 ± 45.41	0.144	38.61 ± 1.62	39.14 ± 1.44	0.248
FU1	1,201.60 ± 40.37	1,226.52 ± 53.09	0.02	38.25 ± 1.54	39.66 ± 0.88	0.057
FU2	1,211.13 ± 43.27	1,288.72 ± 66.59	<0.001	39.70 ± 2.42	44.21 ± 3.35	0.004
FU3	1,210.12 ± 27.73	1,348.01 ± 54.16	<0.001	38.68 ± 1.25	40.51 ± 3.34	0.131
Adjusted *P*-values[b]	NA	>0.99		NA	>0.99	
Adjusted *P*-values[b]	NA	0.006		NA	0.006	
Adjusted *P*-values[b]	NA	<0.001		NA	>0.99	
Percent change (%)						
FU1–FU0	0.05 ± 1.47	1.15 ± 1.87	0.085	−0.84 ± 4.73	1.45 ± 3.94	0.132
FU2–FU0	0.87 ± 3.11	6.29 ± 3.86	0.001	2.89 ± 6.32	13.19 ± 10.63	0.004
FU3–FU0	0.79 ± 1.99	11.24 ± 4.36	<0.001	0.26 ± 3.94	3.57 ± 8.48	0.295

NIA, nonirradiated areas; IA, irradiated areas; NA, not applicable; FU0, baseline; FU1, 2 days post radiotherapy; FU2, 3 months post radiotherapy; FU3, 6 months post radiotherapy.
Unless otherwise specified, data are mean ± SD. Data were compared among baseline and follow-ups by using the Friedman rank test with *post-hoc test* with Bonferroni correction. Data were compared between NIA and IA by using Paired Sample *t*-Test.
[a]$P > 0.05$ using Friedman rank test among baseline and follow-ups.
[b]Adjusted *P*-values by *post-hoc test* with Bonferroni correction between FU1 and FU0, FU2 and FU0, and FU3 and FU0.

In our study, no significant changes in global myocardial strain were found, which may be because the IMRT of our patients affected only the focal myocardium and so had little effect on the global strain. Since that segmental myocardial strain did not have good reproducibility reported (47) and not all of the irradiated field myocardium was distributed according to American Heart Association (AHA) segments, we did not measure segmental myocardial strain. As for the early change in strain in the animal study (46), it may also be because they used whole-heart irradiation, while only the focal myocardium was irradiated in our study. Our study also implied that changes in LVEF and other function parameters were later than changes in native T1 and T2 values, which revealed that CMR has the potential to detect subclinical damage derived from radiotherapy.

There was no significant correlation between irradiation dose and MR parameters (T1 and T2 values) found on IA in our study, and another study (48) was consistent with our results. First, both studies have a small sample size and, second, the difference in the irradiation dose on IA of the heart was small among each patient in our study. So, the correlation between irradiation dose and heart injury degree may have not been ultimately shown in both studies. There was still a study (49) with 6 years of follow-ups that found that areas of high cardiac dose exhibited high T1 values, and no significant changes in NIA in our study also implied that there was a correlation to some degree. However, the detailed information, such as the threshold dose to process heart injury, remains unanswered, which is crucial to the clinic. Then, further investigation is needed.

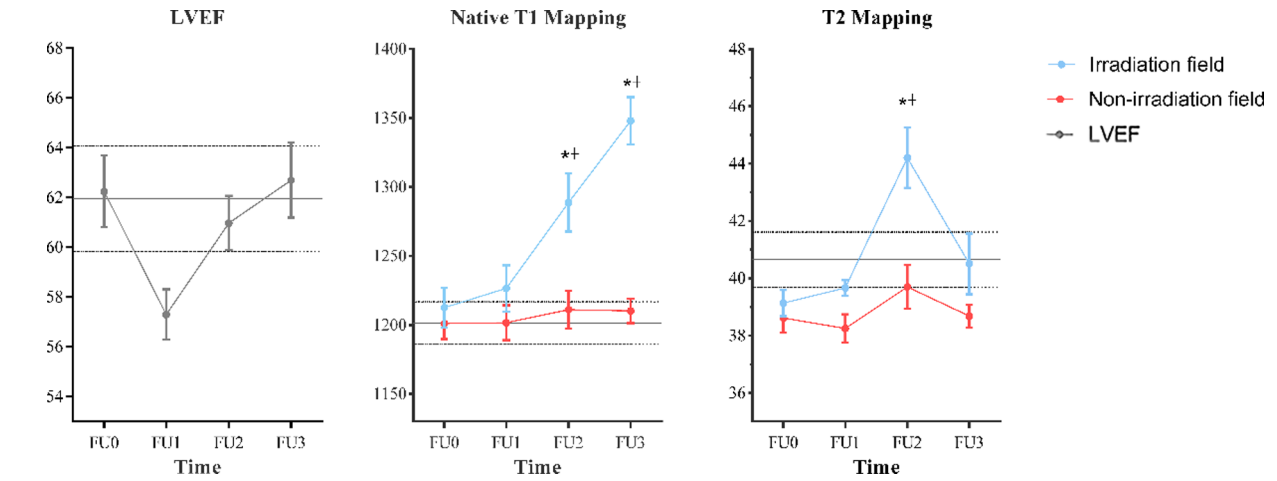

FIGURE 3
Temporal evolution of CMR measurements. Data are represented as mean ± SD. The parallel gray solid lines represent the mean values of age/gender-matched controls and the interval of two parallel gray dotted lines represents their 95% CI. *Statistically significant differences compared with FU0: $P < 0.01$. †Statistically significant differences compared with the values measured in the nonirradiation field: $P < 0.05$. CMR, cardiac magnetic resonance; FU0, baseline.

Our study has several limitations. First, the sample size of this study was small and the follow-up period was short, thus late changes in parameters such as native T1, T2, LV function, and strain were unclear; and no participant had a cardiac event during the follow-up period, so the correlation between MRI performance and cardiac events after chemotherapy–radiotherapy remains unclear. Second, we did not perform enhancement scans, so additional cardiac MR data such as extracellular volume (ECV) and LGE could not be obtained for several reasons: on the one hand, the scans would have been longer and there was concern that the patients would not tolerate them; on the another hand, some of the chemotherapeutic agents may be nephrotoxic to reduce the patient's renal burden as well as to avoid contrast allergy or adverse reactions. Third, all of our participants received radiotherapy and chemotherapy, some of them with paclitaxel, which has been found to cause cardiac rhythm disturbances possibly through mechanisms such as organelle damage and histamine-induced release (50), so it may affect the outcome. However, to exclude interference from chemotherapy, we compared baseline MR data from radiotherapy patients and healthy volunteers and no significant differences were found, so we concluded that chemotherapy did not affect the hearts in our cohort. Finally, all participants did not undergo a myocardial biopsy, so there were no pathological findings to confirm our results.

In conclusion, native T1 and T2 mapping can detect early changes in the myocardium at 3 months after chest radiotherapy, which is earlier than LVEF. This may provide clinical evidence of the time point to early prevent cardiac injury during chest radiotherapy.

Data availability statement

The original contributions presented in the study are included in the article/Supplementary material, further inquiries can be directed to the corresponding author.

Ethics statement

The studies involving human participants were reviewed and approved by Shandong Provincial Hospital Affiliated to Shandong First Medical University. The patients/participants provided their written informed consent to participate in this study.

Author contributions

CW, TW, and YT conceived and designed the experiments.WS provided clinical data. CW, YT, TW, and LT performed the experiments.YT, TW, YY, and CX analyzed the data and created the figures.YT, TW, and LT wrote the paper. CW provided funding. All authors contributed to the article and approved the submitted version.

Funding

This work was supported by the Natural Science Foundation of Shandong Provincial (grant no. ZR2019MH125).

Acknowledgments

We thank all of the volunteers and patients for their participation in our study.

Conflict of interest

The authors declare that the research was conducted in the absence of any commercial or financial relationships that could be construed as a potential conflict of interest.

Publisher's note

All claims expressed in this article are solely those of the authors and do not necessarily represent those of their affiliated organizations, or those of the publisher, the editors and the reviewers. Any product that may be evaluated in this article, or claim that may be made by its manufacturer, is not guaranteed or endorsed by the publisher.

Supplementary material

The Supplementary Material for this article can be found online at: https://www.frontiersin.org/articles/10.3389/fcvm.2023.1085737/full#supplementary-material.

References

1. Sung H, Ferlay J, Siegel RL, Laversanne M, Soerjomataram I, Jemal A, et al. Global Cancer Statistics 2020: GLOBOCAN estimates of incidence and mortality worldwide for 36 cancers in 185 countries. *CA Cancer J Clin*. (2021) 71(3):209–49. doi: 10.3322/caac.21660

2. Miller KD, Fidler-Benaoudia M, Keegan TH, Hipp HS, Jemal A, Siegel RL. Cancer statistics for adolescents and young adults, 2020. *CA Cancer J Clin*. (2020) 70 (6):443–59. doi: 10.3322/caac.21637

3. Delaney G, Jacob S, Featherstone C, Barton M. The role of radiotherapy in cancer treatment: estimating optimal utilization from a review of evidence-based clinical guidelines. *Cancer*. (2005) 104(6):1129–37. doi: 10.1002/cncr.21324

4. van Hagen P, Hulshof MC, van Lanschot JJ, Steyerberg EW, van Berge Henegouwen MI, Wijnhoven BP, et al. Preoperative chemoradiotherapy for esophageal or junctional cancer. *N Engl J Med*. (2012) 366(22):2074–84. doi: 10.1056/NEJMoa1112088

5. Mikhail S, Wei L, Salem ME, Bekaii-Saab T. Outcomes of definitive chemoradiation in patients with esophageal cancer. *Dis Esophagus*. (2017) 30 (2):1–7. doi: 10.1111/dote.12506

6. Benveniste MF, Gomez D, Carter BW, Betancourt Cuellar SL, Shroff GS, Benveniste APA, et al. Recognizing radiation therapy-related complications in the chest. *Radiographics*. (2019) 39(2):344–66. doi: 10.1148/rg.2019180061

7. McGale P, Darby SC, Hall P, Adolfsson J, Bengtsson NO, Bennet AM, et al. Incidence of heart disease in 35,000 women treated with radiotherapy for breast cancer in Denmark and Sweden. *Radiother Oncol*. (2011) 100(2):167–75. doi: 10.1016/j.radonc.2011.06.016

8. Aleman BM, van den Belt-Dusebout AW, Klokman WJ, Van't Veer MB, Bartelink H, van Leeuwen FE. Long-term cause-specific mortality of patients treated for Hodgkin's disease. *J Clin Oncol*. (2003) 21(18):3431–9. doi: 10.1200/JCO.2003.07.131

9. Darby SC, McGale P, Taylor CW, Peto R. Long-term mortality from heart disease and lung cancer after radiotherapy for early breast cancer: prospective cohort study of about 300,000 women in US SEER cancer registries. *Lancet Oncol*. (2005) 6(8):557–65. doi: 10.1016/S1470-2045(05)70251-5

10. Atkins KM, Rawal B, Chaunzwa TL, Lamba N, Bitterman DS, Williams CL, et al. Cardiac radiation dose, cardiac disease, and mortality in patients with lung cancer. *J Am Coll Cardiol*. (2019) 73(23):2976–87. doi: 10.1016/j.jacc.2019.03.500

11. van den Bogaard VA, Ta BD, van der Schaaf A, Bouma AB, Middag AM, Bantema-Joppe EJ, et al. Validation and modification of a prediction model for acute cardiac events in patients with breast cancer treated with radiotherapy based on three-dimensional dose distributions to cardiac substructures. *J Clin Oncol*. (2017) 35(11):1171–8. doi: 10.1200/JCO.2016.69.8480

12. Taylor C, Correa C, Duane FK, Aznar MC, Anderson SJ, Bergh J, et al. Estimating the risks of breast cancer radiotherapy: evidence from modern radiation doses to the lungs and heart and from previous randomized trials. *J Clin Oncol*. (2017) 35(15):1641–9. doi: 10.1200/JCO.2016.72.0722

13. Darby SC, Ewertz M, McGale P, Bennet AM, Blom-Goldman U, Bronnum D, et al. Risk of ischemic heart disease in women after radiotherapy for breast cancer. *N Engl J Med*. (2013) 368(11):987–98. doi: 10.1056/NEJMoa1209825

14. Ferreira VM, Piechnik SK. CMR parametric mapping as a tool for myocardial tissue characterization. *Korean Circ J*. (2020) 50(8):658. doi: 10.4070/kcj.2020.0157

15. Liang YD, Xu YW, Li WH, Wan K, Sun JY, Lin JY, et al. Left ventricular function recovery in peripartum cardiomyopathy: a cardiovascular magnetic resonance study by myocardial T1 and T2 mapping. *J Cardiovasc Magn Reson*. (2020) 22(1):2. doi: 10.1186/s12968-019-0590-z

16. Aikawa Y, Noguchi T, Morita Y, Tateishi E, Kono A, Miura H, et al. Clinical impact of native T1 mapping for detecting myocardial impairment in Takotsubo cardiomyopathy. *Eur Heart J Cardiovasc Imaging*. (2019) 20(10):1147–55. doi: 10.1093/ehjci/jez034

17. Poindron V, Chatelus E, Canuet M, Gottenberg J-E, Arnaud L, Gangi A, et al. T1 mapping cardiac magnetic resonance imaging frequently detects subclinical diffuse myocardial fibrosis in systemic sclerosis patients. *Semin Arthritis Rheum*. (2020) 50 (1):128–34. doi: 10.1016/j.semarthrit.2019.06.013

18. Tahir E, Sinn M, Bohnen S, Avanesov M, Säring D, Stehning C, et al. Acute versus chronic myocardial infarction: diagnostic accuracy of quantitative native T1 and T2 mapping versus assessment of edema on standard T2-weighted cardiovascular MR images for differentiation. *Radiology*. (2017) 285(1):83–91. doi: 10.1148/radiol.2017162338

19. Dabir D, Luetkens J, Kuetting DLR, Feisst A, Isaak A, Schild HH, et al. Cardiac magnetic resonance including parametric mapping in acute Takotsubo syndrome: preliminary findings. *Eur J Radiol*. (2019) 113:217–24. doi: 10.1016/j.ejrad.2019.02.026

20. Krittayaphong R, Zhang S, Saiviroonporn P, Viprakasit V, Tanapibunpon P, Komoltri C, et al. Detection of cardiac iron overload with native magnetic resonance T1 and T2 mapping in patients with thalassemia. *Int J Cardiol*. (2017) 248:421–6. doi: 10.1016/j.ijcard.2017.06.100

21. Bohnen S, Radunski UK, Lund GK, Ojeda F, Looft Y, Senel M, et al. Tissue characterization by T1 and T2 mapping cardiovascular magnetic resonance imaging to monitor myocardial inflammation in healing myocarditis. *Eur Heart J Cardiovasc Imaging*. (2017) 18(7):744–51. doi: 10.1093/ehjci/jex007

22. Shah RV, Kato S, Roujol S, Murthy V, Bellm S, Kashem A, et al. Native myocardial T1 as a biomarker of cardiac structure in non-ischemic cardiomyopathy. *Am J Cardiol*. (2016) 117(2):282–8. doi: 10.1016/j.amjcard.2015.10.046

23. Giusca S, Korosoglou G, Montenbruck M, Gersak B, Schwarz AK, Esch S, et al. Multiparametric early detection and prediction of cardiotoxicity using myocardial strain, T1 and T2 mapping, and biochemical markers: a longitudinal cardiac resonance imaging study during 2 years of follow-up. *Circ Cardiovasc Imaging*. (2021) 14(6):e012459. doi: 10.1161/CIRCIMAGING.121.012459

24. Halliday BP, Senior R, Pennell DJ. Assessing left ventricular systolic function: from ejection fraction to strain analysis. *Eur Heart J*. (2021) 42(7):789–97. doi: 10.1093/eurheartj/ehaa587

25. MacIver DH, Adeniran I, Zhang H. Left ventricular ejection fraction is determined by both global myocardial strain and wall thickness. *Int J Cardiol Heart Vasc*. (2015) 7:113–8. doi: 10.1016/j.ijcha.2015.03.007

26. Schultz-Hector S, Trott KR. Radiation-induced cardiovascular diseases: is the epidemiologic evidence compatible with the radiobiologic data? *Int J Radiat Oncol Biol Phys*. (2007) 67(1):10–8. doi: 10.1016/j.ijrobp.2006.08.071

27. Lauk S, Kiszel Z, Buschmann J, Trott KR. Radiation-induced heart-disease in rats. *Int J Radiat Oncol Biol Phys*. (1985) 11(4):801–8. doi: 10.1016/0360-3016(85)90314-1

28. Fajardo LF, Stewart JR. Capillary injury preceding radiation-induced myocardial fibrosis. *Radiology*. (1971) 101(2):429–33. doi: 10.1148/101.2.429

29. Takagi H, Ota H, Umezawa R, Kimura T, Kadoya N, Higuchi S, et al. Left ventricular T1 mapping during chemotherapy-radiation therapy: serial assessment of participants with esophageal cancer. *Radiology*. (2018) 289(2):347–54. doi: 10.1148/radiol.2018172076

30. Kvernby S, Flejmer AM, Dasu A, Bolger AF, Ebbers T, Engvall JE. T1 and T2 mapping for early detection of treatment-related myocardial changes in breast cancer patients. *J Magn Reson Imaging*. (2022) 55(2):620–2. doi: 10.1002/jmri.27820

31. Tahir E, Azar M, Shihada S, Seiffert K, Goy Y, Beitzen-Heineke A, et al. Myocardial injury detected by T1 and T2 mapping on CMR predicts subsequent cancer therapy–related cardiac dysfunction in patients with breast cancer treated by

epirubicin-based chemotherapy or left-sided RT. *Eur Radiol*. (2022) 32(3):1853–65. doi: 10.1007/s00330-021-08260-7

32. Haslbauer JD, Lindner S, Valbuena-Lopez S, Zainal H, Zhou H, D'Angelo T, et al. CMR imaging biosignature of cardiac involvement due to cancer-related treatment by T1 and T2 mapping. *Int J Cardiol*. (2019) 275:179–86. doi: 10.1016/j.ijcard.2018.10.023

33. Jordan JH, Vasu S, Morgan TM, D'Agostino RB Jr., Melendez GC, Hamilton CA, et al. Anthracycline-associated T1 mapping characteristics are elevated independent of the presence of cardiovascular comorbidities in cancer survivors. *Circ Cardiovasc Imaging*. (2016) 9(8):e004325. doi: 10.1161/CIRCIMAGING.115.004325

34. Safaei AM, Kamangar TM, Asadian S, Rezaeian N, Esmati E, Kolahdouzan K, et al. Detection of the early cardiotoxic effects of doxorubicin-containing chemotherapy regimens in patients with breast cancer through novel cardiac magnetic resonance imaging: a short-term follow-up. *J Clin Imaging Sci*. (2021) 11:33. doi: 10.25259/JCIS_58_2021

35. Melendez GC, Vasu S, Lesnefsky EJ, Kaplan JR, Appt S, D'Agostino RB Jr., et al. Myocardial extracellular and cardiomyocyte volume expand after doxorubicin treatment similar to adjuvant breast cancer therapy. *JACC Cardiovasc Imaging*. (2020) 13(4):1084–5. doi: 10.1016/j.jcmg.2019.10.020

36. Jafari F, Safaei AM, Hosseini L, Asadian S, Kamangar TM, Zadehbagheri F, et al. The role of cardiac magnetic resonance imaging in the detection and monitoring of cardiotoxicity in patients with breast cancer after treatment: a comprehensive review. *Heart Fail Rev*. (2021) 26(3):679–97. doi: 10.1007/s10741-020-10028-y

37. Dabir D, Child N, Kalra A, Rogers T, Gebker R, Jabbour A, et al. Reference values for healthy human myocardium using a T1 mapping methodology: results from the international T1 multicenter cardiovascular magnetic resonance study. *J Cardiovasc Magn Reson*. (2014) 16(1):69. doi: 10.1186/s12968-014-0069-x

38. Alsaied T, Tseng SY, Siddiqui S, Patel P, Khoury PR, Crotty EJ, et al. Pediatric myocardial T1 and T2 value associations with age and heart rate at 1.5 T. *Pediatr Cardiol*. (2021) 42(2):269–77. doi: 10.1007/s00246-020-02479-9

39. Seemann I, Gabriels K, Visser NL, Hoving S, te Poele JA, Pol JF, et al. Irradiation induced modest changes in murine cardiac function despite progressive structural damage to the myocardium and microvasculature. *Radiother Oncol*. (2012) 103 (2):143–50. doi: 10.1016/j.radonc.2011.10.011

40. Mezzaroma E, Di X, Graves P, Toldo S, Van Tassell BW, Kannan H, et al. A mouse model of radiation-induced cardiomyopathy. *Int J Cardiol*. (2012) 156 (2):231–3. doi: 10.1016/j.ijcard.2012.01.038

41. Taunk NK, Haffty BG, Kostis JB, Goyal S. Radiation-induced heart disease: pathologic abnormalities and putative mechanisms. *Front Oncol*. (2015) 5:39. doi: 10.3389/fonc.2015.00039

42. Spetz J, Moslehi J, Sarosiek K. Radiation-induced cardiovascular toxicity: mechanisms, prevention, and treatment. *Curr Treat Options Cardiovasc Med*. (2018) 20:1–11. doi: 10.1007/s11936-018-0627-x

43. Dall'Armellina E, Piechnik SK, Ferreira VM, Si QL, Robson MD, Francis JM, et al. Cardiovascular magnetic resonance by non contrast T1-mapping allows assessment of severity of injury in acute myocardial infarction. *J Cardiovasc Magn Reson*. (2012) 14:15. doi: 10.1186/1532-429X-14-15

44. Jeuthe S, Wassilew K, Oh-Ici D, da Silva TF, Munch F, Berger F, et al. Myocardial T1 maps reflect histological findings in acute and chronic stages of myocarditis in a rat model. *J Cardiovasc Magn Reson*. (2016) 18:19. doi: 10.1186/s12968-016-0241-6

45. Ferreira VM, Schulz-Menger J, Holmvang G, Kramer CM, Carbone I, Sechtem U, et al. Cardiovascular magnetic resonance in nonischemic myocardial inflammation: expert recommendations. *J Am Coll Cardiol*. (2018) 72(24):3158–76. doi: 10.1016/j.jacc.2018.09.072

46. Ibrahim E-SH, Baruah D, Croisille P, Stojanovska J, Rubenstein JC, Frei A, et al. Cardiac magnetic resonance for early detection of radiation therapy-induced cardiotoxicity in a small animal model. *JACC CardioOncol*. (2021) 3(1):113–30. doi: 10.1016/j.jaccao.2020.12.006

47. Mangion K, Burke NMM, McComb C, Carrick D, Woodward R, Berry C. Feature-tracking myocardial strain in healthy adults—a magnetic resonance study at 3.0 tesla. *Sci Rep*. (2019) 9(1):3239. doi: 10.1038/s41598-019-39807-w

48. Ricco A, Slade A, Canada JM, Grizzard J, Dana F, Rezai Gharai L, et al. Cardiac MRI utilizing late gadolinium enhancement (LGE) and T1 mapping in the detection of radiation induced heart disease. *Cardiooncology*. (2020) 6:6. doi: 10.1186/s40959-020-00061-z

49. Tuohinen S, Skytta T, Virtanen V, Nikus K, Kellokumpu-Lehtinen PL, Raatikainen P, et al. Radiotherapy-induced changes in breast cancer patients in extra cellular volume and T1 mapping in cardiac magnetic resonance imaging and in ECG six years after radiotherapy treatment. *Eur Heart J Cardiovasc Imaging*. (2019) 20(Suppl_2):jez111.008. doi: 10.1093/ehjci/jez111.008

50. Rowinsky EK, McGuire WP, Guarnieri T, Fisherman JS, Christian MC, Donehower RC. Cardiac disturbances during the administration of taxol. *J Clin Oncol*. (1991) 9(9):1704–12. doi: 10.1200/JCO.1991.9.9.1704

frontiers | Frontiers in Cardiovascular Medicine

TYPE Original Research
PUBLISHED 25 April 2023
DOI 10.3389/fcvm.2023.996354

OPEN ACCESS

EDITED BY
Rod Skinner,
Newcastle University, United Kingdom

REVIEWED BY
Yue Zheng,
Tianjin Medical University, China
Mirza Pojskic,
University Hospital of Giessen and Marburg, Germany

*CORRESPONDENCE
Mingwei Zhang
zhangmingwei28@sina.cn
Dajun Chai
dajunchai-fy@fjmu.edu.cn
Jinsheng Hong
13799375732@163.com

†These authors have contributed equally to this work and share first authorship

SPECIALTY SECTION
This article was submitted to Cardio-Oncology, a section of the journal Frontiers in Cardiovascular Medicine

RECEIVED 17 July 2022
ACCEPTED 30 March 2023
PUBLISHED 25 April 2023

CITATION
Wang X, Li X, Wu Y, Hong J, Chai D and Zhang M (2023) Risk of cardiac-related death in astrocytoma patients treated with chemotherapy: A competing risk analysis using the SEER database.
Front. Cardiovasc. Med. 10:996354.
doi: 10.3389/fcvm.2023.996354

Risk of cardiac-related death in astrocytoma patients treated with chemotherapy: A competing risk analysis using the SEER database

Xuezhen Wang[1,2†], Xiaoxia Li[1,2†], Yufan Wu[1,2†], Jinsheng Hong[1,2,3*], Dajun Chai[2,4*] and Mingwei Zhang[1,2,3*]

[1]Department of Radiotherapy, Cancer Center, The First Affiliated Hospital, Fujian Medical University, Fuzhou, China, [2]National Regional Medical Center, Binhai Campus of the First Affiliated Hospital, Fujian Medical University, Fuzhou, China, [3]Key Laboratory of Radiation Biology of Fujian Higher Education Institutions, The First Affiliated Hospital, Fujian Medical University, Fuzhou, China, [4]Cardiovascular Department, The First Affiliated Hospital, Fujian Medical University, Fuzhou, China

Purpose: To explore the impact of chemotherapy on the risk of cardiac-related death in astrocytoma patients.
Methods: We retrospectively evaluated astrocytoma patients diagnosed between 1,975 and 2016 in the Surveillance, Epidemiology, and End Results (SEER) database. Using Cox proportional hazards models, we compared the risks of cardiac-related death between a chemotherapy group and non-chemotherapy group. Competing-risks regression analyses were used to evaluate the difference in cardiac-related death. Also, propensity score matching (PSM) was employed to reduce confounding bias. The robustness of these findings was evaluated by sensitivity analysis, and E values were calculated.
Results: A total of 14,834 patients diagnosed with astrocytoma were included. Chemotherapy (HR = 0.625, 95%CI: 0.444–0.881) was associated with cardiac-related death in univariate Cox regression analysis. Chemotherapy was an independent prognostic factor for a lower risk of cardiac-related death before (HR = 0.579, 95%CI: 0.409–0.82, $P = 0.002$) and after PSM (HR = 0.550, 95%CI: 0.367–0.823 $P = 0.004$). Sensitivity analysis determined that the E-value of chemotherapy was 2.848 and 3.038 before and after PSM.
Conclusions: Chemotherapy did not increase the risk of cardiac-related death in astrocytoma patients. This study highlights that cardio–oncology teams should provide comprehensive care and long-term monitoring for cancer patients, especially those with an increased risk of cardiovascular disease.

KEYWORDS
glioma, chemotherapy, cardiac-related death, competing risk analysis, PSM

1. Introduction

Gliomas are the most common primary tumors of the brain. They account for more than half of all primary tumors of the central nervous system (CNS). The World Health Organization classification of tumors of the central nervous system (CNS) (5th Edition) (1) was published in 2021, but the choice of treatment was based on the previous criteria of tumor diagnosis.

The standard treatment for glioma is resection with or without radiotherapy and/or chemotherapy (2, 3). Chemotherapy can prolong the progression-free survival and overall survival (OS) of glioma patients (3). In cases where glioma recurs after standard treatment, there is currently no standard chemotherapy regimen available, and instead an

individualized approach is typically employed. Therefore, careful consideration of the benefits and drawbacks of chemotherapy is crucial (4).

Antineoplastic therapy, such as chemotherapy, is known to prolong the survival of cancer patients. However, it can also induce cardiotoxicity, including cardiomyopathy, arrhythmias and other types of cardiovascular disease (CVD) (5, 6). CVD has become the second leading cause of death in patients with CNS tumors (7–9). A study on the Wales-based Secure Anonymous Information Linkage (SAIL) and US Surveillance, Epidemiology, and End Results (SEER) databases showed that the standardized mortality ratio (SMR) for CVD in patients with gliomas was 2.24 and 1.98, respectively (8).

However, evidence that clinical, imaging or laboratory parameters could identify astrocytoma patients at a higher cardiac risk is lacking. Studies on the risk of CVD or mortality for people with a glioma have reported overall findings without revealing histologic subtypes. This scenario may mask tumor heterogeneity, which could lead to different impacts on CVD mortality (8). Additionally, previous studies have focused on the effect of chemotherapy on all-cause mortality, with little attention given to the effect of chemotherapy on cardiac-related death in patients with astrocytoma. A better understanding of the risk factors associated with cardiac-related death and risk stratification in astrocytoma could help facilitate targeted interventions to lengthen survival.

Our study aimed to explore whether chemotherapy increases the risk of cardiac-related death in patients with astrocytoma based on a cohort from the SEER database. We used competing-risks regression analysis and sensitivity analysis. Our findings could aid clinicians in making informed treatment decisions by providing a better understanding of the risks associated with chemotherapy, as well as enabling more precise predictions of outcome in patients with astrocytoma.

2. Materials and methods

2.1. Study population

This retrospective study was undertaken with data from the SEER database using SEER*Stat 8.3.8. Our selected data source was the "Incidence—SEER 18 Regs Research Data + Hurricane Katrina Impacted Louisiana Cases, Nov 2018 Sub (1975–2016 varying)" database.

The inclusion criteria were: (1) the primary site of the tumor was the brain; (2) the histologic type was based on the International Classification of Diseases, 3rd edition (ICD-O-3), including 9400/3 [astrocytoma, not otherwise specified (NOS)], 9410/3 (protoplasmic astrocytoma), 9410/3 (protoplasmic astrocytoma) or 9420/3 (fibrillary astrocytoma); (3) the year of the diagnosis was between 1975 and 2016.

The exclusion criteria were: (1) unknown survival time; (2) missing important clinical data (e.g., age, sex, race, primary site of tumor and cause of death).

2.2. Selection of variables

The study variables provided by the SEER database were: demographic variable ("age at diagnosis", "sex", "race", "marital status at diagnosis", "year of the diagnosis"), clinicopathologic variables ("primary site", "histologic type ICD-O-3", "tumor size", "sequence number"), treatment status ("radiation recode", "chemotherapy recode", "surgery record", "surgical method") and survival status ("survival months", "SEER cause-specific death classification", "SEER other cause of death classification").

2.3. Endpoint definition

Cardiac-related death was the primary endpoint. Deaths resulting from accidents or diseases other than cardiac-related death was considered to be the competing risks. The data of cardiac-related death and non-cardiac-related death were extracted from the variables "SEER cause-specific death classification" and "SEER other cause of death classification" in the SEER database (https://seer.cancer.gov/causespecific/).

2.4. PSM

Propensity-score matching (PSM) was done using the nearest-neighbor-matching method with a caliper of 0.1 on the propensity scale with logistic regression. PSM was undertaken to match different variables between patients who underwent chemotherapy vs. patients who did not undergo chemotherapy. The variables were age, sex, race, marital status, year of diagnosis, primary site of tumor, histologic type of tumor, radiotherapy and surgery, and we used a 1:1 ratio for patients.

2.5. Statistical analyses

R 4.0.1 (R Foundation for Statistical Computing, Vienna, Austria; www.r-project.org/) was used for statistical analyses. Statistical analyses of categorical data were done using the chi-square test. "Cardiac-related death" was defined as any death caused by a heart disease. To gain a first insight into the relationship between chemotherapy and cardiac-related disease-specific survival, Kaplan–Meier survival curves were estimated and compared by the log-rank test. The association between chemotherapy and the risk of cardiac-related death was assessed by univariable and multivariable Cox proportional hazards regression models. The competing risks model was employed with a cumulative incidence function (CIF) to estimate the cumulative probability of cardiac-related death and non-cardiac-related death. The CIF was compared among subgroups by the Gray test. The Fine–Gray proportional hazards model was employed to analyze competing risks using "cmprsk" within R. Adopt E-value (10) was used to evaluate the extent of unmeasured confounding factors that could have influenced the results. $P < 0.05$ (two-sided) was considered significant.

3. Results

3.1. Patient characteristics before PSM

A total of 14,834 patients diagnosed with astrocytoma before 2016 were identified. Patients were divided into a chemotherapy group ($n = 3832$) and non-chemotherapy group ($n = 11{,}002$). The median duration of survival among the whole group was 25 [interquartile range (IQR): 7–96] months. The median duration of survival in the chemotherapy group was 18 (IQR: 8–52) months, and that in non-chemotherapy group was 30 (IQR: 7–114.75) months. The demographic and clinicopathological data of the two groups are shown in **Table 1**.

3.2. Patient characteristics after PSM

PSM was conducted to minimize possible confounding effects. We discovered that 3,349 pairs of patients who underwent chemotherapy vs. those who did not receive chemotherapy were matched by a 1:1 ratio, respectively. The standard mean difference of all parameters after matching was <0.1 (**Supplementary Figure S1**). No significant differences in characteristics at baseline were observed in the two cohorts except for sex, grade and surgery method (**Table 1**).

3.3. Survival analyses

Patients who underwent chemotherapy had a higher prevalence of cardiac-related disease-specific survival compared to those who did not receive chemotherapy (**Figure 1A**). A univariate Cox regression model was established to identify potential prognostic factors. Our findings showed that chemotherapy (hazard ratio [HR] = 0.625, 95% confidence interval [CI]: 0.444–0.881), age (31–50 vs. ≤30 years: HR = 6.564, 95%CI: 3.743–11.51; 51–70 vs. ≤30 years: HR = 41.38, 95%CI: 23.775–72.021; ≥71 vs. ≤ 30 years: HR = 161.748, 95%CI: 90.175–290.13), race (others *vs.* black: HR = 0.266, 95%CI: 0.111–0.638; white *vs.* black: HR = 0.627, 95%CI: 0.432–0.912), marital status (single/unmarried *vs.* divorced/separated: HR = 0.147, 95%CI: 0.088–0.245; widowed/others *vs.* divorced/separated: HR = 2.482, 95%CI: 1.575–3.91), primary site (HR = 1.985, 95%CI: 1.305–3.02), surgery (HR = 0.388, 95%CI: 0.25–0.601) and sequence number (HR = 1.961, 95%CI: 1.263–3.043) were associated with cardiac-related death (**Table 2**). However, upon multivariable Cox regression analysis, chemotherapy was not an independent factor for patients with astrocytoma.

After PSM, the cardiac-related disease-specific survival outcome between the chemotherapy group and non-chemotherapy group was the same, with a *P*-value of 0.038 (**Figure 2**).

3.4. Competing-risks regression analysis before PSM

We aimed to address the issue of competing risk bias, so we utilized the Fine–Gray model to evaluate the risks of independent prognostic variables with non-cardiac-related death as a competing risk. Among the 10,602 deaths events, 277 were attributed to cardiac-related death. The cumulative incidence of cardiac-related death and non-cardiac-related death is demonstrated in **Figure 3**. The univariate analysis results are displayed in **Figure 4A**. It is found that chemotherapy was associated with a lower risk of cardiac-related death (HR = 0.491, 95%CI: 0.35–0.688, $P < 0.001$). The multivariate competing-risks proportional hazards model included the same covariates as the univariate analysis. Chemotherapy remained significant in the multivariate analysis (HR = 0.579, 95%CI: 0.409–0.821, $P = 0.002$) (**Figure 4A**). Subgroups of age (51–70 or ≥71 years), sex (male or female), race (white), marital status (married), diagnosis (before 2005), primary site (supratentorial or others), tumor size (unknown), surgery (no or unknown), surgical method (no surgery or others), radiotherapy (yes or no) and sequence number (yes or no) demonstrated a reduction in the risk of cardiac-related death with chemotherapy. There was no significant interaction between chemotherapy and other study variables ($P_{interaction} > 0.05$) (**Supplementary Figure S2A**).

3.5. Competing-risks regression analysis after PSM

PSM was carried out to eliminate the imbalance of baseline characteristics between groups. After PSM, results based on the competing risk model demonstrated that chemotherapy was associated significantly with cardiac-related death (HR = 0.549, 95%CI: 0.368–0.818, $P = 0.003$) and was an independent prognostic factor of a lower risk of cardiac-related death (HR = 0.55, 95%CI: 0.367–0.823, $P = 0.004$) (**Figure 4B**). The subgroups of sex (male), marital status (married), diagnosis (before 2005), primary site (supratentorial), tumor size (unknown), surgery (unknown), radiotherapy and no sequence number were demonstrated to reduce the risk of cardiac-related death with chemotherapy. No significant interaction between chemotherapy and those variables was found($P_{interaction} > 0.05$) (**Supplementary Figure S2B**).

3.6. Sensitivity analysis

Before PSM, it was found that the relative risk (RR) of death in the chemotherapy group was 0.579, and the E-value (95%CI) was determined to be 2.848 (1.737–4.325) (**Supplementary Figure S3A**). After PSM, the RR was 0.55 and the E-value (95% CI) was determined to be 3.038 (1.726–4.893) for death in the chemotherapy group (**Supplementary Figure S3B**).

TABLE 1 Characteristics of patients before and after PSM.

Variables	Before PSM			After PSM		
	Chemotherapy NO (*n* = 11,002)	Chemotherapy YES (*n* = 3,832)	*P*	Chemotherapy NO (*n* = 3,350)	Chemotherapy YES (*n* = 3,349)	*P*
Age, *n* (%)			<0.001			0.482
~30	3,166 (29)	748 (20)		683 (20)	715 (21)	
31–50	3,067 (28)	1,248 (33)		1,078 (32)	1,026 (31)	
51–70	3,057 (28)	1,500 (39)		1,272 (38)	1,274 (38)	
71~	1,712 (16)	336 (9)		317 (9)	334 (10)	
Sex, *n* (%)			<0.001			0.034
Female	4,978 (45)	1,574 (41)		1,435 (43)	1,348 (40)	
Male	6,024 (55)	2,258 (59)		1,915 (57)	2,001 (60)	
Race, *n* (%)			0.101			0.331
Black	758 (7)	232 (6)		238 (7)	227 (7)	
Others	528 (5)	204 (5)		164 (5)	190 (6)	
White	9,716 (88)	3,396 (89)		2,948 (88)	2,932 (88)	
Marital_status, *n* (%)			<0.001			0.094
Divorced/separated	765 (7)	286 (7)		231 (7)	273 (8)	
Married	5,549 (50)	2,357 (62)		2,034 (61)	1,949 (58)	
Single/Unmarried	3,497 (32)	938 (24)		858 (26)	881 (26)	
Widowed/Others	1,191 (11)	251 (7)		227 (7)	246 (7)	
Diagnosis, *n* (%)			<0.001			0.268
~2005	8,252 (75)	2,001 (52)		2,041 (61)	1,995 (60)	
2005–2016	2,750 (25)	1,831 (48)		1,309 (39)	1,354 (40)	
Grade, *n* (%)			<0.001			<0.001
1	830 (8)	104 (3)		197 (6)	92 (3)	
2	3,426 (31)	609 (16)		962 (29)	548 (16)	
3	2,016 (18)	1,011 (26)		577 (17)	945 (28)	
4	1,199 (11)	898 (23)		374 (11)	768 (23)	
Unknown	3,531 (32)	1,210 (32)		1,240 (37)	996 (30)	
Primary.Site, *n* (%)			<0.001			0.373
Infratentorial	1,399 (13)	275 (7)		255 (8)	271 (8)	
Others	2,557 (23)	870 (23)		789 (24)	826 (25)	
Supratentorial	7,046 (64)	2,687 (70)		2,306 (69)	2,252 (67)	
Hist.Type, *n* (%)			<0.001			0.592
Fibrillary astrocytoma	1,035 (9)	570 (15)		430 (13)	430 (13)	
Gemistocytic astrocytoma	543 (5)	421 (11)		338 (10)	317 (9)	
NOS	9,326 (85)	2,827 (74)		2,574 (77)	2,589 (77)	
Protoplasmic astrocytoma	98 (1)	14 (0)		8 (0)	13 (0)	
Tumor_Size, *n* (%)			<0.001			0.464
~4	1,141 (10)	606 (16)		466 (14)	452 (13)	
4~	792 (7)	600 (16)		394 (12)	426 (13)	
Unknown	9,069 (82)	2,626 (69)		2,490 (74)	2,471 (74)	
Surgery, *n* (%)			<0.001			0.108
NO	1,801 (16)	871 (23)		842 (25)	847 (25)	
Unknown	6,276 (57)	1,424 (37)		1,500 (45)	1,423 (42)	
YES	2,925 (27)	1,537 (40)		1,008 (30)	1,079 (32)	
Surgery. Method, *n* (%)			<0.001			0.01
Biopsy&Local excision	851 (8)	457 (12)		311 (9)	332 (10)	
Gross total resection	1,132 (10)	469 (12)		337 (10)	301 (9)	
No surgery	1,801 (16)	871 (23)		842 (25)	847 (25)	
Others	6,352 (58)	1,451 (38)		1,519 (45)	1,446 (43)	
Subtotal resection	866 (8)	584 (15)		341 (10)	423 (13)	
Radiation, *n* (%)			<0.001			0.65
NO	7,357 (67)	1,593 (42)		1,591 (47)	1,571 (47)	
YES	3,645 (33)	2,239 (58)		1,759 (53)	1,778 (53)	

(*continued*)

TABLE 1 Continued

Variables	Before PSM			After PSM		
	Chemotherapy NO (*n* = 11,002)	Chemotherapy YES (*n* = 3,832)	*P*	Chemotherapy NO (*n* = 3,350)	Chemotherapy YES (*n* = 3,349)	*P*
Sequence. Number, *n* (%)			0.145			0.816
NO	10,281 (93)	3,553 (93)		3,104 (93)	3,109 (93)	
YES	721 (7)	278 (7)		246 (7)	240 (7)	

Note: Sequence number, previous history of malignancy.

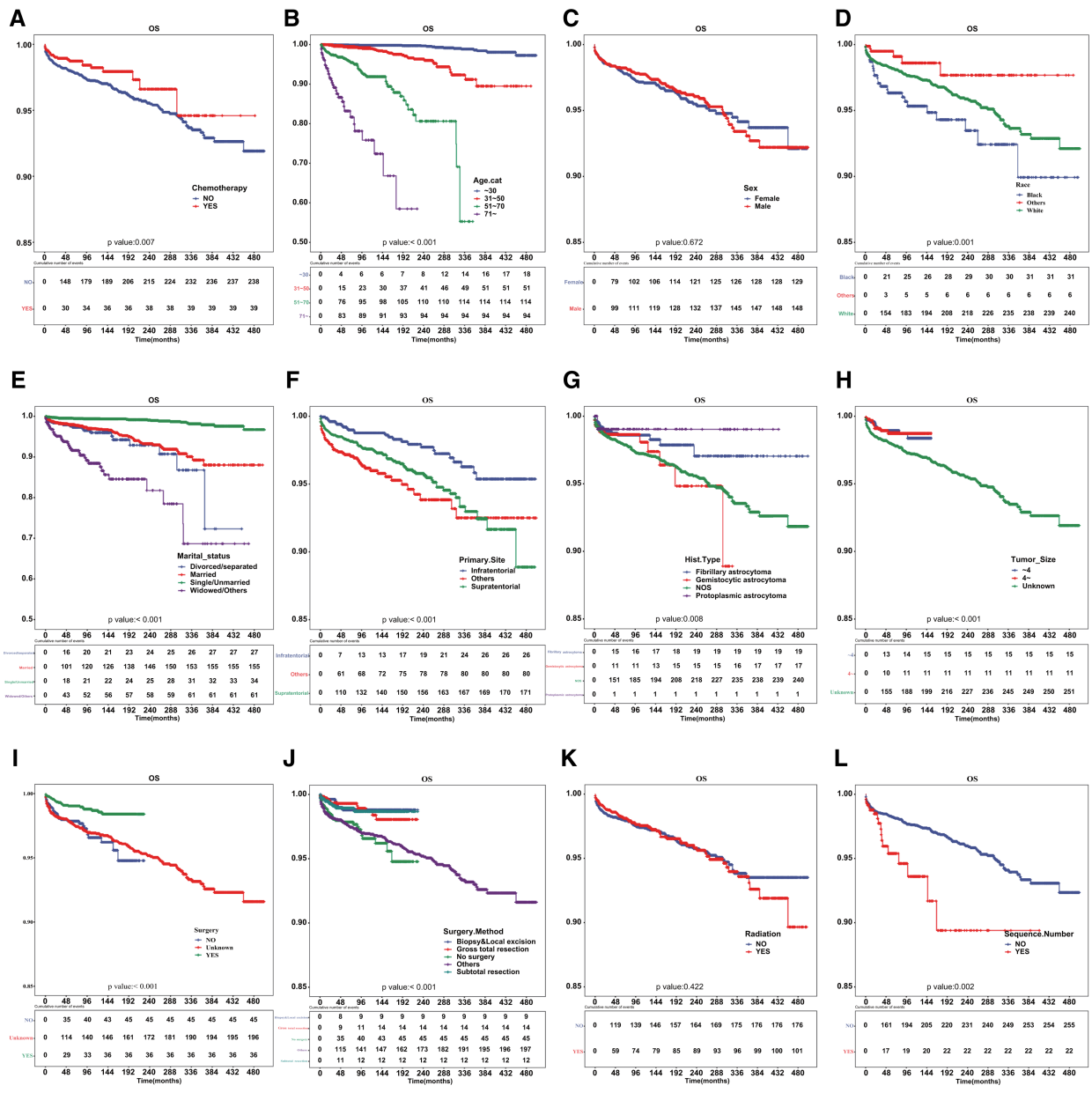

FIGURE 1
Cardiac disease-specific survival curve according to patient characteristics. Cardiac disease-specific survival curve of (A) chemotherapy, (B) age, (C) sex, (D) race, (E) marital status, (F) primary site of tumor, (G) histologic type, (H) tumor size, (I) surgery, (J) surgical method, (K) radiotherapy and (L) sequence number.

10.3389/fcvm.2023.996354

TABLE 2 Univariate and multivariate Cox regression analysis.

	Univariate analysis		Multivariate analysis	
	HR (95%CI)	*P*	HR (95%CI)	*P*
Age. cat				
31–50 vs. ~30	6.564 (3.743–11.51)	<0.001	5.989 (3.136–11.434)	<0.001
51–70 vs. ~30	41.38 (23.775–72.021)	<0.001	37.376 (19.438–71.866)	<0.001
71~ vs. ~30	161.748 (90.175–290.13)	<0.001	130.233 (64.925-261.234)	<0.001
Sex				
Male vs. female	0.95 (0.75–1.204)	0.672	1.24 (0.969–1.588)	0.088
Race				
Others vs. black	0.266 (0.111–0.638)	0.003	0.192 (0.08–0.462)	<0.001
White vs. black	0.627 (0.432–0.912)	0.015	0.41 (0.28–0.599)	<0.001
Marital status				
Married vs. divorced/ separated	0.776 (0.515–1.168)	0.224	0.718 (0.474–1.086)	0.117
Single/unmarried vs. divorced/separated	0.147 (0.088–0.245)	<0.001	0.599 (0.34–1.056)	0.077
Widowed/others vs. divorced/separated	2.482 (1.575–3.91)	<0.001	1.098 (0.684–1.765)	0.698
Primary site of tumor				
Others vs. infratentorial	2.936 (1.876–4.595)	<0.001	1.247 (0.783–1.985)	0.352
Supratentorial vs. infratentorial	1.985 (1.305–3.02)	0.001	0.997 (0.645–1.542)	0.991
Histologic type				
Gemistocytic astrocytoma vs. fibrillary astrocytoma	1.731 (0.9–3.332)	0.1	1.537 (0.794–2.976)	0.202
NOS vs. fibrillary astrocytoma	1.732 (1.086–2.765)	0.021	1.246 (0.778–1.996)	0.36
Protoplasmic astrocytoma vs. fibrillary astrocytoma	0.523 (0.07–3.91)	0.528	0.587 (0.078–4.405)	0.604
Tumor size				
4~ vs. ~4	0.96 (0.441–2.091)	0.919	1.018 (0.466–2.22)	0.965
Unknown vs. ~4	2.026 (1.198–3.426)	0.008	1.389 (0.782–2.469)	0.263
Surgery				
Unknown vs. NO	1.034 (0.741–1.443)	0.843	1.309 (0.895–1.914)	0.165
YES vs. NO	0.388 (0.25–0.601)	<0.001	0.654 (0.411–1.042)	0.074
Radiotherapy				
YES vs. NO	0.904 (0.708–1.156)	0.422	1.005 (0.765–1.32)	0.971
Chemotherapy				
YES vs. NO	0.625 (0.444–0.881)	0.007	0.703 (0.491–1.006)	0.054
Sequence number				
YES vs. NO	1.961 (1.263–3.043)	0.003	0.857(0.549–1.337)	0.496

Note: Sequence number, previous history of malignancy.

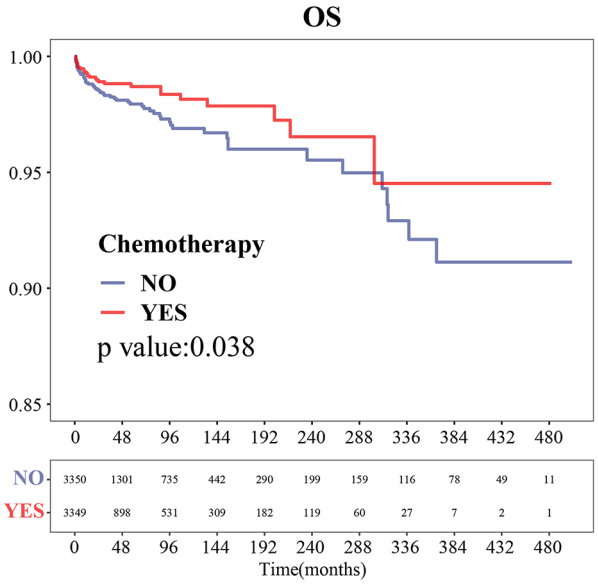

FIGURE 2
Cardiac disease-specific survival curve of chemotherapy after PSM.

4. Discussion

Cancer treatment-related cardiotoxicity has gained increasing attention recently. Chemotherapy plays an important role in the treatment of patients with high-risk, low-grade gliomas (11, 12). However, the evidence regarding whether chemotherapy increases the risk of cardiac-related death in patients with astrocytoma is not yet conclusive.

We investigated the impact of chemotherapy on cardiac-related death in patients with astrocytoma based on clinicopathological characteristics and the survival data of 14,834 patients with astrocytoma in the SEER database. With cardiac-related death as the endpoint, the Kaplan–Meier curve showed longer cardiac-related disease-specific survival in patients receiving chemotherapy than those who did not. However, a correlation between chemotherapy and cardiac-related death was not found upon multivariable Cox regression analysis. As retrospective observational studies cannot eliminate the influence of confounding factors on the outcome through randomization, we conducted PSM to achieve the effect of "post-randomization". Before and after PSM, patients who received chemotherapy had significantly longer cardiac-related disease-specific survival compared with those who did not receive chemotherapy. The competing risk regression model showed an independent prognostic role of chemotherapy for cardiac-related death. Furthermore, E-values were calculated in order to evaluate the influence of unmeasured confounding factors. The E-value of chemotherapy was 2.848 and 3.038 before and after PSM indicating that an unmeasured confounding factor exhibiting an extremely powerful association strength is required to overturn the obtained results. However, this type of factor is almost non-existent in this study.

One strength of our study is that it relates the risk of cardiac-related death in astrocytoma patients to whether they received chemotherapy or not during the disease course. Another strength of our study is that it was population-based, involving all patients with astrocytoma in the SEER database who had or did not have chemotherapy during the study period, thereby increasing the generalizability of our findings. Also, the cohort

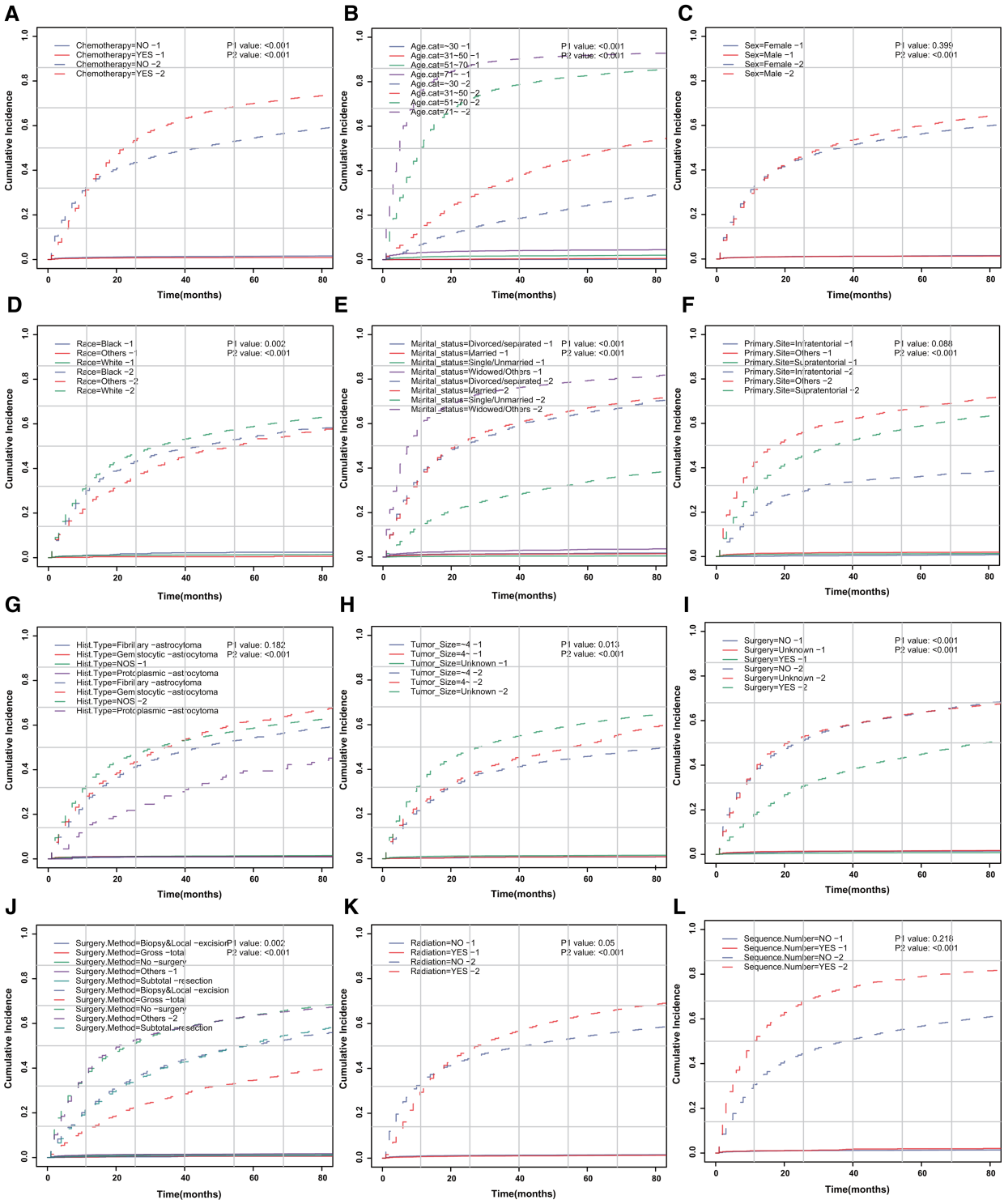

FIGURE 3
CIF curve of death according to patient characteristics. CIF curve of (A) chemotherapy, (B) age, (C) sex, (D) race, (E) marital status, (F) primary site of tumor, (G) histologic type, (H) tumor size, (I) surgery, (J) surgical method, (K) radiotherapy and (L) sequence number.

size was large, which aided robust statistical analyses. Our study also avoided the tendency in randomized clinical trials to omit patients in poor health. We minimized the potential for bias caused by a lack of information by only enrolling patients for whom detailed information on chemotherapy was available. However, because it was a retrospective study, we cannot rule out the possibility of confounding factors that may have influenced our results. To mitigate this, we used PSM for post-randomization to reduce the influence of confounding factors. In addition, E-value was used to assess the effect of unknown

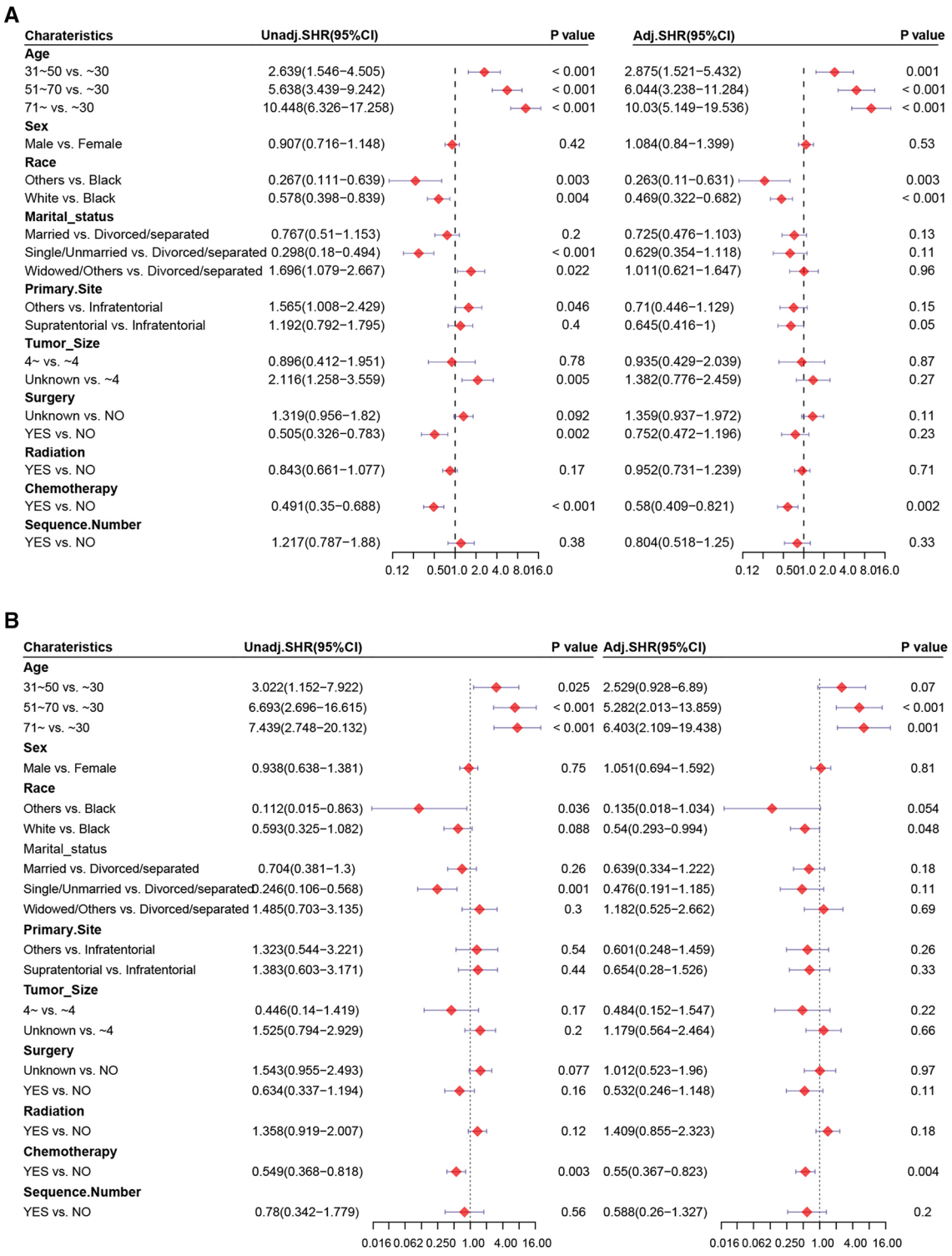

FIGURE 4
Forest plots of univariate and multivariate Cox regression analysis. Univariate and multivariate Cox regression analysis of chemotherapy (A) before and (B) after PSM.

confounding factors on the results to evaluate the robustness of these findings. No prospective clinical studies have explored the correlation between chemotherapy and cardiac-related death in astrocytoma patients, so our results based on a large cohort after PSM provide valuable guidance (13).

CVD is an important cause of death in cancer survivors (7). Many studies have discussed the risk of antineoplastic therapy-related cardiac diseases among survivors of breast cancer (14), lung cancer (15), and hematologic malignancies (15), but the risk of cardiac disease in patients with astrocytoma is not known.

The study conducted by Matthews and colleagues, which included 1,005 postmenopausal breast cancer patients in the UK and 22,027 patients in the USA, found that women treated with aromatase inhibitors showed a higher risk of several cardiovascular outcomes compared with those in users of tamoxifen. A study by Sun (15) indicated that of all competing causes of death in non-small-cell lung cancer, CVD resulted in the highest cumulative mortality (with the exception of lung cancer). Chemotherapy is considered to be a risk factor for CVD in cancer patients (14, 16). Platinum-based chemotherapy is a cardiovascular risk factor for survivors of testicular cancer (17), mainly due to drug toxicity. In the competing risk regression model, patients receiving chemotherapy (HR = 0.55, 95%CI: 0.367–0.823) had a lower risk of cardiac-related death than others, which is consistent with previous findings (15). In the absence of specific chemotherapy regimens, it is difficult to determine whether this effect is related to drug toxicity is not possible because clinicians may have assessed the potential combined risk before chemotherapy so that patients with high risk of CVD are excluded from treatment due to contraindications to chemotherapy. Patients with good cardiac function, excellent physical status and few contraindications to chemotherapy are more likely to receive chemotherapy, which could also influence the results.

A better understanding of the risk factors contributing to cardiac disease in cancer patients can aid in preventing and reducing avoidable morbidity and mortality, ultimately improving prognosis. Factors associated with CVD mortality in the CNS cancers include age, sex, ethnicity, economic deprivation, and no surgical procedure (8). One study focusing on cardiac mortality among 200,000 cancer patients aged 15–39 years who survived 5 years indicated that the number of cardiac-related deaths expected was 1.4-times greater than that of CNS tumors survivors. Additionally, the study suggested that the age at diagnosis plays a crucial role in determining the risk of subsequent cardiac-related death (7). Stratified analysis based on sex revealed that male patients with malignant glioma had a CVD mortality rate of over twofold higher in the SAIL (SMR = 2.66, 95% CI = 1.77–3.82) and SEER (SMR = 2.09, 95%CI = 1.89–2.31) databases compared to female patients (8). In our study, the HR for cardiac-related death in male patients was 0.448 (95%CI: 0.260–0.771). The reason for the discrepancy in values may be due to the inclusion of all histologic types of gliomas in the SAIL and SEER studies (e.g., glioblastoma), whereas we targeted the specific histologic type of astrocytoma. In addition, the risk of cardiotoxicity is associated with the type of chemotherapeutic agent used, as well as other factors such as anthracyclines, anthraquinones, miscellaneous drugs (18), dose (19), hypertension, previous cardiac disease (19), and radiation exposure (20).

For patients at high risk of astrocytoma, the most commonly used chemotherapy regimens are temozolomide (TMZ), procarbazine, lomustine, and vincristine (PCV) (21, 22). The main toxicities of procarbazine and lomustine (CCNU) are myelosuppression and gastrointestinal symptoms, while vincristine is neurotoxic and hepatotoxic, and has been reported to induce ischemic events due to its neurotoxicity (23). Additionally, chronic vincristine treatment may induce cardiovascular toxicity (5). TMZ is a type of oral alkylating agent with the most common side-effects being gastrointestinal and hematologic toxicity (24). Severe hematologic toxicity can lead to life-threatening infections (25), and cardiotoxicity occurs in a small number of patients who experience palpitations and hypertension. It has been reported that alkylating agents can cause direct endothelial damage to cardiomyocytes (26). Given the potential for cardiotoxicity associated with chemotherapeutic agents, the Cardio-Oncology Study Group of the Heart Failure Association of the European Society of Cardiology in collaboration with the International Cardio-Oncology Society Cardiology recommends cardiovascular-risk assessment at baseline for patients scheduled for cancer treatment to minimize the risk of cardiovascular toxicity (27). Meanwhile, the European Society for Medical Oncology consensus also defines cardiovascular toxicity associated with cancer and its treatment, and provides management strategies for prevention, screening, monitoring and treatment of cardiovascular toxicity (28). In the era of "personalized" medicine and the coexistence of multiple treatment modalities for oncology, collaboration between oncology and cardiology departments will facilitate more comprehensive treatment plans for cancer patients.

Our study had five main limitations. Firstly, the lack of detailed information on chemotherapy regimens, doses, frequencies or cycles and radiation dose/fraction in the SEER database prevented a more comprehensive analysis. Secondly, the SEER database does not include records of targeted therapy, immunotherapy and other antineoplastic treatments, the aim of curative or palliative treatment or prognosis-related molecular pathological status which could have influenced the accurate judgment of the prognosis of astrocytoma patients. Thirdly, the survival analysis of subgroups of different types of cardiac disease-related death was not explored due to the variability of heart diseases among patients with cardiac-related disease. Fourthly, the absence of a documented history of previous cardiac disease and assessment of risk factors for cardiac disease (e.g., tobacco smoking, obesity and diabetes mellitus) hampered subgroup analyses. Finally, as this was a retrospective, population-based study, we could only access data from the database up to 2016, which was the entry time for patients with information on adjuvant treatment that could be updated in the database to date. Despite these limitations, our study shed light on the persistent challenge of cardiac-related deaths in astrocytoma patients receiving chemotherapy. These results must be confirmed by further high-level evidence from prospective, multicenter, large-cohort clinical studies.

5. Conclusions

We revealed that cardiac-related deaths of astrocytoma patients treated with chemotherapy remain a clinical challenge. Several risk factors for cardiac-related death were identified by using the competing risk regression model. This study highlights that cardio–oncology teams must provide comprehensive care and long-term monitoring for cancer patients, especially those at an increased risk of CVD.

Data availability statement

Publicly available datasets were analyzed in this study. This data can be found here: SEER*Stat 8.3.8, https://seer.cancer.gov/causespecific/, and https://seer.cancer.gov/seerstat/.

Author contributions

The study design was decided by MZ, DC and JH. MZ: carried out data extraction. XW: carried out all analyses. YW: created graphs. XL: wrote the first draft. All authors contributed to the article and approved the submitted version.

Acknowledgments

We thank the members of Professor Hong's team (Department of Radiotherapy, Cancer Center, The First Affiliated Hospital, Fujian Medical University, Fuzhou, China) for their helpful discussions and critical reading of our manuscript.

Conflict of interest

The authors declare that the research was conducted in the absence of any commercial or financial relationships that could be construed as a potential conflict of interest.

Publisher's note

Supplementary material

The Supplementary Material for this article can be found online at: https://www.frontiersin.org/articles/10.3389/fcvm.2023.996354/full#supplementary-material.

References

1. Gritsch S, Batchelor TT, Gonzalez Castro LN. Diagnostic, therapeutic, and prognostic implications of the 2021 world health organization classification of tumors of the central nervous system. *Cancer*. (2022) 128:47–58. doi: 10.1002/cncr.33918

2. Stupp R, Mason WP, van den Bent MJ, Weller M, Fisher B, Taphoorn MJ, et al. Radiotherapy plus concomitant and adjuvant temozolomide for glioblastoma. *N Engl J Med*. (2005) 352:987–96. doi: 10.1056/NEJMoa043330

3. Stupp R, Hegi ME, Mason WP, van den Bent MJ, Taphoorn MJ, Janzer RC, et al. Effects of radiotherapy with concomitant and adjuvant temozolomide versus radiotherapy alone on survival in glioblastoma in a randomised phase III study: 5-year analysis of the EORTC-NCIC trial. *Lancet Oncol*. (2009) 10:459–66. doi: 10.1016/s1470-2045(09)70025-7

4. McDuff SGR, Dietrich J, Atkins KM, Oh KS, Loeffler JS, Shih HA. Radiation and chemotherapy for high-risk lower grade gliomas: choosing between temozolomide and PCV. *Cancer Med*. (2020) 9:3–11. doi: 10.1002/cam4.2686

5. Herradon E, Gonzalez C, Gonzalez A, Uranga JA, Lopez-Miranda V. Cardiovascular toxicity induced by chronic vincristine treatment. *Front Pharmacol*. (2021) 12:692970. doi: 10.3389/fphar.2021.692970

6. Huang G, Zhang N, Bi X, Dou M. Solid lipid nanoparticles of temozolomide: potential reduction of cardial and nephric toxicity. *Int J Pharm*. (2008) 355:314–20. doi: 10.1016/j.ijpharm.2007.12.013

7. Henson KE, Reulen RC, Winter DL, Bright CJ, Fidler MM, Frobisher C, et al. Cardiac mortality among 200 000 five-year survivors of cancer diagnosed at 15 to 39 years of age: the teenage and young adult cancer survivor study. *Circulation*. (2016) 134:1519–31. doi: 10.1161/circulationaha.116.022514

8. Jin K, Brennan PM, Poon MTC, Sudlow CLM, Figueroa JD. Raised cardiovascular disease mortality after central nervous system tumor diagnosis: analysis of 171,926 patients from UK and USA. *Neuro-oncol Adv*. (2021) 3:vdab136. doi: 10.1093/noajnl/vdab136

9. Sturgeon KM, Deng L, Bluethmann SM, Zhou S, Trifiletti DM, Jiang C, et al. A population-based study of cardiovascular disease mortality risk in US cancer patients. *Eur Heart J*. (2019) 40:3889–97. doi: 10.1093/eurheartj/ehz766

10. Haneuse S, VanderWeele TJ, Arterburn D. Using the E-value to assess the potential effect of unmeasured confounding in observational studies. *JAMA*. (2019) 321:602–3. doi: 10.1001/jama.2018.21554

11. Bell EH, Zhang P, Shaw EG, Buckner JC, Barger GR, Bullard DE, et al. Comprehensive genomic analysis in NRG oncology/RTOG 9802: a phase III trial of radiation versus radiation plus procarbazine, lomustine (CCNU), and vincristine in high-risk low-grade glioma. *J Clin Oncol*. (2020) 38:3407–17. doi: 10.1200/jco.19.02983

12. Fisher BJ, Pugh SL, Macdonald DR, Chakravatri A, Lesser GJ, Fox S, et al. Phase 2 study of a temozolomide-based chemoradiation therapy regimen for high-risk, low-grade gliomas: long-term results of radiation therapy oncology group 0424. *Int J Radiat Oncol Biol Phys*. (2020) 107:720–5. doi: 10.1016/j.ijrobp.2020.03.027

13. Hwang ES, Wang X. Value of propensity score matching to study surgical outcomes. *Ann Surg*. (2017) 265:457–8. doi: 10.1097/sla.0000000000002125

14. Matthews AA, Peacock Hinton S, Stanway S, Lyon AR, Smeeth L, Lund JL, et al. Endocrine therapy use and cardiovascular risk in postmenopausal breast cancer survivors. *Heart*. (2021) 107:1327–35. doi: 10.1136/heartjnl-2020-317510

15. Sun JY, Zhang ZY, Qu Q, Wang N, Zhang YM, Miao LF, et al. Cardiovascular disease-specific mortality in 270,618 patients with non-small cell lung cancer. *Int J Cardiol*. (2021) 330:186–93. doi: 10.1016/j.ijcard.2021.02.025

16. Padegimas A, Clasen S, Ky B. Cardioprotective strategies to prevent breast cancer therapy-induced cardiotoxicity. *Trends Cardiovasc Med*. (2020) 30:22–8. doi: 10.1016/j.tcm.2019.01.006

17. Gugic J, Zaletel LZ, Oblak I. Treatment-related cardiovascular toxicity in long-term survivors of testicular cancer. *Radiol Oncol*. (2017) 51:221–7. doi: 10.1515/raon-2016-0021

18. McGowan JV, Chung R, Maulik A, Piotrowska I, Walker JM, Yellon DM. Anthracycline chemotherapy and cardiotoxicity. *Cardiovasc Drugs Ther*. (2017) 31:63–75. doi: 10.1007/s10557-016-6711-0

19. Babiker HM, McBride A, Newton M, Boehmer LM, Drucker AG, Gowan M, et al. Cardiotoxic effects of chemotherapy: a review of both cytotoxic and molecular targeted oncology therapies and their effect on the cardiovascular system. *Crit Rev Oncol Hematol*. (2018) 126:186–200. doi: 10.1016/j.critrevonc.2018.03.014

20. Darby SC, Ewertz M, McGale P, Bennet AM, Blom-Goldman U, Brønnum D, et al. Risk of ischemic heart disease in women after radiotherapy for breast cancer. *N Engl J Med*. (2013) 368:987–98. doi: 10.1056/NEJMoa1209825

21. Fisher BJ, Hu C, Macdonald DR, Lesser GJ, Coons SW, Brachman DG, et al. Phase 2 study of temozolomide-based chemoradiation therapy for high-risk low-grade gliomas: preliminary results of radiation therapy oncology group 0424. *Int J Radiat Oncol Biol Phys*. (2015) 91:497–504. doi: 10.1016/j.ijrobp.2014.11.012

22. van den Bent MJ, Carpentier AF, Brandes AA, Sanson M, Taphoorn MJ, Bernsen HJ, et al. Adjuvant procarbazine, lomustine, and vincristine improves progression-free survival but not overall survival in newly diagnosed anaplastic oligodendrogliomas and oligoastrocytomas: a randomized European organisation for research and treatment of cancer phase III trial. *J Clin Oncol*. (2006) 24:2715–22. doi: 10.1200/jco.2005.04.6078

23. Al-Mahayri ZN, AlAhmad MM, Ali BR. Long-term effects of pediatric acute lymphoblastic leukemia chemotherapy: can recent findings inform old strategies? *Front Oncol.* (2021) 11:710163. doi: 10.3389/fonc.2021.710163

24. Scaringi C, De Sanctis V, Minniti G, Enrici RM. Temozolomide-related hematologic toxicity. *Onkologie*. (2013) 36:444–9. doi: 10.1159/000353752

25. Stepanovic A, Nikitovic M. Severe hematologic temozolomide-related toxicity and lifethreatening infections. *J BUON*. (2018) 23:7–13.

26. Morandi P, Ruffini PA, Benvenuto GM, Raimondi R, Fosser V. Cardiac toxicity of high-dose chemotherapy. *Bone Marrow Transplant*. (2005) 35:323–34. doi: 10.1038/sj.bmt.1704763

27. Lyon AR, Dent S, Stanway S, Earl H, Brezden-Masley C, Cohen-Solal A, et al. Baseline cardiovascular risk assessment in cancer patients scheduled to receive cardiotoxic cancer therapies: a position statement and new risk assessment tools from the cardio-oncology study group of the heart failure association of the European society of cardiology in collaboration with the international cardio-oncology society. *Eur J Heart Fail.* (2020) 22:1945–60. doi: 10.1002/ejhf.1920

28. Curigliano G, Lenihan D, Fradley M, Ganatra S, Barac A, Blaes A, et al. Management of cardiac disease in cancer patients throughout oncological treatment: eSMO consensus recommendations. *Ann Oncol.* (2020) 31:171–90. doi: 10.1016/j.annonc.2019.10.023

frontiers | Frontiers in Cardiovascular Medicine

TYPE Original Research
PUBLISHED 27 April 2023
DOI 10.3389/fcvm.2023.980101

OPEN ACCESS

EDITED BY
Antonella Lombardo,
Agostino Gemelli University Polyclinic (IRCCS), Italy

REVIEWED BY
Zoltan Varga,
Semmelweis University, Hungary
Teodora Donisan,
Mayo Clinic, United States

*CORRESPONDENCE
Tung-Hsin Wu
✉ tung@ym.edu.tw
Hon-Yi Lin
✉ doc16021@gmail.com

†These authors have contributed equally to this work

RECEIVED 28 June 2022
ACCEPTED 17 April 2023
PUBLISHED 27 April 2023

CITATION
Lee M-S, Tsai W-T, Yang H-J, Hung S-K, Chiou W-Y, Liu D-W, Chen L-C, Chew C-H, Yu B-H, Hsu F-C, Wu T-H and Lin H-Y (2023) Hazard-based risk grouping effectively stratifying breast cancer patients in post-irradiation long-term heart diseases: a population-based cohort study.
Front. Cardiovasc. Med. 10:980101.
doi: 10.3389/fcvm.2023.980101

Hazard-based risk grouping effectively stratifying breast cancer patients in post-irradiation long-term heart diseases: a population-based cohort study

Moon-Sing Lee[1,2†], Wei-Ta Tsai[1,3†], Hsuan-Ju Yang[1†], Shih-Kai Hung[1,2], Wen-Yen Chiou[1,2], Dai-Wei Liu[2,4], Liang-Cheng Chen[1,2,5], Chia-Hui Chew[1], Ben-Hui Yu[1], Feng-Chun Hsu[1], Tung-Hsin Wu[3*] and Hon-Yi Lin[1,2,6*]

[1]Department of Radiation Oncology, Dalin Tzu Chi Hospital, Buddhist Tzu Chi Medical Foundation, Chiayi, Taiwan, [2]School of Medicine, Tzu Chi University, Hualien, Taiwan, [3]Department of Biomedical Imaging and Radiological Sciences, National Yang Ming Chiao Tung University, Taipei, Taiwan, [4]Departments of Radiation Oncology, Hualien Tzu Chi Hospital, Buddhist Tzu Chi Medical Foundation, Chiayi, Taiwan, [5]Department of Computer Science and Information Engineering, National Cheng Kung University, Chiayi, Taiwan, [6]Department of Biomedical Sciences, National Chung Cheng University, Chia-Yi, Taiwan

Background: Even though advanced radiotherapy techniques provide a better protective effect on surrounding normal tissues, the late sequelae from radiation exposure to the heart are still considerable in breast cancer patients. The present population-based study explored the role of cox-regression-based hazard risk grouping and intended to stratify patients with post-irradiation long-term heart diseases.

Materials and methods: The present study investigated the Taiwan National Health Insurance (TNHI) database. From 2000 to 2017, we identified 158,798 breast cancer patients. Using a propensity score match of 1:1, we included 21,123 patients in each left and right breast irradiation cohort. Heart diseases, including heart failure (HF), ischemic heart disease (IHD), and other heart diseases (OHD), and anticancer agents, including epirubicin, doxorubicin, and trastuzumab, were included for analysis.

Results: Patients received left breast irradiation demonstrated increased risks on IHD (aHR, 1.16; 95% CI, 1.06–1.26; $p < 0.01$) and OHD (aHR, 1.08; 95% CI, 1.01–1.15; $p < 0.05$), but not HF (aHR, 1.11; 95% CI, 0.96–1.28; $p = 0.14$), when compared with patients received right breast irradiation. In patients who received left breast irradiation dose of >6,040 cGy, subsequent epirubicin might have a trend to increase the risk of heart failure (aHR, 1.53; 95% CI, 0.98–2.39; $p = 0.058$), while doxorubicin (aHR, 0.59; 95% CI, 0.26–1.32; $p = 0.19$) and trastuzumab (aHR, 0.93; 95% CI, 0.33–2.62; $p = 0.89$) did not. Older age was the highest independent risk factor for post-irradiation long-term heart diseases.

Conclusion: Generally, systemic anticancer agents are safe in conjunction with radiotherapy for managing post-operative breast cancer patients. Hazard-based risk grouping may help stratify breast cancer patients associated with post-irradiation long-term heart diseases. Notably, radiotherapy should be performed cautiously for elderly left breast cancer patients who received epirubicin. Limited irradiation dose to the heart should be critically considered. Regular monitoring of potential signs of heart failure may be conducted.

KEYWORDS

synergic effect, heart failure, cardiovascular disease, breast cancer, epirubicin, radiotherapy

Introduction

Cardiovascular diseases (CVDs), including heart disease, cerebrovascular disease, atherosclerosis, and aortic aneurysm/dissection, are recognized as potential long-term sequelae in cancer survivors (1, 2). Among 28 cancer diseases, 38.0% of patients died from cancer, and 11.3% died from CVDs. Breast cancer patients demonstrated a higher (11.7%) than average (11.3%) risk of death from CVDs (2). Regarding CVDs, 76.3% of deaths were due to heart disease (2).

The risk of treatment-associated heart diseases in breast cancer patients is a particular issue in current clinical medicine. Anthracycline chemotherapy, targeted therapy, and radiation therapy are treatment modalities at risk for heart diseases (3, 4), and they may limit the overall treatment effectiveness (3, 5). Clinically, treatment-associated cardiotoxicity gains significant concern in breast cancer patients (4, 6–8). However, few studies comprehensively demonstrated the synergic effect of anticancer agents and radiotherapy on heart toxicities in breast cancer patients. Even though advanced irradiation techniques have provided better protective effects for the heart, the risk of long-term heart disease in patients who received left breast irradiation is still a considerable concern. Clinically, a potential synergic effect of anticancer agents and radiotherapy on heart toxicities may exist in patients with left breast irradiation. However, the actual hazard sizes of combined treatments are rarely demonstrated, especially in the real-world setting.

In the present study, we extensively explored the events of long-term heart sequelae, including heart failure, ischemic heart disease, and other heart diseases, such as acute pericarditis, cardiomyopathy, and arrhythmia. Anticancer agents, including epirubicin, doxorubicin, and trastuzumab, were selected to examine the synergic effect of radiotherapy on cardiac toxicities in patients who received left breast irradiation. Notably, hazard-based risk grouping was applied to stratify patients.

Materials and methods

Ethic consideration and research database

The present population-based cohort study utilized the national database of the Taiwan National Health Insurance (TNHI). The TNHI database contained comprehensive information, including the records of diagnosis and treatment of approximately 99% of people in Taiwan (9), and this database was evaluated strictly and regularly by the National Health Insurance Administration (NHIA) (5). The Institute Review Board (IRB) of the Dalin Tzu-Chi Hospital, Buddhist Tzu Chi Medical Foundation, approved the protocol before the study initiation (B10404014). The IRB waived the requirement for informed consent due to the absolutely de-identified data nature.

This is a 17-year long-term follow-up cohort study. **Figure 1** presents the patient flow chart. From 2000 to 2017, female patients diagnosed with breast cancer aged 20–80 were identified from the TNHI database. We excluded patients with incomplete data, non-irradiation, and a follow-up period of less than 1 year. For balancing the pre-analysis patient population, we used a propensity score match (PSM) to pair patients into two groups: left and right breast irradiation. The match-paired ratio was 1:1. The PSM is a statistical method based on multiple regression analysis. In this study, we used the basic characteristics of the subjects as independent variables, including age, radiation doses, clinical and pathological stage, surgery type, chemotherapy, hormone therapy, ant-cancer agents, comorbidities, family income, urbanization level, geographic region, and the group as the dependent variable, left-sided and right-sided breast irradiation groups (see **Table 1**). Each subject was assigned a propensity score, which represents the probability of being assigned to either left-sided or right-sided breast irradiation group, and we further utilized the propensity scores of each subject to perform two-group matching in order to reduce bias caused by potential confounding factors. The detail of propensity score calculated was as follows:

1. Individual propensity score (PS) was calculated from a multivariate Logistic regression model with response variable laterality coded as 0 for the right and 1 for the left while predictors including all the confounding factors listed in the baseline characteristic summary table (see **Table 1**). The PS indicated how likely an individual with the given covariates was a sample from the cohort of laterality 1.
2. For each individual with a value of PS, for example, ps1 in cohort of laterality 1, an individual from cohort of laterality 0 with PS value closest to the ps1 was selected as a match. Random selection was made when tied. The distance of the two PS values must be ≤ 0.0001; otherwise, no match was made.

After a 1:1 propensity score match for two groups, there were 21,123 patients were included in the left and right breast irradiation group, respectively.

Three systemic anticancer agents, including epirubicin, doxorubicin, and trastuzumab, were selected to investigate each drug's independent effect under different radiation dose levels. Other agents, such as docetaxel, paclitaxel, carboplatin, cyclophosphamide, fluorouracil, and methotrexate, were included as covariates for analysis to examine their potential association with the risk of heart diseases. Radiation doses were defined into three levels, ranging from 3,000 to 5,040 cGy, from 5,040 to 6,040 cGy, and >6,040 cGy. According to the International Classification of Disease, Ninth Revision, Clinical Modification (ICD-9-CM codes), heart diseases are categorized as a diagnosis of heart failure (HF), ischemic heart disease (IHD), and other heart diseases (OHD). The code of ICD-9-CM for heart failure was 428. The code for ischemic heart disease was 410–414, including acute and subacute myocardial infarction. We defined the codes for other heart diseases, including pericarditis (420), endocarditis (421), other diseases of pericarditis and endocarditis (423–424), myocarditis (422), cardiomyopathy (425), conduction disorders (426), cardiac dysrhythmias (427), and ill-defined descriptions and complications of heart disease (429).

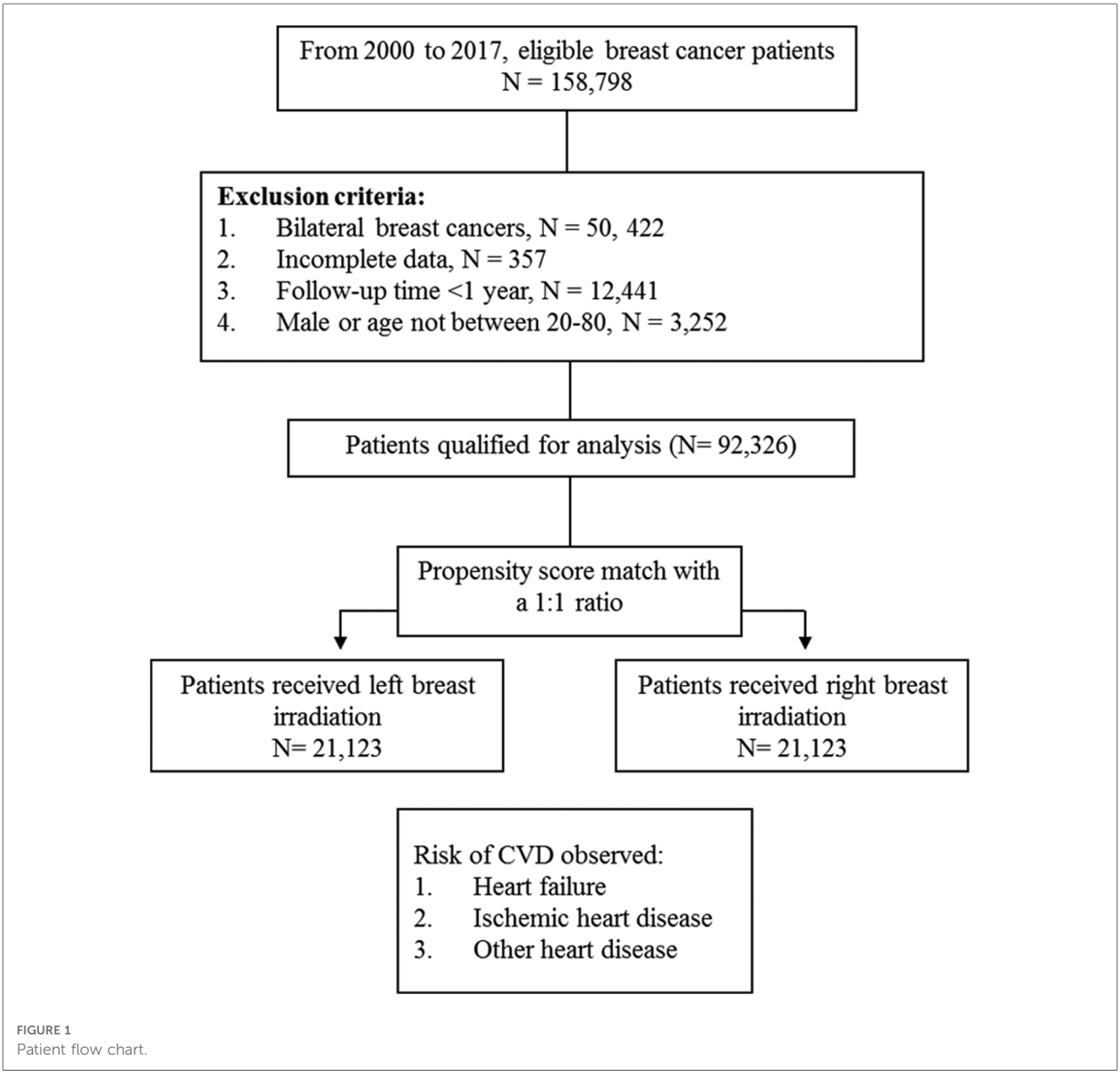

FIGURE 1
Patient flow chart.

Other factors, including age, diabetes mellitus (including type I and type II), hypertension, surgery type, clinical and pathological staging, chemotherapy, and hormone therapy, were also applied as covariates for data analysis. In addition, socioeconomic variables, including geographic region, urbanization level, and monthly income-based insurance premiums, were included in the analysis to reduce bias from lifestyle.

Statistical analysis

Cox proportional hazard regression was performed to estimate the adjusted hazard ratio (aHR) with a 95% confidence interval (CI) to examine the independent effect of left breast irradiation, when compared with right breast irradiation, on the risk of heart diseases.

In addition, Cox regression was also utilized to estimate the individual hazard based on all covariates for risk grouping and explore the synergic effect of anticancer agents and irradiation dose on heart disease risk. We estimated individual hazard by using the COX regression method with the following formula: $y = \exp(aX + bY + cZ\ldots)$; a, b, c = log (aHR); X, Y, Z = covariate variable. All included patients were allocated equally in number into 2, 3, 4, or 5 sub-groups, according to the order of each individual hazard ratios, which were based on parameters including all covariates and socioeconomic variables to assess the risks of IHD, OHD, and HF. The 1/2, 1/3, 1/4, and 1/5 risk subgroups denote the lowest risk subgroup, while the 2/2, 3/3, 4/4, and 5/5 subgroups denote the highest risk subgroup.

A two-sided p-value of <0.05 was considered statistically significant. The SAS software (version 9.2; SAS Institute, Inc., Cary, NC) was used for all statistical analyses.

TABLE 1 Patient characteristics.

Variables	Breast cancer patients received radiotherapy after propensity score 1:1 match		Absolute standardized mean difference
	Right	Left	
	$N = 21,123$ (%)	$N = 21,123$ (%)	
Age group (years)			0.0014
20–46	6,890 (32.6)	6,918 (32.8)	
47–53	6,024 (28.5)	6,011 (28.5)	
54–62	5,346 (25.3)	5,336 (25.3)	
>62	2,863 (13.6)	2,858 (13.5)	
RT dose (cGy)			0.0017
3,000–5,040	6,328 (30.0)	6,311 (29.9)	
5,040–6,040	9,755 (46.2)	9,780 (46.3)	
>6,040	5,040 (23.9)	5,032 (23.8)	
C-stage			0.0004
0	1,433 (6.8)	1,440 (6.8)	
I	6,642 (31.4)	6,637 (31.4)	
II	7,871 (37.3)	7,888 (37.3)	
III	2,118 (10.0)	2,114 (10.0)	
IV	640 (3.0)	641 (3.0)	
Unknown	2,419 (11.5)	2,403 (11.4)	
P-stage			0.0018
0	1,640 (7.8)	1,635 (7.7)	
I	7,090 (33.6)	7,077 (33.5)	
II	6,778 (32.1)	6,797 (32.2)	
III	4,490 (21.3)	4,480 (21.2)	
IV	434 (2.1)	434 (2.1)	
Unknown	691 (3.3)	700 (3.3)	
Chemotherapy	14,946 (70.8)	14,965 (70.9)	0.0020
Hormone therapy	15,048 (71.2)	15,098 (71.5)	0.0053
Anti-cancer agents			
Doxorubicin	3,964 (18.8)	3,953 (18.7)	0.0015
Epirubicin	8,622 (40.8)	8,661 (41.0)	0.0037
Trastuzumab	2,154 (10.2)	2,154 (10.3)	0.0043
Docetaxel	6,756 (32.0)	6,803 (32.2)	0.0049
Paclitaxel	1,441 (6.8)	1,432 (6.8)	0.0016
Carboplatin	55 (0.3)	50 (0.2)	0.0040
Cyclophosphamide	14,175 (67.1)	14,192 (67.2)	0.0017
Fluorouracil	9,415 (44.6)	9,432 (44.7)	0.0016
Methotrexate	1,221 (5.8)	1,199 (5.7)	0.0043
Surgery type			0.0014
BCS	12,616 (59.7)	12,603 (59.7)	
MRM	6,401 (30.3)	6,413 (30.4)	
None	2,106 (10.0)	2,107 (10.0)	
Comorbidities			
Hypertension	3,464 (16.4)	3,506 (16.6)	0.0054
Diabetes mellitus	1,605 (7.6)	1,610 (7.6)	0.0008
Family income (NTD per month)			0.0012
<20,100	4,275 (20.2)	4,277 (20.3)	
20,101–22,800	6,556 (31.0)	6,541 (31.0)	
22,801–42,000	5,253 (24.9)	5,268 (24.9)	
>42,000	5,039 (23.9)	5,037 (23.9)	
Urbanization level			0.0011
City	5,629 (26.7)	5,619 (26.6)	
Satellite cities	11,099 (52.5)	11,092 (52.5)	
Rural areas	4,395 (20.8)	4,412 (20.9)	
Geographic region			0.0010
North	10,631 (50.3)	10,641 (50.4)	
Central	4,741 (22.4)	4,747 (22.5)	
South	5,336 (25.3)	5,326 (25.2)	
East	415 (2.0)	409 (1.9)	

RT, radiotherapy; C-stage, clinical stage; P-stage, pathological stage; BCS, breast conserving surgery; MRM, modified radical mastectomy; NTD, New Taiwan dollar; Insurance premium for National Health Insurance is according to family income. Absolute standardized mean difference less than 0.1 is considered as covariates balance between groups after propensity score matching.

Results

From 2000 to 2017, 158,798 breast cancer patients were identified, and 92,326 cases were qualified (Figure 1). After a 1:1 propensity score match, 42,246 patients with left ($n = 21,123$) and right ($n = 21,123$) breast irradiation were included for final analysis. The mean ages of the two cohorts who received left and right breast irradiation were 51.20 and 51.17 years old, respectively. After PSM, the two cohorts' pre-analysis clinical and demographic variables are comparable (Table 1).

Table 2 presents the aHRs of CVD after adjusting covariates. Patients with left breast irradiation had trends in risks of ischemic heart disease (aHR, 1.16; 95% CI, 1.06–1.26; $p < 0.01$) and other heart diseases (aHR, 1.08; 95% CI, 1.01–1.15; $p < 0.05$), but not heart failure (aHR, 1.11; 95% CI, 0.96–1.28; $p = 0.14$). Regarding the risk of all heart diseases, the adjusted hazard ratio showed an increasing curve with age. Patients aged >62 years tended to have elevated risks of HF (aHR, 4.11; 95% CI, 3.22–5.24), IHD (aHR, 4.26; 95% CI, 3.65–4.98), and OHD (aHR, 2.34; 95% CI, 2.09–2.62), respectively.

Surprisingly, radiation dosage did not statistically significantly influence the risk of heart diseases (Table 2). On the other hand, among anticancer drugs, epirubicin was statistically significantly associated with an increased risk of heart failure (aHR, 1.40; 95% CI, 1.04–1.89; $p < 0.05$), but not doxorubicin and trastuzumab. No significant relationship was presented regarding other systemic anticancer agents such as docetaxel, paclitaxel, carboplatin, cyclophosphamide, fluorouracil and methotrexate for the risks of heart failure, ischemic heart disease and other heart diseases.

Regarding the influence of comorbidities, both hypertension and diabetes mellitus were markedly associated with high risks of heart diseases (for heart failure, aHR of 1.75 and 1.79; for ischemic heart disease, 1.78 and 1.49; for other heart diseases, 1.44 and 1.16, respectively).

For socioeconomic variables, including family income, urbanization level, and geographic region, only rural areas were

10.3389/fcvm.2023.980101

TABLE 2 Adjusted hazard ratios for heart diseases in breast cancer patients received radiotherapy.

	Heart failure (HF)		Ischemic heart disease (IHD)		Other heart diseases (OHD)	
	aHR	95% CI	aHR	95% CI	aHR	95% CI
Left breast RT (right breast RT as ref.)	1.11	0.96–1.28	1.16**	1.06–1.26	1.08*	1.01–1.15
Age (20–47 as ref.)						
47–53	1.58***	1.25–1.99	2.01***	1.75–2.32	1.33***	1.21–1.46
54–62	2.05***	1.63–2.58	2.88***	2.51–3.32	1.63***	1.48–1.80
>62	4.11***	3.22–5.24	4.26***	3.65–4.98	2.34***	2.09–2.62
RT dose (3,000–5,040 as ref.)						
5,040–6,040	0.88	0.73–1.08	0.93	0.82–1.05	0.89*	0.81–0.98
>6,040	0.84	0.67–1.06	1.00	0.87–1.15	1.01	0.90–1.12
C-stage (stage 0 as ref.)						
I	0.94	0.59–1.50	1.00	0.80–1.26	1.16	0.97–1.40
II	0.92	0.58–1.47	0.95	0.76–1.21	1.04	0.86–1.27
III	1.33	0.80–2.18	0.88	0.66–1.16	1.18	0.95–1.46
IV	1.02	0.41–2.54	0.75	0.41–1.38	1.04	0.67–1.60
P-stage (stage 0 as ref.)						
I	1.37	0.86–2.18	1.03	0.83–1.28	1.02	0.86–1.22
II	1.80*	1.11–2.90	0.97	0.77–1.22	0.99	0.82–1.20
III	1.88*	1.14–3.09	0.99	0.77–1.28	1.08	0.88–1.33
IV	1.61	0.59–4.37	0.63	0.30–1.32	0.96	0.59–1.56
Chemotherapy	1.28	0.84–1.95	0.77	0.56–1.05	0.89	0.71–1.11
Anti-hormone therapy	0.95	0.81–1.12	0.87**	0.78–0.95	0.88***	0.81–0.95
Systemic anti-cancer agents						
Doxorubicin	1.09	0.80–1.50	0.99	0.81–1.20	1.02	0.87–1.18
Epirubicin	1.40*	1.04–1.89	0.92	0.76–1.11	1.08	0.93–1.24
Trastuzumab	1.10	0.86–1.42	0.90	0.74–1.08	1.06	0.93–1.22
Docetaxel	0.97	0.79–1.20	0.98	0.85–1.12	0.87**	0.78–0.96
Paclitaxel	0.98	0.74–1.31	1.12	0.92–1.36	0.96	0.82–1.11
Carboplatin	0.82	0.20–3.31	0.53	0.13–2.15	1.19	0.59–2.40
Cyclophosphamide	0.69	0.46–1.02	1.06	0.77–1.46	1.03	0.82–1.30
Fluorouracil	1.04	0.84–1.28	1.12	0.91–1.39	1.01	0.85–1.19
Methotrexate	0.89	0.62–1.29	1.12	0.92–1.36	0.96	0.82–1.11
Surgery type (BCS as ref.)						
MRM	1.12	0.89–1.41	1.07	0.92–1.24	1.13*	1.01–1.26
None	1.14	0.83–1.56	1.07	0.90–1.26	1.16*	1.01–1.33
Comorbidities						
Hypertension	1.75***	1.48–2.07	1.78***	1.61–1.97	1.44***	1.32–1.57
Diabetes mellitus	1.79***	1.48–2.18	1.49***	1.31–1.68	1.16**	1.04–1.30
Family income (NTD per month) (<20,100 as ref.)						
20,101–22,800	0.87	0.72–1.05	0.87*	0.77–0.97	0.88**	0.80–0.97
22,801–42,000	0.81	0.66–1.01	0.80***	0.70–0.90	0.88*	0.79–0.97
>42,000	0.84	0.68–1.04	0.80***	0.70–0.91	0.91	0.82–1.00
Urbanization level (City as ref.)						
Satellite cities	0.98	0.82–1.17	0.90*	0.81–0.99	0.89**	0.82–0.97
Rural areas	1.32*	1.06–1.65	1.04	0.90–1.91	0.98	0.88–1.10
Geographic region (North, as ref.)						
Central	0.85	0.70–1.04	1.05	0.93–1.18	0.94	0.86–1.03
South	0.76	0.62–0.92	0.91	0.81–1.02	0.85***	0.78–0.93
East	1.42	0.95–2.13	0.92	0.67–1.26	1.12	0.89–1.41

RT, radiotherapy; aHR, adjusted hazard ratio; 95% CI, 95% confidence interval; C-stage, clinical stage; P-stage, pathological stage; BCS, breast conserving surgery; MRM, modified radical mastectomy; NTD, New Taiwan Dollar; ref., reference (HR = 1).

*$p < 0.05$.

**$p < 0.01$.

***$p < 0.001$.

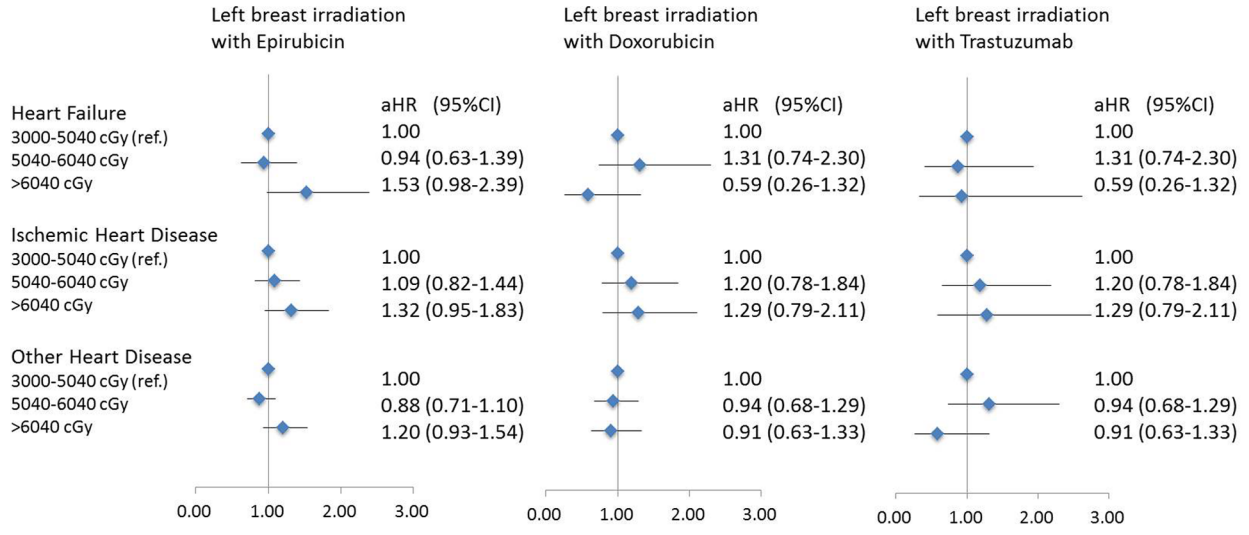

FIGURE 2
A forest plot for demonstrating heart disease risk in patients with left breast irradiation according to three main systemic anti-cancer agents and different radiation dose.

statistically significantly associated with an increased risk of heart diseases. Breast cancer patients who lived in rural areas had a higher risk of heart failure (aHR, 1.32; 95% CI, 1.06–1.65; $p < 0.05$) than those who lived in the city. However, there was no apparent influence from different urbanization levels on ischemic and other heart diseases.

Incidentally, we observed that anti-hormone therapy seemly showed risk reduction in IHD (aHR, 0.87; 95% CI, 0.78–0.95) and OHD (aHR, 0.88; 95% CI, 0.81–0.95; Table 2).

Figure 2 demonstrated the risk of CVDs in breast cancer patients who received left breast irradiation by each anticancer agent, i.e., epirubicin, doxorubicin, and trastuzumab. Notably, patients who received left breast irradiation dosage of >6,040 cGy, epirubicin increased heart failure risk, which reached a marginal statistical significance (aHR, 1.53; 95% CI, 0.98–2.39; $p = 0.058$), while doxorubicin (aHR, 0.59; 95% CI, 0.26–1.32; $p = 0.19$) and trastuzumab (aHR, 0.93; 95% CI, 0.33–2.62; $p = 0.89$) did not. Besides, there was no similar finding for the risk of ischemic and other heart diseases. This observation indicated a particular association between epirubicin and left breast irradiation on the risk of heart failure.

Table 3 shows hazard-based risk sub-grouping. According to the order of the individual hazard, all included patients were allocated equally in number into 2, 3, 4, or 5 sub-groups based on parameters including all covariates and socioeconomic variables showed in Table 2 to assess the risks of IHD, OHD, and HF.

We observed that hazard-based risk grouping effectively stratified irradiated breast cancer patients in the endpoints of IHD (Figure 3), OHD (Figure 4), and HF (Figure 5). Note that statistical significances are found in two, three, four, and five risk-grouping in all three types of heart diseases ($p < 0.0001$).

TABLE 3 Hazard-based risk-group stratification.

Divided to subgroups[a]		IHD (*N*)	OHD (*N*)	HF (*N*)
Two risk groups	1/2	21,132	21,122	21,120
	2/2	21,114	21,124	21,126
Three risk groups	1/3	14,081	14,083	14,082
	2/3	14,054	14,078	14,081
	3/3	14,111	14,085	14,083
Four risk groups	1/4	10,566	10,562	10,561
	2/4	10,566	10,560	10,559
	3/4	10,553	10,562	10,564
	4/4	10,561	10,562	10,562
Five risk groups	1/5	8,450	8,450	8,449
	2/5	8,449	8,448	8,449
	3/5	8,449	8,449	8,450
	4/5	8,448	8,450	8,449
	5/5	8,450	8,449	8,449

IHD, ischemic heart disease; OHD, other heart disease; HF, heart failure; N, patient number. Note that the each patient's individual hazard is estimated according to Table 2. The individual hazard is estimated by using the COX regression method with the following formula: y = exp (aX + bY + cZ....); a, b, c = log (aHR); X, Y, Z = covariate variable. According to the order of the individual hazard, all included patients were allocated equally in number into 2, 3, 4, or 5 sub-groups.

Discussion

The present population-based cohort study utilized Cox regression to estimate hazards for risk grouping and stratify breast cancer patients in post-irradiation long-term heart diseases. The risk of treatment-associated heart disease from the synergic effect of anticancer drugs and left-sided breast irradiation was also examined. Our study confirmed the previous observation that breast cancer patients had an elevated risk of treatment-associated heart disease (3, 10), especially for those who received left-sided irradiation (3, 11, 12). Moreover, when it

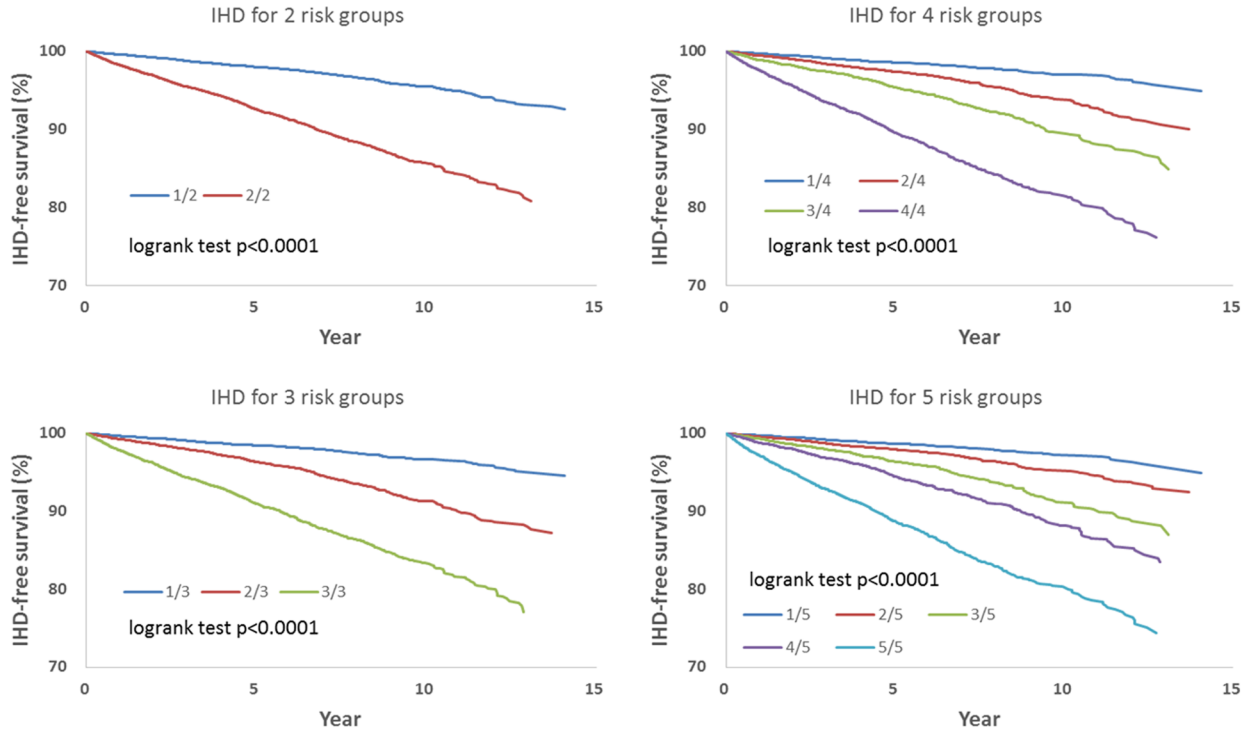

FIGURE 3
Based on Tables 2, 3, the hazard-based risk grouping effectively stratified irradiated breast cancer patients in the endpoint of ischemic heart disease (IHD, $p < 0.0001$ in all sub-grouping). Note that the each patient's individual hazard is estimated according to Table 2. According to the order of the individual hazard, all included patients were allocated equally in number into 2, 3, 4, or 5 sub-groups based on parameters including all covariates and socioeconomic variables showed in Table 2 to assess the risks of IHD, OHD, and HF.

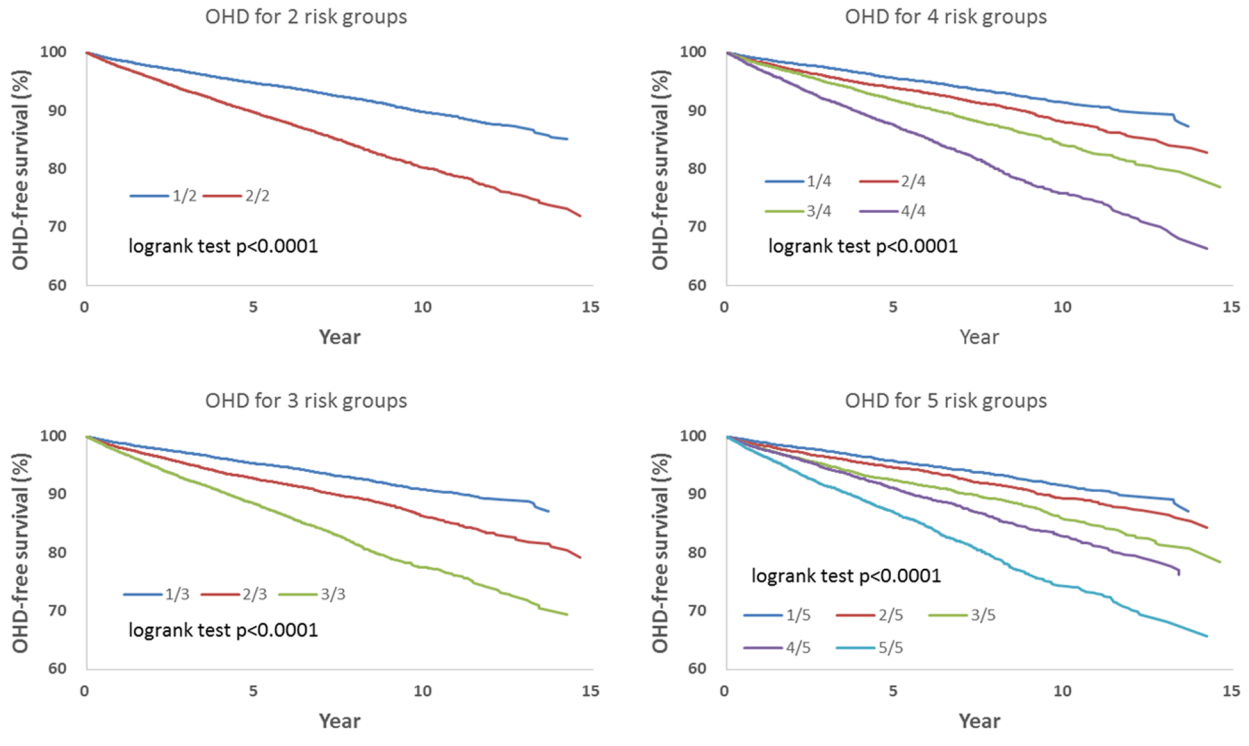

FIGURE 4
Based on Tables 2, 3, the hazard-based risk grouping effectively stratified irradiated breast cancer patients in the endpoint of other heart diseases (OHD; $p < 0.0001$ in all sub-grouping).

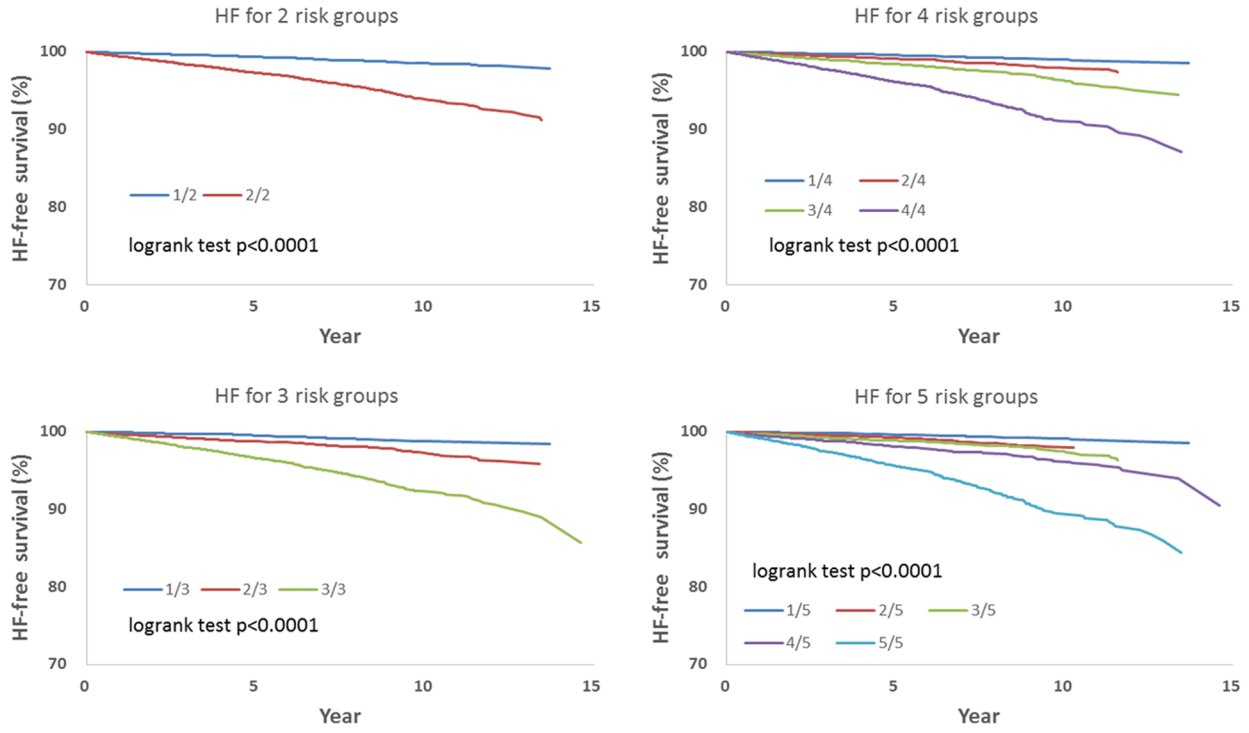

FIGURE 5
Based on Tables 2, 3, the hazard-based risk grouping effectively stratified irradiated breast cancer patients in the endpoint of heart failure (HF; $p < 0.0001$ in all sub-grouping).

comes to the synergic effect of treatment-associated cardiac injury, the role of epirubicin and left-sided breast irradiation in heart failure is highlighted in the present study, especially in the elderly population. Among breast cancer patients who were given both epirubicin and radiation therapy, the risk of heart failure was elevated when left-sided irradiation with a total dose of >6,040 cGy was given. Our observation suggested that among drugs of anticancer therapy, epirubicin may increase the effect of radiotherapy-associated cardiac injury in breast cancer survivors.

A well-known population-based case-control study of breast cancer patients in Sweden and Denmark by Darby et al. demonstrated that major coronary events increased linearly with the dosage of irradiation to the heart, increasing by 7.4% (95% CI = 2.9–14.5, $p < 0.001$) per gray in the mean radiation dose, and they found the significant radiation-related increase in the risk of ischemic heart disease (10). Similar to the study of Darby et al., our results found a high risk of IHD and OHD when left-sided breast irradiation was given (**Table 2**). Indeed, the increased risks of coronary heart disease and myocardial infarction observed evidently in patients received left-sided irradiation have been reported previously (13–15). Radiation therapy for left-sided breast cancer patients may cause irradiation-associated perfusion defects and possible wall-motion abnormalities (16). The anterior portions of the left ventricle were indicated to associate with wall-motion defects, which correspond to the heart region within the radiotherapy field (16). In addition, it has been reported that receiving left-sided breast irradiation may result in high-grade stenosis of the left-anterior artery (LAD) when compared with right-sided breast irradiation (17), which cannot be avoided entirely during radiotherapy.

Compared with ischemic heart disease or other heart diseases, the risk of heart failure may be more susceptible to the anthracycline chemotherapy agents (18, 19). Compared with other anticancer drugs, our study showed that epirubicin was statistically significantly related to the risk of heart failure (**Table 2**) instead of the risk of ischemic heart disease and other heart diseases. More interestingly, the synergic effect of epirubicin-induced and left-sided breast irradiation-induced on heart failure was found in our study. The risk of heart failure emerged as the role of epirubicin under a high dosage of radiotherapy was considered (**Figure 2**). This observation suggested that the risk of treatment-associated heart failure may be multifactorial; the risk of anthracycline-induced cardiac dysfunction needs to be noted when patients who were under the circumstance of a high dosage of left-sided breast irradiation. Although epirubicin has been announced with a low cardiac toxicity profile (20, 21), epirubicin-associated heart failure is still a concern in breast cancer survivors (22, 23). A 20-year follow-up study indicated that the cumulative incidence of heart failure was higher (up to a three-fold increased risk) in the epirubicin treatment group when compared with the non-epirubicin group (22). Although both epirubicin and doxorubicin are members of the anthracycline family and demonstrate the dose-dependent effect of early- and late-onset chronic cardiotoxicity (24–26), clinical trials with the direct head-to-head comparisons between doxorubicin and epirubicin are still needed (clinical trial: NCIC

CTG MA.21) (27). Our results demonstrated that the magnitude of radiotherapy-associated cardiac dysfunction may be enhanced by epirubicin when the total dose of radiation was up to >6,040 cGy and increase the risk of heart failure further. The mechanism of this increased long-term risk of heart failure is uncertain, but the insights of mitochondrial dysfunctions (28–30) and the production of free radicals (28, 31) have been proposed.

Trastuzumab did not show a significant association with the risk of CVDs, nor did it have a synergic effect with radiotherapy in patients with left-sided irradiation in the present study. This finding implies that trastuzumab-related cardiovascular events are relatively low and not apparent relative to anthracycline chemotherapy. The HER2 receptors are reported to be expressed in cardiomyocytes (32), and the alteration in cellular metabolic pathways in cardiomyocytes was indicated as a critical mechanism underlying the development of cardiac dysfunction (33). However, it was reported that the cardiac dysfunction associated with trastuzumab mainly occurs during trastuzumab-treatment (34) and is considered reversible (35, 36) and tolerated (37). Besides, having prior anthracycline treatment is identified for trastuzumab-associated cardiotoxicity (6, 38), in which the incidence of cardiac dysfunction was reported to be 4% with trastuzumab alone and 27% with the combination of anthracycline and cyclophosphamide (39). Even with a median follow-up of 3.6 years, severe chronic heart failure in the trastuzumab group remained low at 0.8% (34).

For risk factors associated with the risk of heart diseases, our study showed that the elevated risk of heart diseases was significant across age groups, and high risk existed in patients aged >62 years in particular, with up to the 4-fold increased risk of heart failure and ischemic heart disease (**Table 2**). Consistent with previous studies (40, 41), the increased age is related to the elevated risk of fatal myocardial infarction after left-sided post lumpectomy radiotherapy. The increased likelihood of mortality had been observed in patients aged 60 years and older ($p = 0.01$) (40). In addition, a previous study showed that preexisting hypertension is highly associated with increased CVDs risk, with the risk ratio for the development of coronary artery disease being 1.59 for left- versus right-irradiated patients (42), which is not far from our reported risk ratio (range, 1.44–1.78). A relationship between a history of diabetes and the risk of CVD-related mortality was reported in breast cancer patients (43). Diabetic patients had significantly high baseline CVD risks (range, 11.8%–24.2%), and the mean 10-year cumulative risk was 3.7% and 3.9% in patients using the DIBH-technique and free-breathing technique, respectively (44). It suggested that caring for breast cancer patients with diabetes should include attention to CVD risk factors (45).

Strengths and limitations

We comprehensively investigated the risk of heart diseases, including ischemic heart disease, heart failure, and other heart diseases, among patients who received left-sided breast irradiation. The strength of the present study is that this is a nationwide cohort study with a 17-year long-term follow-up in Taiwan. In addition, by examining the risk of heart diseases by each anticancer drug under different levels of left-sided breast irradiation dose, our observation provides further information concerning the synergic effect of chemotherapy- and radiotherapy-associated cardiotoxicity among breast cancer survivors. Finally, we used a propensity score to match all the covariates, including clinical information, comorbidities, and socioeconomic variables, to reduce potential bias before statistical analysis.

Regarding this study's limitation, some information is unavailable in our database. For example, the mean heart dose and other heart dose parameters, such as the mean dose to the left anterior descending artery, are unavailable from our database, which may influence assessing the extent of radiotherapy-associated cardiac injury. In addition, we lack some information in our data analysis, such as a history of tobacco use, body mass index, familial history of myocardial infarction, or other cardiovascular diseases, which are reported as preexisting risk factors related to the incidence of CVDs (1, 14, 46–48).

Conclusion

Hazard-based risk grouping may help stratify breast cancer patients at risk of post-irradiation long-term heart diseases. Generally, systemic anticancer agents, including chemotherapy and targeted therapy, are safe in conjunction with radiotherapy for managing post-operative breast cancer patients. However, radiotherapy should be performed cautiously for elderly left breast cancer patients who received epirubicin. Decreasing the irradiation dose to the heart should be critically considered, and regular monitoring of potential signs of heart failure may be conducted.

Data availability statement

The raw data supporting the conclusions of this article will be made available by the authors, without undue reservation.

Author contributions

All authors contributed to the brainstorming of the ideas generation: M-SL, H-JY, S-KH, W-YC, D-WL, L-CC, C-HC, B-HY, F-CH, and H-YL. M-SL and H-JY also contributed to the first draft writing. S-KH, W-YC, D-WL, L-CC, C-HC, B-HY, and F-CH also contributed to the literature review and data interpretation. B-HY, H-JY, and F-CH performed the statistical analyses. H-YL corresponded to overall manuscript communication and final approval. All authors contributed to the article and approved the submitted version.

Funding

We appreciate the research grants from the Dalin Tzu Chi Hospital, Buddhist Tzu Chi Medical Foundation

(grant number: DTCRD110-I-13, TCMF-A 111-10, TCMF-A 112-04).

Conflict of interest

The authors declare that the research was conducted in the absence of any commercial or financial relationships that could be construed as a potential conflict of interest.

Publisher's note

References

1. Rothe D, Paterson I, Cox-Kennett N, Gyenes G, Pituskin E. Prevention of cardiovascular disease among cancer survivors: the role of Pre-existing risk factors and cancer treatments. *Curr Epidemiol Rep*. (2017) 4(3):239–47. doi: 10.1007/s40471-017-0117-9

2. Sturgeon KM, Deng L, Bluethmann SM, Zhou S, Trifiletti DM, Jiang C, et al. A population-based study of cardiovascular disease mortality risk in US cancer patients. *Eur Heart J*. (2019) 40(48):3889–97. doi: 10.1093/eurheartj/ehz766

3. Zagar TM, Cardinale DM, Marks LB. Breast cancer therapy-associated cardiovascular disease. *Nat Rev Clin Oncol*. (2016) 13(3):172–84. doi: 10.1038/nrclinonc.2015.171

4. Martel S, Maurer C, Lambertini M, Pondé N, De Azambuja E. Breast cancer treatment-induced cardiotoxicity. *Expert Opin Drug Saf*. (2017) 16(9):1021–38. doi: 10.1080/14740338.2017.1351541

5. Cheng TM. Taiwan's new national health insurance program: genesis and experience so far. *Health Aff*. (2003) 22(3):61–76. doi: 10.1377/hlthaff.22.3.61

6. Ewer MS, Ewer SM. Cardiotoxicity of anticancer treatments: what the cardiologist needs to know. *Nat Rev Cardiol*. (2010) 7(10):564–75. doi: 10.1038/nrcardio.2010.121

7. Higgins AY, O'Halloran TD, Chang JD. Chemotherapy-induced cardiomyopathy. *Heart Fail Rev*. (2015) 20(6):721–30. doi: 10.1007/s10741-015-9502-y

8. Caron J, Nohria A. Cardiac toxicity from breast cancer treatment: can we avoid this? *Curr Oncol Rep*. (2018) 20(8):61. doi: 10.1007/s11912-018-0710-1

9. Lu JF, Hsiao WC. Does universal health insurance make health care unaffordable? Lessons from Taiwan. *Health Aff*. (2003) 22(3):77–88. doi: 10.1377/hlthaff.22.3.77

10. Darby SC, Ewertz M, McGale P, Bennet AM, Blom-Goldman U, Brønnum D, et al. Risk of ischemic heart disease in women after radiotherapy for breast cancer. *N Engl J Med*. (2013) 368(11):987–98. doi: 10.1056/NEJMoa1209825

11. Piroth MD, Baumann R, Budach W, Dunst J, Feyer P, Fietkau R, et al. Heart toxicity from breast cancer radiotherapy: current findings, assessment, and prevention. *Strahlenther Onkol*. (2019) 195(1):1–12. doi: 10.1007/s00066-018-1378-z

12. Rehammar JC, Jensen MB, McGale P, Lorenzen EL, Taylor C, Darby SC, et al. Risk of heart disease in relation to radiotherapy and chemotherapy with anthracyclines among 19,464 breast cancer patients in Denmark, 1977-2005. *Radiother Oncol*. (2017) 123(2):299–305. doi: 10.1016/j.radonc.2017.03.012

13. Paszat LF, Vallis KA, Benk VMA, Groome PA, Mackillop WJ, Wielgosz A. A population-based case-cohort study of the risk of myocardial infarction following radiation therapy for breast cancer. *Radiother Oncol*. (2007) 82(3):294–300. doi: 10.1016/j.radonc.2007.01.004

14. Hooning MJ, Botma A, Aleman BMP, Baaijens MHA, Bartelink H, Klijn JGM, et al. Long-term risk of cardiovascular disease in 10-year survivors of breast cancer. *J Natl Cancer Inst*. (2007) 99(5):365–75. doi: 10.1093/jnci/djk064

15. Correa CR, Litt HI, Hwang WT, Ferrari VA, Solin LJ, Harris EE. Coronary artery findings after left-sided compared with right-sided radiation treatment for early-stage breast cancer. *J Clin Oncol*. (2007) 25(21):3031–7. doi: 10.1200/JCO.2006.08.6595

16. Marks LB, Yu X, Prosnitz RG, Zhou S-M, Hardenbergh PH, Blazing M, et al. The incidence and functional consequences of RT-associated cardiac perfusion defects. *Int J Radiat Oncol Biol Phys*. (2005) 63(1):214–23. doi: 10.1016/j.ijrobp.2005.01.029

17. Nilsson G, Holmberg L, Garmo H, Duvernoy O, Sjögren I, Lagerqvist B, et al. Distribution of coronary artery stenosis after radiation for breast cancer. *J Clin Oncol*. (2012) 30(4):380–6. doi: 10.1200/JCO.2011.34.5900

18. Appel JM, Nielsen D, Zerahn B, Jensen BV, Skagen K. Anthracycline-induced chronic cardiotoxicity and heart failure. *Acta Oncologica*. (2007) 46(5):576–80. doi: 10.1080/02841860601156165

19. Agunbiade TA, Zaghlol RY, Barac A. Heart failure in relation to anthracyclines and other chemotherapies. *Methodist Debakey Cardiovasc J*. (2019) 15(4):243–9. doi: 10.14797/mdcj-15-4-243

20. Untch M, Muscholl M, Tjulandin S, Jonat W, Meerpohl HG, Lichinitser M, et al. First-line trastuzumab plus epirubicin and cyclophosphamide therapy in patients with human epidermal growth factor receptor 2-positive metastatic breast cancer: cardiac safety and efficacy data from the herceptin, cyclophosphamide, and epirubicin (HERCULES) trial. *J Clin Oncol*. (2010) 28(9):1473–80. doi: 10.1200/JCO.2009.21.9709

21. Khasraw M, Bell R, Dang C. Epirubicin: is it like doxorubicin in breast cancer? A clinical review. *Breast*. (2012) 21(2):142–9. doi: 10.1016/j.breast.2011.12.012

22. Banke A, Fosbøl EL, Møller JE, Gislason GH, Andersen M, Bernsdorf M, et al. Long-term effect of epirubicin on incidence of heart failure in women with breast cancer: insight from a randomized clinical trial. *Eur J Heart Fail*. (2018) 20(10):1447–53. doi: 10.1002/ejhf.1168

23. Mahmood SS, Patel RB, Butler J, Vaduganathan M. Epirubicin and long-term heart failure risk in breast cancer survivors. *Eur J Heart Fail*. (2018) 20(10):1454–6. doi: 10.1002/ejhf.1215

24. Cardinale D, Iacopo F, Cipolla CM. Cardiotoxicity of anthracyclines. *Front Cardiovasc Med*. (2020) 7:26. doi: 10.3389/fcvm.2020.00026

25. Steinherz LJ, Steinherz PG, Tan CT, Heller G, Murphy ML. Cardiac toxicity 4 to 20 years after completing anthracycline therapy. *J Am Med Assoc*. (1991) 266(12):1672–7. doi: 10.1001/jama.1991.03470120074036

26. Giantris A, Abdurrahman L, Hinkle A, Asselin B, Lipshultz SE. Anthracycline-induced cardiotoxicity in children and young adults. *Crit Rev Oncol Hematol*. (1998) 27(1):53–68. doi: 10.1016/S1040-8428(97)10007-5

27. Kaklamani VG, Gradishar WJ. Epirubicin versus doxorubicin: which is the anthracycline of choice for the treatment of breast cancer? *Clin Breast Cancer*. (2003) 4(Suppl 1):S26–33. doi: 10.3816/CBC.2003.s.012

28. Vejpongsa P, Yeh ET. Prevention of anthracycline-induced cardiotoxicity: challenges and opportunities. *J Am Coll Cardiol*. (2014) 64(9):938–45. doi: 10.1016/j.jacc.2014.06.1167

29. Brown DA, Perry JB, Allen ME, Sabbah HN, Stauffer BL, Shaikh SR, et al. Mitochondrial function as a therapeutic target in heart failure. *Nat Rev Cardiol*. (2017) 14(4):238–50. doi: 10.1038/nrcardio.2016.203

30. Rosca MG, Hoppel CL. Mitochondrial dysfunction in heart failure. *Heart Fail Rev*. (2013) 18(5):607–22. doi: 10.1007/s10741-012-9340-0

31. Radulescu D, Pripon S, Parv A, Duncea C, Ciuleanu TE, Radulescu LI. Altered left ventricular diastolic performance in oncologic patients treated with epirubicin. *Congest Heart Fail*. (2007) 13(4):215–20. doi: 10.1111/j.1527-5299.2007.07122.x

32. Crone SA, Zhao YY, Fan L, Gu Y, Minamisawa S, Liu Y, et al. Erbb2 is essential in the prevention of dilated cardiomyopathy. *Nat Med*. (2002) 8(5):459–65. doi: 10.1038/nm0502-459

33. Kitani T, Ong SG, Lam CK, Rhee JW, Zhang JZ, Oikonomopoulos A, et al. Human-induced pluripotent stem cell model of trastuzumab-induced cardiac dysfunction in patients with breast cancer. *Circulation*. (2019) 139(21):2451–65. doi: 10.1161/CIRCULATIONAHA.118.037357

34. Procter M, Suter TM, de Azambuja E, Dafni U, van Dooren V, Muehlbauer S, et al. Longer-term assessment of trastuzumab-related cardiac adverse events in the herceptin adjuvant (HERA) trial. *J Clin Oncol*. (2010) 28(21):3422–8. doi: 10.1200/JCO.2009.26.0463

35. Harbeck N, Ewer MS, De Laurentiis M, Suter TM, Ewer SM. Cardiovascular complications of conventional and targeted adjuvant breast cancer therapy. *Ann Oncol*. (2011) 22(6):1250–8. doi: 10.1093/annonc/mdq543

36. Suter TM, Procter M, van Veldhuisen DJ, Muscholl M, Bergh J, Carlomagno C, et al. Trastuzumab-associated cardiac adverse effects in the herceptin adjuvant trial. *J Clin Oncol*. (2007) 25(25):3859–65. doi: 10.1200/JCO.2006.09.1611

37. Ewer MS, Vooletich MT, Durand JB, Woods ML, Davis JR, Valero V, et al. Reversibility of trastuzumab-related cardiotoxicity: new insights based on clinical course and response to medical treatment. *J Clin Oncol*. (2005) 23(31):7820–6. doi: 10.1200/JCO.2005.13.300

38. Suter TM, Ewer MS. Cancer drugs and the heart: importance and management. *Eur Heart J*. (2013) 34(15):1102–11. doi: 10.1093/eurheartj/ehs181

39. Keefe DL. Trastuzumab-associated cardiotoxicity. *Cancer*. (2002) 95 (7):1592–600. doi: 10.1002/cncr.10854

40. Paszat LF, Mackillop WJ, Groome PA, Schulze K, Holowaty E. Mortality from myocardial infarction following postlumpectomy radiotherapy for breast cancer: a population-based study in Ontario, Canada. *Int J Radiat Oncol Biol Phys*. (1999) 43 (4):755–62. doi: 10.1016/S0360-3016(98)00412-X

41. Hooning MJ, Aleman BM, van Rosmalen AJ, Kuenen MA, Klijn JG, van Leeuwen FE. Cause-specific mortality in long-term survivors of breast cancer: a 25-year follow-up study. *Int J Radiat Oncol Biol Phys*. (2006) 64(4):1081–91. doi: 10.1016/j.ijrobp.2005.10.022

42. Harris EE, Correa C, Hwang WT, Liao J, Litt HI, Ferrari VA, et al. Late cardiac mortality and morbidity in early-stage breast cancer patients after breast-conservation treatment. *J Clin Oncol*. (2006) 24(25):4100–6. doi: 10.1200/JCO.2005.05.1037

43. Rodriguez LA, Bradshaw PT, Parada H, Khankari NK, Wang T, Cleveland RJ, et al. Diabetes and cardiovascular disease mortality among a population-based cohort of women with and without breast cancer. *Cancer Causes Control*. (2020) 31 (5):517–24. doi: 10.1007/s10552-020-01292-2

44. Gaasch A, Schönecker S, Simonetto C, Eidemüller M, Pazos M, Reitz D, et al. Heart sparing radiotherapy in breast cancer: the importance of baseline cardiac risks. *Radiat Oncol*. (2020) 15(1):117. doi: 10.1186/s13014-020-01520-8

45. Luo J, Virnig B, Hendryx M, Wen S, Chelebowski R, Chen C, et al. Diabetes, diabetes treatment and breast cancer prognosis. *Breast Cancer Res Treat*. (2014) 148 (1):153–62. doi: 10.1007/s10549-014-3146-9

46. Wilson PW, D'Agostino RB, Levy D, Belanger AM, Silbershatz H, Kannel WB. Prediction of coronary heart disease using risk factor categories. *Circulation*. (1998) 97 (18):1837–47. doi: 10.1161/01.CIR.97.18.1837

47. Grundy SM, Pasternak R, Greenland P, Smith S Jr, Fuster V. Assessment of cardiovascular risk by use of multiple-risk-factor assessment equations: a statement for healthcare professionals from the American heart association and the American college of cardiology. *Circulation*. (1999) 100(13):1481–92. doi: 10.1161/01.CIR.100.13.1481

48. Ridker PM, Buring JE, Rifai N, Cook NR. Development and validation of improved algorithms for the assessment of global cardiovascular risk in women: the reynolds risk score. *J Am Med Assoc*. (2007) 297(6):611–9. doi: 10.1001/jama.297.6.611

Frontiers in
Cardiovascular Medicine

Innovations and improvements in cardiovascular treatment and practice

Focuses on research that challenges the status quo of cardiovascular care, or facilitates the translation of advances into new therapies and diagnostic tools.

Discover the latest Research Topics

See more →

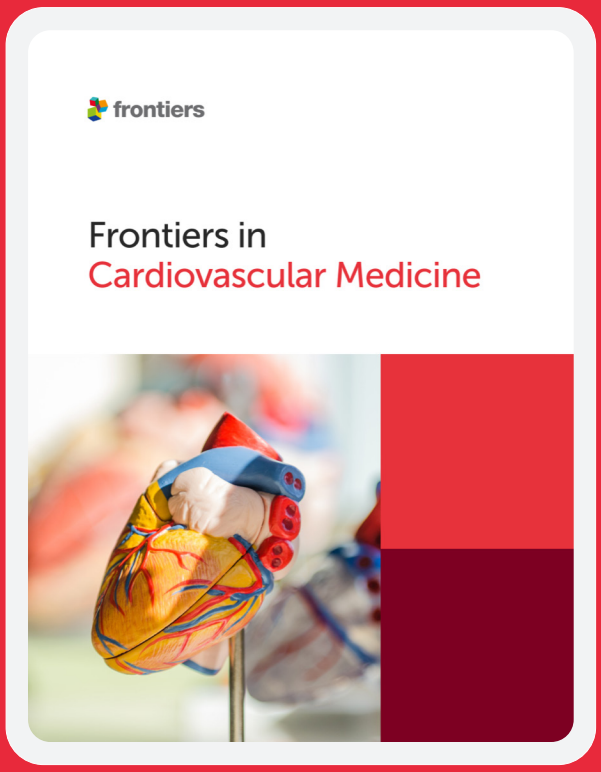

Frontiers

Avenue du Tribunal-Fédéral 34
1005 Lausanne, Switzerland
frontiersin.org

Contact us

+41 (0)21 510 17 00
frontiersin.org/about/contact